

UNCLASSIFIED

AD NUMBER
AD234980
NEW LIMITATION CHANGE
TO Approved for public release, distribution unlimited
FROM Distribution authorized to U.S. Gov't. agencies and their contractors; Administrative/Operational Use; FEB 1960. Other requests shall be referred to Army Corps of Engineers, Washington, DC 20310.
AUTHORITY
wes d/a ltr 11 jul 1975

THIS PAGE IS UNCLASSIFIED

UNCLASSIFIED

AD

234 980

Reproduced

Armed Services Technical Information Agency

ARLINGTON HALL STATION; ARLINGTON 12 VIRGINIA

NOTICE: WHEN GOVERNMENT OR OTHER DRAWINGS, SPECIFICATIONS OR OTHER DATA ARE USED FOR ANY PURPOSE OTHER THAN IN CONNECTION WITH A DEFINITELY RELATED GOVERNMENT PROCUREMENT OPERATION, THE U. S. GOVERNMENT THEREBY INCURS NO RESPONSIBILITY, NOR ANY OBLIGATION WHATSOEVER; AND THE FACT THAT THE GOVERNMENT MAY HAVE FORMULATED, FURNISHED, OR IN ANY WAY SUPPLIED THE SAID DRAWINGS, SPECIFICATIONS, OR OTHER DATA IS NOT TO BE REGARDED BY IMPLICATION OR OTHERWISE AS IN ANY MANNER LICENSING THE HOLDER OR ANY OTHER PERSON OR CORPORATION, OR CONVEYING ANY RIGHTS OR PERMISSION TO MANUFACTURE, USE OR SELL ANY PATENTED INVENTION THAT MAY IN ANY WAY BE RELATED THERETO.

UNCLASSIFIED

AD No. 234980
ASTIA FILE COPY

FLOODS RESULTING FROM SUDDENLY BREACHED DAMS

CONDITIONS OF MINIMUM RESISTANCE

Hydraulic Model Investigation

234980

10



XEROX

MISCELLANEOUS PAPER NO. 2-374

Report I

February 1960

FILE COPY

Return to

ASTIA

ARLINGTON HALL STATION

ARLINGTON 12, VIRGINIA

Attn: TISSS

ASTIA
RECEIVED
APR 15 1960
RESERVED
TIPDR

U. S. Army Engineer Waterways Experiment Station
CORPS OF ENGINEERS

Vicksburg, Mississippi

FLOODS RESULTING FROM SUDDENLY BREACHED DAMS

CONDITIONS OF MINIMUM RESISTANCE

Hydraulic Model Investigation



MISCELLANEOUS PAPER NO. 2-374

Report I

February 1960

U. S. Army Engineer Waterways Experiment Station
CORPS OF ENGINEERS
Vicksburg, Mississippi

ARMY-NRC VICKSBURG, MISS.

Preface

This report is the first of a series relating to the problem of dam-breach floods, and describes the procedures and summarizes the results of tests made in a model flume involving its natural roughness condition. A second report will contain additional data of a similar nature for tests with an artificial roughness added to the flume. It is planned to publish a final report which will summarize, further analyze, and correlate the data previously presented in the preliminary reports. The final report will also present a method of predicting the stage and discharge hydrographs of floods released by the sudden breaching of dams.

The investigation was authorized by the Office, Chief of Engineers, as a part of R&D Project 8-12-95-420 in November 1955. The experiments reported herein were conducted during the period July 1956 to July 1958 by personnel of the Hydraulics Division under the general supervision of Messrs. E. P. Fortson, Jr., and F. R. Brown. Mr. G. L. Arbuthnot, Jr., was directly in charge of the study and was assisted by Mr. J. N. Strange. Design of the test facilities, evaluation of measuring techniques, operation of the model, data analysis, and correlation of results were accomplished by the following personnel: Cpl. D. J. Sadar (deceased), SP-4 H. B. Spalding, SP-4 J. D. Laarman, SP-4 T. Schmidgall, SP-4 N. J. Ferrell, and Messrs. S. H. Halper, B. B. Boggan, and G. A. Wilkerson.

Programs for the IBM 650 computer, used in certain of the numerical procedures, were written by Mr. J. M. Pinkston, SP-4 S. Closs, and SP-4 J. D. Laarman.

The consultative services of Drs. G. H. Keulegan, R. F. Dressler, H. Rouse, A. T. Ippen, and Messrs. R. L. Irwin and F. P. Barklow are gratefully acknowledged.

Directors of the Waterways Experiment Station during the tests reported herein and preparation of this report were Col. A. P. Rollins, Jr., CE, and Col. Edmund H. Lang, CE. Technical Director was Mr. J. B. Tiffany.

Contents

	<u>Page</u>
Preface	iii
Notations	vii
Summary	ix
Introduction	1
General history	1
Purpose of the investigation	3
Scope of the investigation and this report	3
Description of Test Facilities	4
Test flume	4
Water supply	5
Dam-ejection mechanism	7
Test Conditions	8
Non-base flow tests	8
Base flow tests	10
Adjustment and Calibration of Flume	11
Grading of flume	11
Calibration of flume roughness	11
Means of Measuring the Stage-Time Hydrograph	12
Staff gages	13
Provision of a time reference	16
Method of Determining Discharge-Time Hydrographs	16
Discharge at the dam (non-base flow tests)	16
Discharge at the dam (base flow tests)	17
Discharge at stations downstream of dam	18
Test Procedures	21
Discussion of Test Results	22
Stage-time hydrographs	22
Discharge-time hydrograph at dam	24

Contents (Continued)

	<u>Page</u>
Discharge-time hydrographs for stations downstream from the dam	29
The upstream negative wave (non-base flow tests)	30
The upstream negative wave (base flow tests)	31
The downstream positive wave (flood wave), non-base flow tests	32
The downstream positive wave (flood wave), base flow tests	33
Conclusions	33
Data-gathering techniques	33
Stage-time measurements	33
Discharge-time measurements	34
Negative wave	35
Positive wave (downstream flood wave)	35
Application to prototype situations	36
List of References	36
Tables 1-21	
Plates 1-110	

Notations

A	Area of flow, sq ft
D_b	Distance from original water surface to bottom of breach (depth of breach), ft
g	Acceleration of gravity, 32.2 ft/sec ²
L	Length of reservoir, 200 ft
n	Manning's coefficient of roughness, sec/ft ^{1/3}
Q	Discharge at dam, cu ft/sec
Q_b	Base flow discharge, cu ft/sec
Q_{max}	Maximum discharge at dam, cu ft/sec
Q_d	Discharge at station downstream of dam, cu ft/sec
R	Hydraulic radius, ft
S	Slope of energy gradient, dimensionless
S_f	Slope of flume, $S_f = 0.005$, dimensionless
t	Time after breach, sec
t_a	Arrival time of negative or positive wave, sec
t_f	Duration of flood wave, sec
t_o	Time of outflow, sec
v	Velocity of flow (average), ft/sec
v_c	Velocity of confetti (surface velocity), ft/sec
V_o	Volume of outflow, cu ft
V_b	Volume of reservoir above breach level, cu ft
V_s	Storage volume of reservoir, cu ft
W_b	Width of breach at original water surface, ft
W_d	Width of dam at original water surface, ft
X_d	Distance downstream from dam, ft
X_u	Distance upstream from dam, ft

y Depth of water, ft
 y_{av} Average depth of water, ft
 y_d Depth of water (stage) downstream from dam, ft
 y_o Depth of water (at the dam) that lies above the breach level at time t after breach, ft
 y_u Depth of water (stage) upstream from dam, ft
 Y_o Depth of water at dam before breach, ft

Summary

The purpose of this study was to obtain experimental stage and discharge data resulting from dam breaches in a model flume. This information, along with that from subsequent tests, will be used to verify or assess the reliability of theoretical and analytical methods developed to predict the flood magnitudes resulting from dam breaches in prototype conditions.

The experimental tests were conducted in a sloped, rectangular flume with the dam located midway of its length, thus permitting both upstream and downstream observations.

Twelve test conditions, each representing a different breach pattern, were simulated with no base flow, and five test conditions were simulated with a base flow included. For each test condition, readings were made to obtain stage-time records at various stations both upstream and downstream from the dam and velocity-time records at three downstream stations. From these records, discharge-time hydrographs were calculated for flow through the breached section and for 3 downstream stations.

The methods used in obtaining these measurements were found to be satisfactory.

As a result of these tests, conclusions were reached regarding the maximum flow through a given breach, the maximum stage at the dam and downstream stations, the propagation of the negative wave, and the shape, velocity, and duration of the positive wave. ©

FLOODS RESULTING FROM SUDDENLY BREACHED DAMS

CONDITIONS OF MINIMUM RESISTANCE

Hydraulic Laboratory Investigation

Introduction

General history

1. During the Second World War, the deliberate breaching of the Mohne and Eder Dams^{6*} in Germany created disastrous flood waves which produced severe damage to most all manmade facilities that lay in the flood plains of both reservoirs. As a result of the breaching of the Mohne Dam, production in the heavily industrialized Ruhr Valley was seriously curtailed, thereby affecting the flow of vital war materiel. Furthermore, transportation and communication facilities were comparatively inoperable throughout much of the region. Prolonged inundation denied the enemy direct access to the area; consequently, recovery and rehabilitational efforts were seriously delayed. Sober reflection on this single event points beyond question to the fact that floods resulting from suddenly breached dams can be effectively used either in offensive or defensive situations.

2. The degree and extent of the damage that accompanies a major flood are proportional to the height, duration, and speed with which the flood wave is propagated. These factors vary with the characteristics of the river channel and the rate of flow from the breached dam, the latter being affected principally by the size/shape of the breach and the volume/shape of the reservoir. In essence, this implies the larger the breach, the more severe the flood.

3. The ability to extensively breach or completely destroy a given dam was multiplied a thousandfold with the advent of the nuclear-thermonuclear family of weapons. By utilizing these energy sources, entire dams can be removed almost instantaneously, thus releasing the highest flood wave a given reservoir is capable of producing. Consideration of the experiences derived from World War II, plus the added capability to more extensively breach a given dam, led to the realization that a means of estimating the depth, duration, and extent of a flood wave thus created was extremely desirable. The ability to forecast the magnitude and extent of

* Raised numbers refer to similarly numbered items in the List of References that follows the text of this report.

an anticipated flood would permit the execution of countermeasures that might obviate or alleviate some of the damaging effects.

4. Until recently, little experimental work had been accomplished with regard to floods resulting from suddenly breached dams. Barré de Saint Venant,¹ a 19th century engineer-mathematician, considered theoretically the dam-breach problem and formulated an equation of the free surface of the water at any time t for the case where friction was neglected, where the entire dam was instantly removed, and where the slope of the two-dimensional flume was zero. The expression developed by St. Venant is given in equation 1.

$$\frac{X_d \text{ (or } X_u)}{t \sqrt{g Y_o}} = z - 3 \sqrt{\frac{y}{Y_o}} \quad (1)$$

With $X_d = 0$ and $t = 1$, the depth of flow at the dam is equal to $4/9 Y_o$. St. Venant also determined that the maximum discharge flowing through the breach was related to initial depth of reservoir at the dam and the width of the dam (equation 2).

$$Q_{\max} = \frac{8}{27} W_d \sqrt{g} Y_o^{3/2} \quad (2)$$

5. Approximately twenty years later, A. Ritter,¹⁰ using the previous work of St. Venant, developed an explicit solution of the problem for a two-dimensional configuration, a horizontal stream bed with no water in the channel below the dam, and with the water above the dam at rest. Some twenty-five years later, Dr. Armin Schoklitsch¹² conducted experimental studies in an effort to evaluate resistance effects and to adequately describe just how they affect the dam-breach problem.

6. During the next twenty-five years a few other researchers intermittently studied the problem without making major contributions to its general solution. In 1952, Dr. Robert F. Dressler prepared a paper² which discussed the work of St. Venant, Ritter, and Equiazaroff, and presented the results of additional theoretical analyses along with the results of rather extensive laboratory experiments. As a result of this work, certain refinements to the general theoretical solution were realized by taking into account the resistance to flow. Subsequent theoretical and experimental work by Dressler³ contributed substantially toward an

understanding of the behavior of the flood-wave tip, which is grossly influenced by the turbulence that is common to this region of the flood wave.

7. Several years ago, the Military Hydrology Branch (MHB) of the Washington District, Corps of Engineers,* was requested to pursue a line of study that would provide the Corps of Engineers with a feasible solution to the dam-breach problem, a solution that would lend itself to ready use by field units, and one that would satisfactorily estimate the extent and magnitude of a flood arising from an assumed breach. A thorough review of literature dealing with the dam-break problem was made, and findings were abstracted. Using the knowledge gained in the literature search and the laws and axioms of classical hydrology, an analytical solution was evolved wherein breaches of varying size and shape were assumed. Various channel slopes were treated for a single channel roughness ($n = 0.03$). A number of reports were published; however, the main effort is reflected in two reports, both entitled Flow Through a Breached Dam.^{13,14} These reports utilized the basic principles of hydrology to formulate a method of predicting, with limited accuracy, flows through a breached dam.

Purpose of the investigation

8. Because only a limited amount of experimental data was available on which to base an empirical approach to the problem, it was decided that a broad laboratory investigation was needed in order to assess the reliability of the theoretical work and to evaluate the exactitude of the analytical approach formulated by the MHB. Accordingly, the U. S. Army Engineer Waterways Experiment Station was authorized to conduct the study as a part of Research and Development Project 8-12-95-420.

Scope of the investigation and this report

9. The study was to include determination of the stage and discharge hydrographs at the dam, and at several stations downstream from the dam, for various sizes and patterns of breach and for several degrees of channel roughness. However, because of fund limitations and an underestimation of the time required to accomplish the investigation, data will be obtained for only two roughnesses.

* MHB is now attached to Army Map Service, CE.

10. This report describes the test facilities, the test procedures, the data-recording system, the data-reduction techniques, the test conditions, and the experimental results obtained without the addition of artificial roughness ($n \sim 0.009$). A second preliminary report will publish additional data from tests of a similar nature but with roughness added to the bottom and sides of the flume ($0.02 < n < 0.15$ depending on the depth of flow). A final report is planned that will more extensively analyze and interpret the data presented in the preliminary reports and will present a method for estimating the magnitude of a flood resulting from the sudden failure of a given dam or portion thereof.

Description of Test Facilities

Test flume

11. The experiments were conducted in a wooden flume 4 ft wide and 400 ft long, constructed on a slope equal to 0.005 (fig. 1). Water was

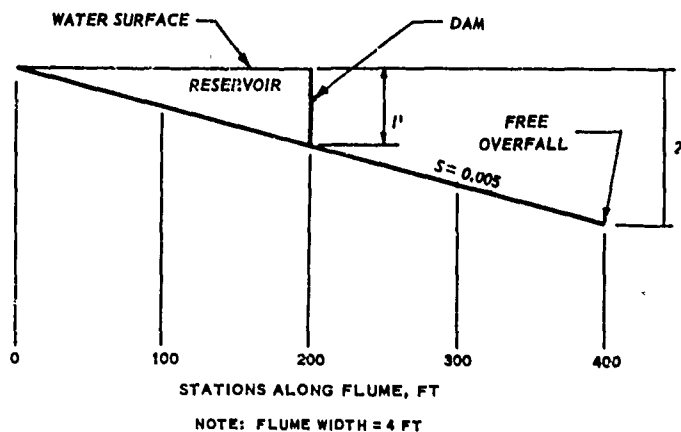


Fig. 1. Schematic diagram of flume

impounded at station* 200 by a simulated dam (hereafter referred to as model dam) to a depth of 1 ft. The side walls of the flume were 21 in high from sta 0 to sta 208, and 16 in. high from sta 208 to sta 400. The right wall of the flume from sta 172 to sta 208 was fabricated of glass panels

* The term station refers to distances that are measured horizontally from the upstream end of the flume (upper end of model reservoir).

4 ft long and 21 in. high so that visual observation of flow patterns beneath the water surface could be determined in this section. The glass panels also made possible more accurate monitoring of the stage gages in the region near the dam, where changes in the water surface elevation with time were most acute. The flume was lined with 3/8-in. plastic-coated plywood (GPX tan 60/60). This material was selected because of its ability to resist warping and deterioration. From the upstream end of the flume (sta 0) down to sta 100, the flume was supported on 4-in.-diameter pipes partially



Fig. 2. Headbay foundation and upper end of flume during construction

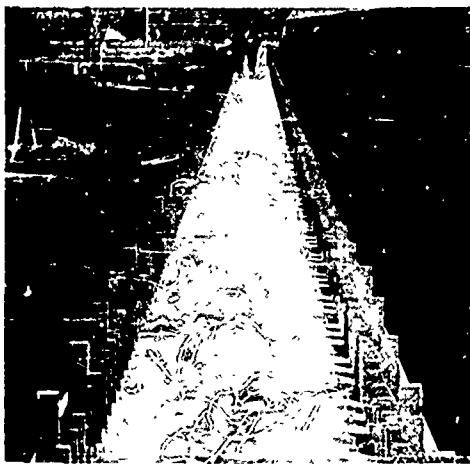


Fig. 3. Upstream view of flume showing aligned buttresses before side wall were placed

imbedded in concrete footings. The remainder of the flume (sta 100 to sta 400) utilized the side walls of an existing concrete sump as continuous footings upon which were placed the supporting and framing members of the flume. Figs. 2, 3, and 4 show the flume at various stages of construction.

Water supply

12. Water, for operation of the flume, was supplied from an existing recirculating system. To begin operations, it was necessary to tap the main pressure

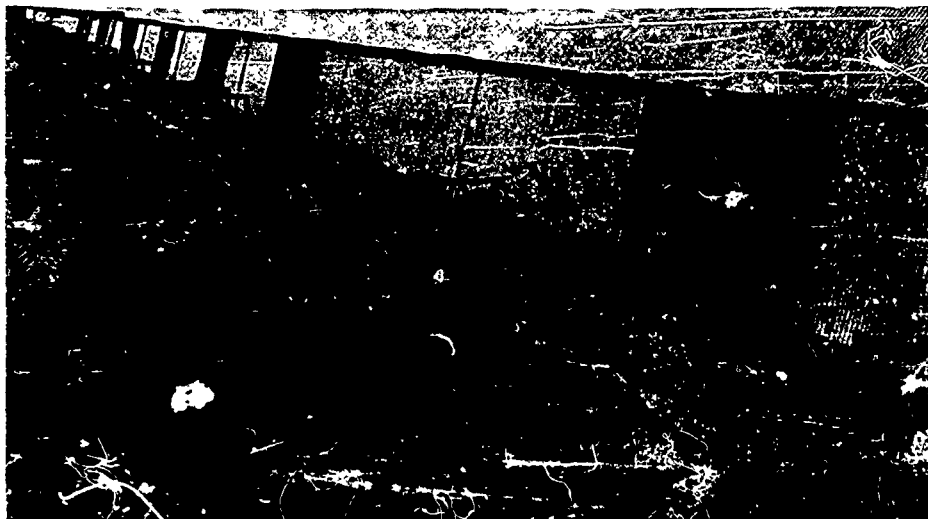


Fig. 4. Upstream view of a portion of the completed flume.



Fig. 5. Water-supply system
tively. After flowing through the flume, the water was returned to the central pumping system.

header with appropriate size feed pipes, and to introduce into the feed system flow-control and flow-measuring equipment (fig. 5). Inflow was controlled by hand-operated gate valves. The various discharges needed to calibrate flume roughness at various depths and to provide appropriate base flows were measured by two types of flow-measuring devices. The low flows ($Q \leq 2.5$ cfs) were measured through a 90° V-notch weir. Higher flows (up to approximately 25 cfs) were measured through either a 9- or 15-in. orifice plate mounted in the 12- and 20-in. supply lines, respec-

Dam-ejection mechanism

13. To simulate the breaching of a dam by explosive attack, it was necessary to remove the entire model dam or portion thereof almost instantaneously. Several different methods of accomplishing this were considered. The method selected as offering the most economic and yet satisfactory way of removing the dam makes use of a falling weight (100 lb) to furnish the kinetic energy for removal of the dam. The dam-ejection mechanism is shown in fig. 6. High-speed motion pictures of this system showed



Fig. 6. Dam-ejection mechanism

that the model dam was jerked vertically upward and free of the water surface in the order of $1/30$ of a second. For test conditions involving small breaches (test conditions 4.1, 5.1, 6.1, 9.1, 10.1, and 12.1), the time of ejection was more in the order of $1/100$ of a second.

Test Conditions

14. In order to assess the extent and magnitude of floods induced by breaching actions, it was necessary to determine the stage and discharge hydrographs when various size breaches were created in the model dam. Breach patterns were chosen so as to simulate the removal of the entire dam, the failure of single or multiple monoliths, and the removal of gated bays across the top of a dam. A few of the model dams used during the study are shown in figs. 7-10. Some of these tests were made for the condition when the channel downstream of the dam was dry (non-base flow tests) and some were made when a known flow was passed beneath the dam (base flow tests), simulating routine flood flow over a spillway and/or discharge through flood conduits and penstocks.

Non-base flow tests

15. Twelve test conditions were employed to document the stage and discharge hydrographs and to assess the behavior of the flood wave as it traverses the downstream channel when it is "essentially dry" (no water flowing in the exit channel). The test conditions are identified and described in table A. The decimal system is used in numbering the test conditions; the whole number refers to the test condition (breach pattern and orientation) while the decimal refers to the condition of roughness, i.e., the point 1 refers to the natural roughness of the flume ($n \sim 0.009$).

Table A
Description of Non-Base Flow Test Conditions

Test Conditions	Width of Breach, ft	Depth of Breach, ft	$\frac{W_b}{W_d}$	$\frac{D_b}{Y_o}$	$\frac{W_b}{W_d} \cdot \frac{D_b}{Y_o}$
1.1	4.00	1.00	1.00	1.00	1.00
2.1	2.40	1.00	0.60	1.00	0.60
3.1	1.20	1.00	0.30	1.00	0.30
4.1	0.60	1.00	0.15	1.00	0.15
5.1	0.40	1.00	0.10	1.00	0.10
6.1	0.24	1.00	0.06	1.00	0.06
7.1	4.00	0.60	1.00	0.60	0.60
8.1	4.00	0.30	1.00	0.30	0.30
9.1	4.00	0.15	1.00	0.15	0.15
10.1	4.00	0.10	1.00	0.10	0.10
11.1	2.40	0.60	0.60	0.60	0.36
12.1	1.20	0.30	0.30	0.30	0.09



Fig. 7. Model dam for test conditions 1.1, 1.1(10), and 1.1(20)



Fig. 8. Model dam for test condition 6.1



Fig. 9. Model dam for test condition 8.1



Fig. 10. Model dam for test condition 11.1

Base flow tests

16. Five test conditions were set up from conditions 1.1, 2.1, and 3.1 to determine the hydrographs and flood wave action when a base flow is passed beneath the dam. A schematic diagram of the base flow conditions is shown in fig. 11. The base flow test conditions are identical in breach

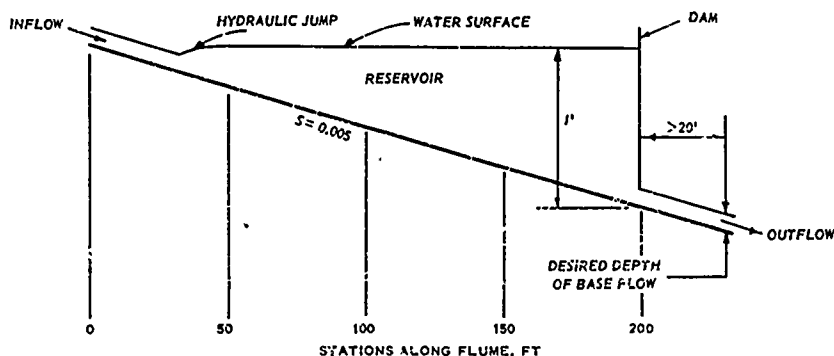


Fig. 11. Schematic diagram of base flow conditions

pattern with those itemized in table A except that a number in parentheses is added to identify the magnitude of the base flow. For example, 1.1(10) means that the depth of the base flow, at a station sufficiently distant downstream so as to permit the flow to become completely stable and uniform, is equal to 10 per cent of the water depth at the dam before breaching occurred (Y_0). The depth Y_0 is equal to 1 ft for both the non-base flow and base flow tests. Fig. 12 illustrates the base flow breach for

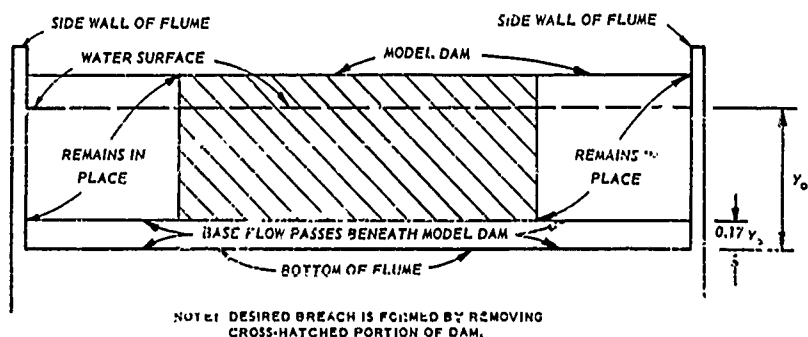


Fig. 12. Base flow breach, test condition 2.1(20)

test condition 2.1(20). The base flow test conditions were: 1.1(10), 1.1(20), 2.1(10), 2.1(20), and 3.1(10). In each of the base flow test conditions, the depth of breach (D_b) was equal to 1 ft and the total volume within the reservoir was equal to 400 cu ft. For the 10 per cent base flow, $Q_b = 1.00$, and for the 20 per cent base flow, $Q_b = 3.07$.

Adjustment and Calibration of Flume

Grading of flume

17. Before each test series was begun and approximately once each month during the tests, a complete level survey at intervals of 5 or 10 ft was made along the entire flume to assure that the flume was at proper grade and slope. Because the flume was constructed almost entirely of wood, and therefore subject to shrinking and swelling cycles, it was impossible to grade the flume precisely. Hence, the flume was considered to be near enough proper grade when its actual elevation was within the limits of the desired grade elevation ± 0.01 ft. Grade elevations in error by an amount greater than 0.01 ft were adjusted to proper elevation.

Calibration of flume roughness

18. The natural flume (without the addition of artificial roughness) was calibrated for roughness as a function of depth of flow ($0.05 < y < 1.0$) under conditions of uniform flow. Knowing the discharge and depth of flow, the roughness n was determined from Manning's equation,

$$n = \frac{1.486 R^{2/3} S^{1/2} A}{Q}$$

where Q is the discharge in cu ft per sec, R is the hydraulic radius in ft, S is the slope of the energy gradient which in this case is equal to the slope of the flume (true only for uniform flow), and A is the area of flow ($4y$). A number of test runs were made to evaluate roughness as a function of depth of flow, the results of which are presented in fig. 13. From these data, it is obvious that the roughness remained essentially constant over the range of depths considered. Hereafter, the flume roughness will be assumed equal to 0.009 regardless of the depth of flow.

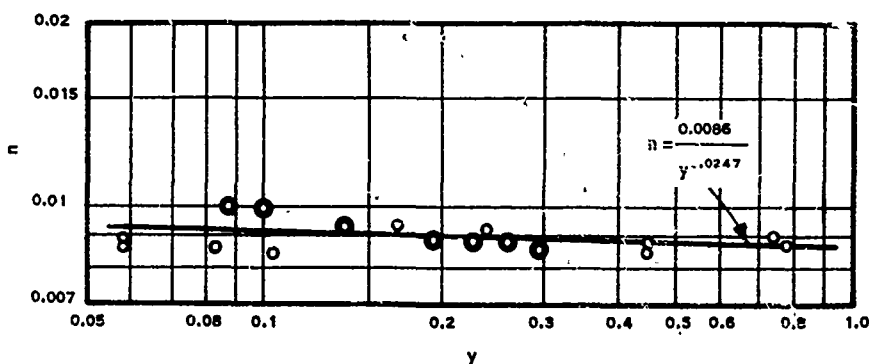


Fig. 13. Variation of roughness with depth of flow

Means of Measuring the Stage-Time Hydrograph

19. For both the non-base flow and base flow test conditions, it was necessary to determine the variation of depth of water at stations along the flume with time. In most instances these observations were made at approximately 20 different recording stations for both the non-base flow and base flow tests. Several different methods of obtaining the stage-time hydrograph were considered. The possibility of using stereophotogrammetry was the first method considered. After careful investigation and consultation with appropriate personnel at the Army Map Service as to what was involved in obtaining stereoshots at frequent time intervals, due consideration of the equipment needed, and the time required for processing and interpreting the shots, the method was abandoned as being too costly. Repeated attempts were made to electronically record on an oscillogram the depth of water versus time by using several styles of resistance- and inductance-type wave rods. The major objection to using these rods arose from the fact that appreciable build-up of the water surface occurred on the upstream edge of the rod due to velocities that were generally critical or supercritical at some time during the test run. The parallel-wire wave rod was entirely satisfactory as far as the "build-up" was concerned; however, the nonlinearity of the calibration over the range of depths involved made its use objectionable also.

20. A third technique which involved photographing, with 16mm movie

cameras, staff gages with time indicators in the fields of view, was tried and found to be satisfactory. This method involved essentially no instrumentation, required no calibration, and gave directly the stage and the time after breach. A sufficient number of cameras were available (generally six) to permit simultaneous shooting of several stations along the flume; however, repeated runs were necessary in order to photograph all specified stations. Plate 1 shows the reproducibility of stage as a function of time experienced at station 185 (test condition 1.1) for several repeated runs. Cameras were normally operated at 8 to 12 frames per second. Observations of stage and time are presented in tables 1-17. Stage-time hydrographs determined from these data are shown in plates 2-81.

Staff gages

21. Description. The three types of staff gages used in measuring the depth of flow (stage) are shown in fig. 14. The gages are presented (left to right) in the order of their development. Since the negative film was projected, the gage on the extreme right highlighted the water surface and was much easier to read than the previous types. The gages were made from sheet metal 0.04 in. thick. Strips were cut to the proper length but twice as wide as the finished gage. The strip was then folded lengthwise and the rounded edge was oriented upstream when placed in the flume. Placing the gage in this manner minimized flow disturbance around the gage, which



Fig. 14. Typical staff gages

in turn minimized "pile-up." Divisions along the gage were marked at 0.05-ft intervals. After the gages were properly marked and painted, they were sprayed with a clear plastic so as to reduce roughness and protect the finish.

22. Calibration tests, to determine the accuracy to which the staff gage recorded the water depth, were made using the regular point gage under conditions of uniform flow as a standard. These tests showed that the staff gage could be read accurately enough to bracket the point gage reading, ± 0.01 ft. Velocities experienced in these tests were of the same order of magnitude as those experienced in actual test runs so that "pile-up" on the nose of the staff gage was comparable. Considering that the water surface was not perfectly smooth but was marked with standing waves and local disturbances, the accuracy of the staff gage was believed satisfactory.

23. Mounting and placement. The staff gages were initially mounted as shown in fig. 15; however, this system was changed to a more versatile

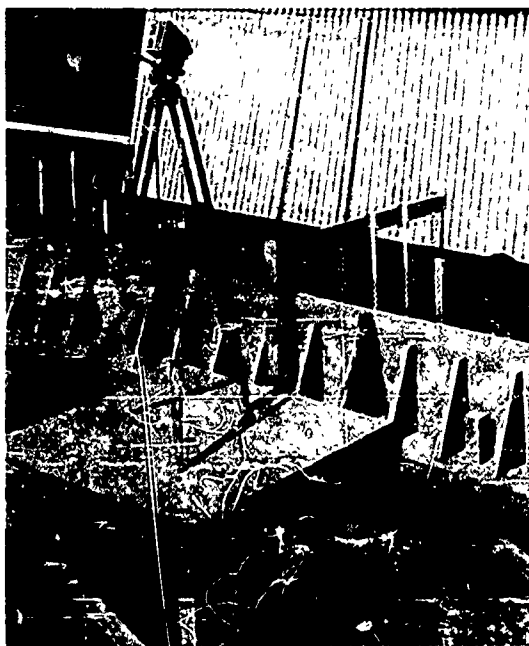


Fig. 15. Setup for recording stage at sta 160

mounting wherein the gages were attached to several 3-ft rails running lengthwise of the flume. The latter mounting system was conveniently portable and was particularly useful in the region from sta 180 to sta 200 where the intervals at which stage-time measurements were required were generally small. Where single recording stations were used, such as sta 40 and 70, the gages were attached to angle-iron clips that were mounted on 2-by-4's about 4.5 ft long.

24. Staff gages were distributed across the flume

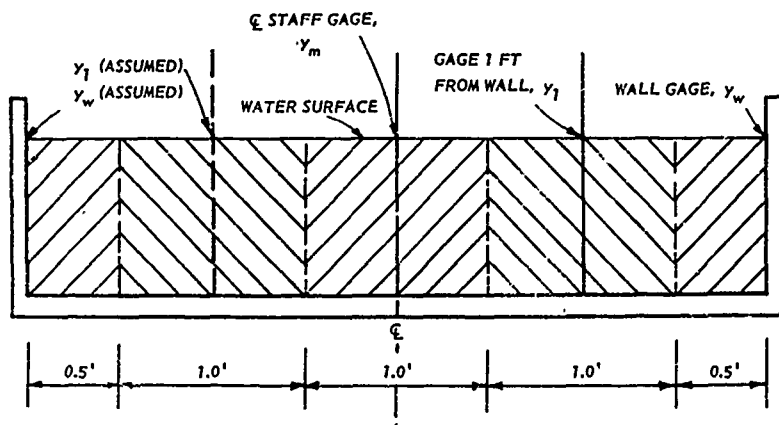


Fig. 16. Distribution of gages across flume

as shown in figs. 15 and 16. Since flow was considered symmetrical about the center line, the gages marked " y_1 (assumed)" and " y_w (assumed)" are considered in the computation of the average stage. The area of flow A equals:

$$A = 0.5y_w + y_1 + y_m + y_1(\text{assumed}) + 0.5y_w(\text{assumed})$$

also,

$$A = 4y_{av}$$

$$4y_{av} = 0.5y_w + y_1 + y_m + y_1(\text{assumed}) + 0.5y_w(\text{assumed})$$

but

$$y_1(\text{assumed}) = y_1 \text{ and } y_w(\text{assumed}) = y_w$$

hence

$$y_{av} = \frac{y_w + 2y_1 + y_m}{4} \quad (3)$$

The average stage was computed from equation 3 for all test conditions. Very little difference in stage was noted regardless of the gage's position laterally across the flume. The location and number of stations photographed varied with the test condition; but generally, staff gages were photographed at stations 40, 70, 100, 120, 140, 150, 160, 172, 181, 189, 191, 195, 197, 199, 200, 220, 225, 230, 275, 280, 285, 345, 350, and 355.

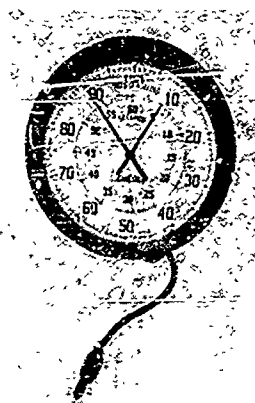


Fig. 17. Clock used to provide time scale (reading = 4.894 sec)

Provision of a time reference

25. The time reference for all tests was provided by the timer shown in fig. 17. This timer is manufactured by the Standard Electric Time Company. The outer dial is divided to read directly to $1/100$ of a second while the inner dial records time in seconds. Each timer is equipped with manually operated start, stop, and reset switches; however, in these tests, the timers were started by the closing of a microswitch that was triggered by ejection of the model dam (see fig. 6). The initial upward displacement of the dam closed the microswitch, completing the circuit to all timers in use on the particular test.

Method of Determining Discharge-Time Hydrographs

Discharge at the dam (non-base flow tests)

26. The discharge through the various breaches as a function of time was determined by cross-plotting the stage-time data (tables 1-17) to plots of stage versus station for different times. A typical plot of this type is shown in plate 82. Since all stages plotted thereon were referenced to the flume bottom, the plate shows the water-surface profiles upstream of the dam for the various times indicated. The difference in the original cross-sectional area of the reservoir (taken lengthwise of the flume) and that remaining in the reservoir at time t , when multiplied by the flume width, equals the volume of outflow that has occurred up until time t . Plots similar to this were made for each test condition and for the times indicated in tables 1-17. From these plots, volume-of-outflow-as-a-function-of-time curves were developed for each test condition. Plate 83 shows the volume-time plot for test condition 1.1 as developed from the plot shown in plate 82. The desired discharge-time hydrograph for each test condition was determined by differentiation of the respective volume-time functions. Efforts were made to determine the equations of each

volume-time curve so that a mathematical differentiation could be performed; however, most of the curves proved difficult to fit throughout the time range covered by the data without resorting to at least a 4th order polynomial or even more complex functions. Hence, it was felt that the effort required to determine the equations would be too costly and time consuming. The volume-time curves were therefore differentiated by numerical methods. Plots of the discharge-time hydrographs through the various breach patterns are shown in plates 84-86 for test conditions 1.1 through 12.1.

Discharge at the dam
(base flow tests)

27. Plots of stage versus station for various times and for each test condition were made for the base flow tests also. A typical plot of this type is shown in plate 87. Fig. 18 illustrates the base flow geometry

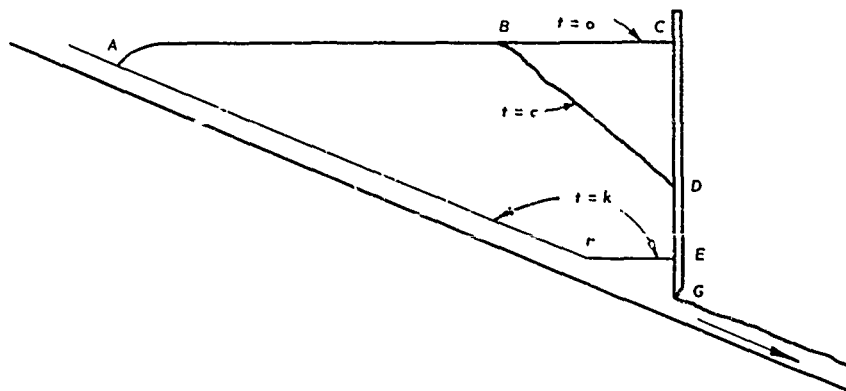


Fig. 18. Base flow geometry before and after breach,
test conditions 2.1(10), 2.1(20), and 3.1(10)

that is characteristic of condition 2.1(10), 2.1(20), and 3.1(10) at three different times. The water-surface profile at $t = 0$ is defined by ABC; at $t = c$, it is defined by ABD; and at $t = k$, where k is sufficiently large so that the reservoir storage has emptied and the base flow has become stable (water-surface profile does not change with time), is defined by AFEG. When $t = k$, the stable water-surface profile appears as AFG for test conditions 1.1(10) and 1.1(20). Using this identification system, the initial reservoir storage for 2.1(10), 2.1(20), and 3.1(10) is defined as

$(ABCDEF) \times 4$ when the base flow is neglected, while for conditions 1.1(10) and 1.1(20) it is defined as $(ABCDEGF) \times 4$, again neglecting base flow. The total volume within the reservoir (reservoir storage plus base flow) in all cases is, as was true in the non-base flow tests, 400 cu ft. The total volume of outflow at $t = c$ is given by

$$V_o = \text{Area BCD} \times \text{width of flume} + Q_b(t)$$

or

$$V_o = 4(BCD) + Q_b(c)$$

From this relation, total volume of outflow as a function of time was determined for each base flow test condition, an example of which is presented in plate 88. The total volume-of-outflow-versus-time curves, developed for each base flow test condition, were also differentiated numerically to yield the discharge-time curves shown in plate 89.

Discharge at stations downstream from dam

28. Before the discharge-time hydrograph could be determined at the desired downstream stations, it was necessary to evaluate the velocity-time hydrograph as well as the stage-time hydrograph. Several methods of measuring the average velocity at the selected downstream stations were tried. Trial runs were made with pitot tubes, pressure cells, and Gurley flowmeters. These means proved unsatisfactory for the following reasons:

Pitot tubes: Poor response to the flood wave and undesirable fluctuations of the water column.

Pressure cells: Too insensitive to change in velocity at low flows.

Gurley flowmeters: Slightly insensitive plus the undesirable recording and interpretation of oscillograph records, whereon was recorded the number of revolutions per sec as a function of time.

29. A photographic method of obtaining the velocity was suggested by Dr. R. F. Dressler.³ The method was used by Dressler in some experimental studies conducted in a glass flume approximately 9 in. wide and 12 in. deep. It consisted of photographing particles in suspension using a time exposure. The length of the trace divided by the exposure time gave the particle velocity. By using particles of very nearly the same density as water, it was possible to keep them in suspension and at the same time

neglect inertial effects without appreciable error. The method was tried using several different particles made from different materials, but without success. The fact that the 4-ft width of the flume made it impossible to properly light the medium in such a way as to highlight the particles in suspension was the major reason for not using the method.

30. After the unsuccessful attempts described above, the problem of measuring the velocity-time hydrograph was discussed independently with Dr. A. T. Ippen and Hunter Rouse.* Both suggested that time exposures of confetti floating on the water surface be used to evaluate the surface velocity. It was further suggested that the surface velocities then be calibrated using conditions of uniform flow as the standard where the average velocity could be easily determined as

$$V = \frac{Q}{A}$$

Calibrations were made and the results indicated that the average velocity was 0.8 that of the surface velocity. This relation is in exact agreement with the hydraulic axiom regarding the relation between surface velocity and average velocity for shallow flow. Consequently, the surface velocities observed were reduced 20 per cent to yield the average velocity. The basic velocity-time data were plotted, and a representative curve was drawn through the points to obtain velocity measurements at regular time intervals for all the various test conditions. Tables 18, 19, and 20 give the average velocity-time data for all of the tests. Considering ten typical stations of different test conditions, the average deviation of all the velocity readings from the velocity curves was 3.8 per cent.

31. A 35mm Graflex camera was used to take photographs of the confetti traces from directly overhead. Fig. 19 shows schematically the setup used for determining the surface velocities at sta 225, 280, and 350. A timer (not shown) was also placed in the field of view to provide a time reference. The grid system (each grid measured 6 in. by 12 in.) provided a reference plane to make possible accurate determination of the trace length with insignificant error due to parallax. The confetti particles (1/2 in. square) were normally introduced 5 to 10 ft upstream of sta 225.

* Dr. A. T. Ippen, MIT, and Dr. Hunter Rouse, Iowa Institute of Hydraulic Research.

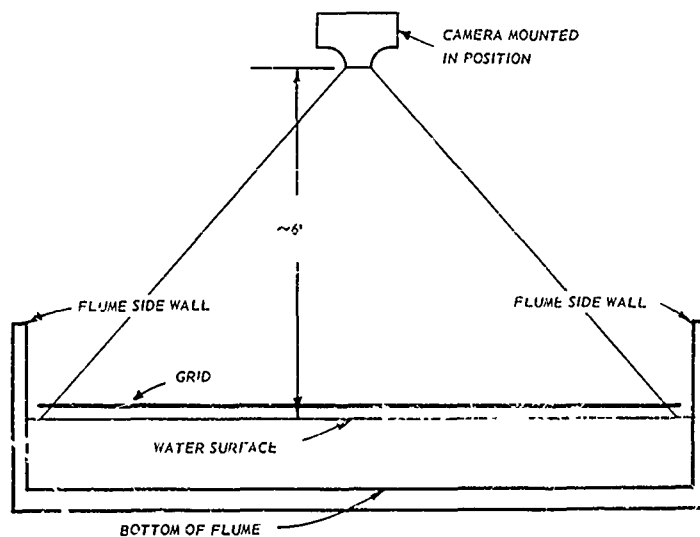


Fig. 19. Setup for obtaining surface velocities at downstream stations

When the confetti entered the grid system, a time exposure was taken (usually 1/10 sec) to provide a measurable trace. Exposures were repeated as often as advancing the film and cocking the shutter would permit. Two independent tests per station were made to insure that an adequate amount of data was obtained.

32. These films were projected frame by frame onto a screen where measurements of the traces were evaluated. To determine the surface velocities, it was necessary to measure the projected length of trace (l_t), ft; the projected width of trace (w_t), ft; the projected length of grid (l_g), ft; and the exposure interval or clock interval (t), sec. The velocity was then determined from:

$$v_c = \frac{0.5(l_t - w_t)}{t(l_g)} \quad (4)$$

where the constant 0.5 is the actual grid interval, ft.

33. The discharge-time hydrograph was determined from the stage-time and velocity-time hydrographs. The area of flow at a given time ($t = c$) is equal to hy_d ; hence,

$$Q(t = c) = 4y_d(t = c) \times v(t = c) \quad (5)$$

The discharge-time curves for the various test conditions thusly determined are shown in plates 90-98.

Test Procedures

34. Available movie cameras were set up to record stage and time at selected stations. The appropriate dam was put into place and the reservoir filled to a depth of 1.0 ft immediately adjacent to the dam. The reservoir was left undisturbed for a sufficient period of time to permit surges or seiches within it to be damped out. The microswitch was then set to initiate all timers in use at the instant of dam release, all timers having been preset to zero. Cameras were started at minus 5 seconds and were operated continuously until plus 90 seconds. Because of the gross difference in the breach and outflow patterns, the recording intervals varied from test to test, but in general, the cameras were operated for a period of 5 seconds at 15- and/or 30-second intervals after the first 90 seconds of the run. The Graflex camera was operated at approximately 4-second intervals beginning with the arrival of the downstream positive wave (flood wave). Since a number of stations had to be covered and it was impossible to record them all simultaneously, it was necessary to make repeated runs. Checks on the reproducibility of repeated runs revealed that the data obtained were in remarkable agreement (see plate 1). Similar checks were made on the arrival times of the negative and positive waves, and reproducibility of results was also found to be satisfactory.

35. When stage-time and velocity-time records had been completed for the selected stations, the films were processed and interpretation commenced. All films were projected onto a rigid screen from which observations were made. Generally the motion picture records of stage versus time were read every second or two for the first 30 to 60 seconds, then observations were made as often as the recording interval, usually 15 to 30 seconds. These data were then plotted for all stations recorded and for all test conditions (plates 2-81). Interpretation of the velocity-time measurements was made from the projected film strips and plotted as shown

in plates 90-98. Also shown on these same plates are the discharge-time hydrographs.

Discussion of Test Results

Stage-time hydrographs

36. The stage-time hydrographs recorded for the various stations both upstream and downstream from the dam and for all test conditions are shown in plates 2-81. Of primary importance is the stage-time hydrograph at the dam and at stations downstream from the dam. The stage-time hydrographs for the upstream stations (station numbers < 200) have their beginning with the arrival of the negative wave, and characteristically exhibit a marked reduction in the water depth over a relatively short time interval followed by a gradual reduction that takes place almost uniformly with time.

37. Stage-time hydrograph at dam. The variation of the depth of flow at the dam with time is presented for each test condition in those plates (2-81) that exhibit the plot for sta 200. When the entire model dam is suddenly removed, the stage drops immediately to one-half its former value, in this case 0.5 ft. This agrees with the experimental work of Schoklitsch mentioned previously, and shows negligible disagreement with the St. Venant equation which for the condition $x = 0$, $s_f = 0$, and $t = 1$, the stage would immediately fall to $4/9$ its former value. From the 0.5-ft depth, the stage progressively decreases with time to zero flow.

38. The effect of the breach opening on the stage at the dam for various times is shown in plate 99 for test conditions 1.1 through 6.1, where for each breach, $\frac{D_b}{Y_0} = 1$ and $\frac{W_b}{W_d} \leq 1$. The work of Schoklitsch (shown also in plate 99) is independent of time, since in his work the reservoir was assumed infinite in length and of constant depth. Deviation of the WES data from this curve qualitatively describes the combined effects of flume slope and the disparity of roughness factors in the WES flume as opposed to the flume used by Schoklitsch. From the family of curves, the stage at the dam can be predicted at various times for any partial width-full depth breach tested in the flume.

39. A similar plot (plate 100) presents the results for test conditions 7.1 through 10.1, where full width-partial depth breaches

$\frac{W_b}{W_d} = 1, \frac{D_b}{Y_o} \leq 1$ were involved. This plot may also be used to predict stage-time relations for any number of full width-partial depth breaches tested in the flume. A similar analysis of the partial width-partial depth breaches (test conditions 11.1 and 12.1) or for the base flow tests could not be made because too few tests were accomplished to permit a quantitative interpretation of results.

40. Stage-time hydrograph downstream from dam, non-base flow tests.

The variation of stage versus time for test conditions 1.1 through 12.1 is shown in those plates (2-81) where the station number is greater than 100. The arrival of the flood wave at a given station marks the beginning of the stage-time hydrograph at that station. Of major importance is the depth of water associated with the maximum downstream stage for each test condition. The downstream flood wave apparently reached a stable flow condition after traveling a distance equivalent to approximately $100 Y_o$, that is, the maximum stage remains constant after reaching this distance. Fig. 20 presents in dimensionless terms the maximum stages noted at sta 350 ($150 Y_o$ downstream). This data tends to fall on three distinct curves representing the three breach regimes; full depth-partial width, full width-partial depth, and partial depth-partial width. When the entire dam was removed, the maximum stage recorded at sta 350 was 0.34 ft. In a more general sense, this implies that since stable flow occurs at roughly $100 Y_o$ downstream from the dam, the maximum height that the flood wave may be expected to attain will be approximately $0.34 Y_o$.

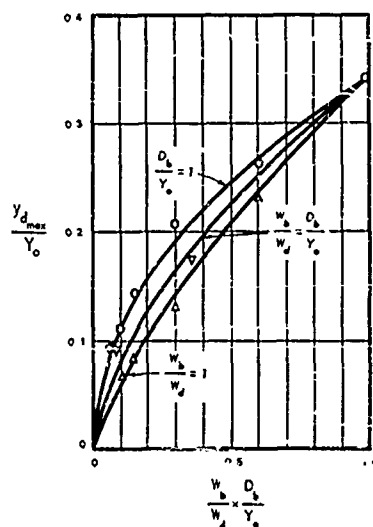


Fig. 20. Maximum downstream stage as a function of breach opening

41. The shape of the downstream flood waves was characterized by an

abrupt initial rise in the stage followed by an irregular increase up to the maximum stage level, which always occurred within 30 seconds of the flood wave arrival time. Should the downstream channel diverge (increase in width with distance downstream) and the alignment remain essentially straight, then the flood wave may be characterized by a more gradual rise and would have a smaller maximum depth. Conversely, should the channel converge and/or meander, then the flood wave may have an even more abrupt rise and would have a greater maximum depth.

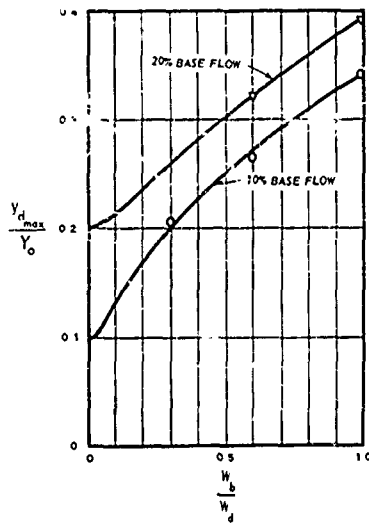


Fig. 21. Maximum downstream stage as a function of breach opening for the base flow tests

base flow being emitted from beneath the dam has not yet reached uniform flow conditions.

Discharge-time hydrograph at dam

43. Non-base flow tests. The discharge-time hydrographs for each of the non-base flow test conditions are presented in plates 84-86. The shapes of the curves are qualitatively similar, exhibiting for the most part a reversed "s" trend. Comparison of these curves at $t + \Delta t$ (where $\Delta t \rightarrow 0$) indicates the effect of breach opening on the maximum discharge observed.

42. Stage-time hydrograph downstream from dam, base flow tests. The variation of stage versus time for the base flow test conditions is shown in plates 65, 68, 69, 75, 76, 77, and 81. Fig. 21 shows graphically and in dimensionless form the maximum downstream stage observed during the base flow test conditions. The maximum stage observed for the 10 per cent base flow was $0.34 Y_0$, and for the 20 per cent base flow, the maximum stage observed was $0.39 Y_0$. The maximum downstream stage for all of the base flow tests occurred within 20 seconds of the wave-front arrival time.

From plates 68 and 76, the original base flow depth at sta 225 is seen to be less than 0.20 ft. This occurs because the

44. Using the equation developed by Schoklitsch,

$$Q_{\max} = \frac{8}{27} W_d \sqrt{g} Y_o^{3/2} \quad (6)$$

it is possible to compute the maximum discharge released by a given dam when the entire dam is instantaneously removed and when frictional effects are neglected. For the condition where partial width-full depth breaches are involved, the following equation may be used to determine Q_{\max}

$$Q_{\max} = \frac{8}{27} W_b \left(\frac{W_d}{W_b} \right)^{1/4} \sqrt{g} Y_o^{3/2} \quad (7)$$

Similarly, the maximum discharge for partial depth-full width breaches is determined from:

$$Q_{\max} = \frac{8}{27} W_d \left(\frac{Y_o}{D_b} \right)^{0.33} \sqrt{g} D_b^{3/2} \quad (8)$$

and for the condition of partial width-partial depth breach patterns,

$$Q_{\max} = \frac{8}{27} W_b \left(\frac{W_d}{W_b} \right)^{1/4} \left(\frac{Y_o}{D_b} \right)^{0.33} \sqrt{g} D_b^{3/2} \quad (9)$$

Equations 7 and 8 are modifications of equation 6 and were also developed empirically by Schoklitsch. Equation 9 is simply a combination of equations 7 and 8 and from the test results presented in table B appears

Table B
Comparison of Q_{\max} for the Various Test Conditions

Test Condition	Q_{\max}	
	Experimental	Schoklitsch's Equations
1.1	6.50	6.72
2.1	4.54	4.57
3.1	2.67	2.72
4.1	1.70	1.62
5.1	1.16	1.20
6.1	0.77	0.81
7.1	3.57	3.70
8.1	1.42	1.66
9.1	0.67	0.73
10.1	0.43	0.46
11.1	2.52	2.52
12.1	0.56	0.67

applicable to the partial depth-partial width breach.

45. Table B lists the measured maximum discharges and the maximum discharges computed from equations 6, 7, 8, and 9 for all of the non-base flow tests. This table shows that the peak discharge exhibits little variation when experimental results are compared with those computed. The variance that is apparent probably stems from the roughness or frictional effects present in the flume but neglected by Schoklitsch. More significant differences may develop when the flume is roughened.

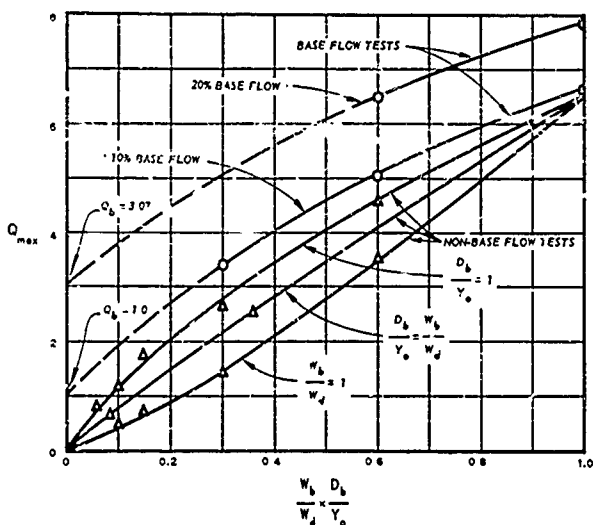


Fig. 22. Variations of Q_{\max} with breach pattern for base flow and non-base flow tests

and ordinate terms were evaluated and are plotted for both the Mohne and Eder breaches. The range of values given agree very well with the curve shown. The mathematical expression for Q_{\max} as determined from this curve is given by equation 10.

$$Q_{\max} = 0.29 \sqrt{g} W_b D_b^{3/2} \left(\frac{W_d}{W_b} \cdot \frac{Y_o}{D_b} \right)^{0.28} \quad (10)$$

From this relation, the value of the maximum discharge through a given breach can be computed provided,

46. Fig. 22 shows a plot of Q_{\max} versus $\frac{W_b}{W_d} \times \frac{D_b}{Y_o}$ for the three types of non-base flow breaches. From the curves presented, the approximate maximum discharge can be determined for any breach pattern tested in the flume. A more generally applicable plot is presented in fig. 23 in dimensionless form. From the data presented in table 21, values of the abscissa

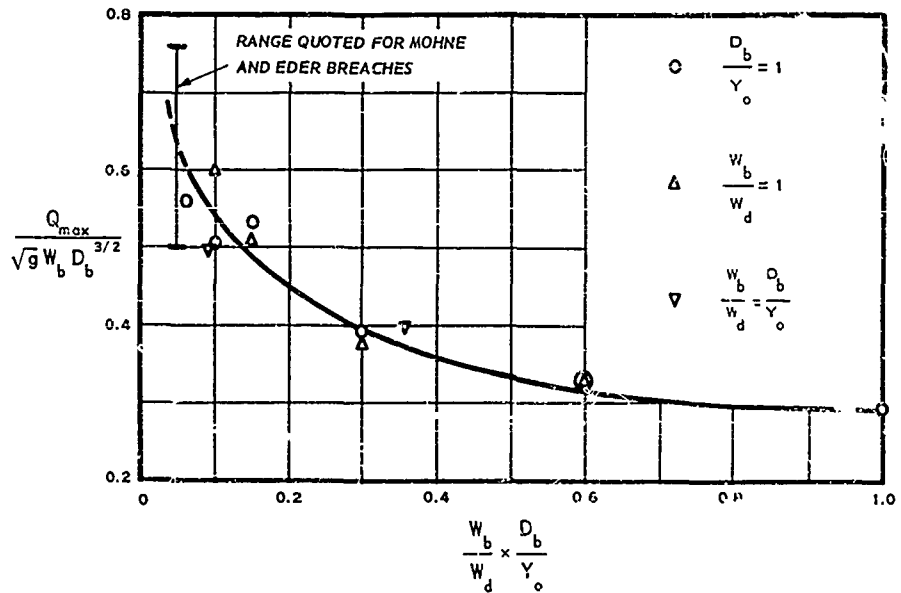


Fig. 23. Effect of breach size on maximum discharge through the breach

$$1.0 \leq \left(\frac{W_d}{W_b} \cdot \frac{Y_o}{D_b} \right) \leq 20$$

The accuracy of predictions derived from equation 10 will improve as $\left(\frac{W_d}{W_b} \cdot \frac{Y_o}{D_b} \right) \rightarrow 1.0$, since less scatter was obtained in this range.

47. When these results (fig. 23) were broken down into the separate breach regimes as was done by Schoklitsch (see equations 7 and 8), the following empirical equations were derived. For the full depth-partial width breaches (test conditions 1.1 through 6.1),

$$Q_{max} = 0.29 \sqrt{g} W_b D_b^{3/2} \left(\frac{W_d}{W_b} \right)^{1/4}$$

which agrees almost exactly with equation 7 since by definition of the breach pattern, $D_b = Y_o$. For the full width-partial depth breaches, the experimental results indicate that

$$Q_{\max} = 0.29 \sqrt{g} W_b D_b^{3/2} \left(\frac{Y_o}{D_b} \right)^{0.3}$$

which agrees very closely with the comparable equation developed by Schoklitsch (equation 8).

48. The discharge-time data (plates 84-86) plainly show that the magnitude of the discharge depends on the elapsed time after breach. Basically, the time of outflow is a function of the total volume of the reservoir that lies above the breach level and the rate at which the outflow takes place, or $t_o = f(Q, V_{+b})$. If Q is replaced with Q_{\max} (which is independent of elapsed time), then a dimensionless time quantity can be easily developed which will give a common time scale for each run belonging to a particular breach regime. The dimensionless time quantity thus developed is $t Q_{\max} / V_{+b}$. Discharges can be made dimensionless simply by dividing the discharge at any time by the maximum discharge observed, or Q/Q_{\max} . Plots of Q/Q_{\max} versus $t Q_{\max} / V_{+b}$ are shown in plates 101-103. These plots provide a means of describing in more general terms the decrease in the discharge as a function of time for the various breach regimes.

49. Base flow tests. The discharge-time hydrographs for the base flow tests are shown in plate 89. These curves also have a characteristic reversed "s" shape, and approach the magnitude of the base flow ($Q_b = 1.0$ for 10 per cent base flow, and $Q_b = 3.06$ for 20 per cent base flow) as a limit with increase in time. The maximum discharge in each case is larger than its counterpart in the non-base flow series of tests; however, the increase is less in each case than the simple addition of the non-base flow maximum discharge plus the base flow. The base flow maximum discharge for various full depth-partial width breaches tested in the flume may be estimated from the base flow curves of fig. 22. The curves are necessarily two and three point curves that have been extrapolated beyond the range of experimental data; nevertheless, they are believed adequate for estimating purposes.

50. Dimensionless plots for the base flow test series are shown in plate 104. For each of these curves, the value of V_{+b} was considered equal to 400 ft^3 , the total volume of the reservoir.

Discharge-time hydrographs for
stations downstream of the dam

51. Plates 90-98 present both the discharge- and velocity-time hydrographs at stations downstream of the dam for all test conditions. Examination of these curves shows that in every case the maximum discharge is reached very early in the time history of the flood wave and gradually decreases to zero or to the base flow discharge level. Further examination of these plates indicates that the maximum velocity decreases uniformly with distance downstream, while the maximum discharge reflects the erratic variations of the maximum stages as indicated in plates 2-61.

52. The order of accuracy of the discharge-time curves is apparent when the Q-t curve is integrated over the time range wherein data were obtained. When the discharge-time curves of ten downstream stations (arbitrarily chosen from different test conditions) were integrated over a time range equivalent to the approximate duration of the flood wave, the integrated volume of outflow differed from the storage volume an average of 7 per cent.

53. Duration of the flood wave is principally a function of the size of breach, the storage volume within the reservoir that lies above the breach level, the distance downstream to the station where evaluation is desired, and the general alignment and roughness pattern encountered by the flow as it moves down the exit channel. Because of the extremely long durations associated with the smaller breach patterns, it was not practical to obtain film records over this length of time. Neither was it possible in most cases to define with any degree of certainty the exact time that the flood wave had passed and the water level receded to normal. Observations were made however of the approximate total time of outflow through each given breach pattern. These times are recorded in table C for the non-base flow tests. Similar observations for the base flow tests were impracticable because it was impossible to ascertain the time of passage with any degree of confidence.

Table C
Total Time of Outflow for the Various Test Conditions

	Test Condition											
	1.1	2.1	3.1	4.1	5.1	6.1	7.1	8.1	9.1	10.1	11.1	12.1
t_o , sec	170	240	450	740	1000	1800	300	500	700	1400	700	1500

The upstream negative wave (non-base flow tests)

54. Immediately after the model dam was breached, a negative wave moved up the reservoir at a velocity dependent upon the reservoir depth. The arrival of this negative wave at stations upstream of the dam was detected by the initial decrease in the stage and by the initial motion of the water surface. By carefully observing both of these effects, the arrival time was determined to the nearest $1/10$ of a second. Arrival times versus distance upstream from the dam were recorded for each test condition. Since propagation of the negative wave is independent of breach pattern, the arrival times for each test condition and for each station were averaged and the results thus obtained are shown in plate 105 as the plotted points. The average of the experimental data agrees very closely with the theoretical curve derived below from the general celerity equation for wave propagation in shallow water. Referring to fig. 24, V_x , the

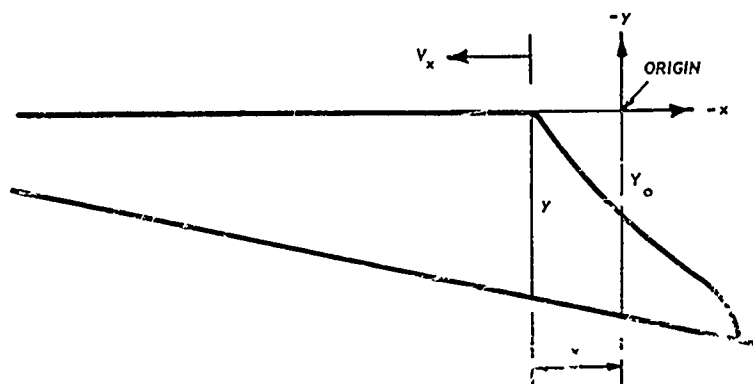


Fig. 24. Schematic diagram of negative wave in motion

upstream velocity of the negative wave equals \sqrt{gy} . The general expression for y in terms of x is: $y = ax + b$ when $x = 0$, $Y_0 = 1$; and then $x = 200$, $y = 0$. Therefore

$$y = 1 - \frac{x}{200}$$

Substituting this expression into $v_x = \sqrt{gy}$ gives

$$v_x = \sqrt{g} \left(1 - \frac{x}{200} \right)^{1/2}$$

but

$$v_x = \frac{dx}{dt}$$

hence,

$$\frac{dx}{dt} = \sqrt{g} \left(1 - \frac{x}{200} \right)^{1/2}$$

or

$$dt = \frac{dx}{\sqrt{g} \left(1 - \frac{x}{200} \right)^{1/2}}$$

$$t_a = \frac{1}{\sqrt{g}} \int_0^x \frac{dx}{(1 - 0.005 x)^{1/2}}$$

which when integrated and simplified yields

$$t_a = -70.6 [(1 - 0.005 x_u)^{1/2} - 1] \quad (11)$$

where t is the arrival time of the negative wave in seconds and x_u is the distance upstream from the dam in feet.

55. A generally applicable solution of the negative wave arrival time for any wedge-shaped reservoir is given in equation 12.

$$t = \frac{2L}{\sqrt{g Y_0}} \left[1 - \left(1 - \frac{x_u}{L} \right)^{1/2} \right] \quad (12)$$

The upstream negative wave (base flow tests)

56. The arrival time of the negative wave at stations upstream from the model dam for the base flow tests exhibited considerably more scatter than was encountered in the non-base flow tests (plate 106). Because of

the nature of the base flow tests, a velocity component in the downstream direction was present at each station. The principal source of the scatter arose from the fact that positive detection of the arrival time of the negative wave was uncertain because of the downstream motion of the water inherent in the base flow. Observing the arrival time of the negative wave over the first 10 ft or so of its motion (approximately sta 200 to sta 190) was impracticable because of the relatively low speed at which the motion picture cameras were operated. The time interval between frames in most cases was in the order of 0.07 to 0.125 second, and since the negative wave in this region is moving at its greatest velocity, the negative wave arrival had very often occurred during this time interval, making interpretation grossly uncertain. Since in this region the downstream velocity attendant to the base flow is a minimum because of the greater depths of flow, little error will result in using the curve derived from the non-base flow tests.

57. If it is assumed that the base flow is distributed uniformly over the entire depth of flow at each station, the magnitude of this component at any station may be determined from the relation $V = Q_b / 4y$. Since Q_b is a constant, the velocity is inversely proportional to the depth at any given station along the reservoir. Based on this assumption, the reservoir velocity retards propagation of the upstream negative wave vectorially. Its influence is apparent in plate 106 where experimental values of the arrival time lie generally above the non-base flow curve shown. For values of $X_u \geq 20$, the experimental results diverge from the curve, indicating that in the shallower reaches of the reservoir, the negative wave is being retarded to a greater degree because of the increase in the reservoir velocity component produced by the base flow.

The downstream positive wave
(flood wave), non-base flow tests

58. The arrival times of the flood wave at selected ranges downstream from the model dam were determined from the stage-time measurements. As was true in the negative wave analysis, the arrival times of the flood waves were also measurable to the nearest tenth of a second. The times of arrival of the flood wave as a function of distance downstream from the dam for the non-base flow tests are shown in plates 107-109. These results

exhibit conclusively that the velocity of the downstream positive wave is markedly influenced by the size of the breach opening, which in turn determines the discharge of the flood wave. To describe this effect in a more generalized manner and to an acceptable degree of accuracy, the slopes of the various curves were made constant by averaging the exponents of the term X_d in the least-squared equations given in plates 107-109. This transformation of the basic data enables the phenomena to be described by the equation:

$$t_a = K (X_d)^{1.16} \quad (13)$$

This equation may be helpful in predicting the flood-wave arrival time at any downstream station for nearly any breach tested in the flume.

The downstream positive wave
(flood wave), base flow tests

59. The arrival times of the flood wave at points downstream from the dam for the base flow tests are presented in plate 110. The right- and left-hand ordinate scales were dispersed by one log cycle in order to separate the curves sufficiently to permit more accurate interpolation. Comparison of these results with the non-base flow test results (plates 107-109) shows that the flood-wave velocity is greater for the base-flow tests. Because of the paucity of the data, it was not possible to analyze these results in the general manner used for the non-base flow tests.

Conclusions

Data-gathering techniques

60. The various methods employed in obtaining the data presented herein are believed satisfactory from the standpoint of accuracy and reproducibility. While other methods of measurement were visualized (some of which were tried during preliminary studies to determine advantages of each system), the method adopted and used throughout the experimental phase of the study is believed to be the most economical of the methods considered, and to be sufficiently precise.

Stage-time measurements

61. At the dam. The depth of water passing through a breach is principally a function of the size and shape of the breach, the volume of reservoir storage that lies above the breach level, and the elapsed time

after occurrence of the breach. Since the reservoir volume and shape remained constant throughout the study, no conclusions can be drawn regarding the effects produced by varying parameters pertinent to the reservoir size or shape. When the entire dam is removed, the initial stage at $t = \Delta t$ (where $\Delta t \rightarrow 0$) is approximately $\frac{Y_0}{2}$. At later times and for other breach patterns, the stage above the bottom of the breach (y_0) may be determined from plates 99 and 100.

62. Downstream from the dam. The depth of flow at points downstream of a breached dam will be influenced by the volume of water passing through the breach, the cross-sectional shape and alignment of the exit channel and the roughness. In this report only the effect of the volume of water entering the exit channel was varied. No definite trend of maximum stage with distance downstream was established; however, the maximum stage recorded was $0.35 Y_0$ for the non-base flow test conditions and $0.40 Y_0$ for the maximum base flow conditions. These stages occurred when the entire dam was removed. Lesser breaches resulted in decreased values of the maximum stage (figs. 20 and 21). A limiting value of the downstream stage can be estimated from the following relation,

$$y_{d_{\max}} < \frac{y_{0_{\max}} W_b}{W_c}$$

where $y_{d_{\max}}$ is the maximum downstream stage, $y_{0_{\max}}$ is the maximum depth of water passing through the breach during the time interval $2 \leq t \leq 5$, W_b is the width of the breach, and W_c is the width of the exit channel at the downstream location where the stage is desired.

63. For all the conditions of this test series, the downstream flood wave initially showed an abrupt rise in stage followed by a more gradual rise up to the maximum stage which always occurred within 30 seconds of the wave arrival time. In general, the flood waves of the base flow tests individually had fewer stage irregularities and collectively followed a more regular shape than those of the non-base flow tests.

Discharge-time measurements

64. At the dam. Experimental results for the non-base flow tests show that the maximum discharge through the breach was obtained when the entire dam was removed. Maximum discharges for less extensive breaches may be determined from fig. 22, while the variation of discharge as a

function of time may be obtained from curves plotted in plates 101-103. Since the reservoir shape remains constant in these tests, it is not possible to determine discharge-time hydrographs for varying reservoir shapes without using distorted scaling.

65. The dam breaches of the base flow tests resulted in a smaller change of discharge at the dam than did the corresponding breaches of the non-base flow tests. However, the total discharge past the dam was always greater in the base flow tests.

66. Downstream from the dam. The maximum discharge at downstream sta 220-355 was less than the maximum discharge at the dam, but no trend of a gradual decrease with distance downstream was indicated. When base flows were introduced, the discharge was generally affected at the downstream stations in the same manner as at the dam (see paragraph 65).

Negative wave

67. Experimental results verify that the propagation of the negative wave as a function of time can be determined analytically when the depth of the reservoir at any point along its length can be expressed as a function of the distance upstream from the dam. Plate 105 shows the agreement between the analytical solution and experiment. Propagation of the negative wave upstream is retarded by the downstream current common to all base flow test conditions. Experimental results plotted in plate 106 show that the retarding effects on the negative wave's propagation are more intense in the upstream end of the reservoir where the water is shallower.

Positive wave (downstream flood wave)

68. The downstream positive wave velocity is dependent on the discharge through the dam breach so that a single arrival-time curve cannot be used to represent all the different test conditions. In each test condition the positive wave decelerated as it progressed downstream. The positive wave arrival time at various stations downstream for the non-base flow tests can be represented by the equation

$$t_a = K (x_a)^{1.16}$$

where K is a constant representing the breach pattern or breach discharge.

Application to prototype situations

69. Extrapolation of these results to prototypes is limited to those situations that are geometrically similar to the conditions characteristic of the model. Significant departures from this restriction may yield completely erroneous results. Even if geometric similarity exists, these data should not be extrapolated to prototype situations where the linear dimensions of the prototype are greater than about 100 times the corresponding model dimension. It is believed that qualitative estimates of flood parameters can be achieved for a scale ratio as high as 200.

70. Procedures for extrapolating these results as well as results now being interpreted will be the subject of a final report. In the final report, studies will be made to assess the possibility of interpreting these data using distorted model scales. Assuming that distorted-scale relations can be developed, then evaluation of reservoirs of different shapes will be possible.

List of References

1. Barré de Saint Venant, A., "Théorie du mouvement non permanent des eaux." Comptes Rendus des Séances de l'Académie des Sciences, vol 73 (1871), pp 147-154, 237-240.
2. Dressler, Robert F., "Hydraulic resistance effect upon the dam-break functions." Journal of Research of the National Bureau of Standards, vol 49 (July-December 1952), pp 217-225.
3. _____, Comparison of Theories and Experiments for the Hydraulic Dam-Break Wave. Publication No. 38, de l'Association Internationale d'Hydrologie (Assemblée générale de Rome, tome III).
4. Frank, Joseph, "Betrachtungen über den Ausfluss beim Bruch von Stauwänden (Consideration on Discharge at Breaks of Dams)." Schweizerische Bauzeitung, vol 69, No. 29 (21 July 1951), pp 401-406.
5. King, Horace Williams Handbook of Hydraulics. Revised edition, McGraw-Hill Book Company, Inc., New York, N. Y., 1954.
6. Kirschmer, Otto, "Zerstörung und Schutz von Talsperren und Dämmen (Destruction and Protection of Dams and Levees)." Schweizerische Bauzeitung, vol 67, No. 20 (14 May 1949), pp 277-281.
7. Levin, L., "Evolution of waves created by the bursting of large dams." Transaction of the Second Meeting of the Yugoslav National Committee on Large Dams (September 1952).
8. Lewin, Joseph D., Report on Study Trip in Europe. November 1948.

9. Quast, Hermann, Zerstörung und Wiederaufbau der Möhne - und Eder - Talsperre. Wasser und Energie Wirtschaft - v.41.
10. Ritter, A., Die Fortpflanzung der Wasser-Wellen. z. Ver deut. Ing. 36, 1892.
11. Rouse, Hunter, Engineering Hydraulics. John Wiley & Sons, Inc., New York, N. Y., 1950.
12. Schoklitsch, Armin, Über Dammbuchwellen. Sitzber. Akad. Wiss. Wien. 126, 1917.
13. U. S. Army Engineer District, Washington, Flow Through a Breached Dam (U). Military Hydrology Manual No. H-2(X) Supplement, June 1955. CONFIDENTIAL.
14. _____, Flow Through a Breached Dam. Military Hydrology Bulletin 9, June 1957.

Table 1
Results of Stage-time Measurements, Test Conditions 1, 2

[illegible]

Table 2

Results of Stage-time Measurement, Test Condition 2.1

Time, seconds Stage, feet

[illegible]

Table 3

[illegible]

Table 4
Results of Stage-time Measurements, Test Credit, m.s.l.

Time	Upstream Stations										Downstream Stations									
	107	110	112	114	116	118	120	122	124	126	128	130	132	134	136	138	140	142	144	146
0	0.20	0.35	0.50	0.60	0.70	0.75	0.80	0.85	0.90	0.95	0.98	1.00	1.02	1.04	1.06	1.08	1.10	1.12	1.14	1.16
1.0	0.21	0.36	0.51	0.61	0.71	0.76	0.81	0.86	0.91	0.96	0.99	1.01	1.03	1.05	1.07	1.09	1.11	1.13	1.15	1.17
1.5	0.22	0.37	0.52	0.62	0.72	0.77	0.82	0.87	0.92	0.97	1.00	1.02	1.04	1.06	1.08	1.10	1.12	1.14	1.16	1.18
2.0	0.23	0.38	0.53	0.63	0.73	0.78	0.83	0.88	0.93	0.98	1.01	1.03	1.05	1.07	1.09	1.11	1.13	1.15	1.17	1.19
2.5	0.24	0.39	0.54	0.64	0.74	0.79	0.84	0.89	0.94	0.99	1.02	1.04	1.06	1.08	1.10	1.12	1.14	1.16	1.18	1.20
3.0	0.25	0.40	0.55	0.65	0.75	0.80	0.85	0.90	0.95	1.00	1.03	1.05	1.07	1.09	1.11	1.13	1.15	1.17	1.19	1.21
3.5	0.26	0.41	0.56	0.66	0.76	0.81	0.86	0.91	0.96	1.01	1.04	1.06	1.08	1.10	1.12	1.14	1.16	1.18	1.20	1.22
4.0	0.27	0.42	0.57	0.67	0.77	0.82	0.87	0.92	0.97	1.02	1.05	1.07	1.09	1.11	1.13	1.15	1.17	1.19	1.21	1.23
4.5	0.28	0.43	0.58	0.68	0.78	0.83	0.88	0.93	0.98	1.03	1.06	1.08	1.10	1.12	1.14	1.16	1.18	1.20	1.22	1.24
5.0	0.29	0.44	0.59	0.69	0.79	0.84	0.89	0.94	0.99	1.04	1.07	1.09	1.11	1.13	1.15	1.17	1.19	1.21	1.23	1.25
5.5	0.30	0.45	0.60	0.70	0.80	0.85	0.90	0.95	1.00	1.05	1.08	1.10	1.12	1.14	1.16	1.18	1.20	1.22	1.24	1.26
6.0	0.31	0.46	0.61	0.71	0.81	0.86	0.91	0.96	1.01	1.06	1.09	1.11	1.13	1.15	1.17	1.19	1.21	1.23	1.25	1.27
6.5	0.32	0.47	0.62	0.72	0.82	0.87	0.92	0.97	1.02	1.07	1.10	1.12	1.14	1.16	1.18	1.20	1.22	1.24	1.26	1.28
7.0	0.33	0.48	0.63	0.73	0.83	0.88	0.93	0.98	1.03	1.08	1.11	1.13	1.15	1.17	1.19	1.21	1.23	1.25	1.27	1.29
7.5	0.34	0.49	0.64	0.74	0.84	0.89	0.94	0.99	1.04	1.09	1.12	1.14	1.16	1.18	1.20	1.22	1.24	1.26	1.28	1.30
8.0	0.35	0.50	0.65	0.75	0.85	0.90	0.95	1.00	1.05	1.10	1.13	1.15	1.17	1.19	1.21	1.23	1.25	1.27	1.29	1.31
8.5	0.36	0.51	0.66	0.76	0.86	0.91	0.96	1.01	1.06	1.11	1.14	1.16	1.18	1.20	1.22	1.24	1.26	1.28	1.30	1.32
9.0	0.37	0.52	0.67	0.77	0.87	0.92	0.97	1.02	1.07	1.12	1.15	1.17	1.19	1.21	1.23	1.25	1.27	1.29	1.31	1.33
9.5	0.38	0.53	0.68	0.78	0.88	0.93	0.98	1.03	1.08	1.13	1.16	1.18	1.20	1.22	1.24	1.26	1.28	1.30	1.32	1.34
10.0	0.39	0.54	0.69	0.79	0.89	0.94	0.99	1.04	1.09	1.14	1.17	1.19	1.21	1.23	1.25	1.27	1.29	1.31	1.33	1.35
10.5	0.40	0.55	0.70	0.80	0.90	0.95	1.00	1.05	1.10	1.15	1.18	1.20	1.22	1.24	1.26	1.28	1.30	1.32	1.34	1.36
11.0	0.41	0.56	0.71	0.81	0.91	0.96	1.01	1.06	1.11	1.16	1.19	1.21	1.23	1.25	1.27	1.29	1.31	1.33	1.35	1.37
11.5	0.42	0.57	0.72	0.82	0.92	0.97	1.02	1.07	1.12	1.17	1.20	1.22	1.24	1.26	1.28	1.30	1.32	1.34	1.36	1.38
12.0	0.43	0.58	0.73	0.83	0.93	0.98	1.03	1.08	1.13	1.18	1.21	1.23	1.25	1.27	1.29	1.31	1.33	1.35	1.37	1.39
12.5	0.44	0.59	0.74	0.84	0.94	0.99	1.04	1.09	1.14	1.19	1.22	1.24	1.26	1.28	1.30	1.32	1.34	1.36	1.38	1.40
13.0	0.45	0.60	0.75	0.85	0.95	1.00	1.05	1.10	1.15	1.20	1.23	1.25	1.27	1.29	1.31	1.33	1.35	1.37	1.39	1.41
13.5	0.46	0.61	0.76	0.86	0.96	1.01	1.06	1.11	1.16	1.21	1.24	1.26	1.28	1.30	1.32	1.34	1.36	1.38	1.40	1.42
14.0	0.47	0.62	0.77	0.87	0.97	1.02	1.07	1.12	1.17	1.22	1.25	1.27	1.29	1.31	1.33	1.35	1.37	1.39	1.41	1.43
14.5	0.48	0.63	0.78	0.88	0.98	1.03	1.08	1.13	1.18	1.23	1.26	1.28	1.30	1.32	1.34	1.36	1.38	1.40	1.42	1.44
15.0	0.49	0.64	0.79	0.89	0.99	1.04	1.09	1.14	1.19	1.24	1.27	1.29	1.31	1.33	1.35	1.37	1.39	1.41	1.43	1.45
15.5	0.50	0.65	0.80	0.90	1.00	1.05	1.10	1.15	1.20	1.25	1.28	1.30	1.32	1.34	1.36	1.38	1.40	1.42	1.44	1.46
16.0	0.51	0.66	0.81	0.91	1.01	1.06	1.11	1.16	1.21	1.26	1.29	1.31	1.33	1.35	1.37	1.39	1.41	1.43	1.45	1.47
16.5	0.52	0.67	0.82	0.92	1.02	1.07	1.12	1.17	1.22	1.27	1.30	1.32	1.34	1.36	1.38	1.40	1.42	1.44	1.46	1.48
17.0	0.53	0.68	0.83	0.93	1.03	1.08	1.13	1.18	1.23	1.28	1.31	1.33	1.35	1.37	1.39	1.41	1.43	1.45	1.47	1.49
17.5	0.54	0.69	0.84	0.94	1.04	1.09	1.14	1.19	1.24	1.29	1.32	1.34	1.36	1.38	1.40	1.42	1.44	1.46	1.48	1.50
18.0	0.55	0.70	0.85	0.95	1.05	1.10	1.15	1.20	1.25	1.30	1.33	1.35	1.37	1.39	1.41	1.43	1.45	1.47	1.49	1.51
18.5	0.56	0.71	0.86	0.96	1.06	1.11	1.16	1.21	1.26	1.31	1.34	1.36	1.38	1.40	1.42	1.44	1.46	1.48	1.50	1.52
19.0	0.57	0.72	0.87	0.97	1.07	1.12	1.17	1.22	1.27	1.32	1.35	1.37	1.39	1.41	1.43	1.45	1.47	1.49	1.51	1.53
19.5	0.58	0.73	0.88	0.98	1.08	1.13	1.18	1.23	1.28	1.33	1.36	1.38	1.40	1.42	1.44	1.46	1.48	1.50	1.52	1.54
20.0	0.59	0.74	0.89	0.99	1.09	1.14	1.19	1.24	1.29	1.34	1.37	1.39	1.41	1.43	1.45	1.47	1.49	1.51	1.53	1.55
20.5	0.60	0.75	0.90	1.00	1.10	1.15	1.20	1.25	1.30	1.35	1.38	1.40	1.42	1.44	1.46	1.48	1.50	1.52	1.54	1.56
21.0	0.61	0.76	0.91	1.01	1.11	1.16	1.21	1.26	1.31	1.36	1.39	1.41	1.43	1.45	1.47	1.49	1.51	1.53	1.55	1.57
21.5	0.62	0.77	0.92	1.02	1.12	1.17	1.22	1.27	1.32	1.37	1.40	1.42	1.44	1.46	1.48	1.50	1.52	1.54	1.56	1.58
22.0	0.63	0.78	0.93	1.03	1.13	1.18	1.23	1.28	1.33	1.38	1.41	1.43	1.45	1.47	1.49	1.51	1.53	1.55	1.57	1.59
22.5	0.64	0.79	0.94	1.04	1.14	1.19	1.24	1.29	1.34	1.39	1.42	1.44	1.46	1.48	1.50	1.52	1.54	1.56	1.58	1.60
23.0	0.65	0.80	0.95	1.05	1.15	1.20	1.25	1.30	1.35	1.40	1.43	1.45	1.47	1.49	1.51	1.53	1.55	1.57	1.59	1.61
23.5	0.66	0.81	0.96	1.06	1.16	1.21	1.26	1.31	1.36	1.41	1.44	1.46	1.48	1.50	1.52	1.54	1.56	1.58	1.60	1.62
24.0	0.67	0.82	0.97	1.07	1.17	1.22	1.27	1.32	1.37	1.42	1.45	1.47	1.49	1.51	1.53	1.55	1.57	1.59	1.61	1.63
24.5	0.68	0.83	0.98	1.08	1.18	1.23	1.28	1.33	1.38	1.43	1.46	1.48	1.50	1.52	1.54	1.56	1.58	1.60	1.62	1.64
25.0	0.69	0.84	0.99	1.09	1.19	1.24	1.29	1.34	1.39	1.44	1.47	1.49	1.51	1.53	1.55	1.57	1.59	1.61	1.63	1.65
25.5	0.70	0.85	1.00	1.10	1.20	1.25	1.30	1.35	1.40	1.45	1.48	1.50	1.52	1.54	1.56	1.58	1.60	1.62	1.64	1.66
26.0	0.71	0.86	1.01	1.11	1.21	1.26	1.31	1.36	1.41	1.46	1.49	1.51	1.53	1.55	1.57	1.59	1.61	1.63	1.65	1.67
26.5	0.72	0.87	1.02	1.12	1.22	1.27	1.32	1.37	1.42	1.47	1.50	1.52	1.54	1.56	1.58	1.60	1.62	1.64	1.66	1.68
27.0	0.73	0.88	1.03	1.13	1.23	1.28	1.33	1.38	1.43	1.48	1.51	1.53	1.55	1.57	1.59	1.61	1.63	1.65	1.67	1.69
27.5	0.74	0.89	1.04	1.14	1.24	1.29	1.34	1.39	1.44	1.49	1.52	1.54	1.56	1.58	1.60	1.62	1.64	1.66	1.68	1.70
28.0	0.75	0.90	1.05	1.15	1.25	1.30	1.35	1.40	1.45	1.50	1.53	1.55	1.57	1.59	1.61	1.63	1.65	1.67	1.69	1.71
28.5	0.76	0.91	1.06	1.16	1.26	1.31	1.36	1.41	1.46	1.51	1.54	1.56	1.58	1.60	1.62	1.64	1.66	1.68	1.70	1.72
29.0	0.77	0.92	1.07	1.17	1.27	1.32	1.37	1.42	1.47	1.52	1.55	1.57	1.59	1.61	1.63	1.65	1.67	1.69	1.71	1.73
29.5	0.78	0.93	1.08	1.18	1.28	1.33	1.38	1.43	1.48	1.53	1.56	1.58	1.60	1.62	1.64	1.66	1.68	1.70	1.72	1.74
30.0	0.79	0.94	1.09	1.19	1.29	1.34	1.39	1.44	1.49	1.54	1.57	1.59	1.61	1.63	1.65	1.67	1.69	1.71	1.73	1.75
30.5	0.80	0.95	1.10	1.20	1.30	1.35	1.40	1.45	1.50	1.55	1.58	1.60	1.62	1.64	1.66	1.68	1.70	1.72	1.74	1.76
31.0	0.81	0.96	1.11	1.21																

Table 5
Results of Stage-time Measurements, Test Condit. of 2.1

[illegible]

Table 6
Results of Stepwise Measurements, Test Condition 6.1

[illegible]

Table 7

[illegible]

Table 8
Results of Stagesize Measurements, Test (Condition 8.1)

Time	Upstream Stations										Downstream Stations										Run	Stage, feet
	70	72	74	76	78	80	82	84	86	88	90	92	94	96	98	100	102	104	106	108		
0																					1.00	
0.5																					0.99	
1.0																					0.92	
1.5																					0.92	
2.0																					0.92	
2.5																					0.92	
3.0																					0.92	
3.5																					0.92	
4.0																					0.92	
4.5																					0.92	
5																					0.92	
5.5																					0.92	
6																					0.92	
6.5																					0.92	
7																					0.92	
7.5																					0.92	
8																					0.92	
8.5																					0.92	
9																					0.92	
9.5																					0.92	
10																					0.92	
10.5																					0.92	
11																					0.92	
11.5																					0.92	
12																					0.92	
12.5																					0.92	
13																					0.92	
13.5																					0.92	
14																					0.92	
14.5																					0.92	
15																					0.92	
15.5																					0.92	
16																					0.92	
16.5																					0.92	
17																					0.92	
17.5																					0.92	
18																					0.92	
18.5																					0.92	
19																					0.92	
19.5																					0.92	
20																					0.92	
20.5																					0.92	
21																					0.92	
21.5																					0.92	
22																					0.92	
22.5																					0.92	
23																					0.92	
23.5																					0.92	
24																					0.92	
24.5																					0.92	
25																					0.92	
25.5																					0.92	
26																					0.92	
26.5																					0.92	
27																					0.92	
27.5																					0.92	
28																					0.92	
28.5																					0.92	
29																					0.92	
29.5																					0.92	
30																					0.92	
30.5																					0.92	
31																					0.92	
31.5																					0.92	
32																					0.92	
32.5																					0.92	
33																					0.92	
33.5																					0.92	
34																					0.92	
34.5																					0.92	
35																					0.92	
35.5																					0.92	
36																					0.92	
36.5																					0.92	
37																					0.92	
37.5																					0.92	
38																					0.92	
38.5																					0.92	
39																					0.92	
39.5																					0.92	
40																					0.92	
40.5																					0.92	
41																					0.92	
41.5																					0.92	
42																					0.92	
42.5																					0.92	
43																					0.92	
43.5																					0.92	
44																					0.92	
44.5																					0.92	
45																					0.92	
45.5																					0.92	
46																					0.92	
46.5																					0.92	
47																					0.92	
47.5																					0.92	
48																					0.92	
48.5																					0.92	
49																					0.92	
49.5																					0.92	
50																					0.92	
50.5																					0.92	
51																					0.92	
51.5																					0.92	
52																					0.92	
52.5																					0.92	
53																					0.92	
53.5																					0.92	
54																					0.92	
54.5																					0.92	
55																					0.92	
55.5			</																			

Table 10

[illegible]

Table 12

[illegible]

Table 13

Results of Stage-time Measurements, Test Condition 1, (10)

Time, seconds Age, feet

[illegible]

46. 1964

[illegible]

Table 16
Results of Stage-time Measurements, Test Condition 2.1(20)
Time, seconds Stage, ft

Time	Upstream Stations										Downstream Stations			
	100	120	140	160	180	190	192	194	196	198	200	202	204	206
0.0											1.00			
0.5											0.65			
1.0											0.68			
1.5											0.70			
2.0											0.76			
2.5											0.70			
3.0											0.70			
3.5											0.73			
4.0											0.72			
4.5											0.73			
5.0											0.73			
5.5											0.73			
6.0											0.73			
6.5											0.73			
7.0											0.73			
7.5											0.73			
8.0											0.73			
8.5											0.73			
9.0											0.73			
9.5											0.73			
10.0											0.73			
10.5											0.73			
11.0											0.73			
11.5											0.73			
12.0											0.73			
12.5											0.73			
13.0											0.73			
13.5											0.73			
14.0											0.73			
14.5											0.73			
15.0											0.73			
15.5											0.73			
16.0											0.73			
16.5											0.73			
17.0											0.73			
17.5											0.73			
18.0											0.73			
18.5											0.73			
19.0											0.73			
19.5											0.73			
20.0											0.73			
20.5											0.73			
21.0											0.73			
21.5											0.73			
22.0											0.73			
22.5											0.73			
23.0											0.73			
23.5											0.73			
24.0											0.73			

Table 17

Stem. feet

Table 18

Downstream Average Velocity* Data
 Non-Ease Flow Test Conditions 1.1 Through 6.1

Time sec	Test Condition 1.1			Test Condition 2.1			Test Condition 3.1			Test Condition 4.1			Test Condition 5.1			Test Condition 6.1		
	Station			Station			Station			Station			Station			Station		
	225	280	350	225	280	350	225	280	350	225	280	350	225	280	350	225	280	350
0	0	0	0	0	0	0	0	0	0	0	0	0	0	0	0	0	0	0
2	0			0			0			0			0			0		
5	4.5			1.6			1.1			0			0			0		
7	4.8			2.8			2.6			1.6			1.4			0		
10	4.7			3.8			3.4			2.6			2.3			1.4		
12	4.6	0		4.0	0		3.5			2.9			2.6			1.7		
15	4.5	2.6		4.2	3.6		3.7	0		3.0			2.6			1.9		
17	4.4	4.0		4.2	4.2		3.8	0.8		3.0			2.7			2.0		
20	4.3	4.6		4.3	4.3		3.8	3.0		3.0	0		2.7			2.0		
22	4.2	4.7	0		4.3			3.4			1.6			0		2.1		
25	4.2	4.7	1.6	4.3	4.3		3.9	3.4		3.0	2.2		2.7	1.3		2.1		
27	4.1	4.6	4.1		4.3	0		3.4			2.5			2.0			0	
30	4.0	4.6	4.4	4.3	4.3	3.8	4.0	3.4		3.0	2.6		2.7	2.1		2.1	1.1	
32	4.0	4.5	4.5			4.0			0		2.6			2.1			1.4	
35	3.9	4.4	4.5	4.3	4.2	4.1	4.0	3.4	2.5	3.0	2.6		2.7	2.1		2.1	1.8	
37	3.9		4.4						3.4									1.8
40	3.9	4.2	4.3	4.2	4.2	4.2	4.0	3.4	3.4	3.0	2.6		2.7	2.1		2.1	1.9	
42	3.9					4.2			3.4			0						1.9
45	3.8	4.1	4.2	4.2	4.1	4.2	4.0	3.4	3.4	3.0	2.6	2.5	2.7	2.1		2.1	2.0	
47											2.6				0			2.0
50	3.8	3.9	4.1	4.1	4.0	4.1	3.9	3.4	5.4	3.0	2.6	2.6	2.7	2.1	1.4	2.1	2.0	
52											2.6				1.7			
55	3.6	3.8	4.0	4.0	3.9	4.0	3.9	3.3	3.4	3.0	2.6	2.6	2.7	2.1	2.0	2.1	2.0	
57															2.0			0
60	3.4	3.7	3.8	4.0	3.8	3.9	3.8	3.3	3.4	3.0	2.6	2.6	2.7	2.1	2.1	2.1	2.0	1.6
62																		1.8
65	3.3	3.5	3.8	3.8	3.7	3.8	3.7	3.2	3.4	2.9	2.6	2.6	2.7	2.1	2.1	2.1	2.0	1.8
67																		1.9
70	3.1	3.4	3.7	3.8	3.5	3.8	3.6	3.2	3.4	2.9	2.6	2.6	2.7	2.1	2.1	2.1	2.0	1.9
72																		2.0
75	3.0	3.4	3.6	3.6	3.4	3.6	3.5	3.1	3.3	2.9	2.6	2.6	2.7	2.1	2.1	2.1	2.0	2.0
77																		2.0
80	2.9	3.2	3.4	3.5	3.4	3.5	3.4	3.1	3.3	2.8	2.6	2.6	2.6	2.1	2.1	2.1	2.0	2.0
85	2.7	3.1	3.2	3.2	3.4	3.3	3.0	3.2	2.8	2.6	2.6	2.6	2.6	2.1	2.1	2.1	2.0	2.0
90	2.6	3.0	3.0	2.2	3.1	3.3	3.2	3.0	3.2	2.7	2.6	2.6	2.6	2.1	2.1	2.1	2.0	2.0
100	2.3	2.6	2.9	2.8	3.0	3.1	3.0	2.9	3.1	2.6	2.6	2.5	2.6	2.0	2.1	2.1	2.0	2.0
110	1.8	2.2	2.6	2.5	2.7	3.0	3.0	2.8	3.0	2.5	2.5	2.4	2.5	2.0	2.1	2.0	2.0	2.0
120	1.5	2.0	2.4	2.2	2.6	2.7	2.9	2.6	2.9	2.4	2.5	2.3	2.5	2.0	2.1	2.0	2.0	2.0
130		1.8	2.1	2.0	2.4	2.6	2.8	2.6	2.8	2.3	2.5	2.2	2.4	1.9	2.1	1.9	1.9	1.9
140		1.6	1.8	1.8	2.2	2.4	2.7	2.6	2.6	2.2	2.4	2.2	2.3	1.9	2.1	1.8	1.9	1.9
150		1.5	1.7	1.7	2.1	2.2	2.6	2.6	2.6	2.2	2.4	2.2	2.2	1.9	2.1	1.8	1.9	1.9
160		1.4	1.5	1.5	1.9	2.1	2.6	2.5	2.6	2.2	2.3	2.2	2.2	1.9	2.0	1.8	1.9	1.9
170		1.4	1.4	1.4	1.8	1.9	2.4	2.4	2.5	2.2	2.3	2.2	2.2	1.9	1.9	1.8	1.8	1.8
180		1.3	1.3	1.3	1.6	1.8	2.2	2.3	2.4	2.1	2.2	2.1	2.2	1.8	1.8	1.8	1.8	1.8
190		1.3	1.2	1.2	1.4	1.7	2.1	2.2	2.4	2.1	2.2	2.1	2.1	1.8	1.8	1.8	1.8	1.8
200		1.2	1.1	1.1	1.4	1.6	1.0	2.2	2.3	2.0	2.2	2.1	2.0	1.8	1.8	1.8	1.8	1.8
210				1.0	1.3	1.4	1.8	2.1	2.2	1.9	2.1	2.0	2.0	1.8	1.8	1.7	1.7	1.8
240					1.0	1.1	1.5	1.9	1.9	1.8	2.0	1.8	1.8	1.8	1.7	1.7	1.7	1.8
270								1.7	1.7	1.7	1.8	1.6	1.8	1.7	1.6	1.7	1.7	1.7
300										1.5	1.8	1.4	1.8	1.6	1.5	1.6	1.6	1.7
360										1.4	1.5	1.4	1.6	1.4	1.4	1.5	1.5	1.7
420										1.3			1.4	1.4	1.3	1.4	1.4	1.6
480													1.3	1.2	1.2	1.2	1.4	1.5
540													1.1	1.1	1.0	1.1	1.3	1.4
600																1.0	1.2	1.4

* Velocity in feet per second.

Table 19

Downstream Average Velocity* Data

Non-Base Flow Test Conditions 7.1 Through 12.1

Time sec	Test Condi- tion 7.1			Test Condi- tion 8.1			Test Condi- tion 9.1			Test Condi- tion 10.1			Test Condi- tion 11.1			Test Condi- tion 12.1		
	Station			Station			Station			Station			Station			Station		
	225	280	350	225	280	350	225	280	350	225	280	350	225	280	350	225	280	350
0	0	0	0	0	0	0	0	0	0	0	0	0	0	0	0	0	0	0
2	0	0	0	0	0	0	0	0	0	0	0	0	0	0	0	0	0	0
5	4.0	↓	↓	0	↓	↓	0	↓	↓	0	↓	↓	2.4	↓	↓	0	↓	↓
7	4.3	↓	↓	1.6	↓	↓	0	↓	↓	0	↓	↓	4.3	↓	↓	0	↓	↓
10	4.5	↓	↓	2.9	↓	↓	1.6	↓	↓	0.5	↓	↓	4.5	↓	↓	1.0	↓	↓
12	4.5	0	↓	3.1	↓	↓	1.8	↓	↓	0.9	↓	↓	4.6	↓	↓	1.8	↓	↓
15	4.5	3.5	↓	3.1	↓	↓	1.8	↓	↓	1.4	↓	↓	4.6	0	↓	2.0	↓	↓
17	4.5	3.9	↓	3.1	↓	↓	---	↓	↓	1.5	↓	↓	---	1.6	↓	2.1	↓	↓
20	4.5	4.2	↓	3.1	0	↓	1.8	↓	↓	1.6	↓	↓	4.6	3.1	↓	2.1	↓	↓
22	---	4.2	↓	---	1.1	↓	---	↓	↓	1.6	↓	↓	---	2.2	↓	---	↓	↓
25	4.4	4.2	↓	3.1	2.2	↓	1.8	↓	↓	1.6	↓	↓	4.6	3.4	↓	2.1	↓	↓
27	---	---	0	---	2.5	↓	---	↓	↓	---	↓	↓	---	3.4	↓	---	↓	↓
30	4.4	4.2	3.7	3.1	2.6	↓	1.8	↓	↓	1.7	↓	↓	4.5	3.4	↓	2.1	↓	↓
32	---	---	3.8	---	2.7	↓	---	0	↓	---	↓	↓	---	---	0	---	---	---
35	4.3	4.2	4.0	3.1	2.7	↓	1.8	1.2	↓	1.7	↓	↓	4.4	3.4	1.6	2.1	1.4	↓
37	---	---	4.0	---	---	↓	---	1.6	↓	---	0	↓	---	---	2.7	---	1.0	↓
40	4.3	4.1	4.0	3.0	2.7	↓	1.8	1.7	↓	1.7	1.2	↓	4.2	3.4	3.0	2.1	1.7	↓
42	---	---	4.0	---	0	↓	---	1.8	↓	---	1.5	↓	---	---	3.0	---	1.3	↓
45	4.2	3.9	3.0	2.7	1.6	↓	1.8	1.8	↓	1.6	1.6	↓	4.2	3.4	3.0	2.1	1.8	↓
47	---	---	---	---	2.2	↓	---	1.8	↓	---	1.7	↓	---	---	---	---	---	---
50	4.2	3.8	3.0	2.7	2.3	↓	1.8	1.8	↓	1.6	1.7	↓	4.2	3.3	3.0	2.1	1.8	↓
52	---	---	---	---	2.4	↓	---	---	↓	---	---	↓	---	---	---	---	---	---
55	4.0	3.7	3.8	2.9	2.7	2.4	1.8	1.8	↓	1.6	1.7	↓	4.1	3.2	3.0	2.1	1.8	↓
57	---	---	---	---	2.4	↓	---	---	↓	---	---	↓	---	---	---	---	---	---
60	3.9	3.5	3.7	2.9	2.6	2.5	1.8	1.8	↓	1.5	1.7	↓	4.0	3.2	3.0	2.1	1.8	↓
62	---	---	---	---	2.5	↓	---	---	0	---	---	↓	---	---	---	---	---	---
65	3.8	3.4	3.6	2.8	2.6	2.5	1.8	1.8	0.6	1.5	1.7	↓	3.9	3.1	3.0	2.1	1.8	↓
67	---	---	---	---	---	---	---	---	1.1	---	---	↓	---	---	---	---	---	0
70	3.7	3.3	3.4	2.7	2.6	2.5	1.7	1.8	1.4	1.4	1.7	↓	3.8	3.0	3.0	2.0	1.8	0
72	---	---	---	---	---	---	---	---	1.5	---	---	↓	---	---	---	---	---	1
75	3.5	3.1	3.4	2.6	2.5	2.5	1.7	1.8	1.6	1.4	1.6	0	3.8	3.0	3.0	2.0	1.8	1
77	---	---	---	---	---	---	---	---	1.6	---	---	0.6	---	---	---	---	---	1
80	3.4	3.0	3.2	2.6	2.5	2.5	1.6	1.8	1.7	1.4	1.6	0.9	3.6	2.9	3.0	2.0	1.8	1
85	3.2	3.0	3.1	2.5	2.4	2.4	1.6	1.8	1.7	1.4	1.6	1.2	3.5	2.8	2.9	2.0	1.8	1
90	3.0	2.9	3.0	2.4	2.3	2.4	1.5	1.8	1.7	1.3	1.6	1.4	3.4	2.7	2.9	1.9	1.8	1
100	2.8	2.7	2.7	2.2	2.2	2.3	1.4	1.8	1.7	1.3	1.6	1.4	3.1	2.6	2.8	1.9	1.7	1
110	2.4	2.6	2.6	2.0	2.2	2.2	1.4	1.7	1.7	1.2	1.5	1.4	2.9	2.5	2.6	1.8	1.7	1
120	2.1	2.3	2.5	1.8	2.1	2.1	1.4	1.6	1.7	1.2	1.5	1.4	2.6	2.4	2.6	1.8	1.6	1
130	2.0	2.1	2.3	1.7	1.9	1.9	1.3	1.6	1.7	1.1	1.4	1.4	2.5	2.2	2.4	1.7	1.6	1
140	1.9	1.9	2.1	1.6	1.8	1.8	1.3	1.5	1.6	1.1	1.4	1.4	2.3	2.1	2.2	1.7	1.5	1
150	1.9	1.8	1.9	1.6	1.8	1.6	1.2	1.4	1.5	1.1	1.4	1.3	2.2	2.0	2.2	1.6	1.5	1
160	1.8	1.8	1.8	1.5	1.8	1.5	1.2	1.4	1.4	1.1	1.3	1.3	2.1	1.9	2.1	1.6	1.5	1
170	1.6	1.7	1.8	1.4	1.7	1.4	1.2	1.3	1.4	1.0	1.3	1.2	1.9	1.9	1.9	1.5	1.4	1
180	1.4	1.7	1.8	1.4	1.7	1.4	1.2	1.3	1.3	1.0	1.2	1.1	1.8	1.9	1.8	1.5	1.4	1
190	1.4	1.6	1.7	1.3	1.6	1.4	1.2	1.3	1.2	1.0	1.2	1.0	1.6	1.8	1.7	1.5	1.4	1
200	1.2	1.5	1.6	1.3	1.6	1.4	1.2	1.2	1.2	1.0	1.2	1.0	1.5	1.8	1.7	1.5	1.4	1
210	1.1	1.4	1.5	1.2	1.5	1.4	1.1	1.2	1.1	1.0	1.1	0.9	1.4	1.7	1.6	1.5	1.4	1
240	1.0	1.3	1.1	1.1	1.4	1.1	1.1	1.2	1.0	0.9	1.0	0.9	1.2	1.6	1.5	1.4	1.4	1
270	0.8	1.1	1.0	1.0	1.2	1.0	1.0	1.1	1.0	0.9	1.0	0.9	1.0	1.4	1.3	1.4	1.3	1
300	---	---	---	0.9	1.1	0.9	0.9	1.1	0.9	0.8	1.0	0.9	1.0	1.3	1.2	1.2	1.3	1
360	---	---	---	0.8	1.0	0.8	0.7	1.0	0.8	0.6	1.0	0.8	---	1.0	0.9	1.0	1.1	1
420	---	---	---	0.8	0.7	---	---	---	---	---	---	0.8	---	---	---	---	---	1

* Velocity in feet per second.

Table 20

Downstream Average Velocity* Data

Base Flow Test Conditions 1.1(10) Through 3.1(10)

Time sec	Test Condi- tion 1.1(10)			Test Condi- tion 1.1(20)			Test Condi- tion 2.1(10)			Test Condi- tion 2.1(20)			Test Condi- tion 3.1(10)		
	Station			Station			Station			Station			Station		
	225	280	350	225	280	350	225	280	350	225	280	350	225	280	350
0	2.5	2.5	2.5	3.8	3.8	3.8	2.5	2.5	2.5	3.8	3.8	3.8	2.5	2.5	2.5
2	2.5	↓	↓	3.6	↓	↓	2.5	↓	↓	3.8	↓	↓	2.5	↓	↓
5	3.5	↓	↓	5.2	↓	↓	4.0	↓	↓	4.9	↓	↓	3.8	↓	↓
7	4.1	↓	↓	5.3	↓	↓	4.2	↓	↓	5.0	↓	↓	4.0	↓	↓
10	4.2	↓	↓	5.3	3.8	↓	4.7	↓	↓	5.1	3.8	↓	4.2	↓	↓
12	4.2	2.5	↓	---	4.8	↓	4.8	2.5	↓	5.2	4.7	↓	4.3	2.5	↓
15	4.2	3.5	↓	5.3	5.0	↓	4.9	3.5	↓	5.2	4.9	↓	4.4	3.8	↓
17	---	3.9	↓	---	5.1	3.8	---	3.9	↓	---	5.0	↓	---	3.9	↓
20	4.2	4.2	↓	5.3	5.2	4.6	4.9	4.1	↓	5.2	5.0	3.8	4.4	4.0	↓
22	---	4.4	2.5	---	---	4.9	---	4.2	2.5	---	---	4.4	---	---	2.5
25	4.1	4.5	4.1	5.2	5.2	5.1	4.8	4.3	4.0	5.1	5.0	4.7	4.4	4.0	1
27	---	4.6	4.3	---	---	5.2	---	4.3	4.2	---	---	4.7	---	---	3.6
30	4.1	4.6	4.4	5.2	5.1	5.2	4.8	4.3	4.2	5.0	4.9	4.8	4.4	4.0	3.7
32	---	---	4.5	---	---	---	---	---	4.3	---	---	---	---	---	---
35	4.0	4.5	4.5	5.1	5.0	5.2	4.7	4.3	4.3	4.9	4.9	4.8	4.4	4.0	3.7
40	3.9	4.6	4.6	5.0	4.9	5.1	4.6	4.4	4.3	4.9	4.8	4.8	4.3	4.0	3.7
45	3.8	4.5	4.6	4.9	4.8	5.0	4.6	4.4	4.3	4.8	4.8	4.7	4.3	4.0	3.6
50	3.7	4.4	4.6	4.8	4.7	4.9	4.4	4.3	4.3	4.7	4.7	4.7	4.3	4.0	3.6
55	3.6	4.3	4.5	4.7	4.7	4.8	4.4	4.3	4.2	4.7	4.6	4.6	4.2	4.0	3.6
60	3.4	4.1	4.4	4.5	4.6	4.8	4.2	4.3	4.2	4.6	4.6	4.6	4.2	3.9	3.5
65	3.3	4.0	4.3	4.4	4.6	4.7	4.1	4.2	4.1	4.5	4.5	4.5	4.1	3.9	3.5
70	3.2	3.8	4.2	4.2	4.6	4.6	4.0	4.2	4.0	4.5	4.4	4.4	4.1	3.9	3.4
75	3.0	3.7	4.1	4.1	4.5	4.6	3.9	4.1	3.9	4.4	4.3	4.4	4.0	3.8	3.4
80	2.9	3.6	4.0	4.0	4.5	4.6	3.8	4.0	3.8	4.4	4.3	4.3	4.0	3.8	3.4
85	2.8	3.5	3.8	3.9	4.5	4.5	3.6	4.0	3.7	4.3	4.2	4.2	3.9	3.7	3.3
90	2.7	3.3	3.7	3.9	4.4	4.4	3.5	3.9	3.6	4.3	4.2	4.2	3.8	3.7	3.3
100	2.6	3.1	3.5	3.8	4.3	4.3	3.2	3.6	3.3	4.2	4.0	4.1	3.7	3.6	3.2
110	2.5	2.9	3.2	---	4.2	4.1	3.0	3.4	3.2	4.1	3.9	4.0	3.6	3.4	3.2
120	---	2.7	2.9	---	4.1	4.0	2.9	3.2	3.0	4.0	3.9	3.9	3.4	3.4	3.1
130	---	2.6	2.8	---	3.9	3.9	2.7	3.0	2.9	4.0	3.9	3.9	3.3	3.3	3.0
140	---	2.5	2.6	---	3.9	3.9	2.6	2.8	2.9	3.9	3.8	3.8	3.1	3.2	3.0
150	---	---	2.5	---	3.8	3.8	2.6	2.7	2.8	3.9	---	---	2.9	3.0	2.9
160	---	---	---	---	---	---	2.6	2.6	2.8	3.9	---	---	2.8	2.9	2.8
170	---	---	---	---	---	---	2.5	2.5	2.7	3.8	---	---	2.6	2.8	2.7
180	---	---	---	---	---	---	---	---	2.6	---	---	---	2.5	2.7	2.6
190	---	---	---	---	---	---	---	---	2.6	---	---	---	---	2.6	2.6
200	---	---	---	---	---	---	---	---	2.5	---	---	---	---	2.5	2.5
210	---	---	---	---	---	---	---	---	2.5	---	---	---	---	2.5	2.5
240	2.5	2.5	2.5	3.8	3.8	3.8	2.5	2.5	2.5	3.8	3.8	3.8	2.5	2.5	2.5

* Velocity in feet per second.

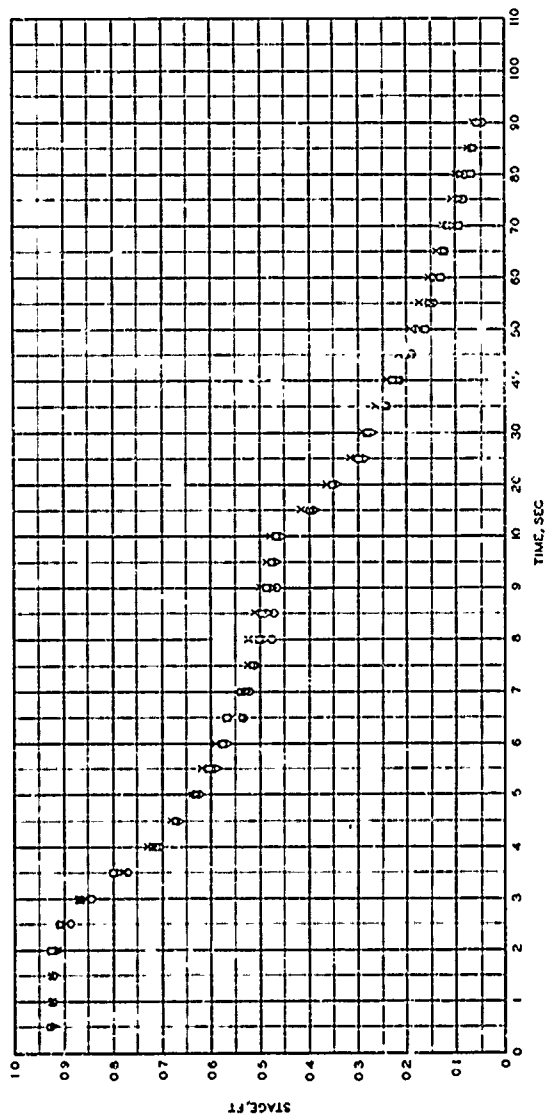
Table 21
Measurements of the Mohne and Eder Dams and Their Breaches

Dimension	Mohne Dam			Eder Dam		
	O. Kirschner	J. D. Levin	L. Levin	O. Kirschner	J. Frank	J. D. Levin L. Levin
<u>Dam</u>						
Height of dam, ft	131	132		157		172
Length of dam along crest, ft	2130	2130		1310		
Width of dam at base, ft	112			115		
Width of dam at top, ft	20.5			19.7		
<u>Reservoir</u>						
Depth of reservoir at time of breach, ft	105			134		
Volume of reservoir at time of breach, cu ft	4.65×10^9	4.79×10^9		7.11×10^9		7.13×10^9
Maximum storage volume of reservoir, cu ft	4.72×10^9			7.11×10^9		
Area of reservoir when full, sq ft	1.1×10^8			1.26×10^8		
Drainage area, sq ft	4.62×10^9					
Annual inflow, cu ft	2.58×10^9			5.37×10^9		
<u>Breach</u>						
Depth of breach below top of dam, ft	72.2			82		82
Width of breach at top of dam, ft	249			164		164
Depth of breach below original water level, ft	46			59		180
Width of breach at original water level, ft	242			154		55.8
Area of breach below water level, sq ft	8.05×10^3			5.91×10^3		
Shape of breach	Parabolic			Semicircular		
Maximum discharge, cu ft/sec	3.1×10^5	3.1×10^5		3.0×10^5		1.41×10^5
Total volume of outflow, cu ft	4.08×10^9			5.44×10^9		

(Continued)

Table 21 (Concluded)

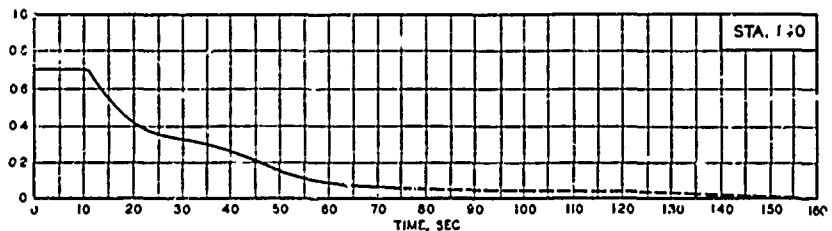
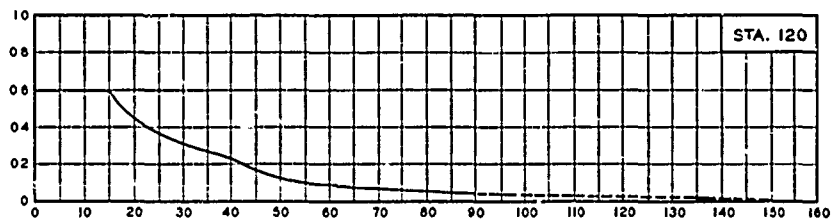
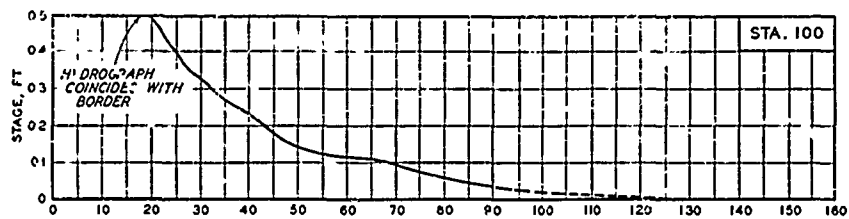
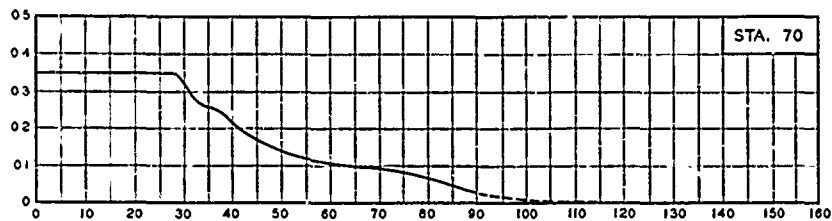
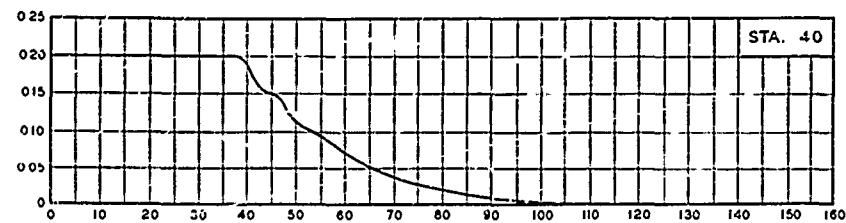
Dimension	Mohne Dam		Eder Dam	
	O. Kirschner	J. D. Lechin	O. Kirschner	J. D. Levin
<u>Breach (Continued)</u>				
Per cent of reservoir emptied	88		76	
Duration of outflow, hr	12		36	
Flood-wave height, ft	33	33		< 20
Average velocity of flood wave, ft/sec:				
Mohne, over 92-mile course	6.2		3.6	
Eder, over 264-mile course	2.88		1.22	
Average velocity of flood-wave tip, ft/sec				
Live. lost	1200			
$\frac{D_b}{Y_0}$	0.44		0.45	
$\frac{W_b}{K^2}$	0.11		0.12	
$\frac{D_b}{Y_0} \cdot \frac{W_b}{K^2}$	0.048		0.054	



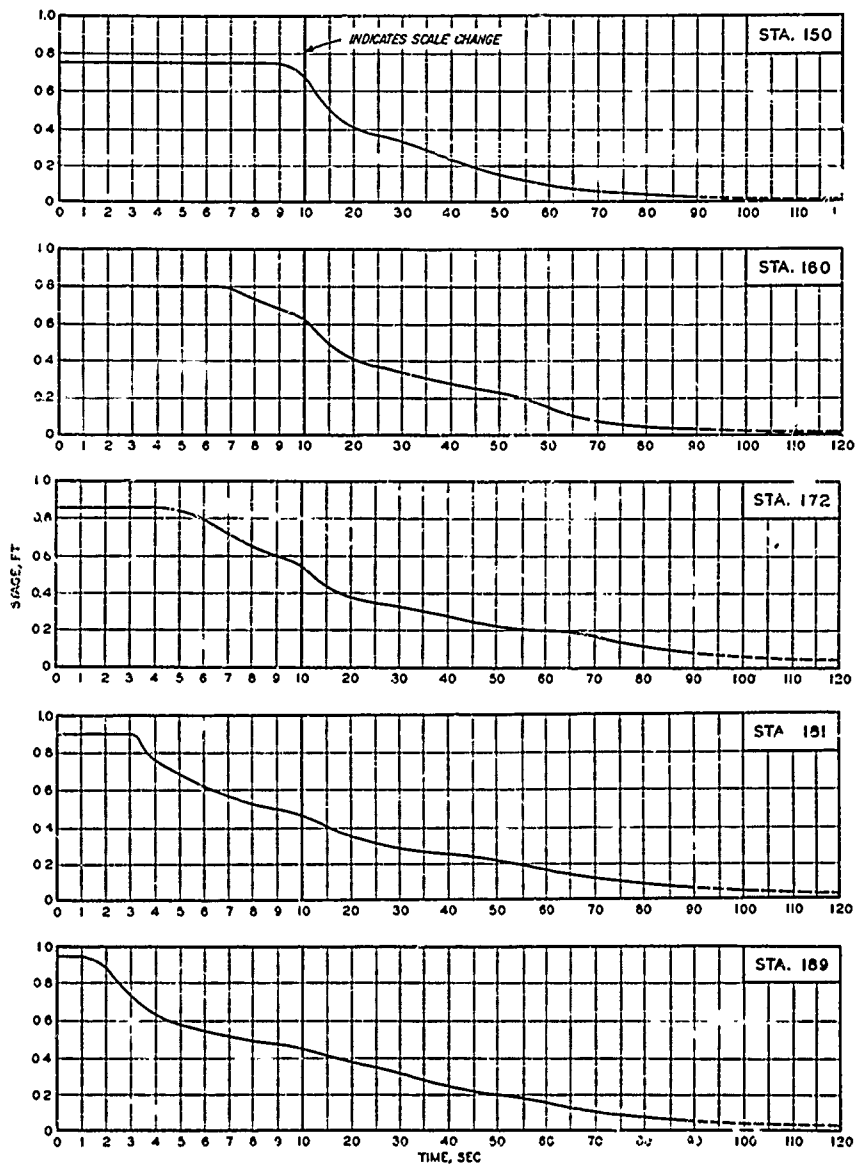
AGREEMENT OF STAGE-TIME HYDROGRAPH WHEN RUNS ARE REPEATED

1ST CONDITION 1.1
STATION 185

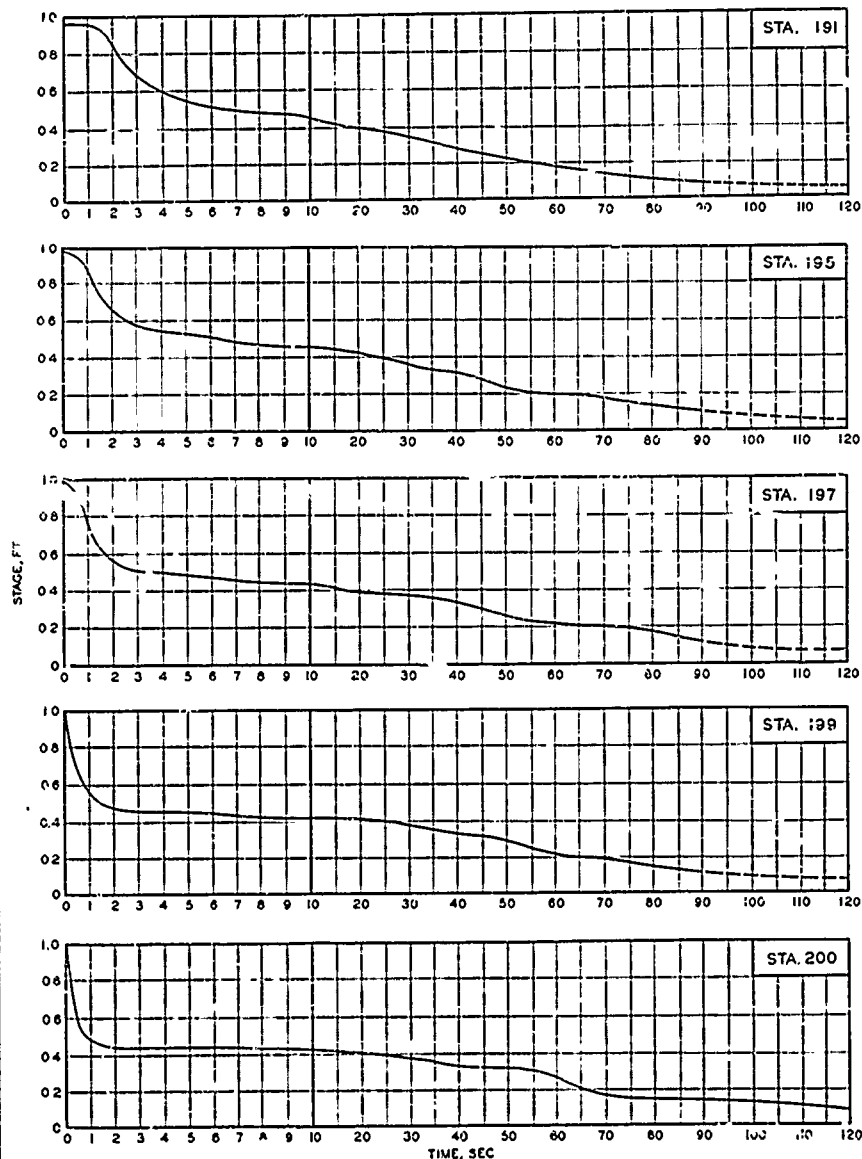
○ FIRST RUN
△ SECOND RUN
▽ THIRD RUN
□ FOURTH RUN



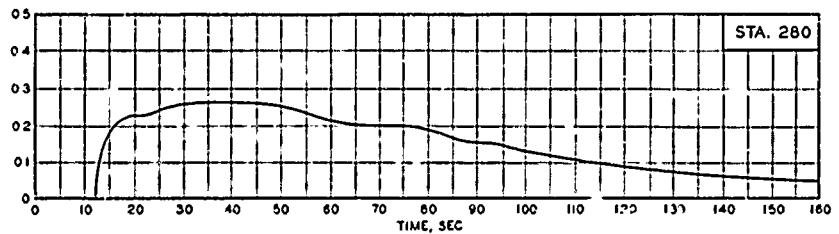
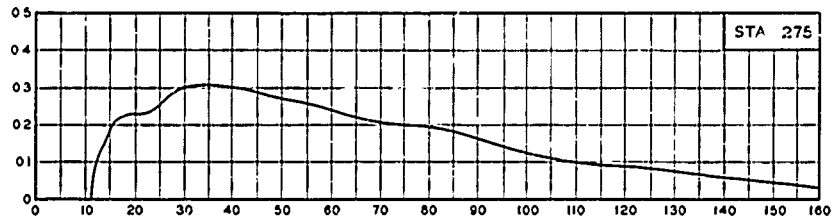
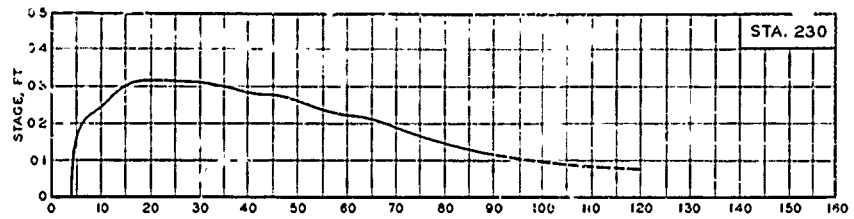
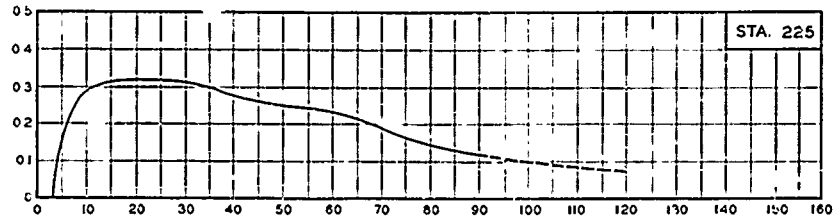
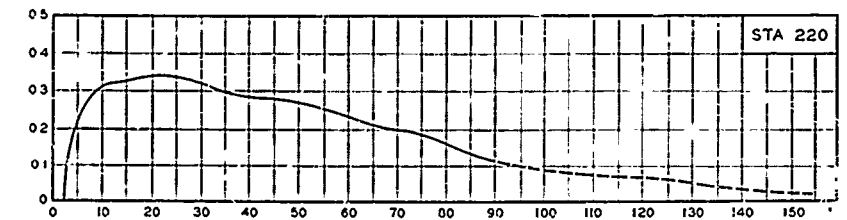
STAGE-TIME HYDROGRAPHS
STATIONS 40, 70, 100, 120, AND 140
TEST CONDITION ...



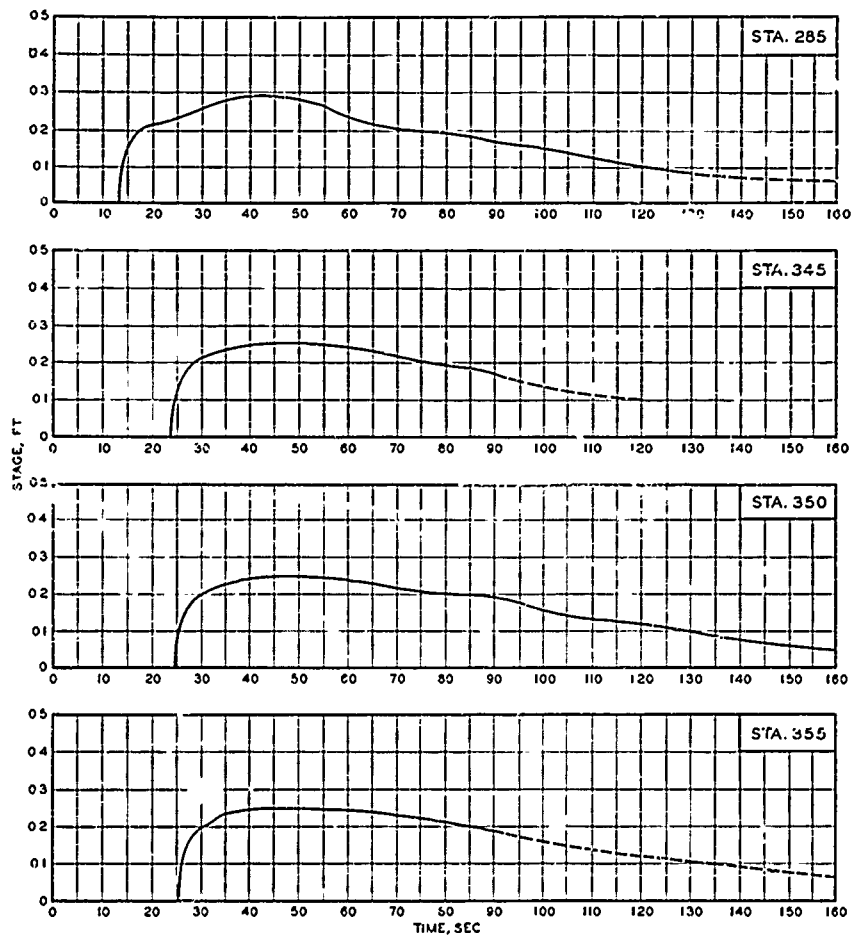
STAGE-TIME HYDROGRAPHS
STATIONS 150, 160, 172, 181, AND 189
TEST CONDITION 1.1



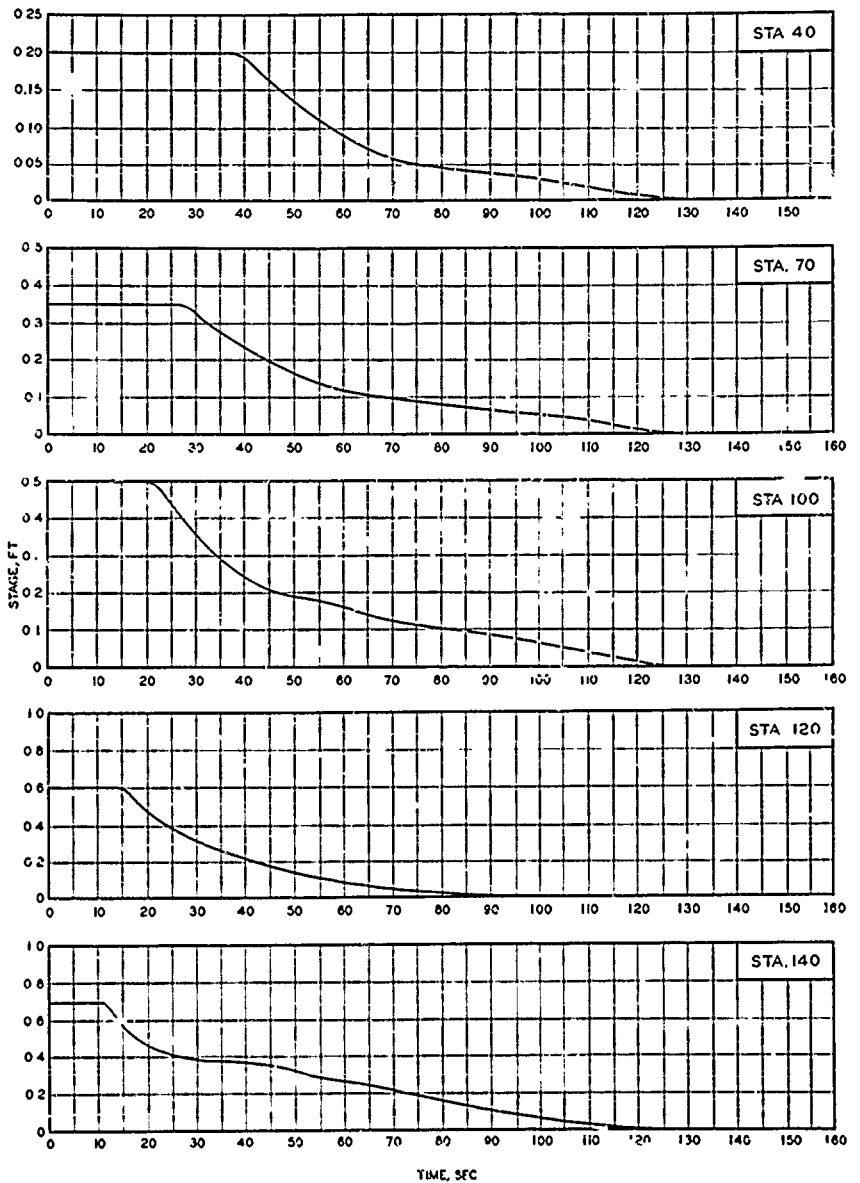
STAGE-TIME HYDROGRAPHS
STATIONS 191, 195, 197, 199 AND 200
TEST CONDITION I.



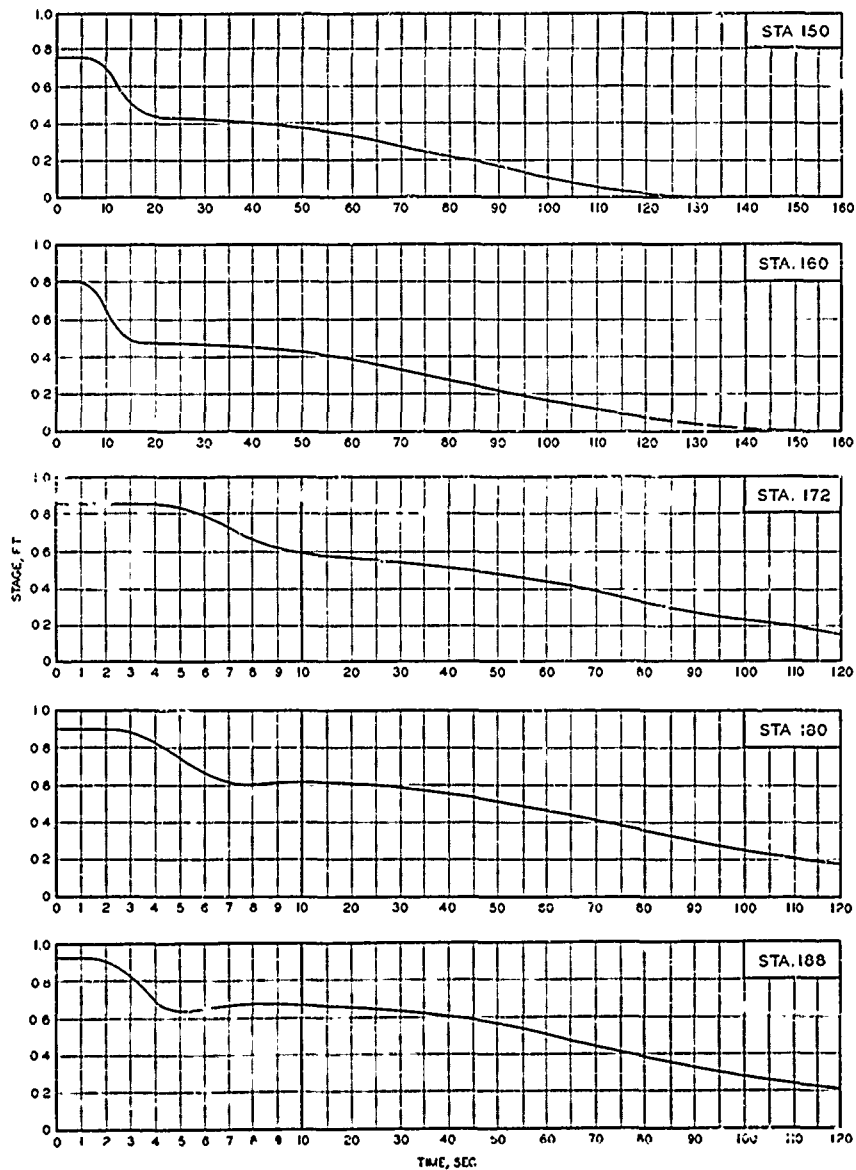
STAGE-TIME HYDROGRAPHS
STATIONS 220, 225, 230, 275, AND 280
TEST CONDITION 1.1



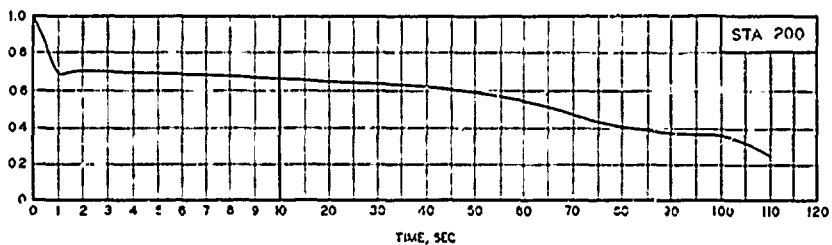
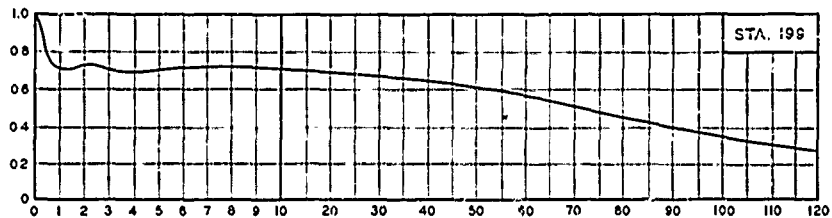
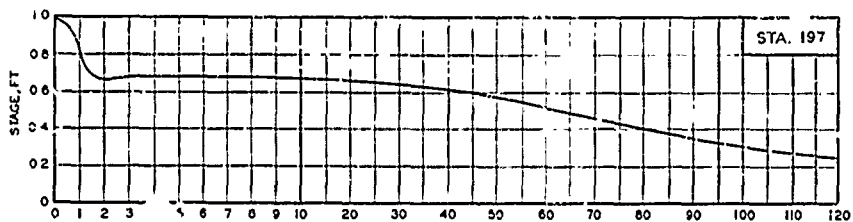
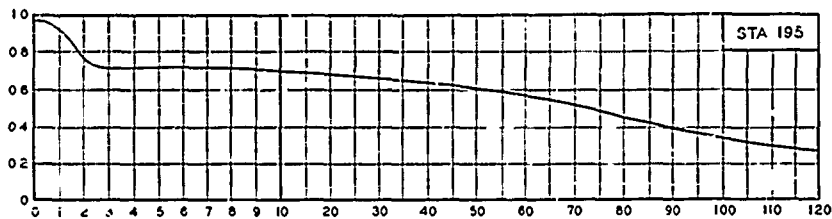
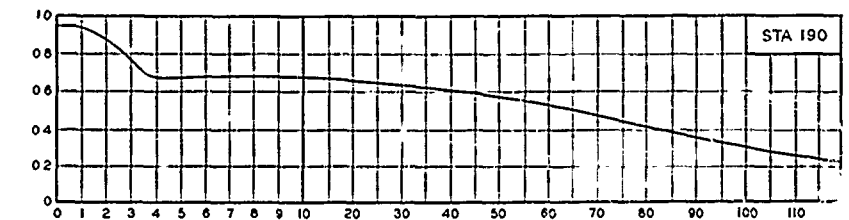
STAGE-TIME HYDROGRAPHS
STATIONS 285, 345, 350 AND 355
TEST CONDITION 1.1



STAGE-TIME HYDROGRAPHS
STATIONS 40, 70, 100, 120 AND 140
TEST CONDITION 2.1



STAGE-TIME HYDROGRAPHS
STATIONS 150, 160, 172, 180, AND 188
TEST CONDITION 21



STAGE-TIME HYDROGRAPHS
STATIONS 190, 195, 197, 198, AND 200
TEST CONDITION 2.1

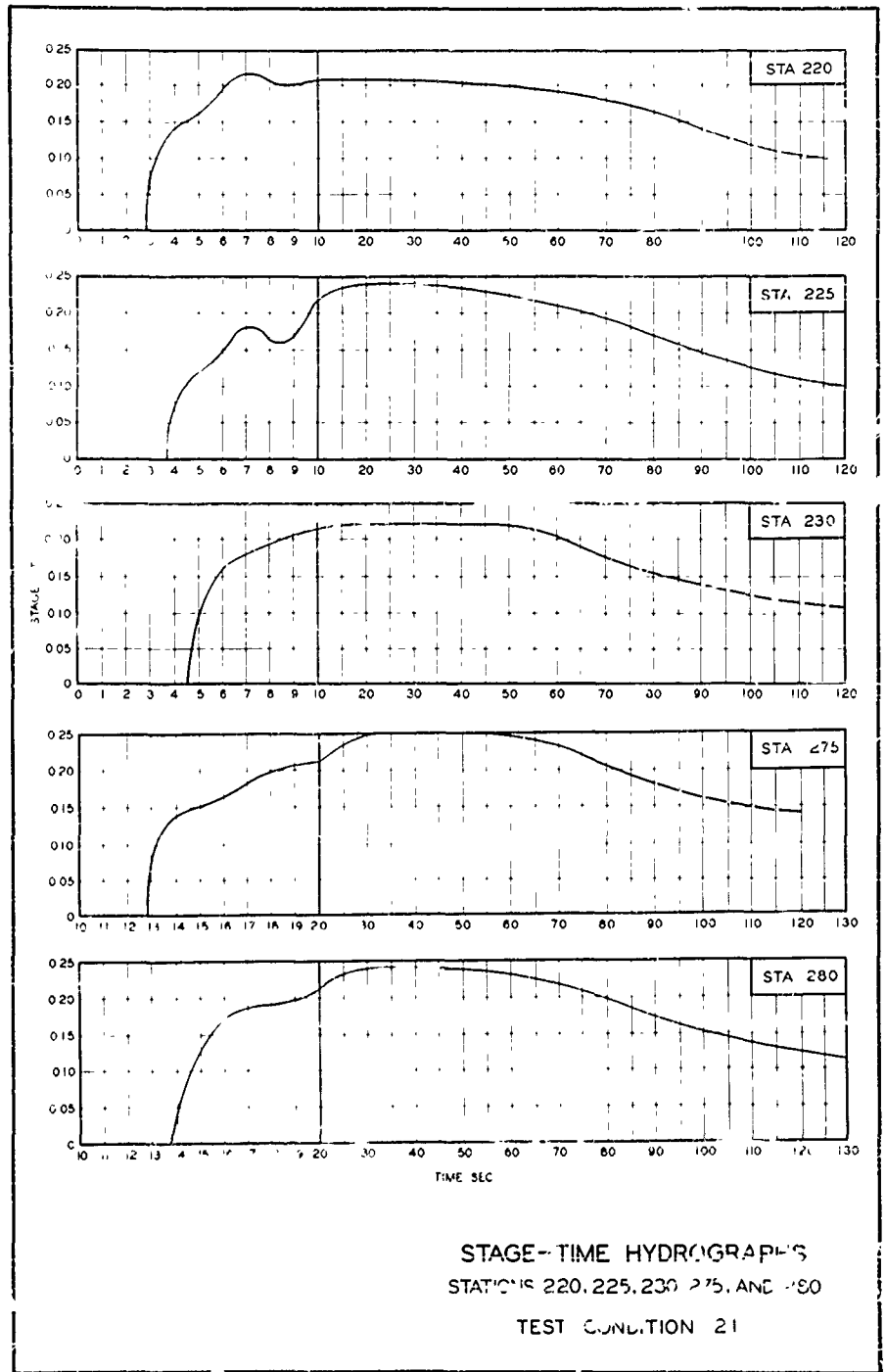
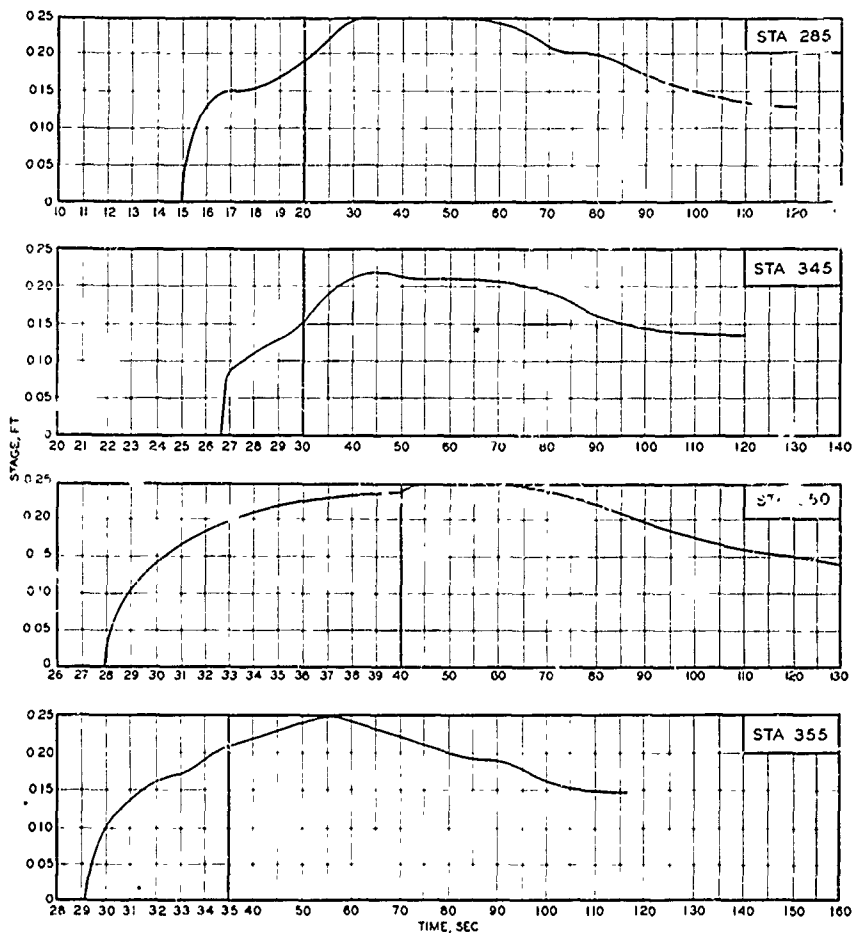


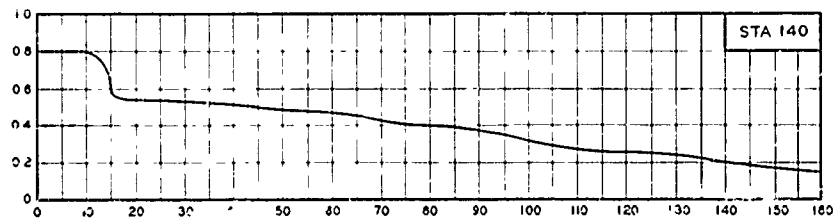
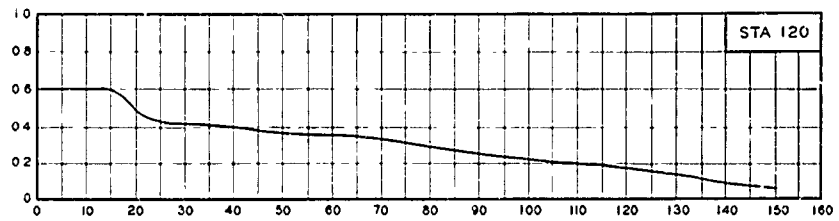
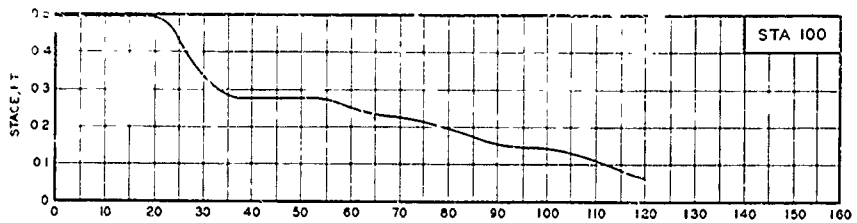
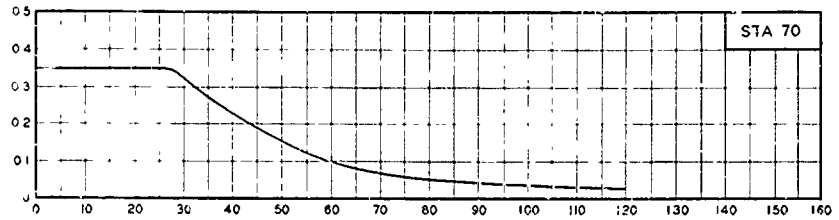
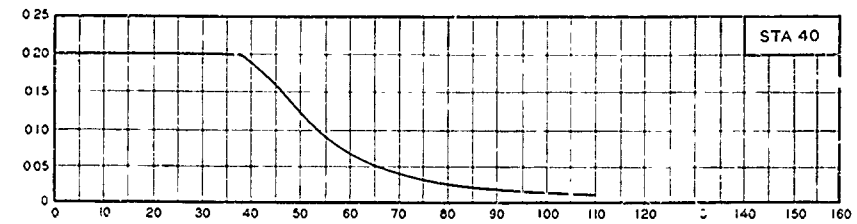
PLATE 10



STAGE-TIME HYDROGRAPHS

STATIONS 285, 345, 350 AND 355

TEST COLLECTION 21

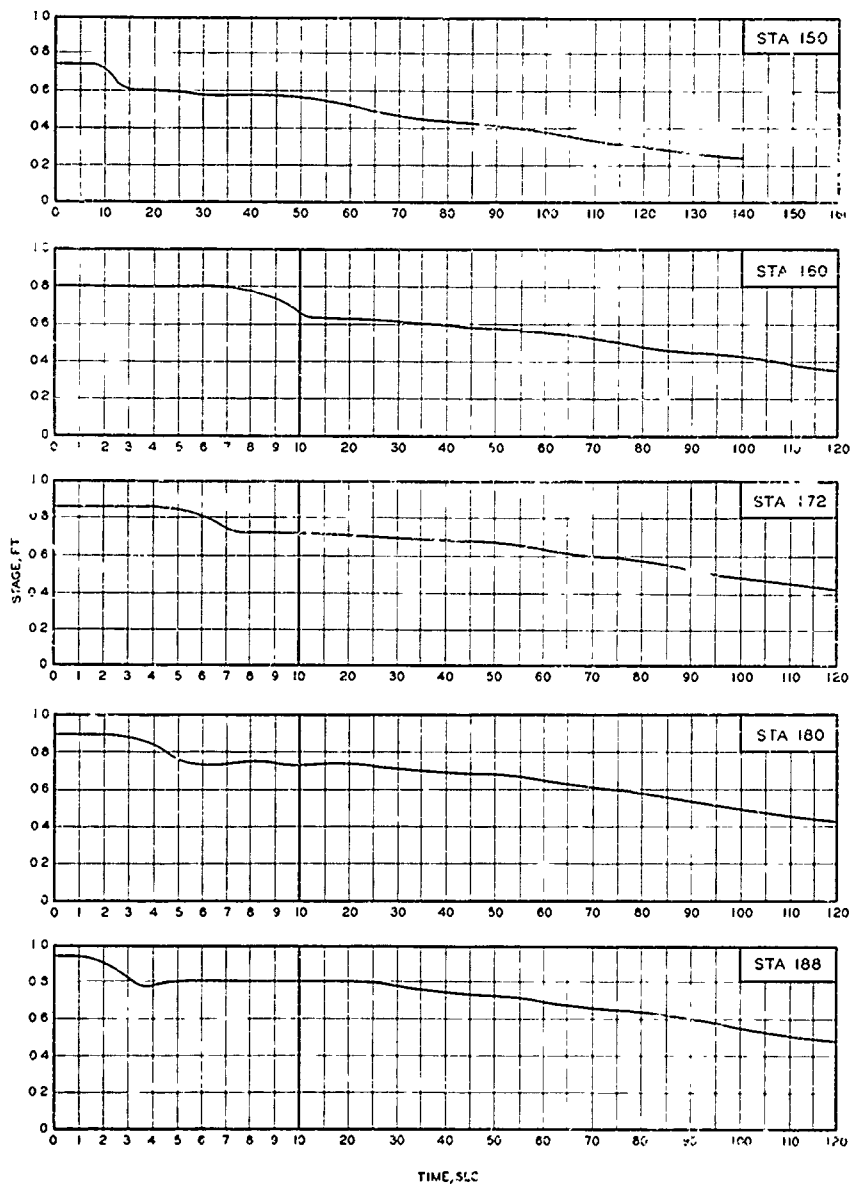


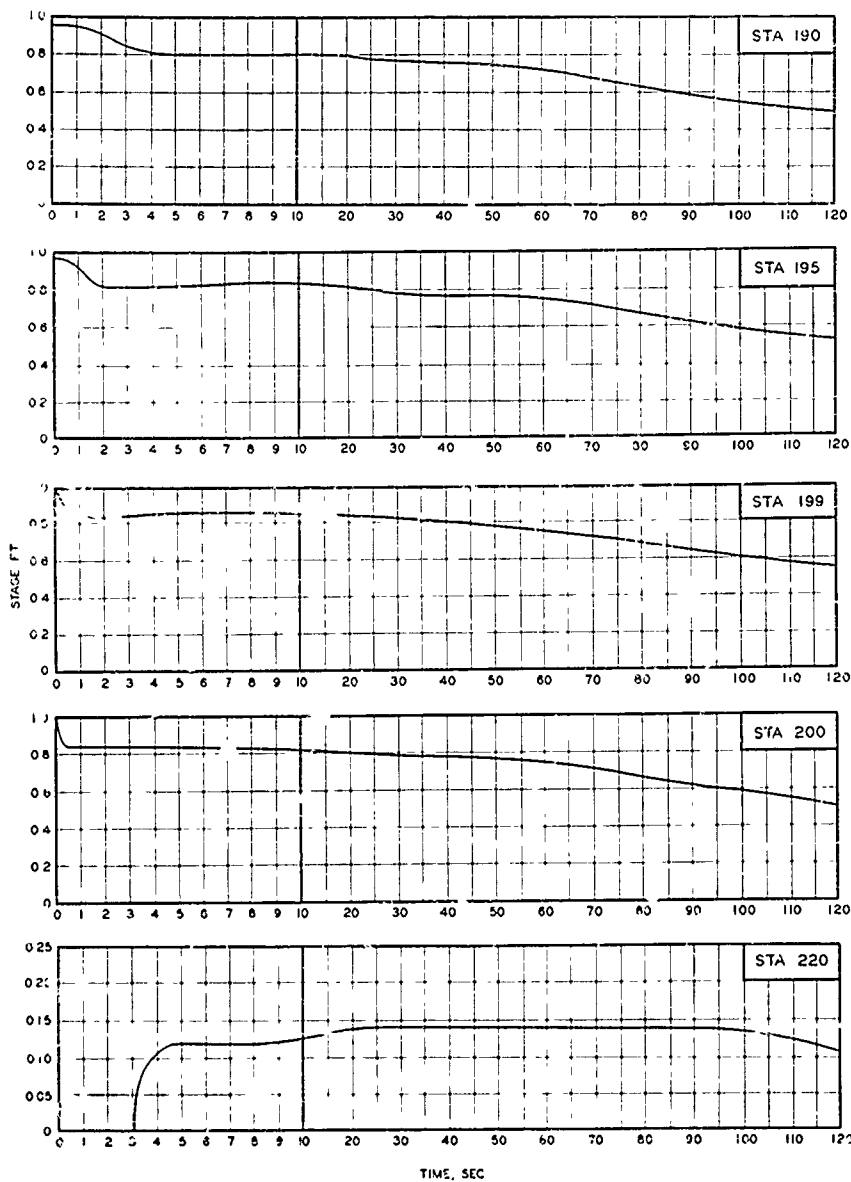
TIME, SEC

STAGE-TIME HYDROGRAPHS

STATIONS 40, 70, 100, 120 AND 140

TEST CONDITION 31

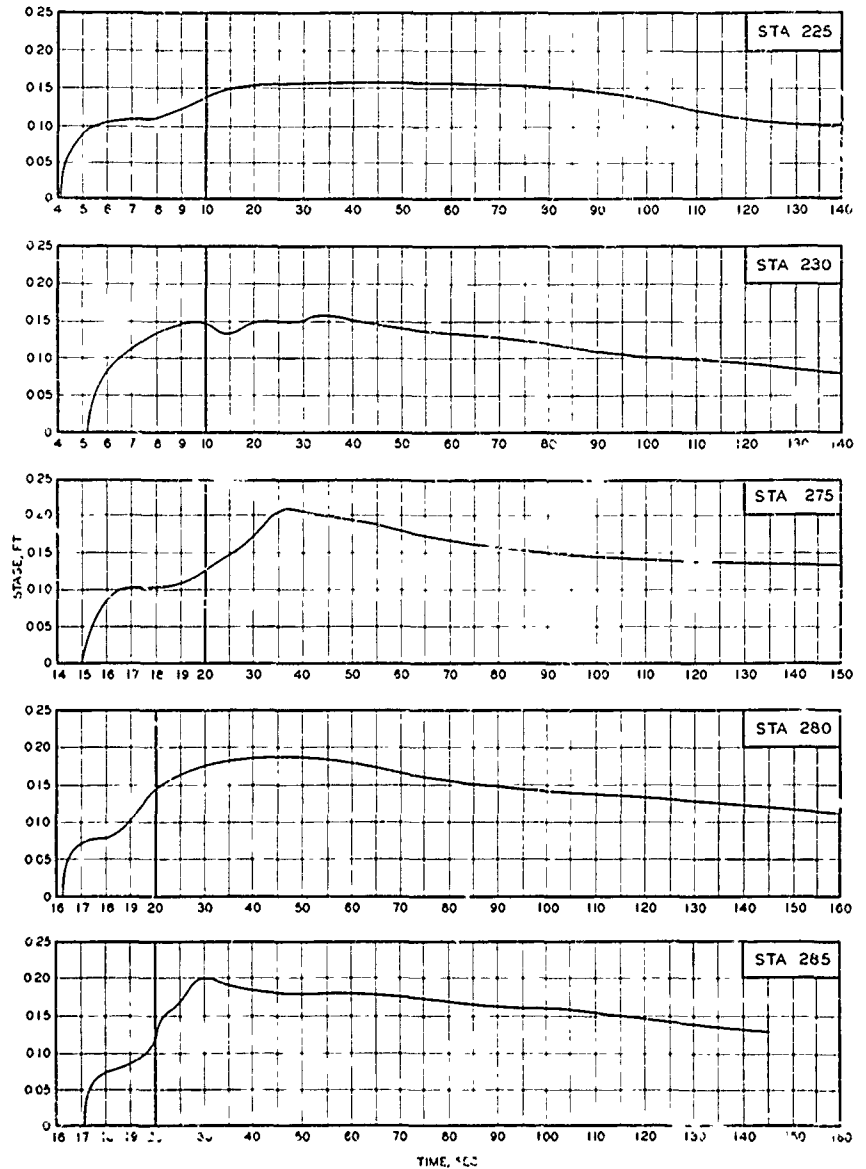




STAGE-TIME HYDROGRAPHS

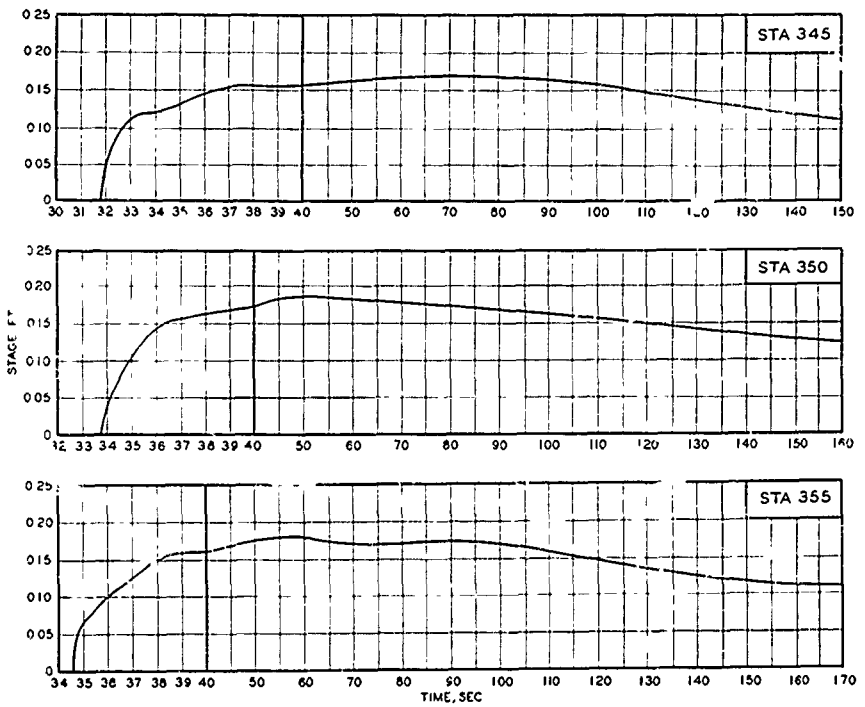
STATIONS 190, 195, 199, 200, AND 220

TEST CONDITION 31



STAGE-TIME HYDROGRAPHS
STATIONS 225, 230, 275, 280, AND 285

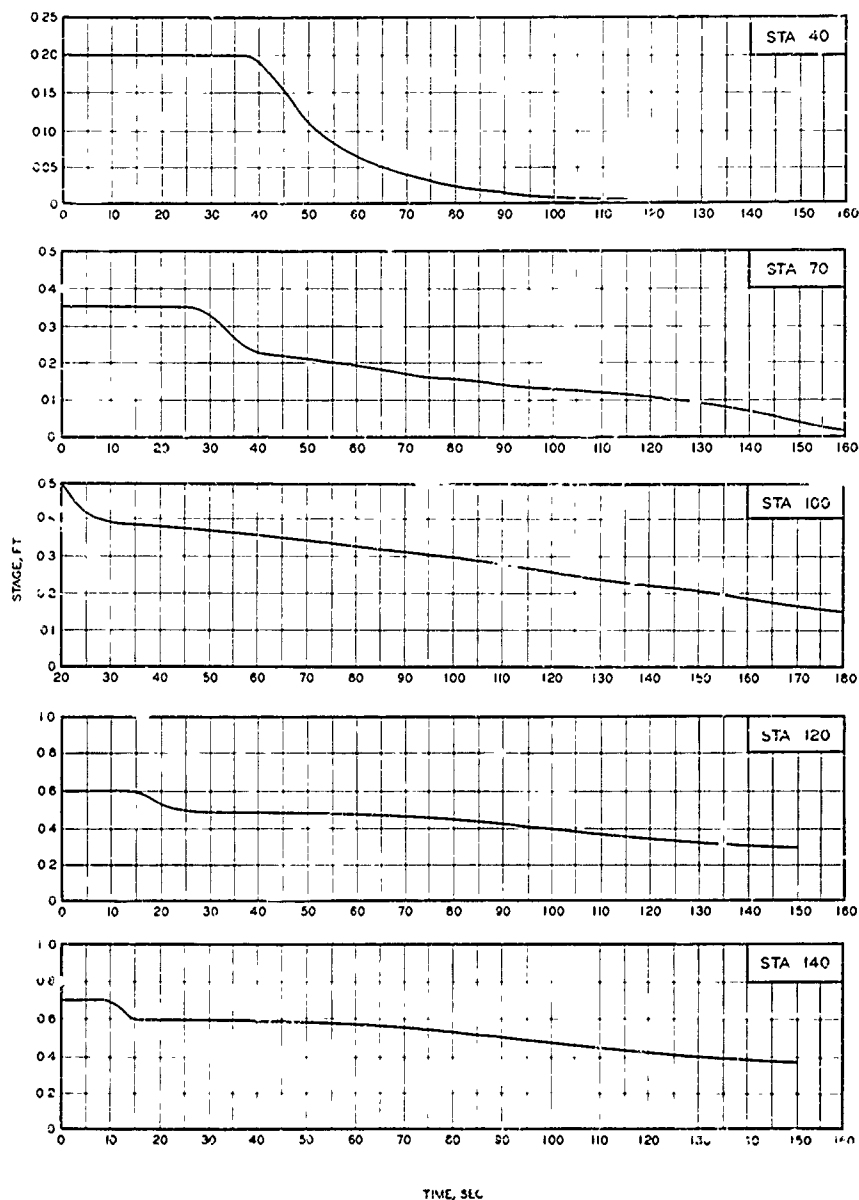
TEST CONDITION 31



STAGE-TIME HYDROGRAPHS

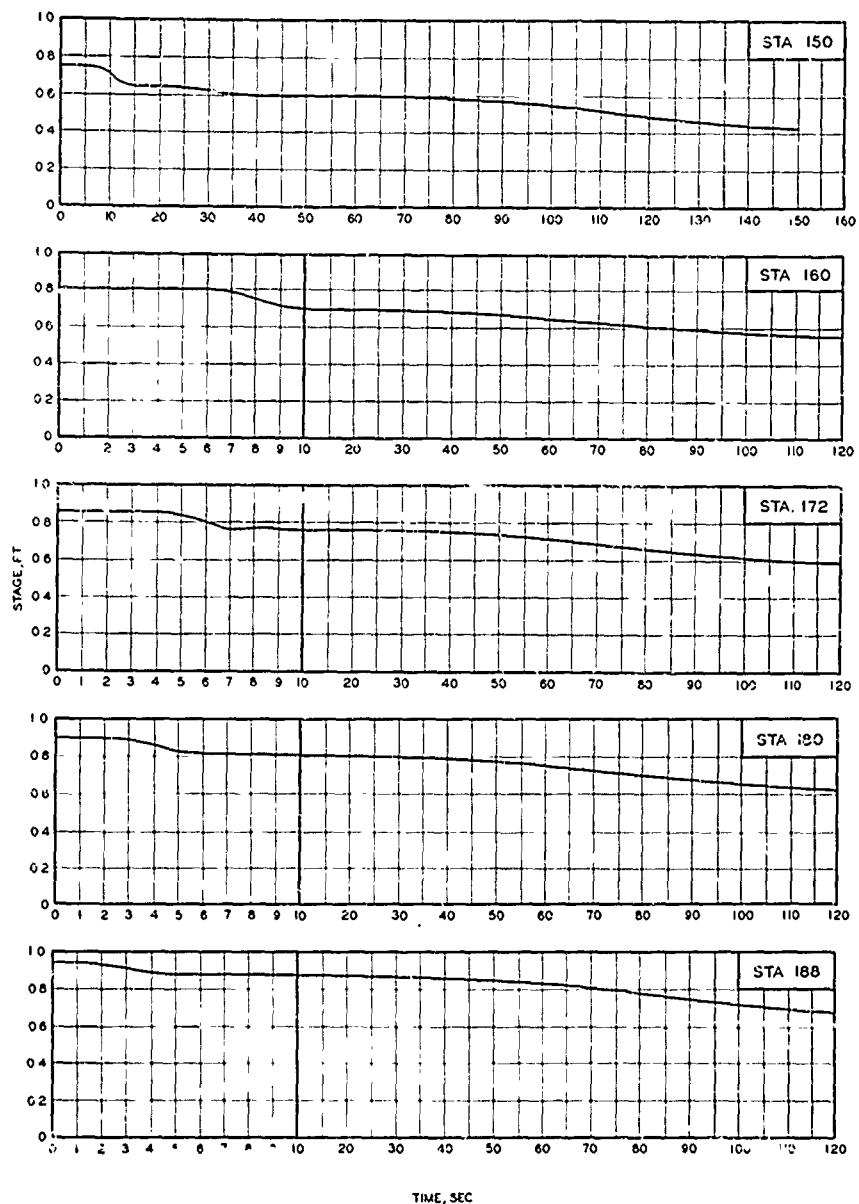
STATIONS 345, 350, AND 355

TEST CONDITION 31



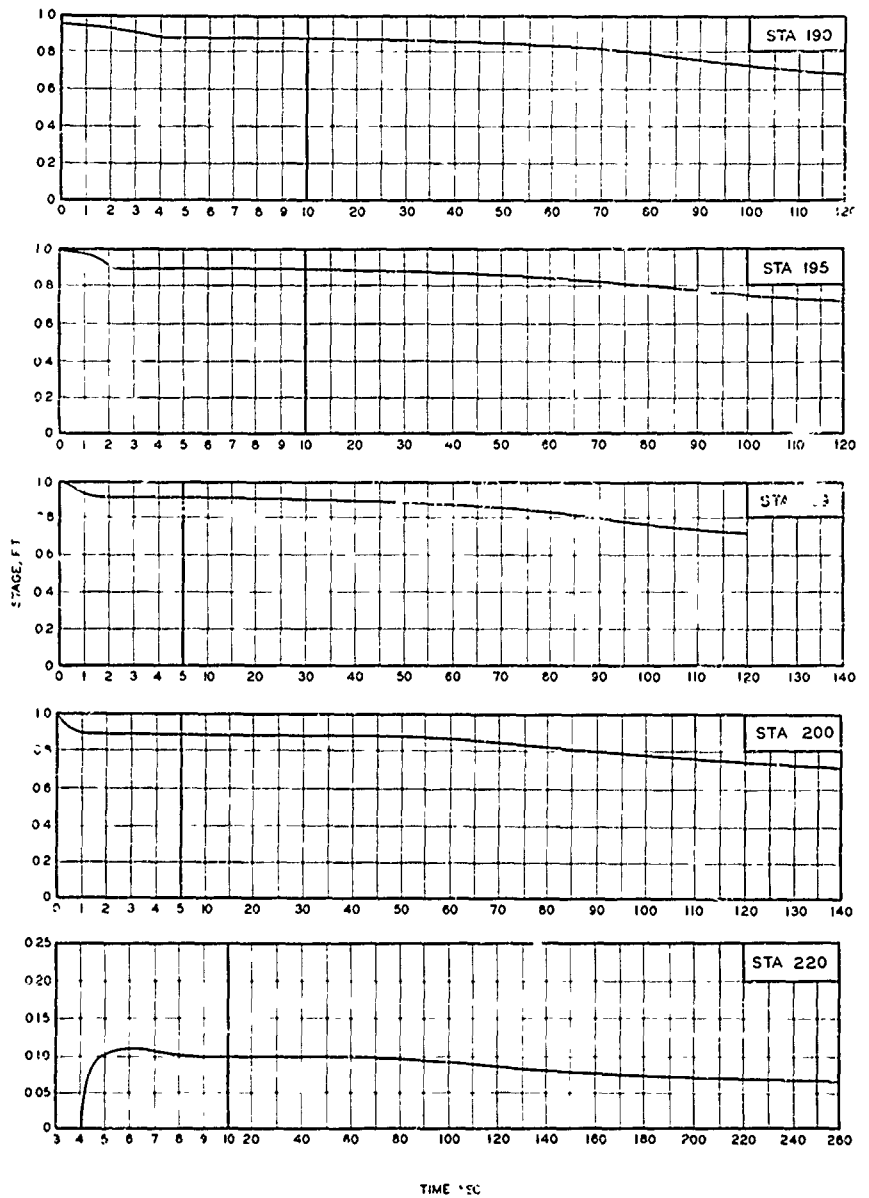
STAGE-TIME HYDROGRAPHS
STATIONS 40, 70, 100, 120, AND 140

TEST CONDITION 41



STAGE-TIME HYDROGRAPHS
STATIONS 150, 160, 172, 180, AND 188

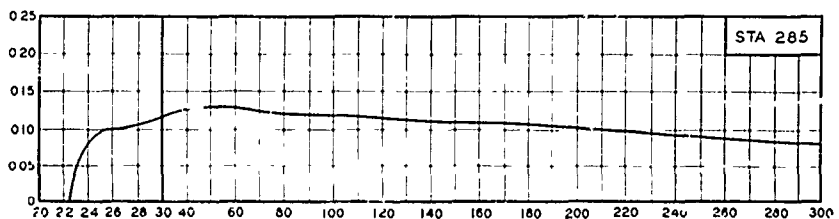
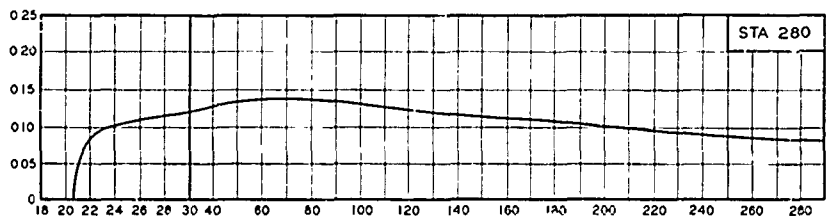
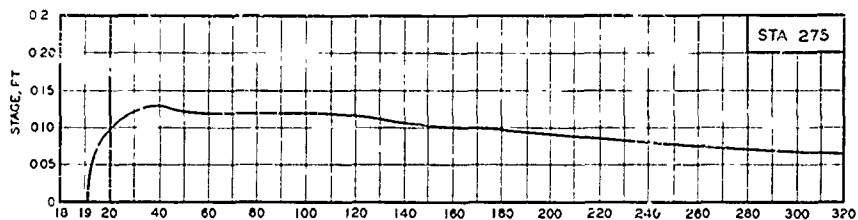
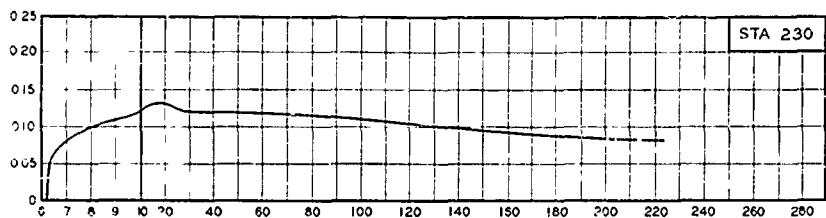
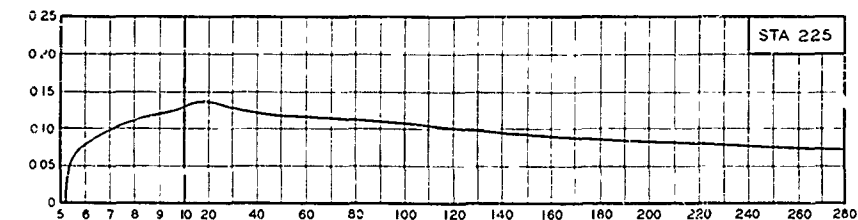
TEST CONDITION 41



TIME, SEC

STAGE-TIME HYDROGRAPHS STATIONS 190, 195, 193, 200 AND 220

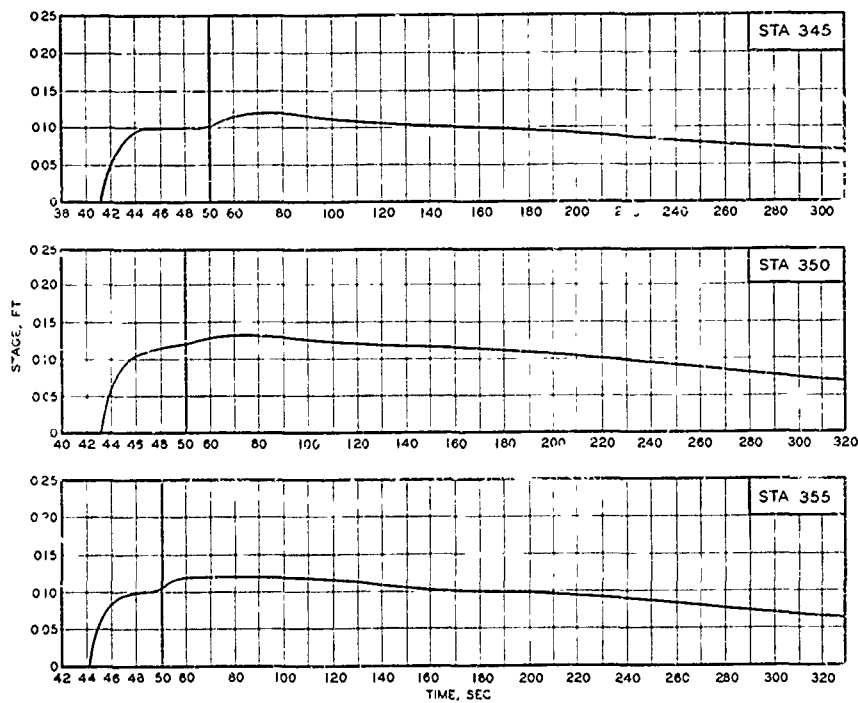
TEST CONDITION 41



TIME, SEC

STAGE-TIME HYDROGRAPHS STATIONS 225, 230, 275, 280, AND 285

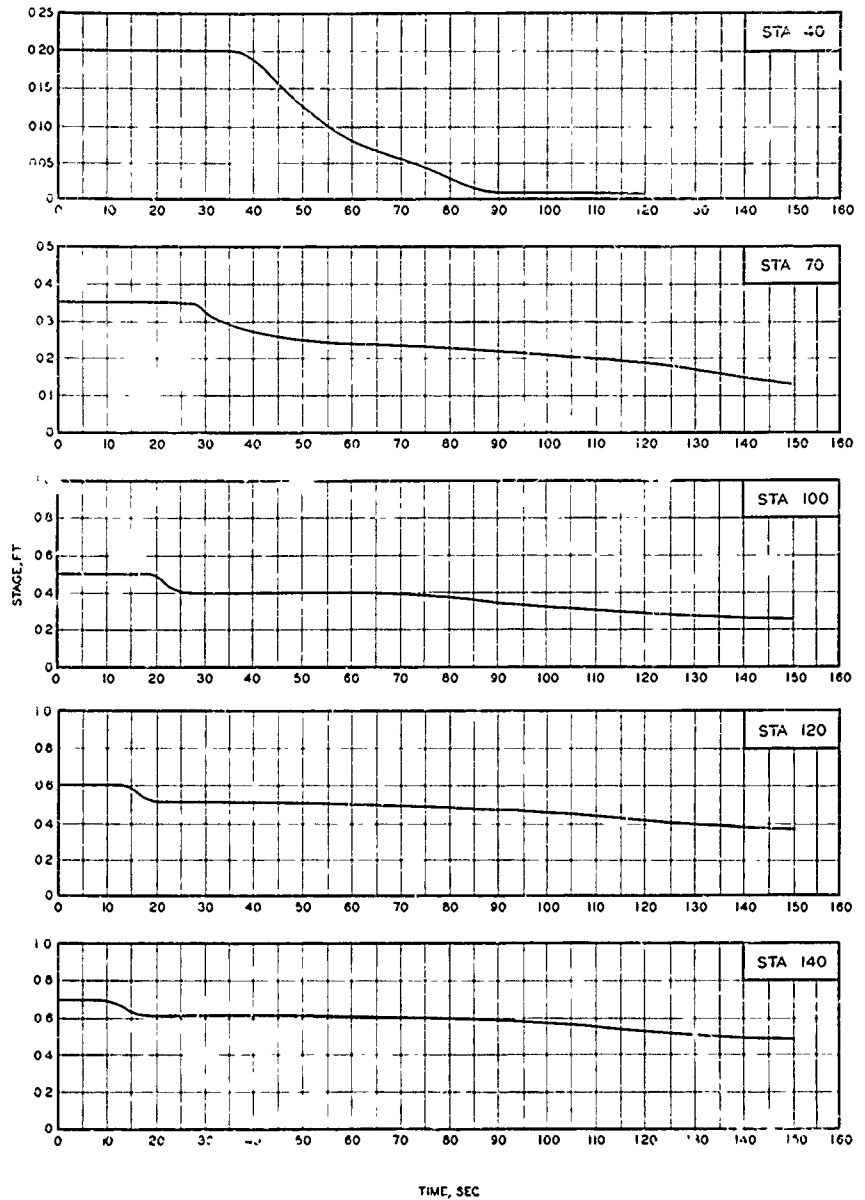
TEST CONDITION 41



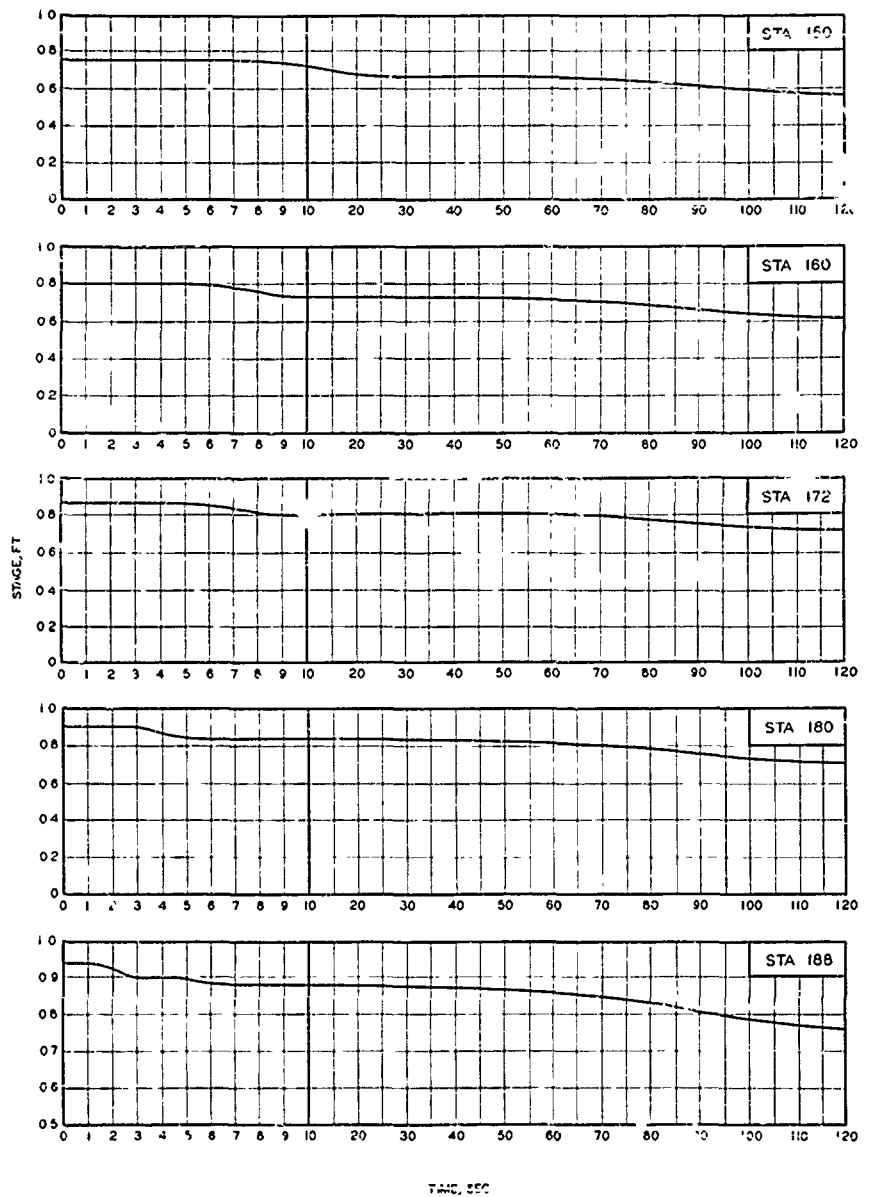
STAGE-TIME HYDROGRAPHS

STATIONS 345, 350, AND 355

TEST CONDITION 41

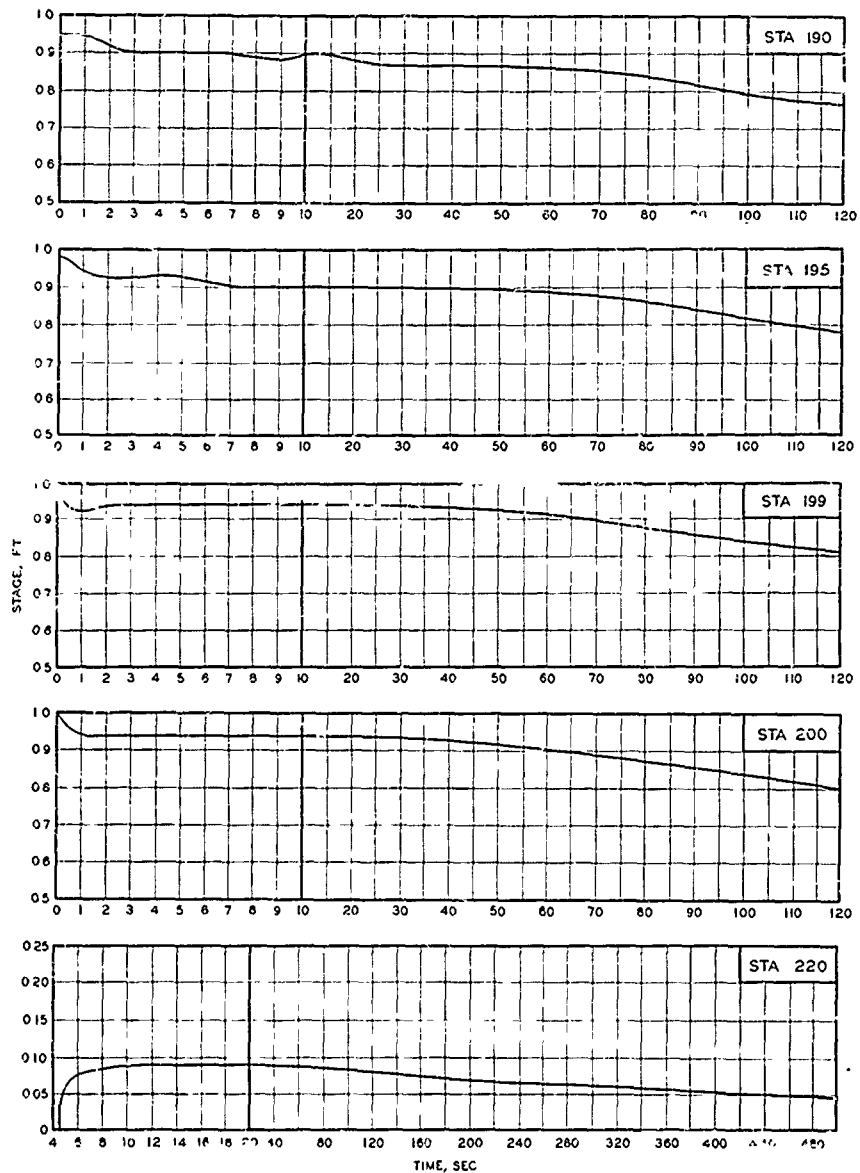


STAGE-TIME HYDROGRAPHS
STATIONS 40, 70, 100, 120, AND 140
TEST CONDITION 5.1

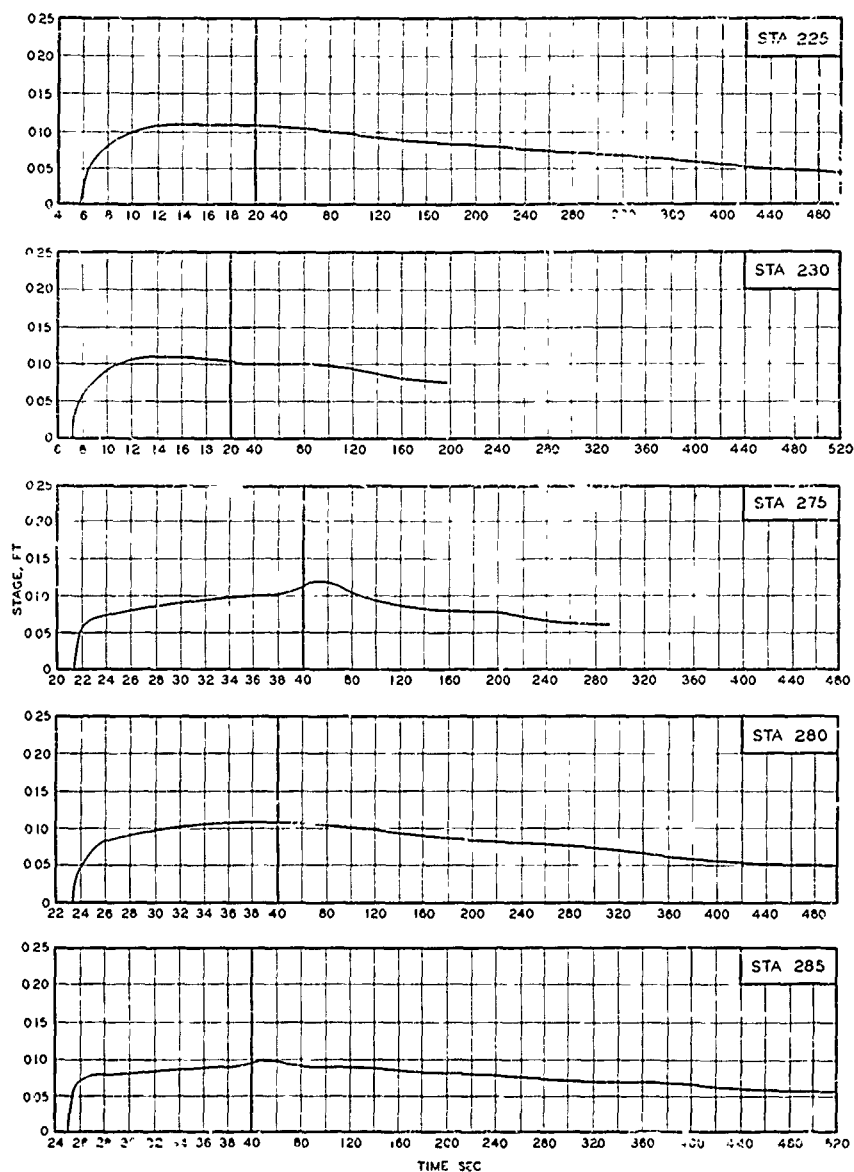


STAGE-TIME HYDROGRAPHS
STATIONS 150, 160, 172, 180, AND 188

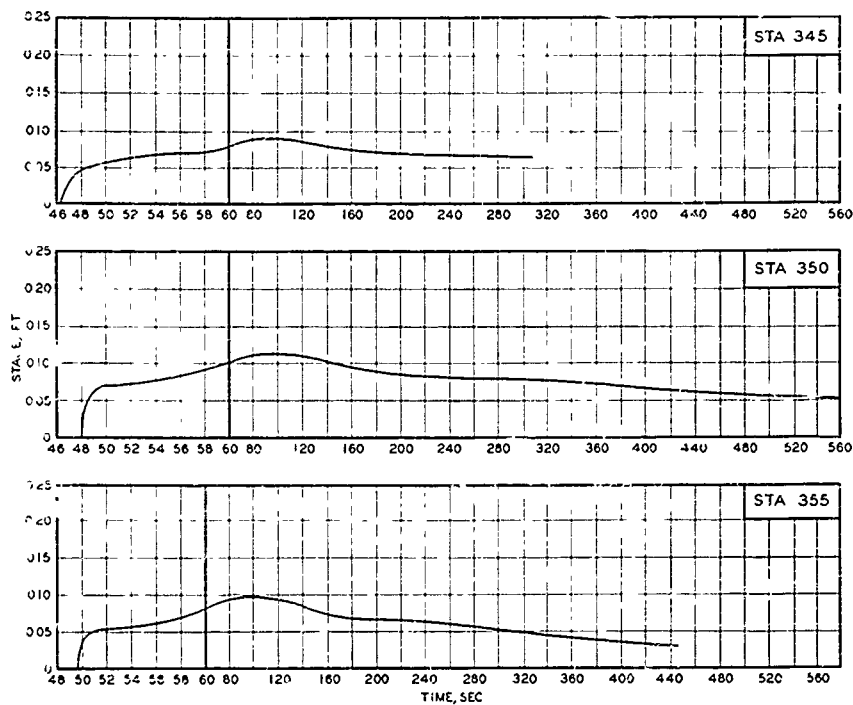
TEST CONDITION 5.1



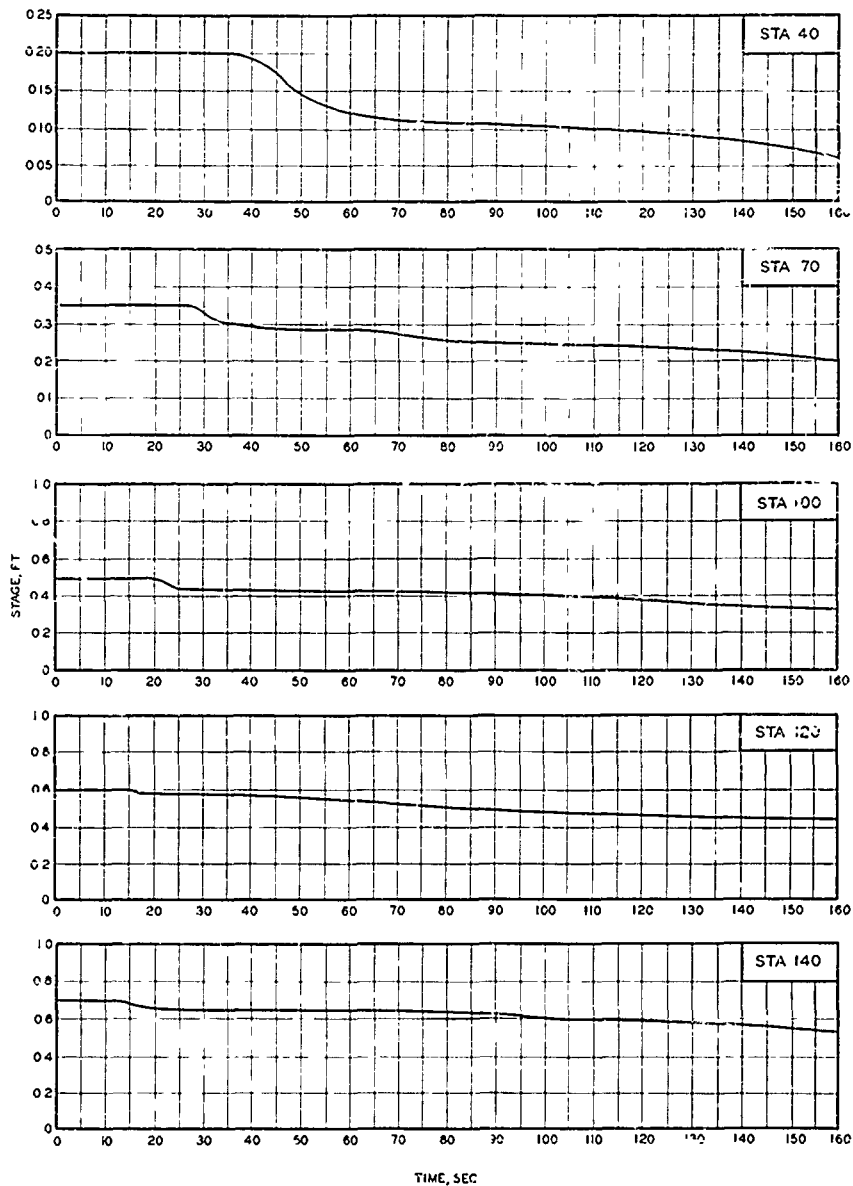
STAGE-TIME HYDROGRAPHS
STATIONS 190, 195, 199, 200, AND 220
TEST CONDITION 51



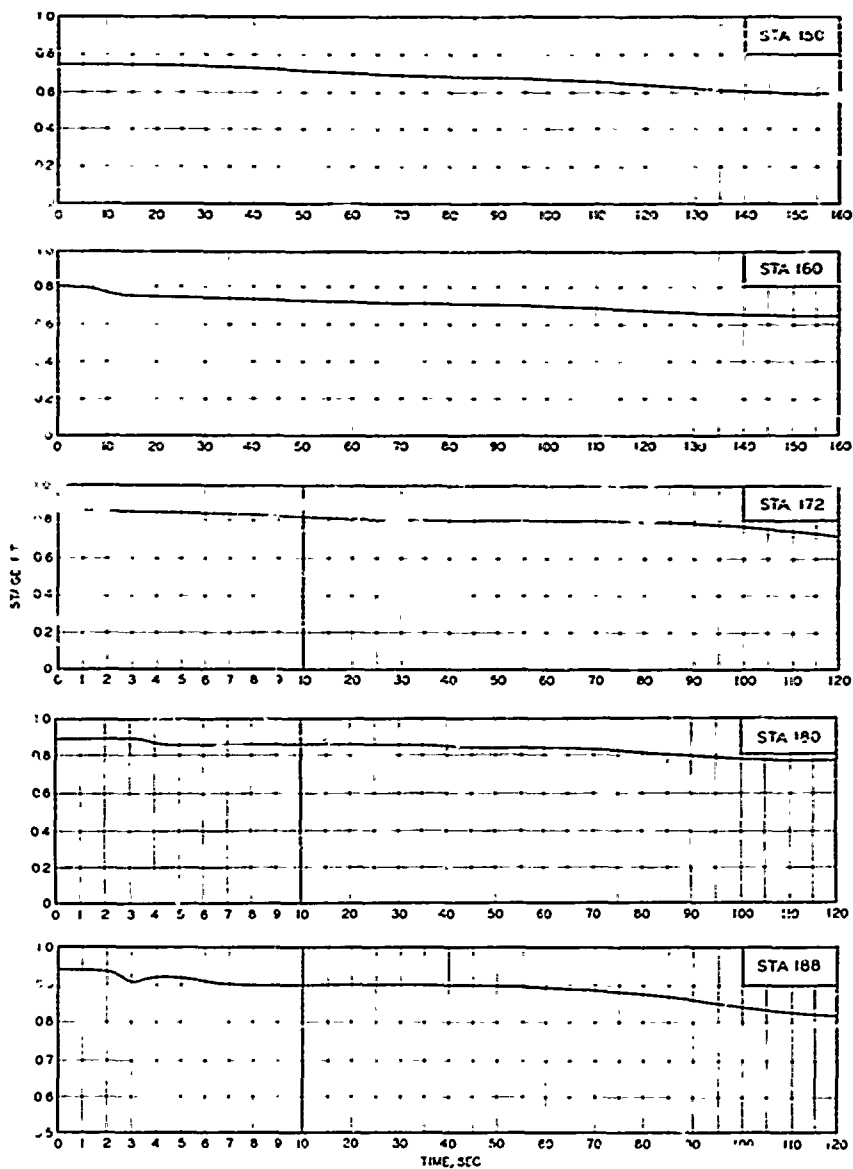
STAGE-TIME HYDROGRAPHS
STATIONS 225, 230, 275, 280, AND 285
"ES" CONDITION 51



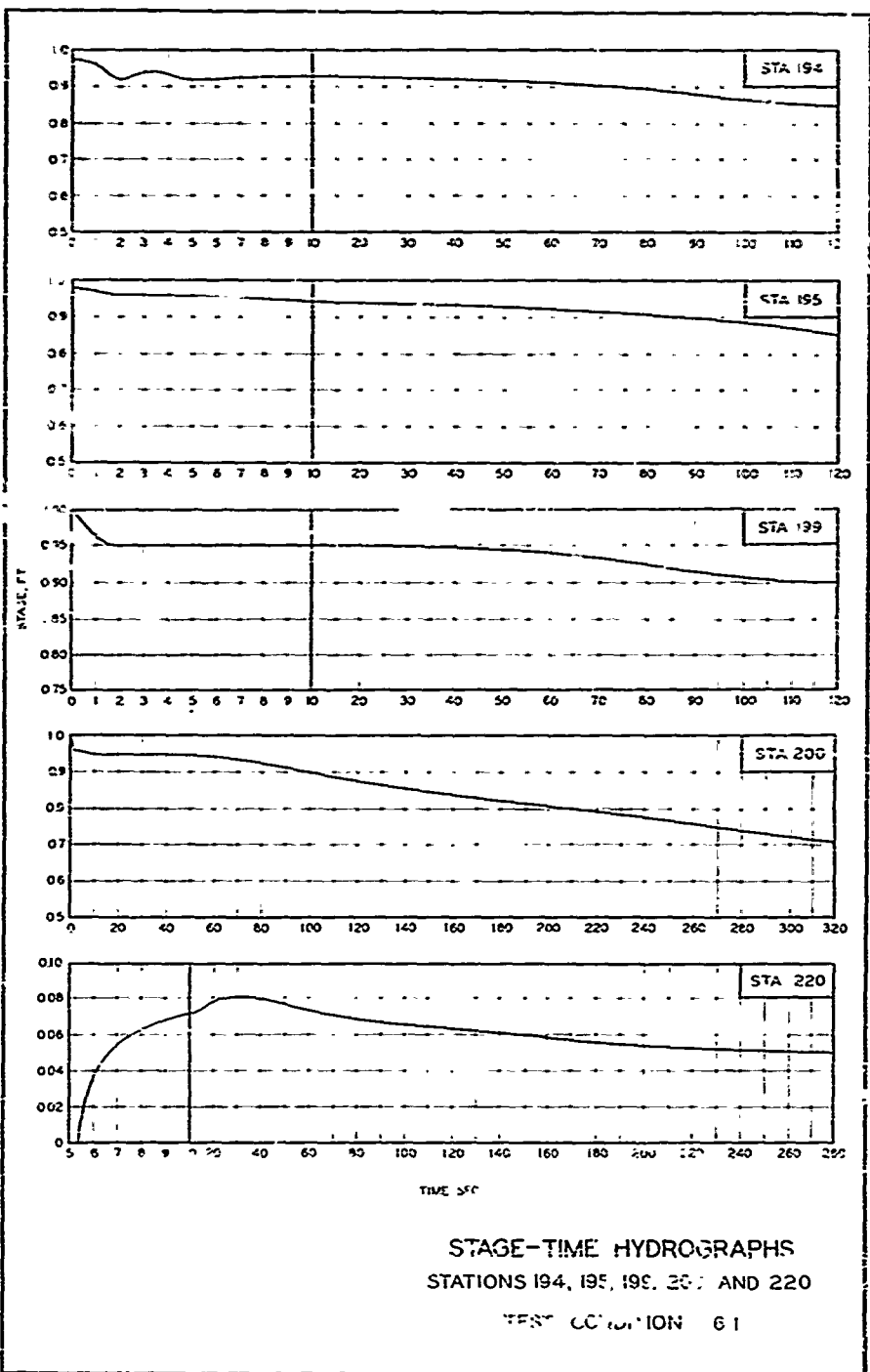
STAGE-TIME HYDROGRAPHS
STATIONS 345, 350, AND 355
TEST CONDITION 51



STAGE-TIME HYDROGRAPHS
STATIONS 40, 70, 100, 120, AND 140
TEST CONDITION 6.1



STAGE-TIME HYDROGRAPHS
STATIONS 150, 160, 172, 180, AND 188
TEST CONDITION: 51



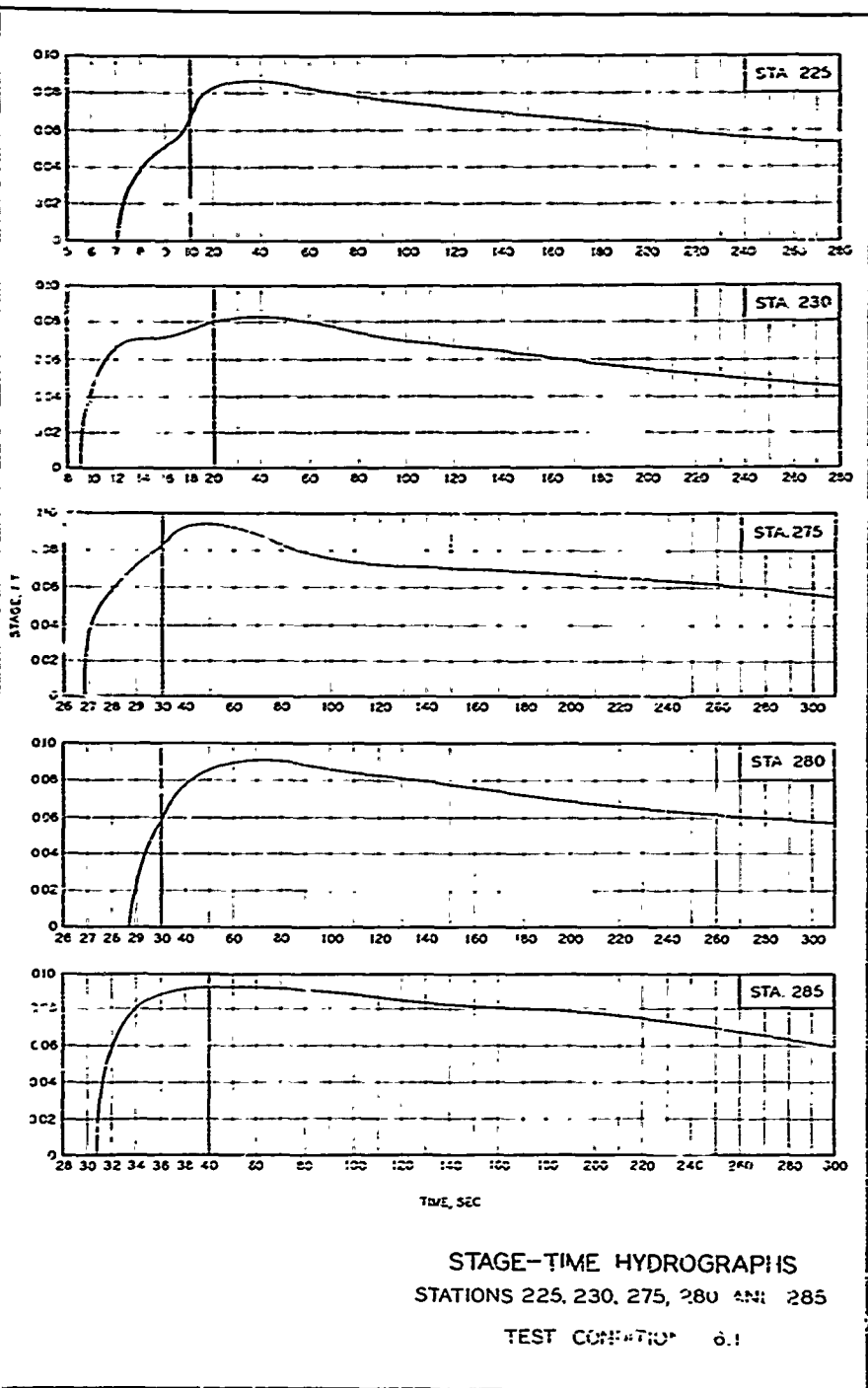
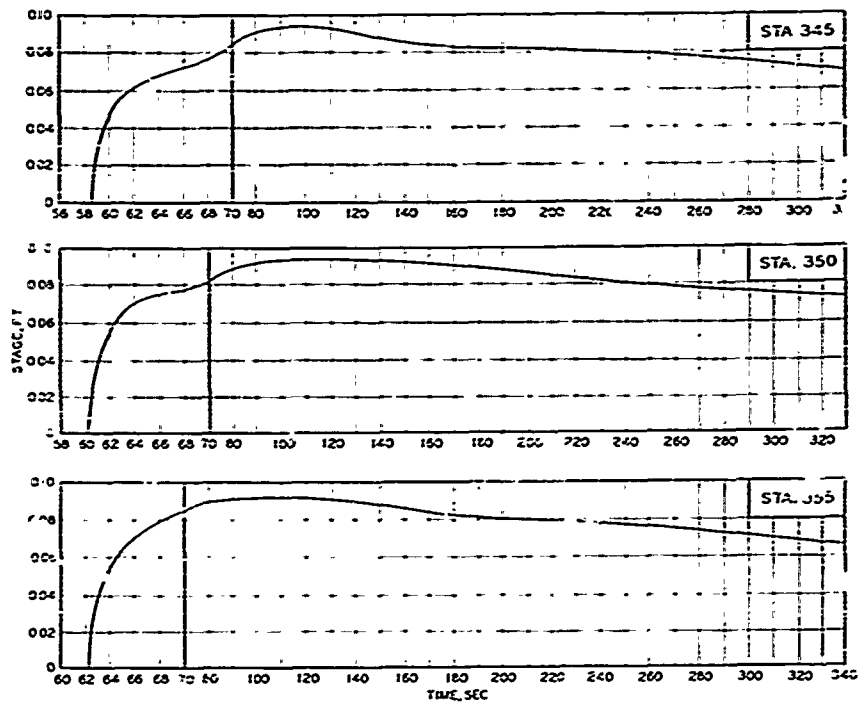


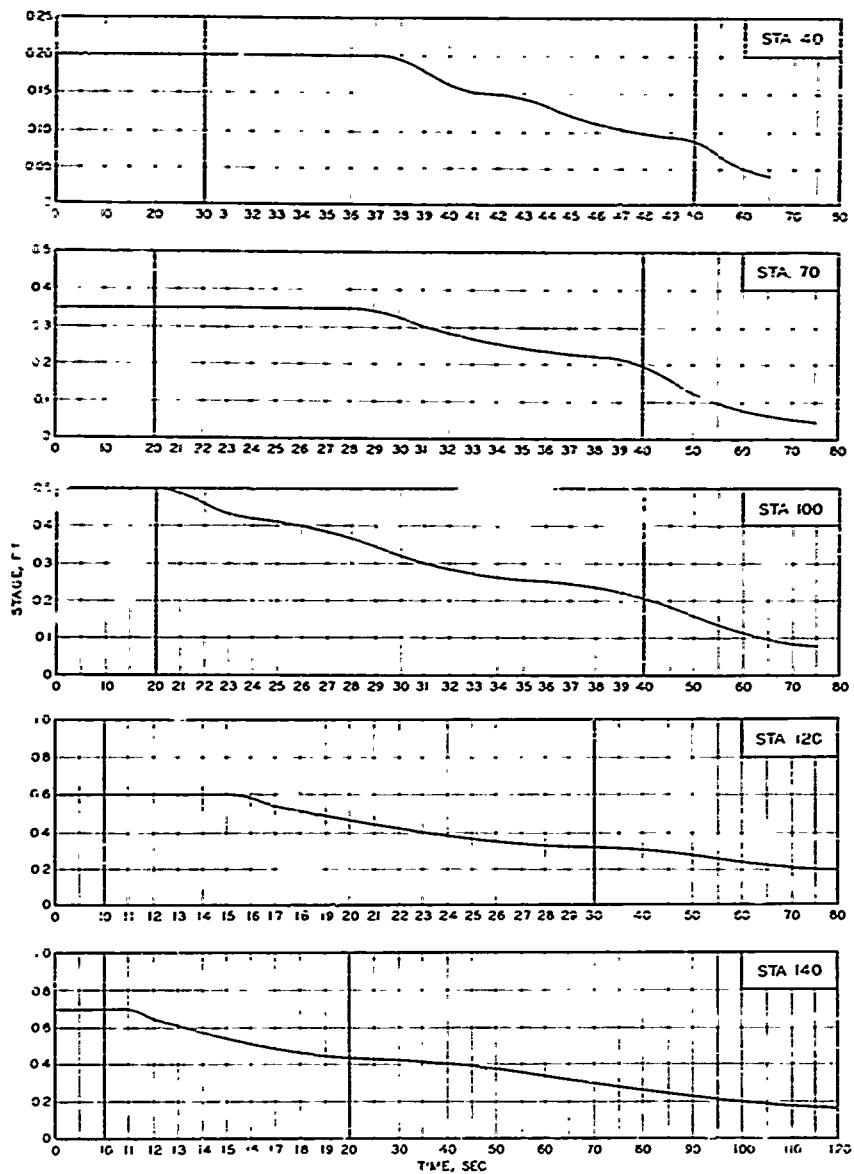
PLATE 30



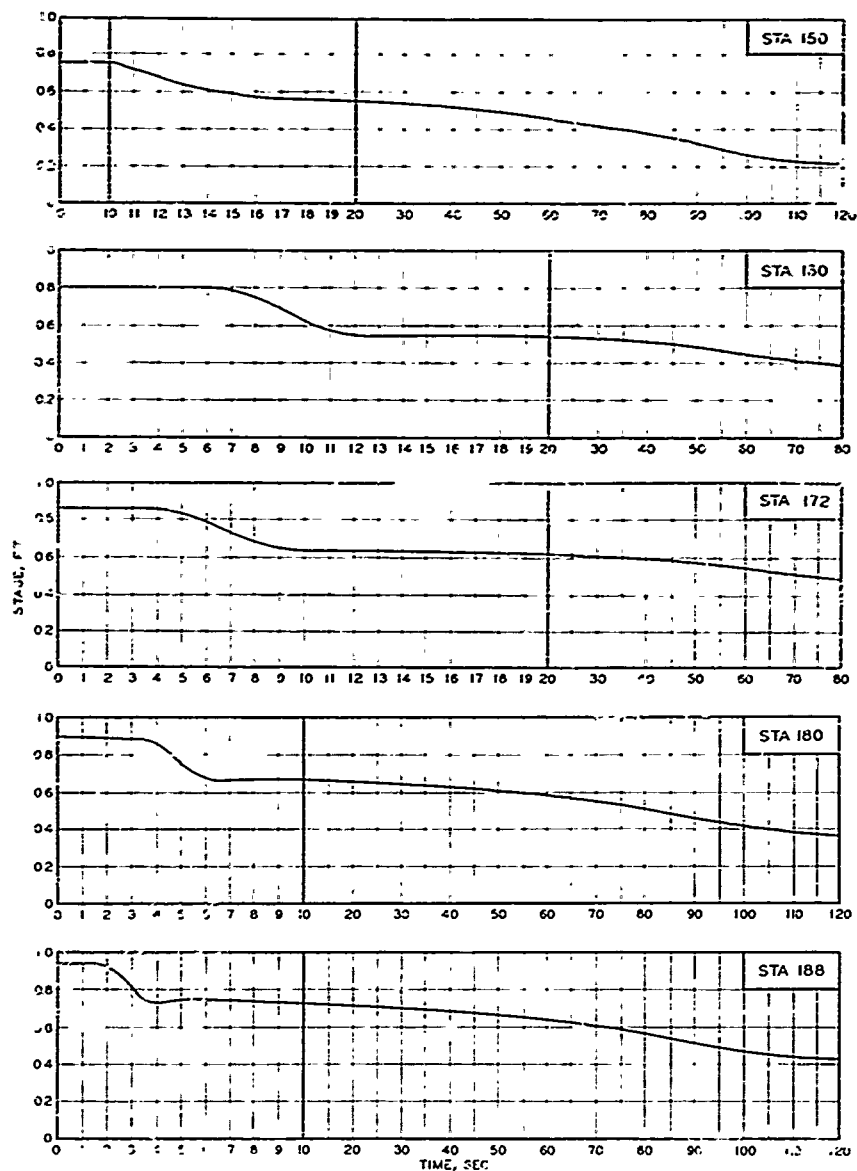
STAGE-TIME HYDROGRAPHS

STATIONS 345, 350, AND 355

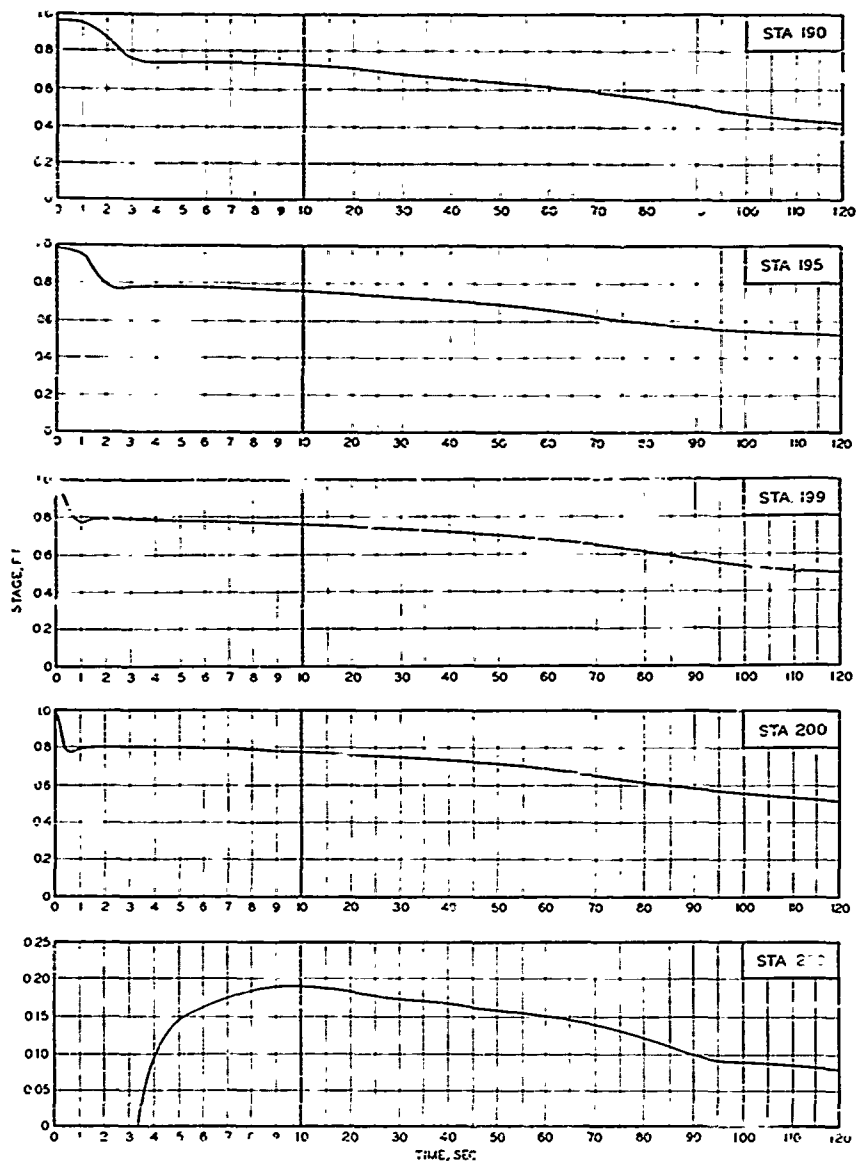
TEST CONDITION 5.1



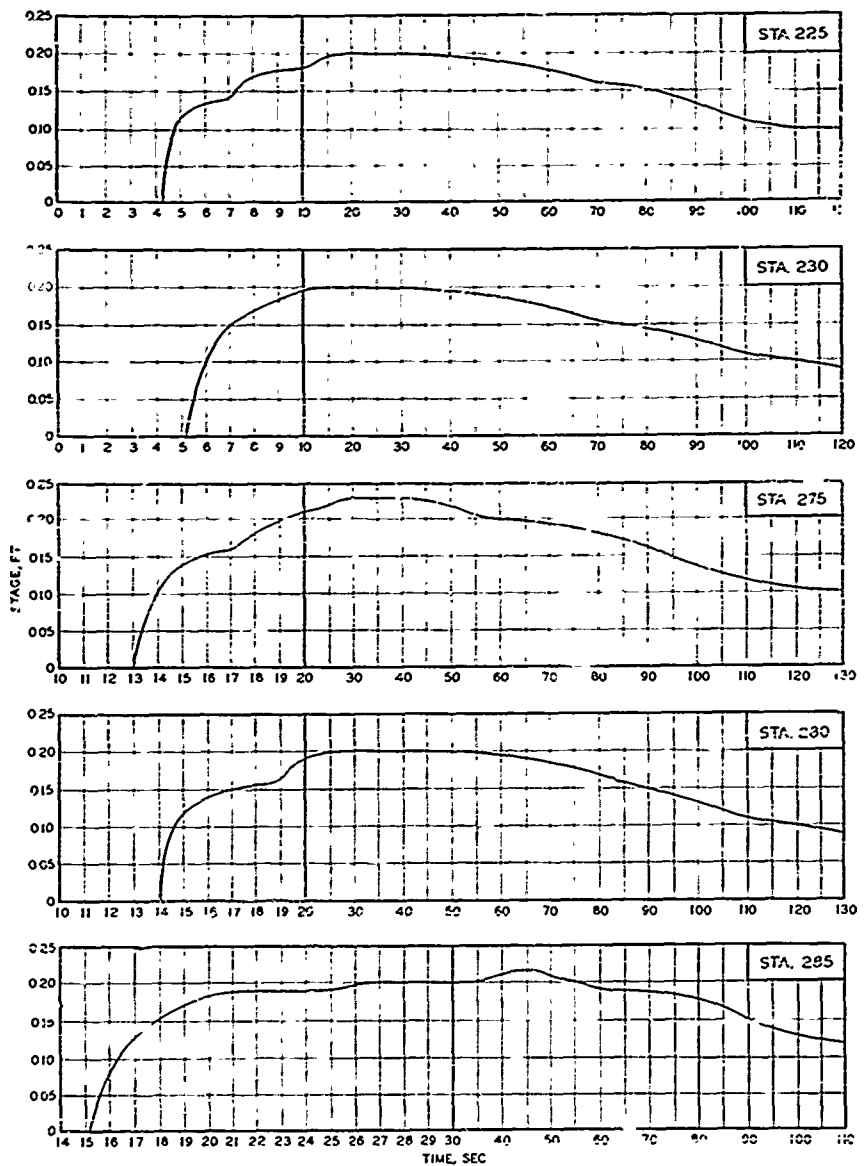
STAGE-TIME HYDROGRAPHS
STATIONS 40, 70, 100, 120, AND 140
TEST CONDITION 71



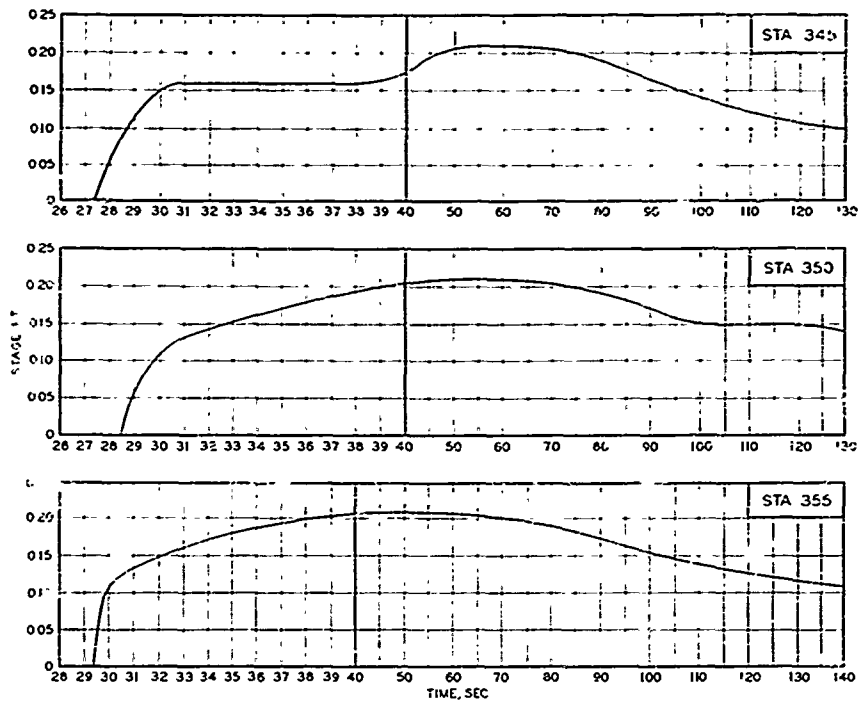
STAGE-TIME HYDROGRAPHS
STATIONS 150, 160, 172, 180, AND 188
TEST CONDITION 71



STAGE-TIME HYDROGRAPHS
STATIONS 190, 195, 199, 200, AND 210
TEST CONDITION 71



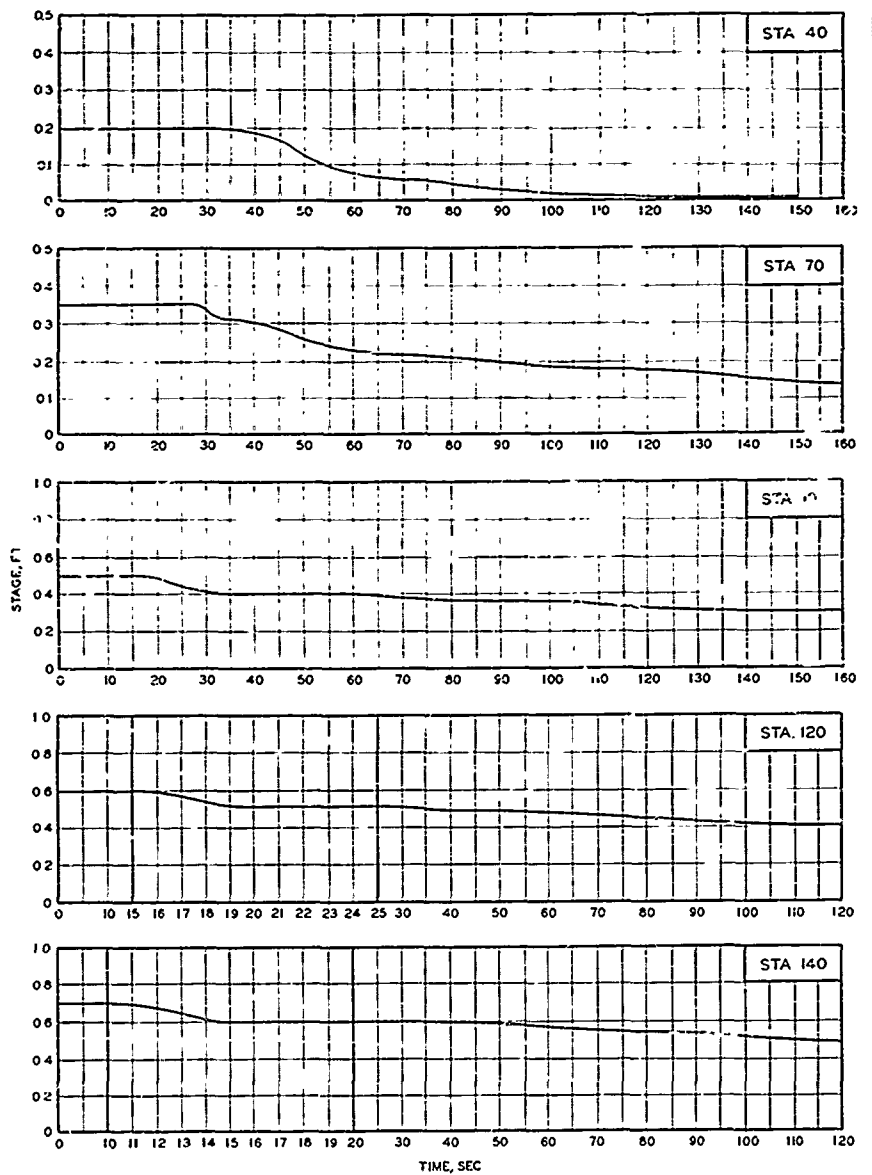
STAGE-TIME HYDROGRAPHS
STATIONS 225, 230, 275, 280 AND 285
TEST CONDITION 41



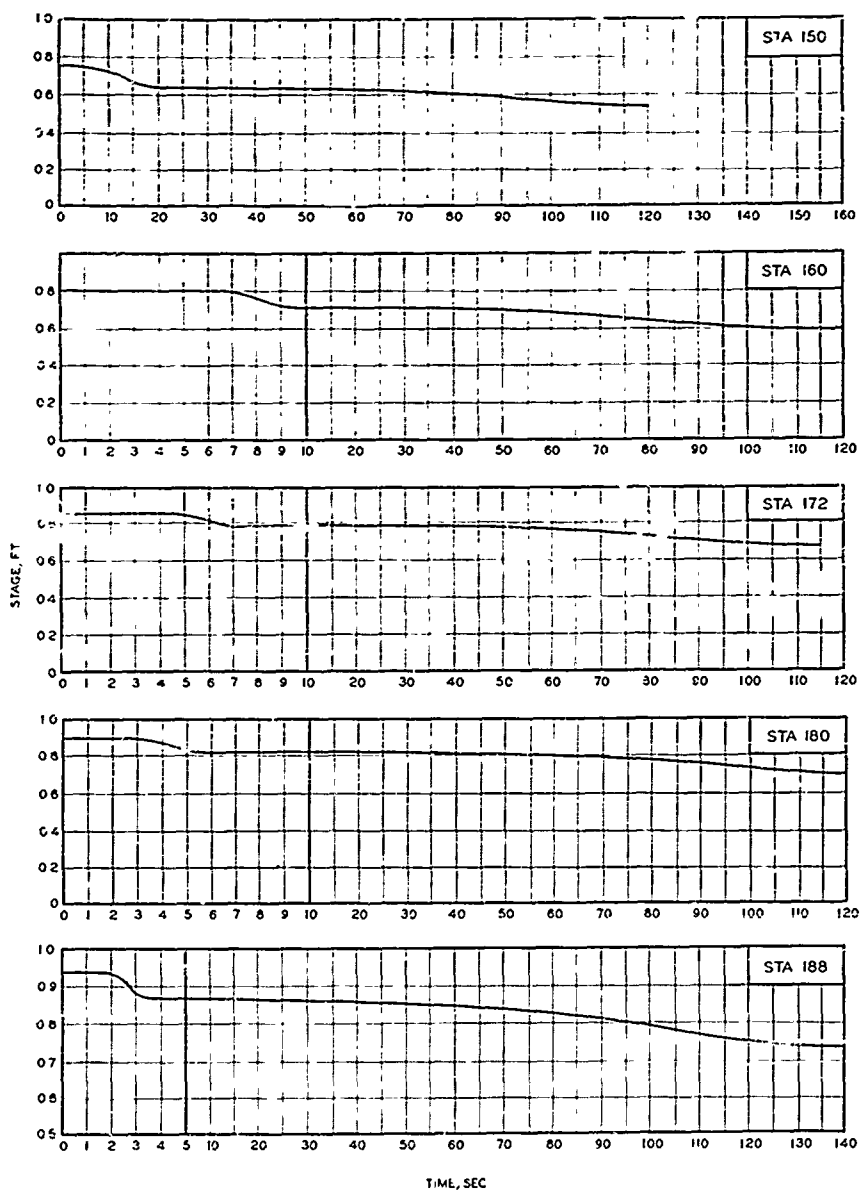
STAGE-TIME HYDROGRAPHS

STATIONS 345, 350 AND 355

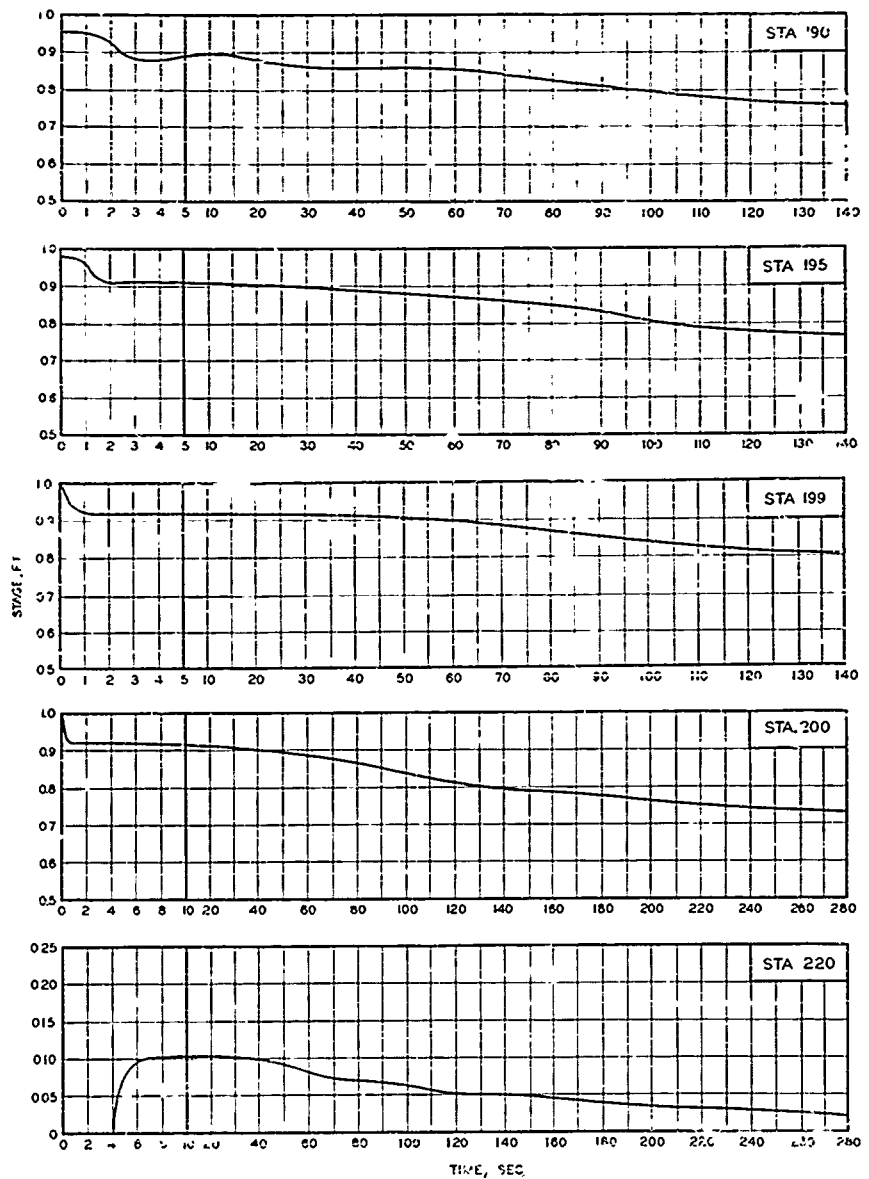
TEST CONDITION 7.1



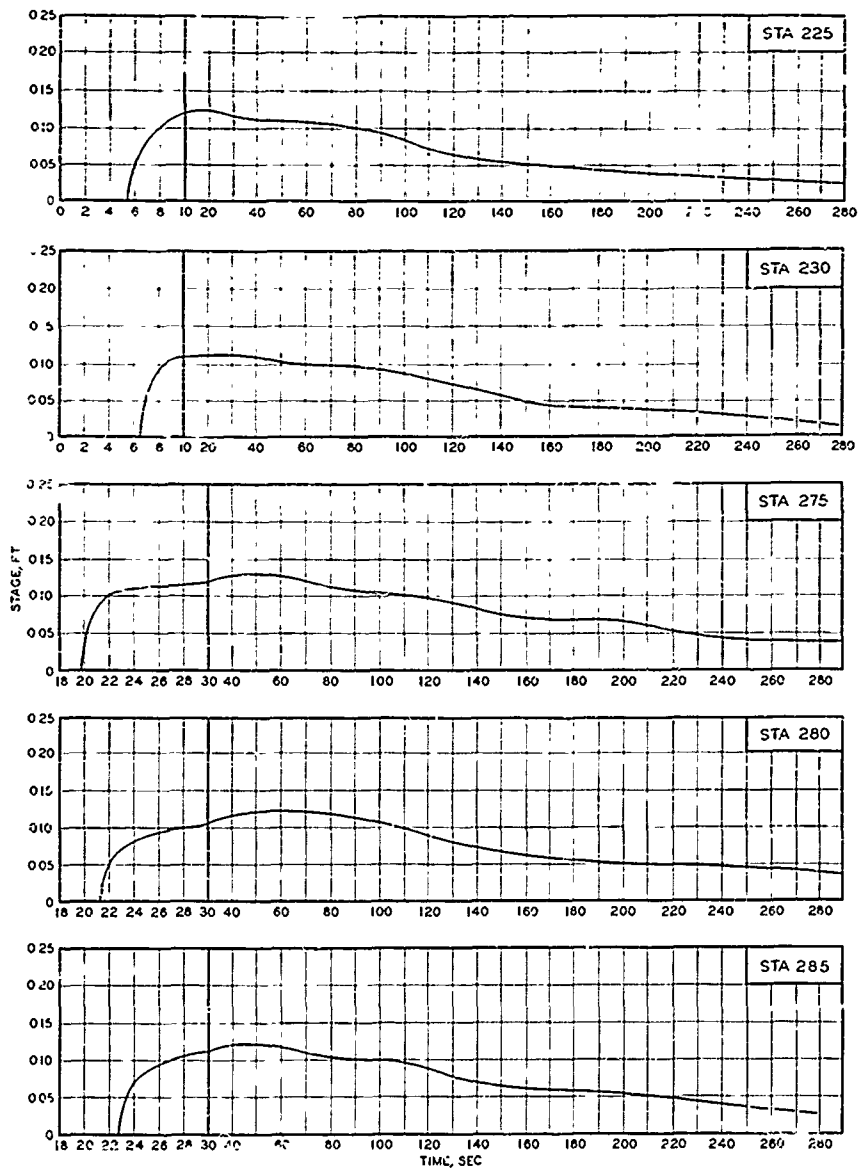
STAGE-TIME HYDROGRAPHS
STATIONS 40, 70, 100, 120, AND 140
TEST CONDUCTION



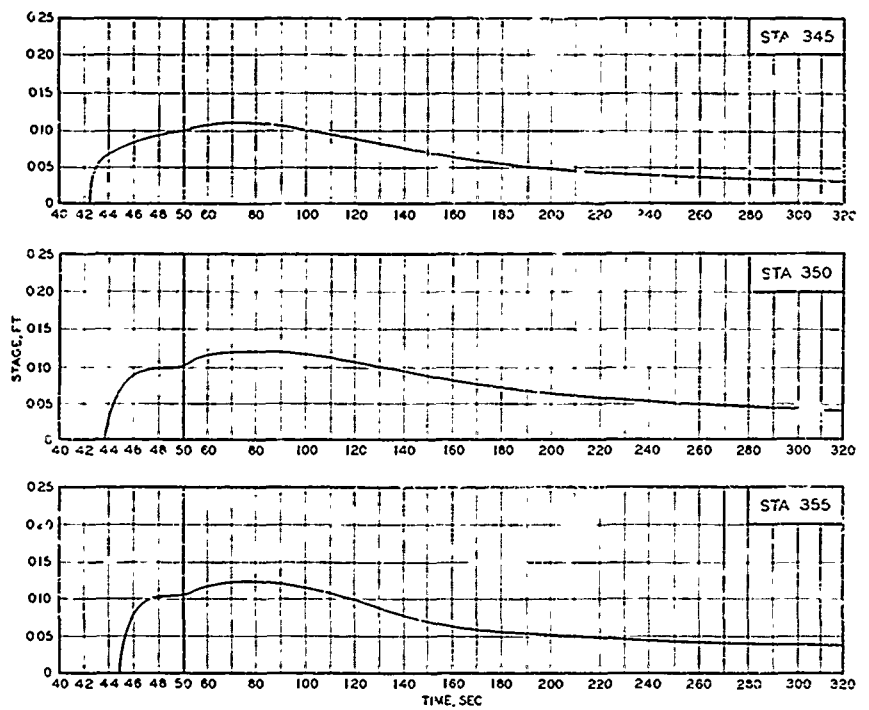
STAGE-TIME HYDROGRAPHS
STATIONS 150, 160, 172, 180, AND 188
TEST CONDITION: 81



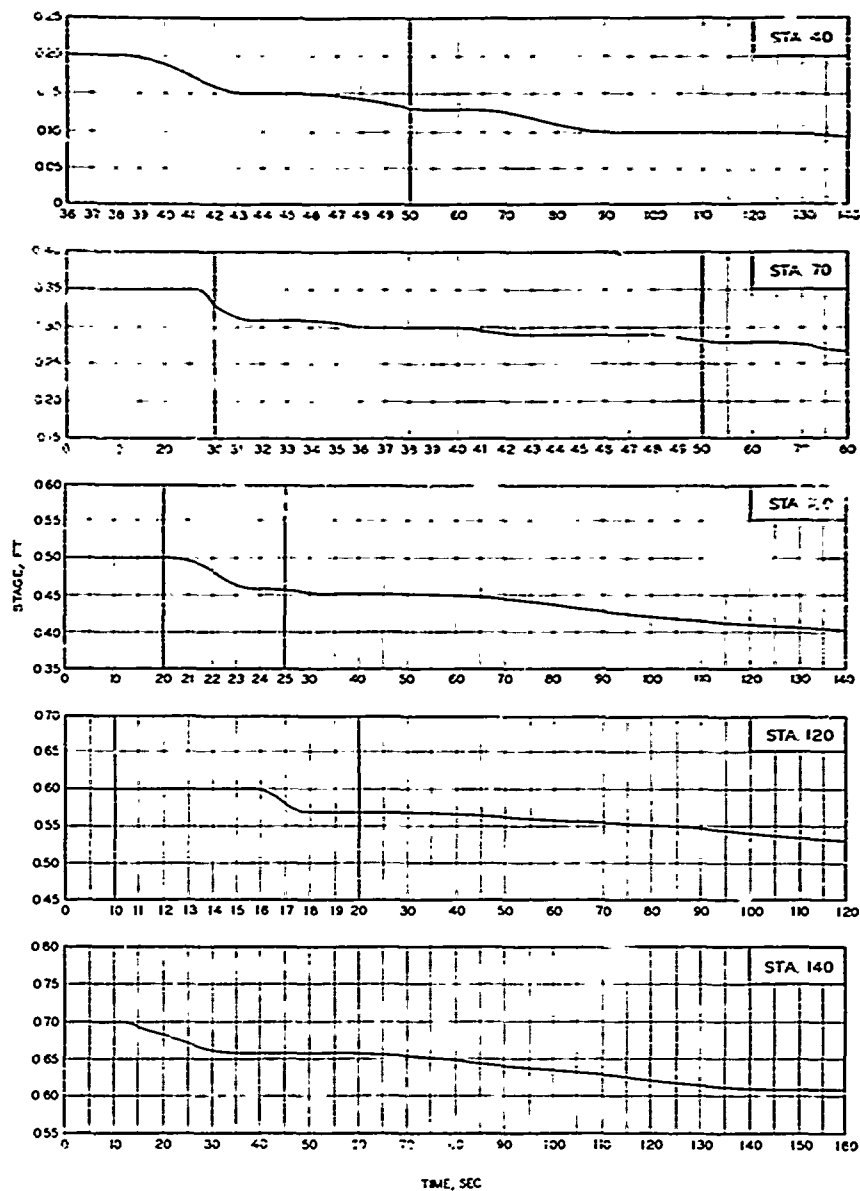
STAGE-TIME HYDROGRAPHS
STATIONS 190, 195, 199, 200 AND 220
TEST CONDITION 81



STAGE-TIME HYDROGRAPHS
STATIONS 225, 230, 275, 280, AND 285
TEST CONDITION 81

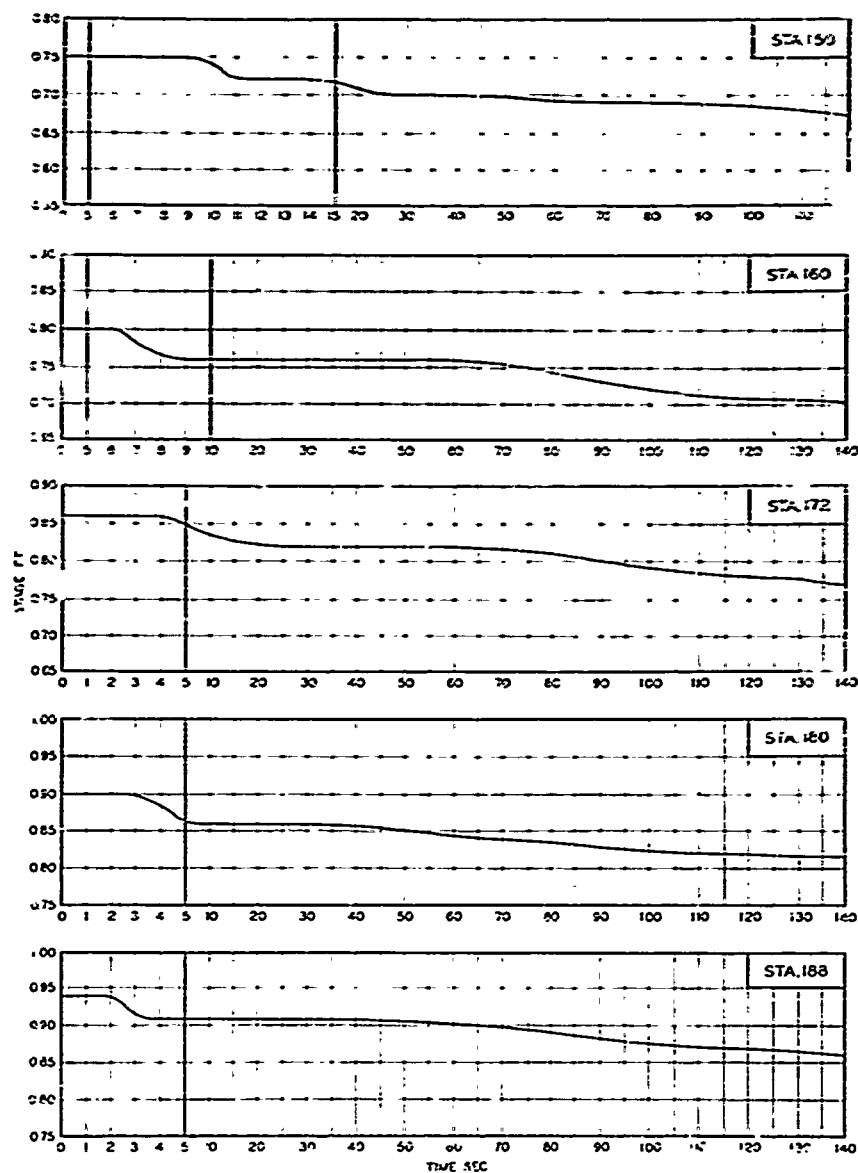


STAGE-TIME HYDROGRAPHS
STATIONS 345, 350, AND 355
TEST CONDITION 81

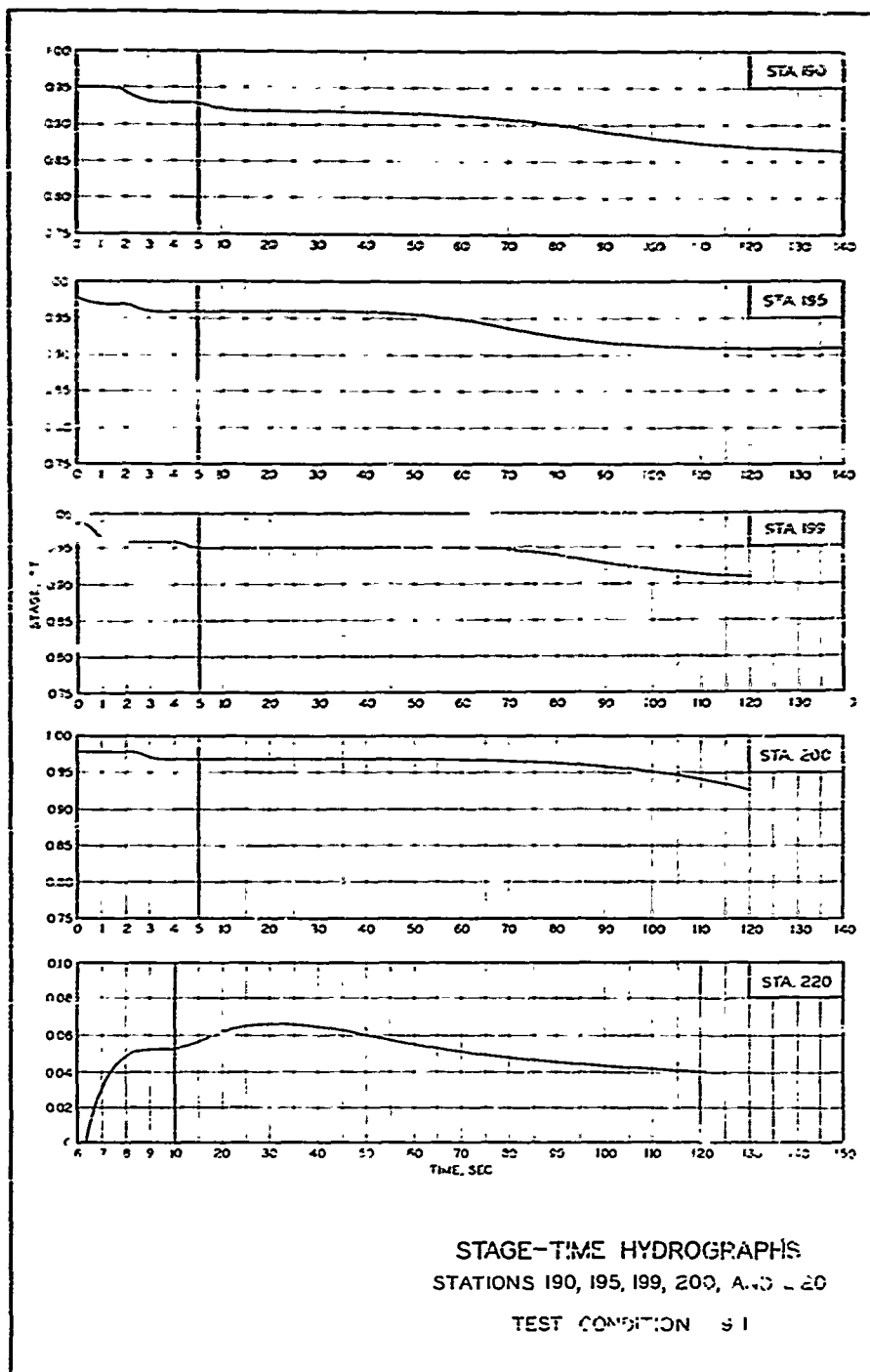


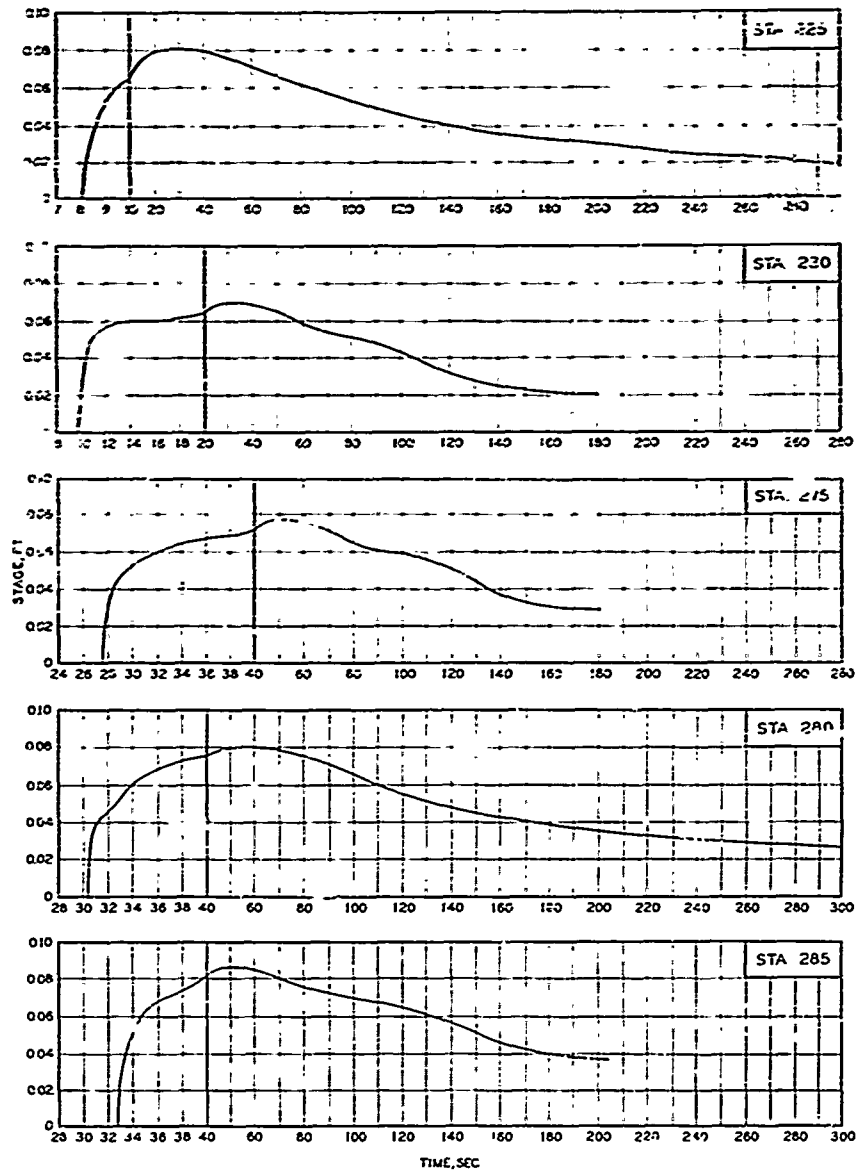
STAGE-TIME HYDROGRAPHS
STATIONS 40 70, 100 120, AND 140

TEST CONDITION 9.1

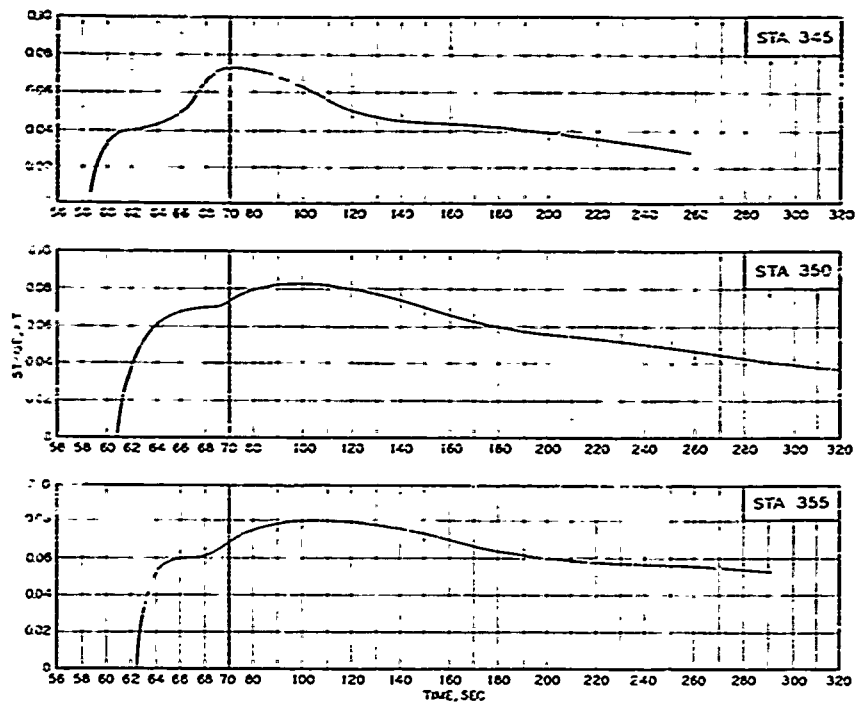


STAGE-TIME HYDROGRAPHS
STATIONS 150, 160, 172, 180, AND 188
TEST CONDITION 9.1



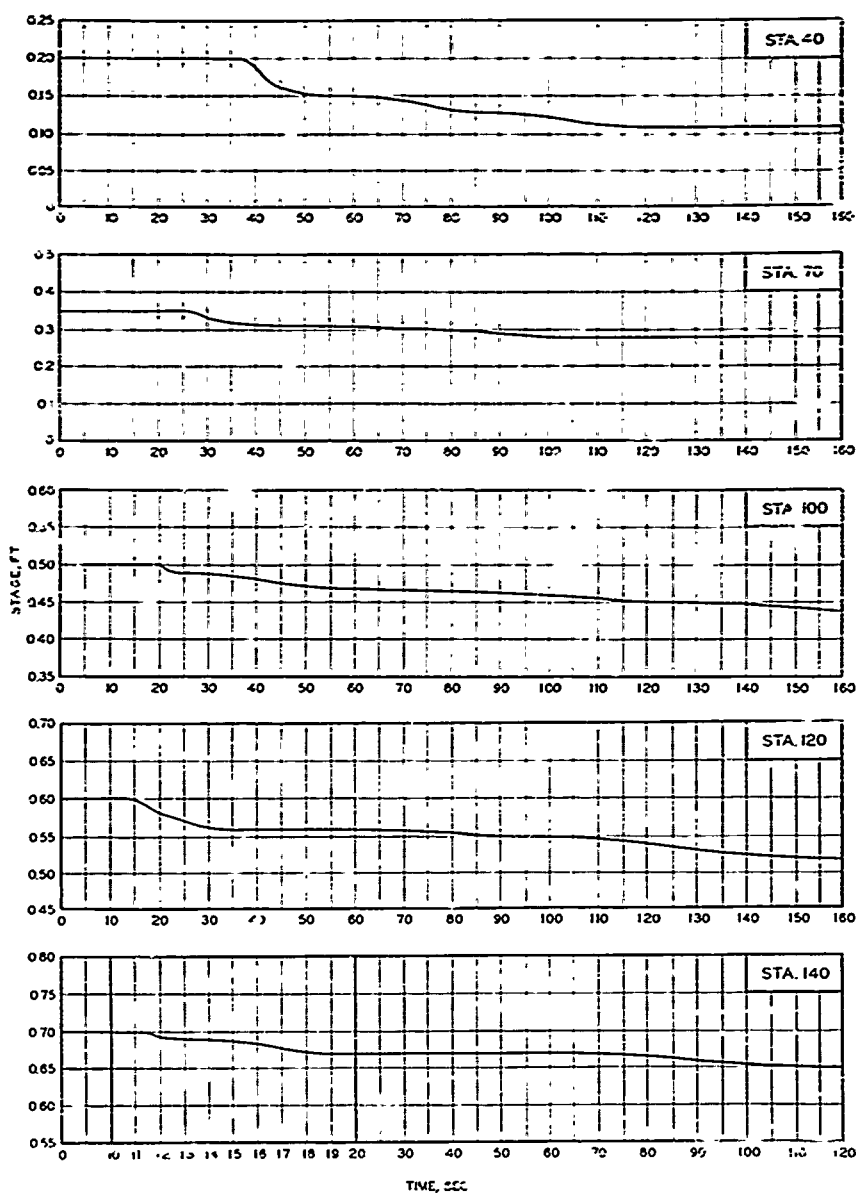


STAGE-TIME HYDROGRAPHS
STATIONS 225, 230, 275, 280 AND 285
TEST CONDITION 5.1

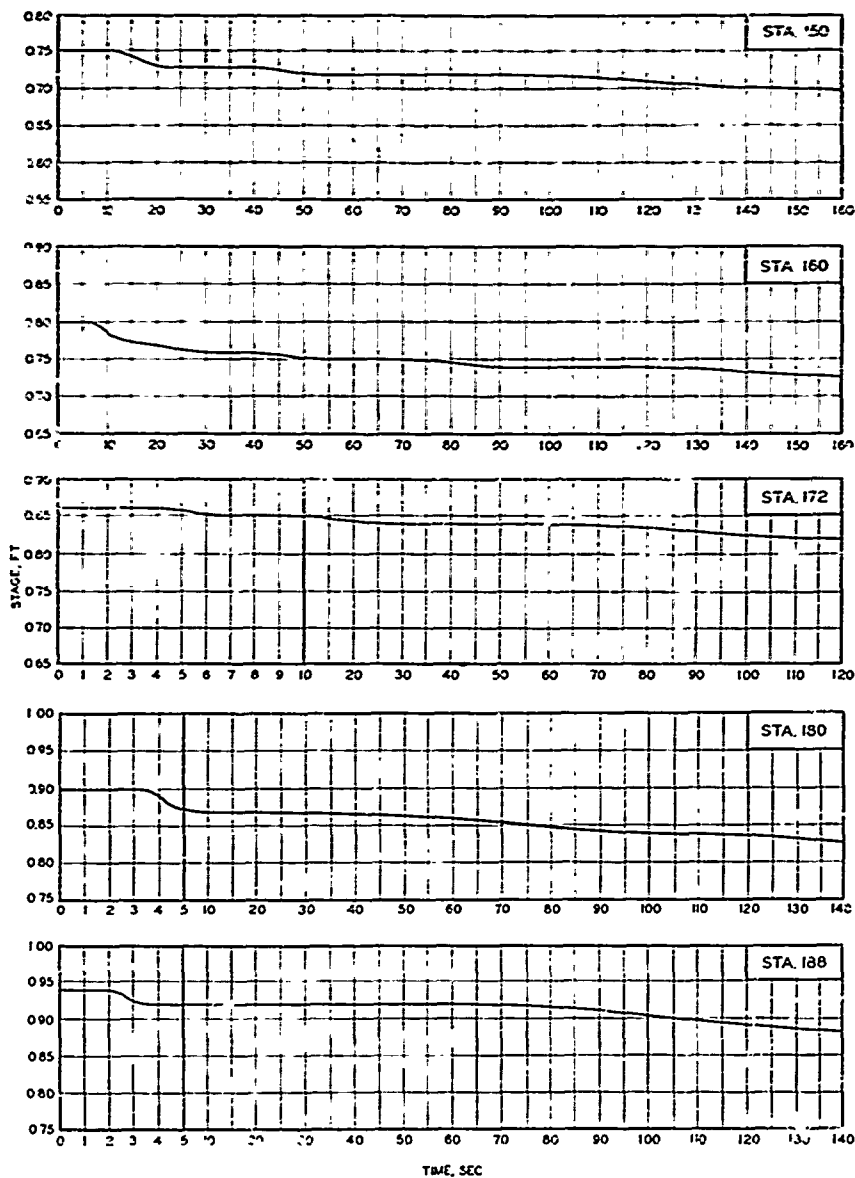


STAGE-TIME HYDROGRAPHS
STATIONS 345, 350, AND 355

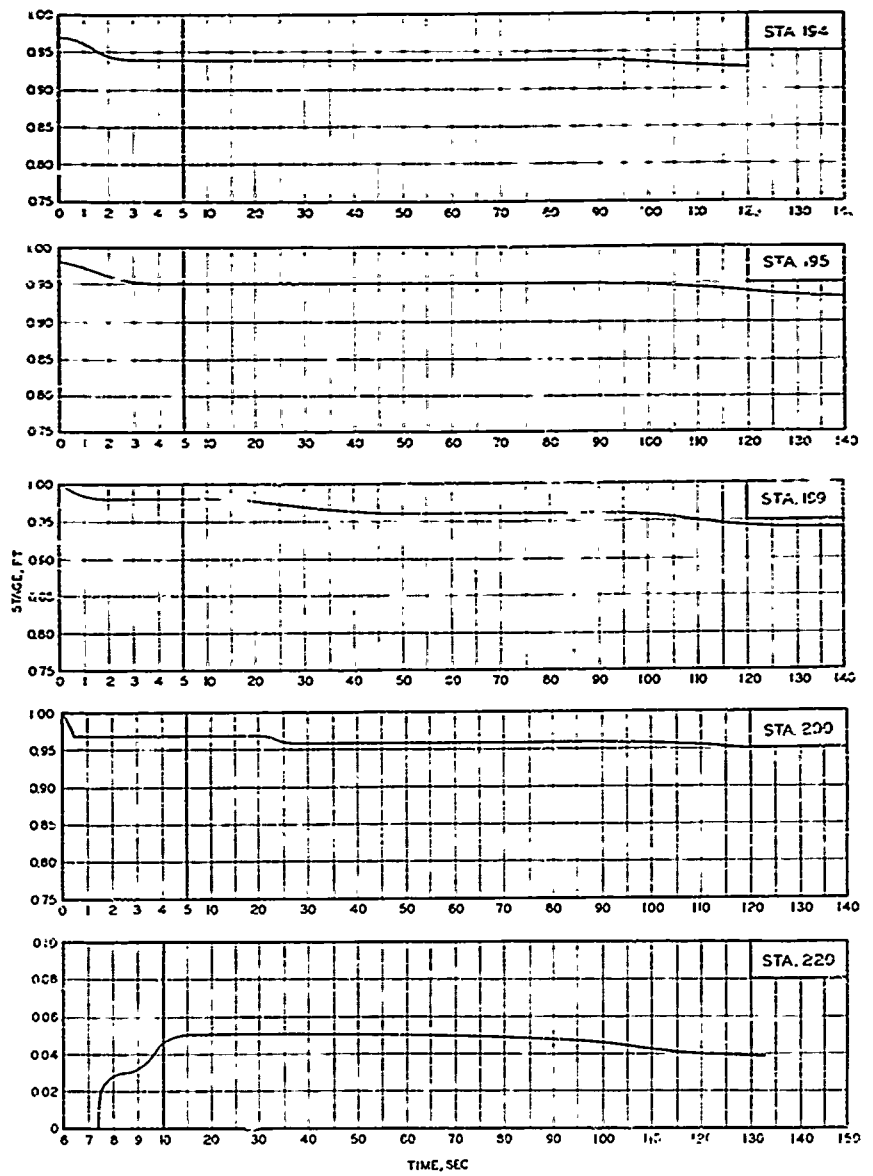
TEST CONDITION 1



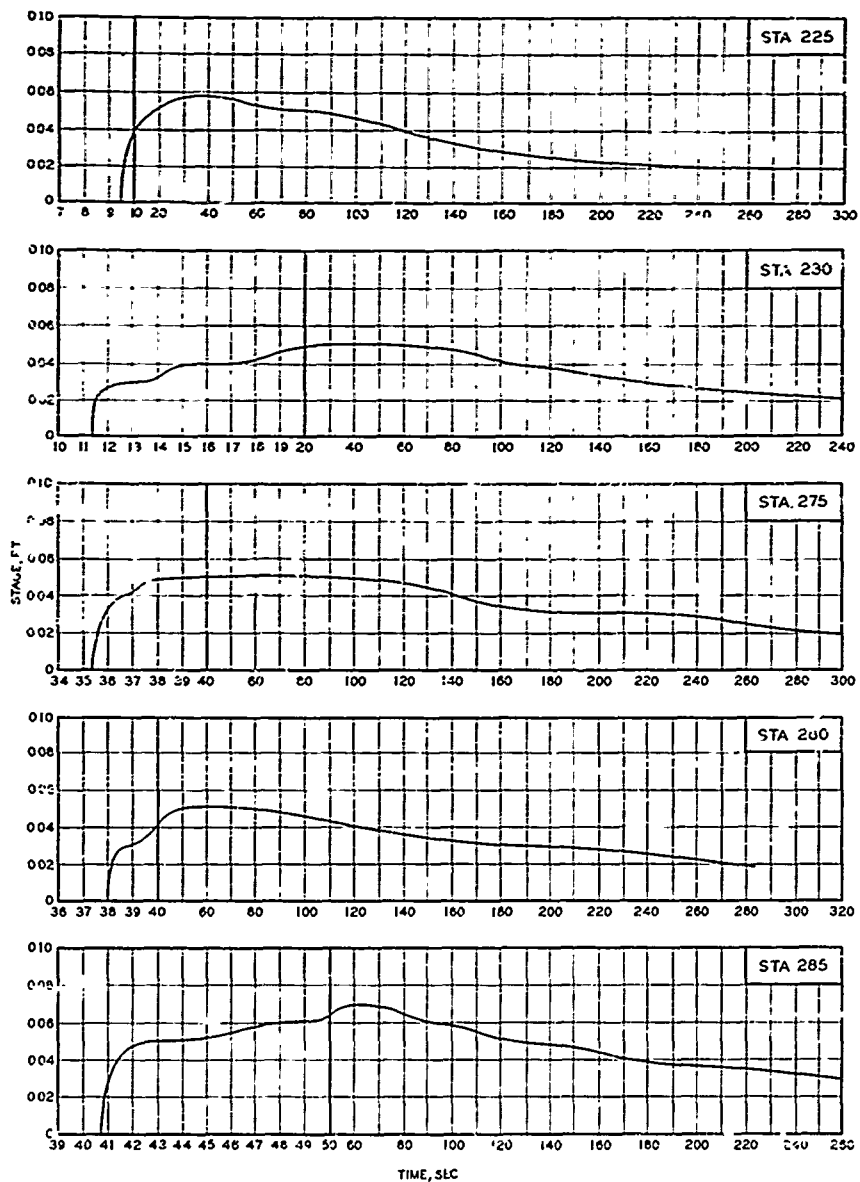
STAGE-TIME HYDROGRAPHS
STATIONS 40, 70, 100, 120, AND 140
TEST CONDITION 10.1



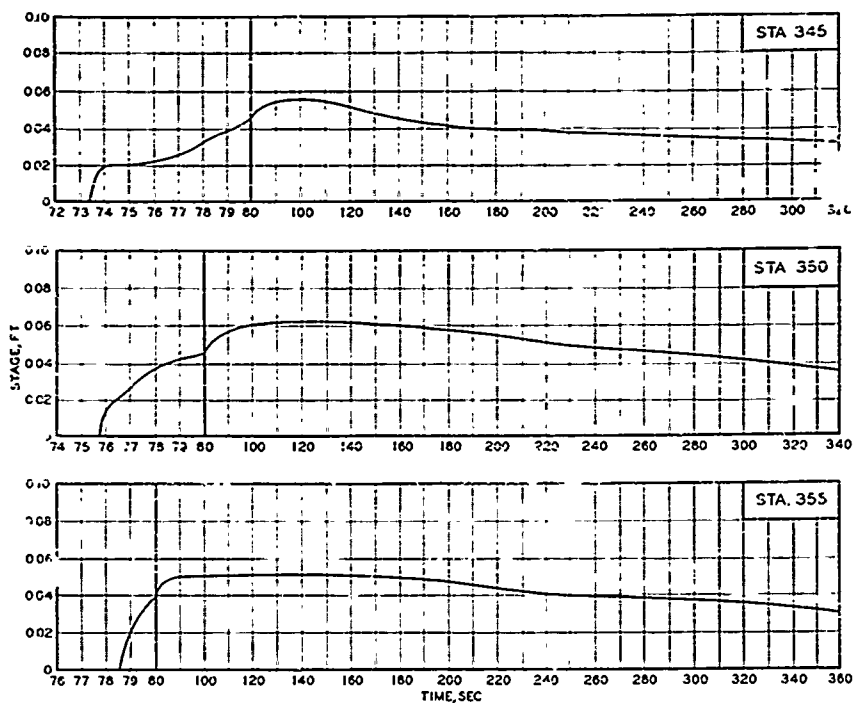
STAGE-TIME HYDROGRAPHIC
STATIONS 150, 160, 172, 180, AND 188
TEST CONDITION 10.1



STAGE-TIME HYDROGRAPHS
STATIONS 194, 195, 199, 200 AND 220
TEST CONVICTION 10.1



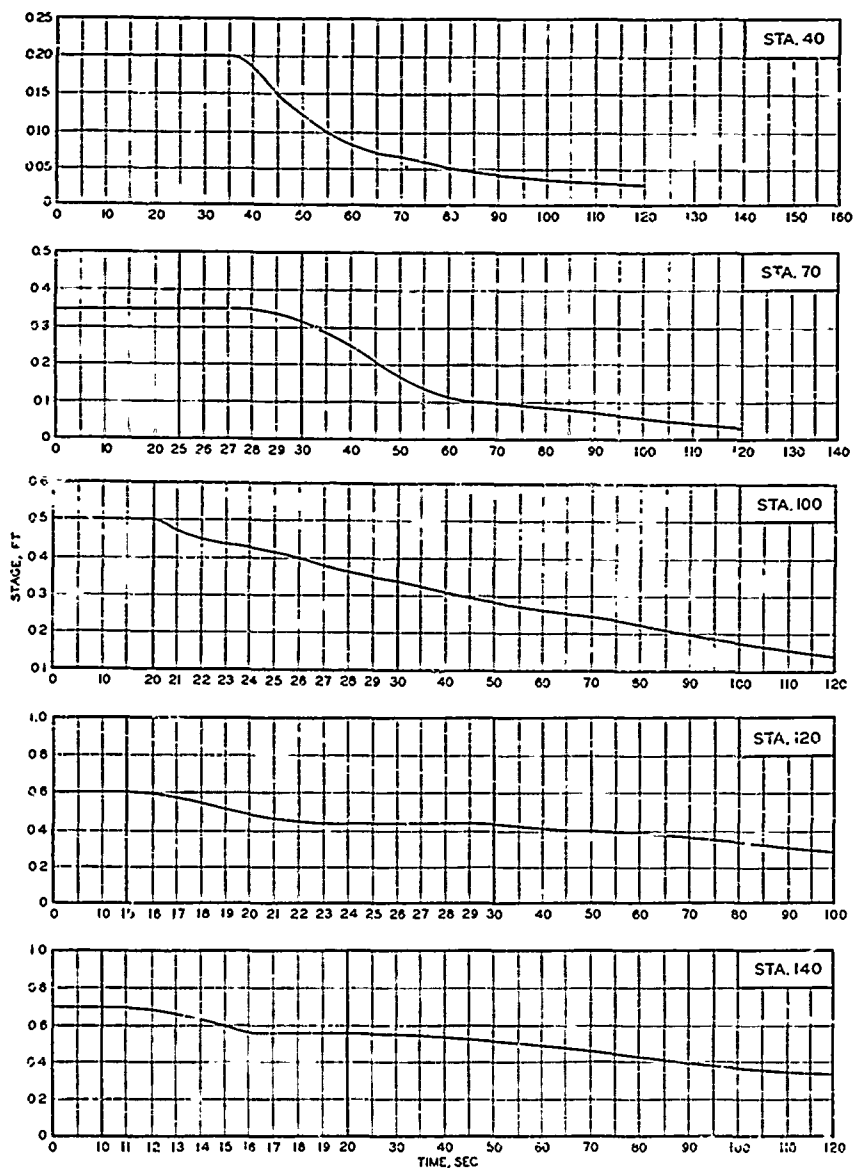
STAGE-TIME HYDROGRAPHS
STATIONS 225, 230, 275, 280, AND 285
TEST CONDITION 101



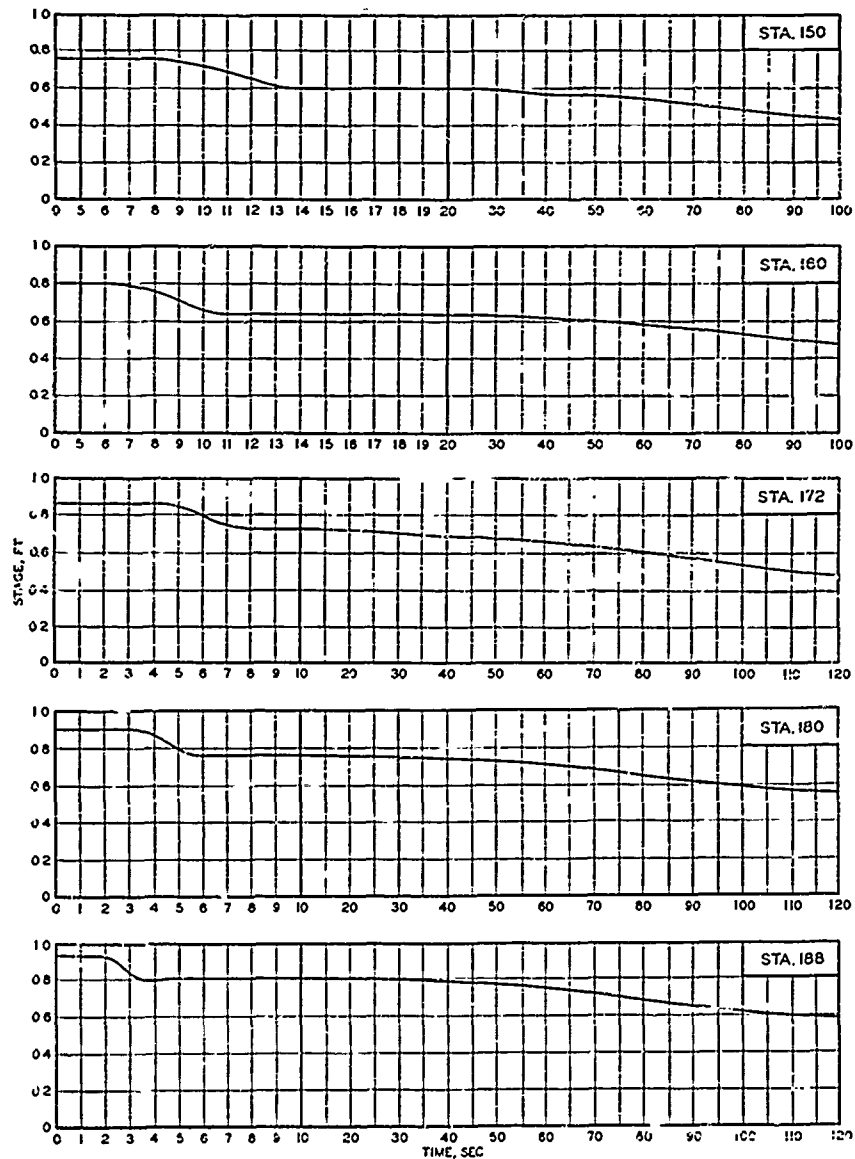
STAGE-TIME HYDROGRAPHS

STATIONS 345, 350, AND 355

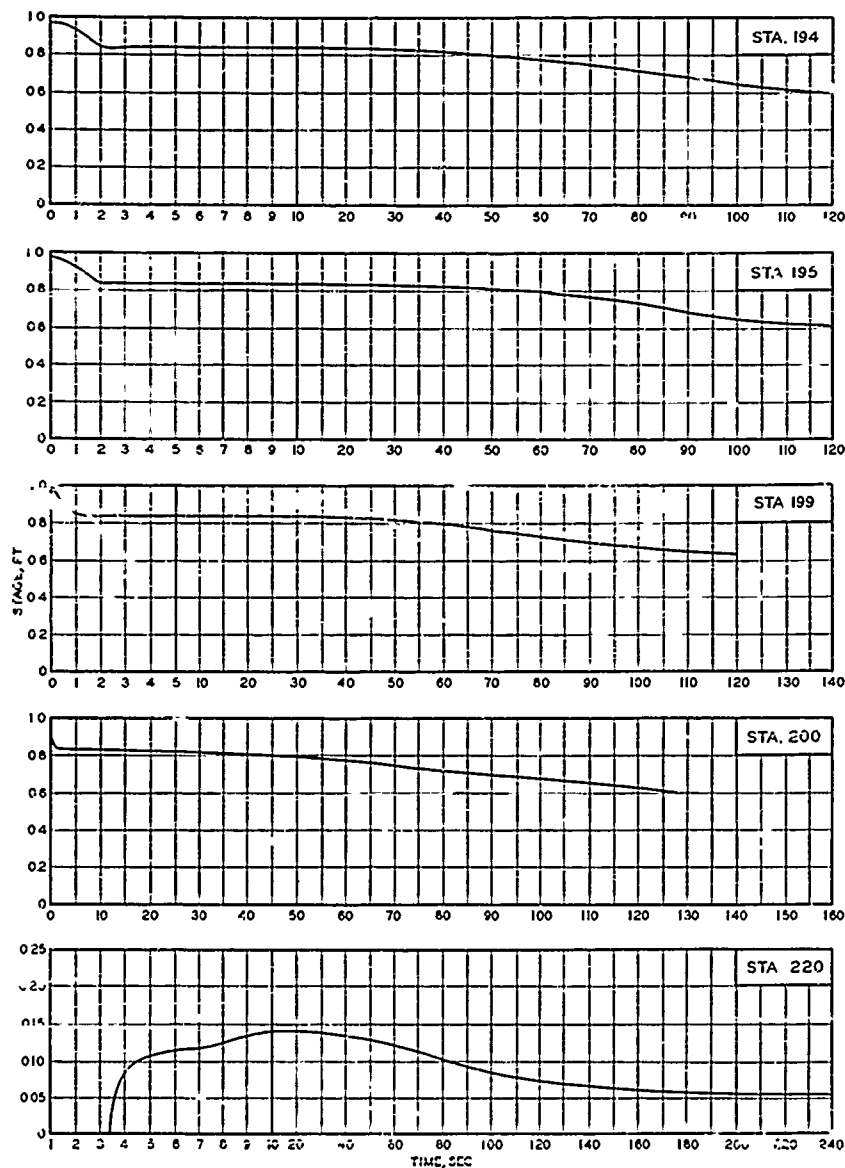
TEST CONDITION 10.1



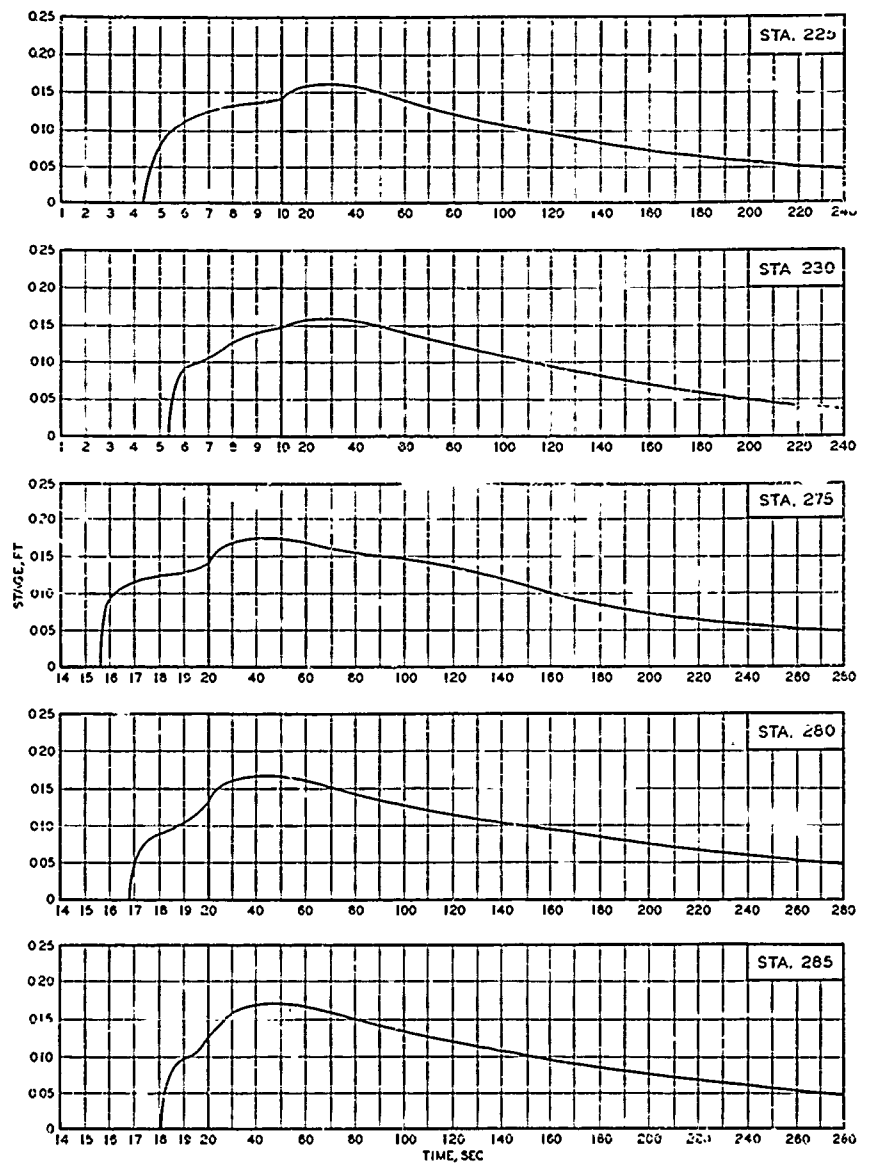
STAGE-TIME HYDROGRAPHS
STATIONS 40, 70, 100, 120, AND 140
TEST CONDITION 111



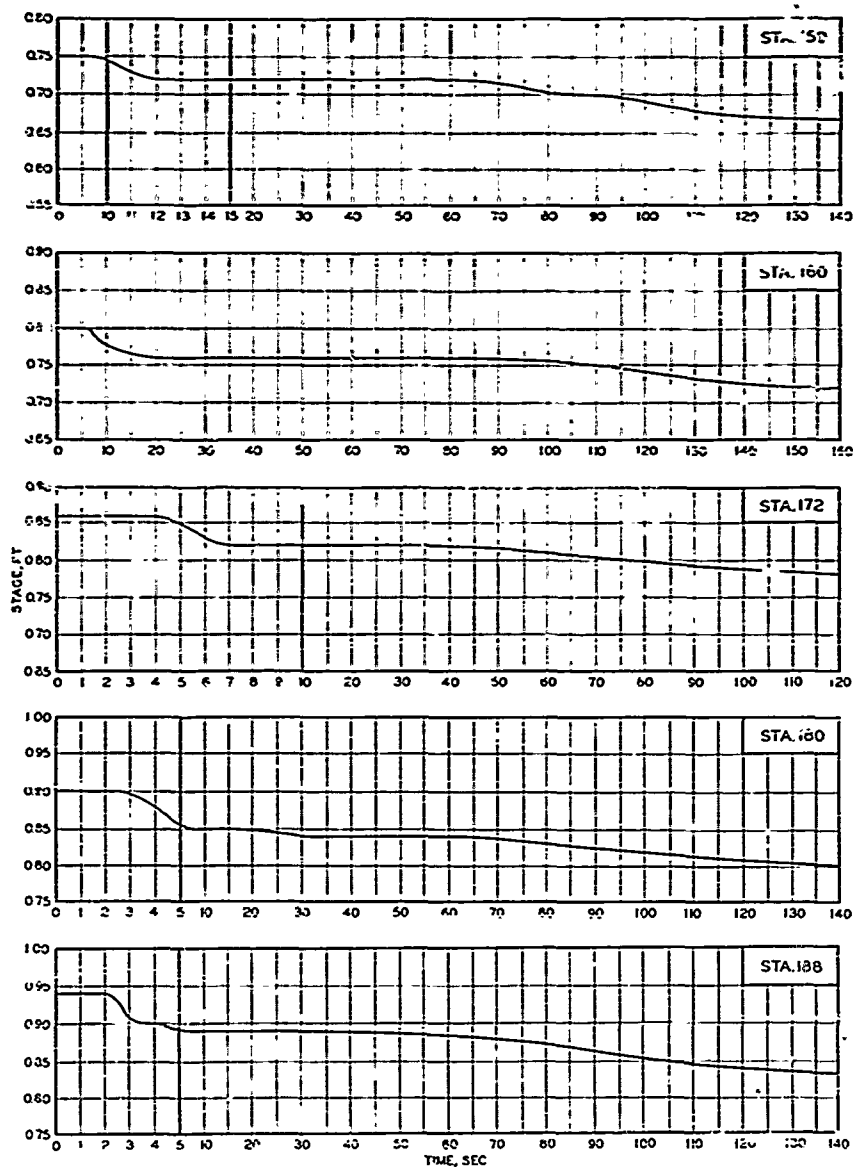
STAGE-TIME HYDROGRAPHS
STATIONS 150, 160, 172, 180, AND 188
TEST CONDITION 11.1



STAGE-TIME HYDROGRAPHS
STATIONS 194, 195, 199, 200, AND 220
TEST CONDITION III

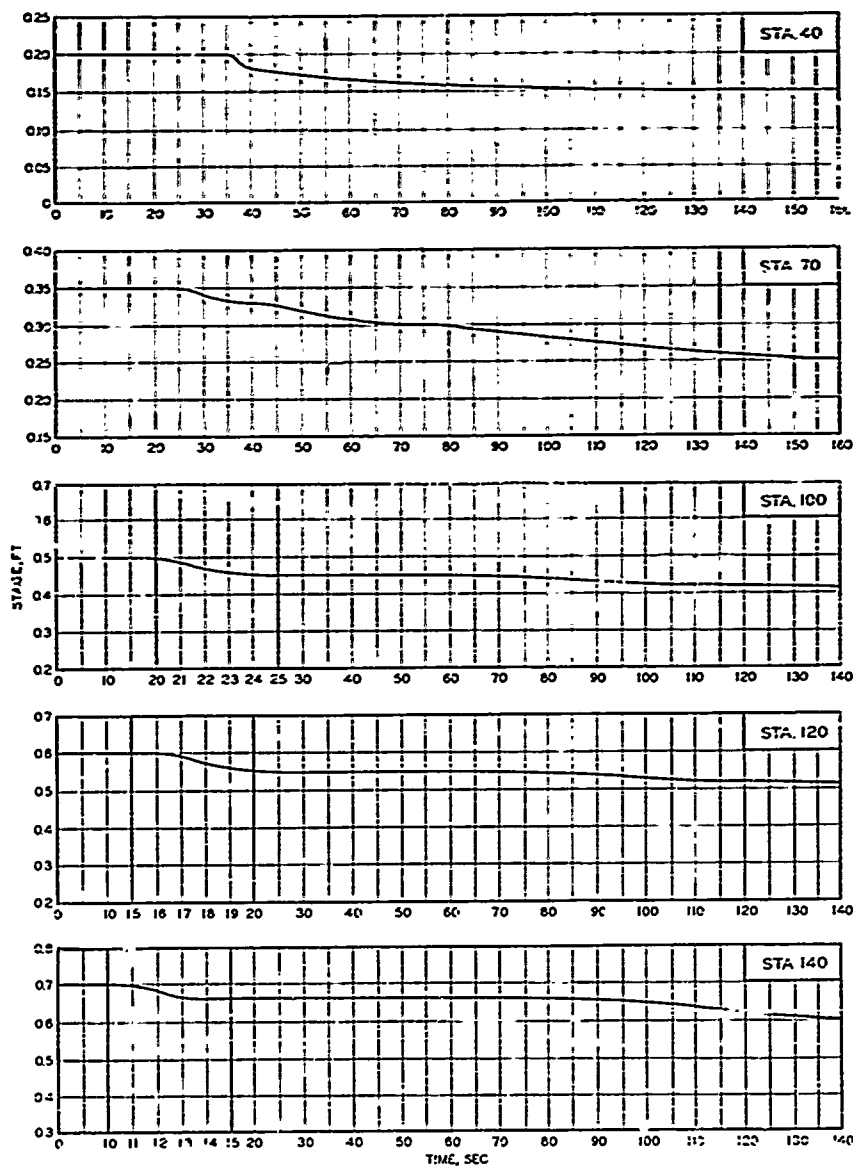


STAGE-TIME HYDROGRAPHS
STATIONS 225, 230, 275, 280, AND 285
TEST CONJUNCTION III

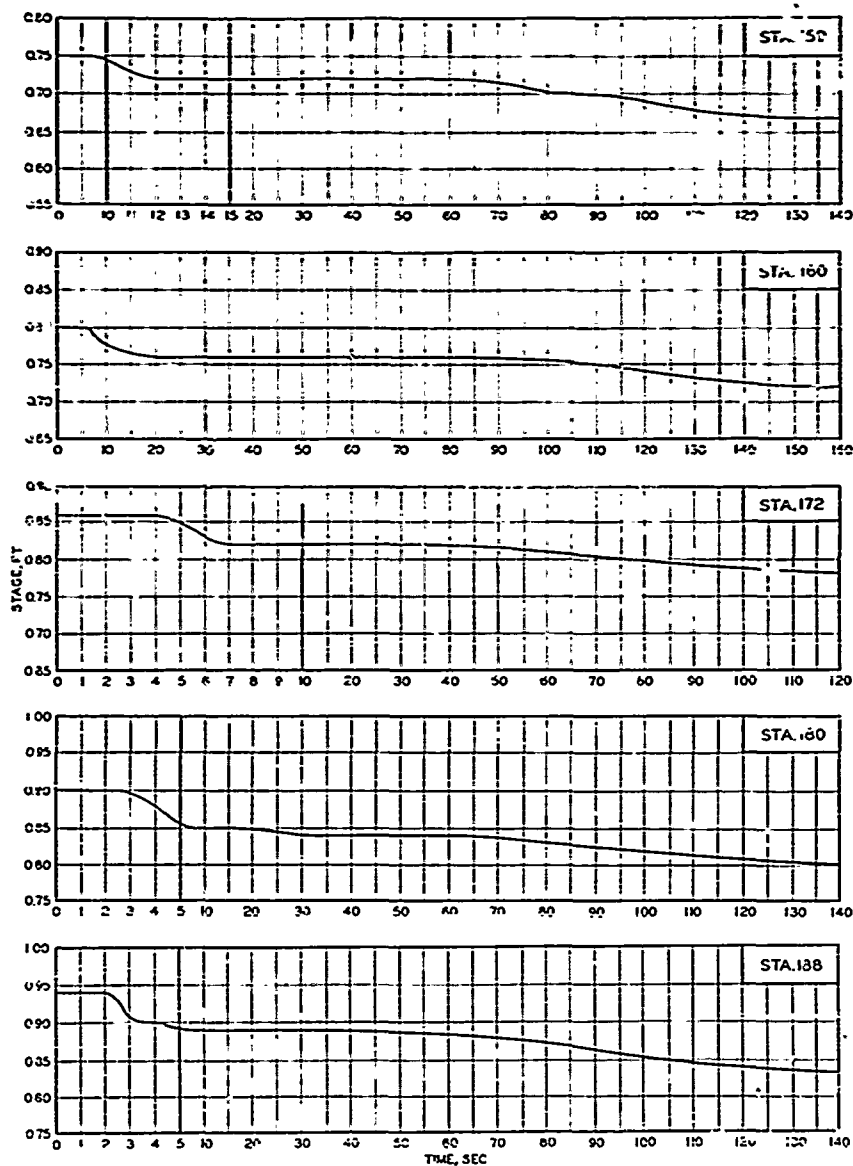


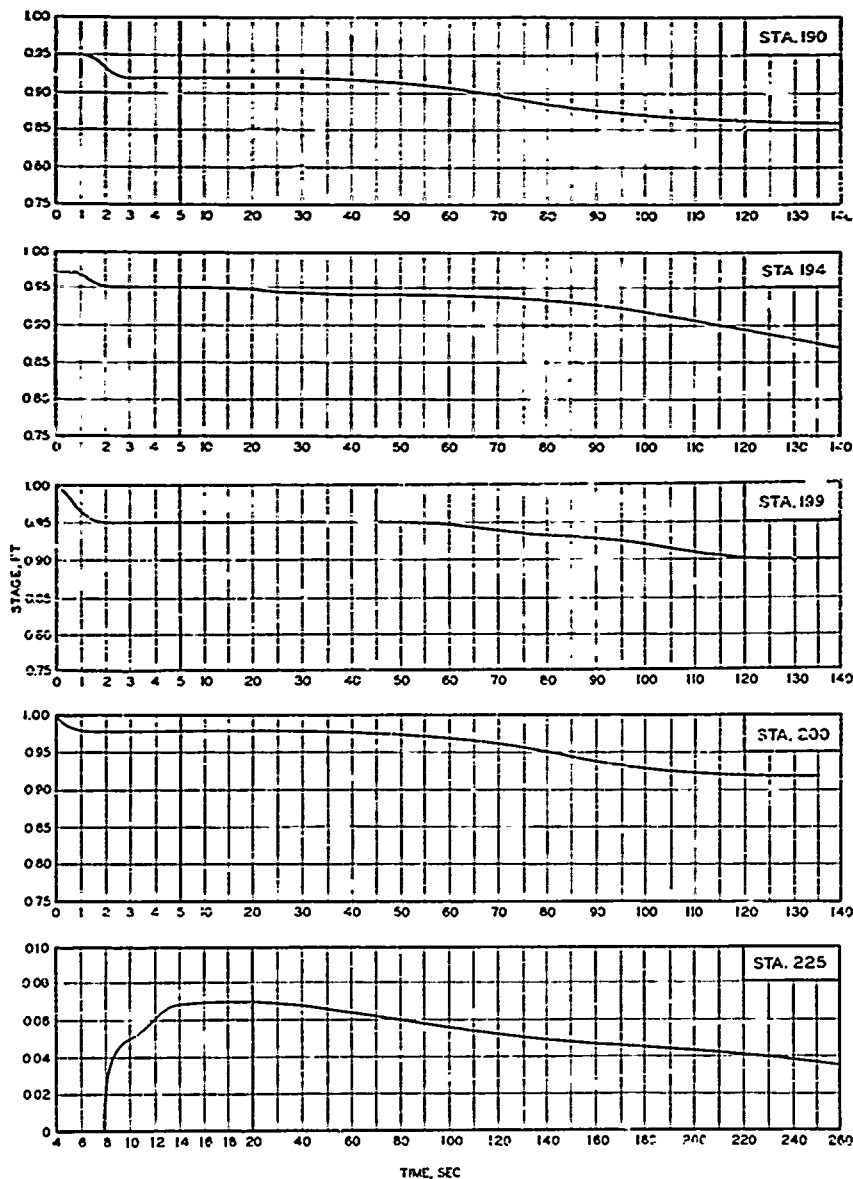
STAGE-TIME HYDROGRAPHS
STATIONS 150, 160, 172, 180, AND 188

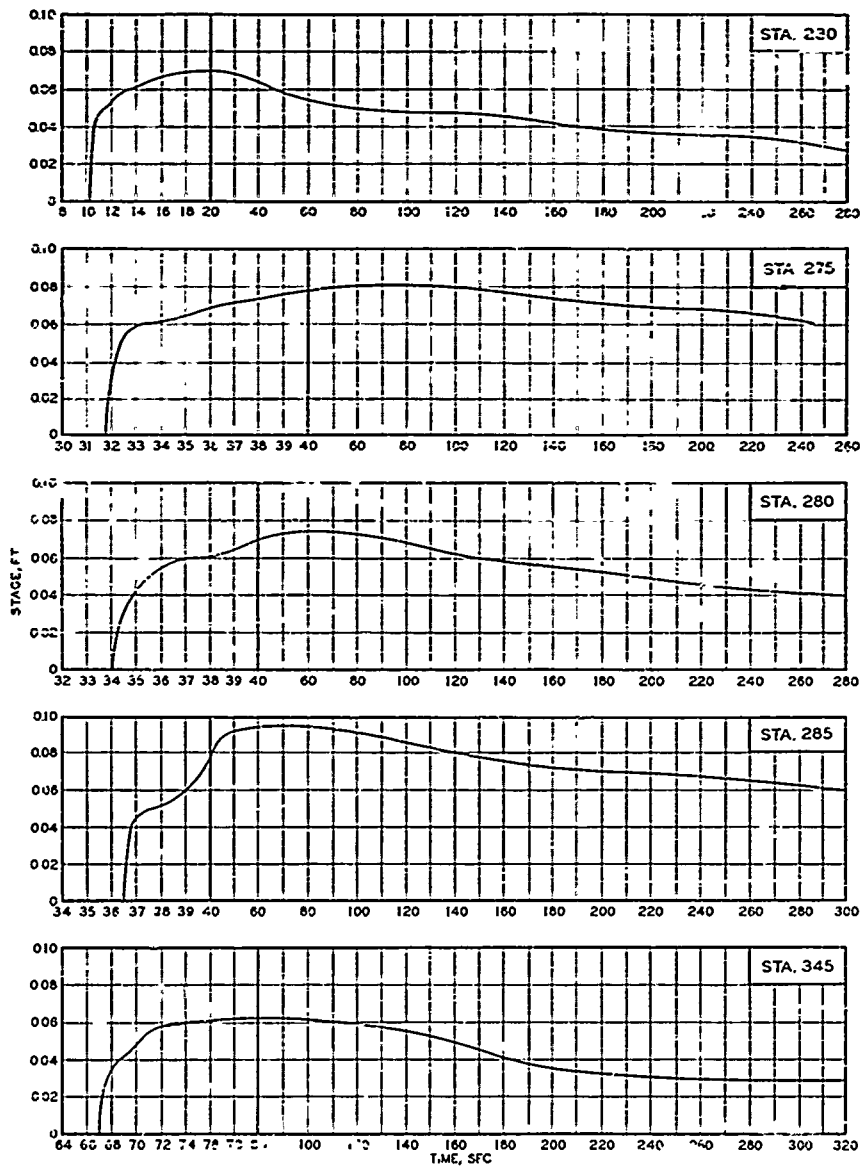
TEST CONDITION 12.1



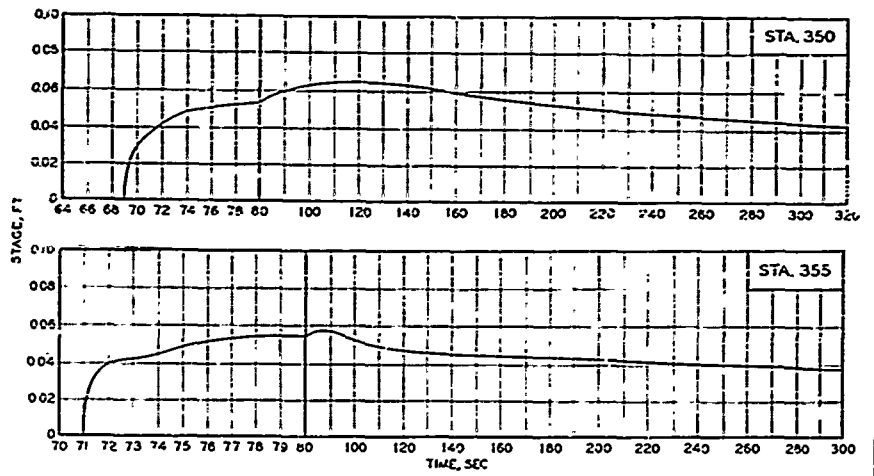
STAGE-TIME HYDROGRAPHS
STATIONS 40, 70, 100, 120, AND 140
TEST CONDITION 12.1







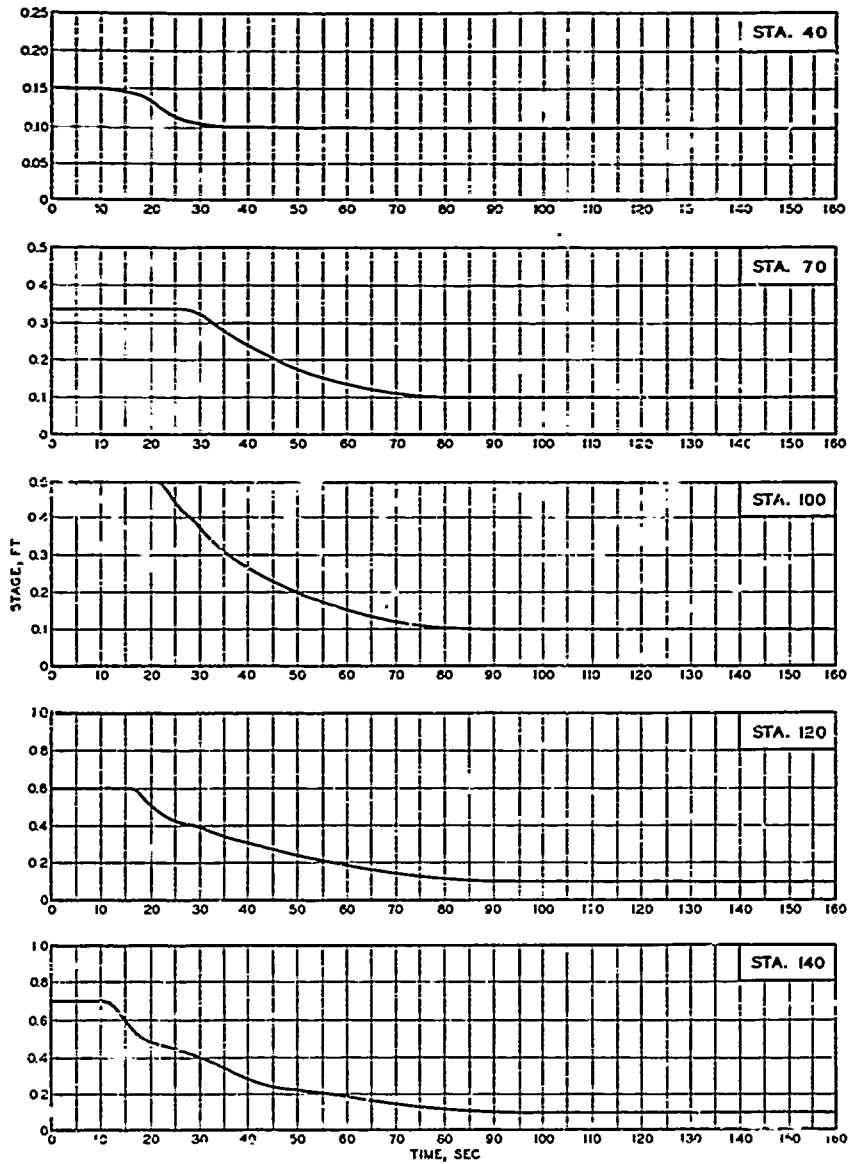
STAGE-TIME HYDROGRAPHS
STATIONS 230, 275, 280, 285, AND 345
TEST CONDITION 12.1



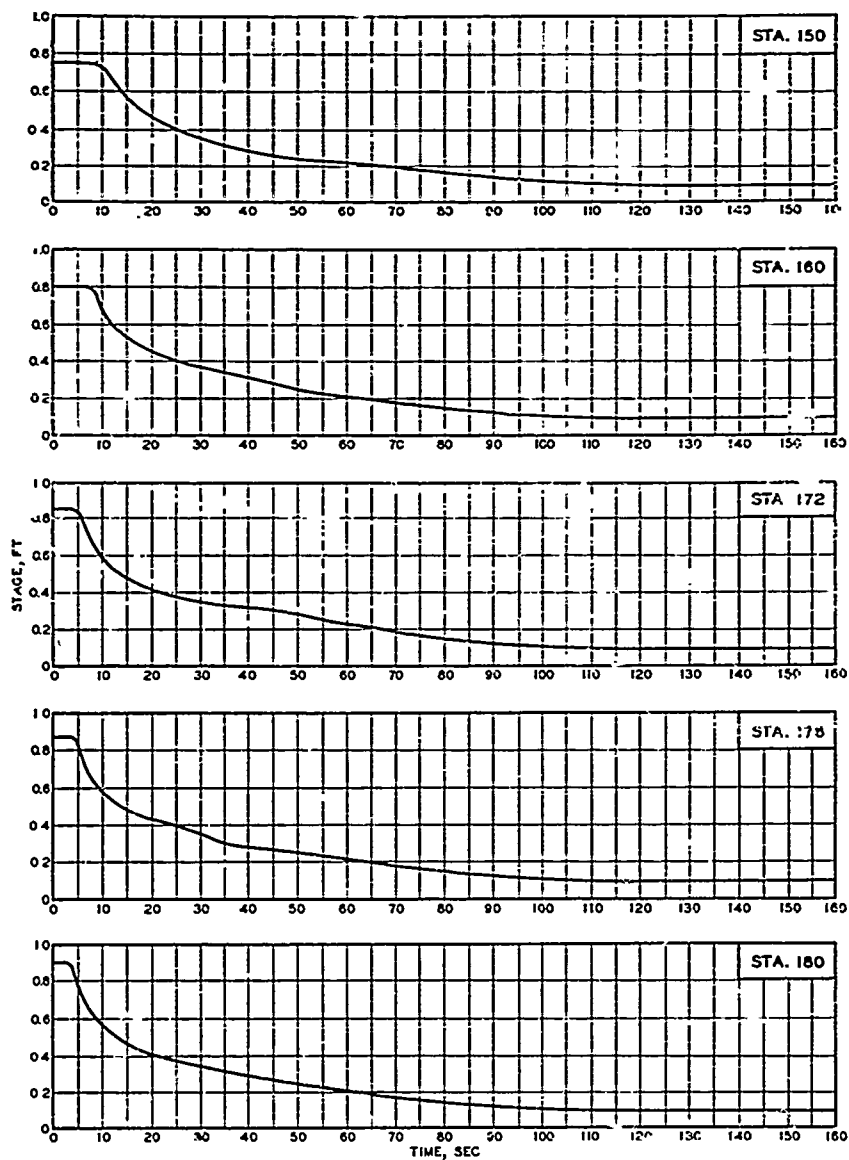
STAGE-TIME HYDROGRAPHS

STATIONS 350 AND 355

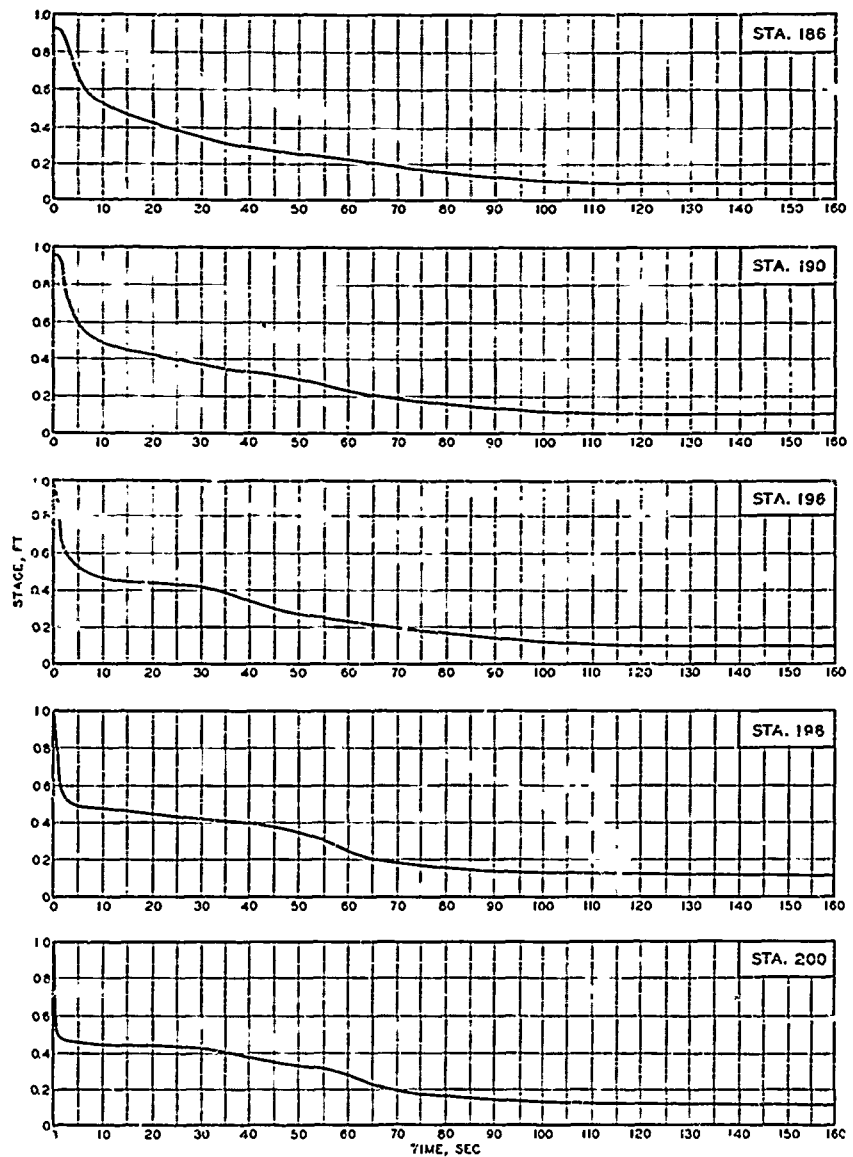
TEST CONDITION 12.1



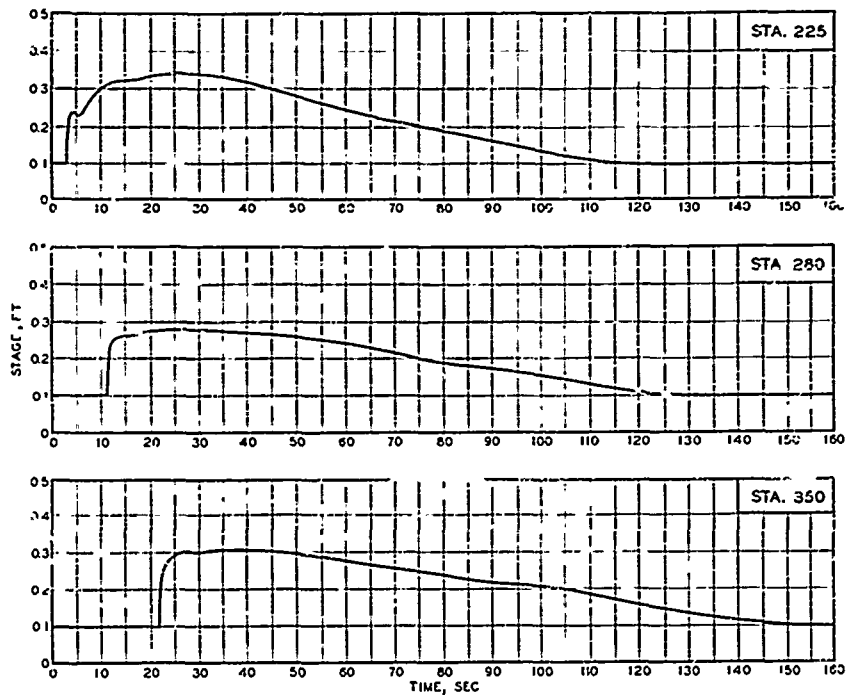
STAGE-TIME HYDROGRAPHS
STATIONS 40, 70, 100, 120 AND 140
TEST CONDITION 1.1 (10)



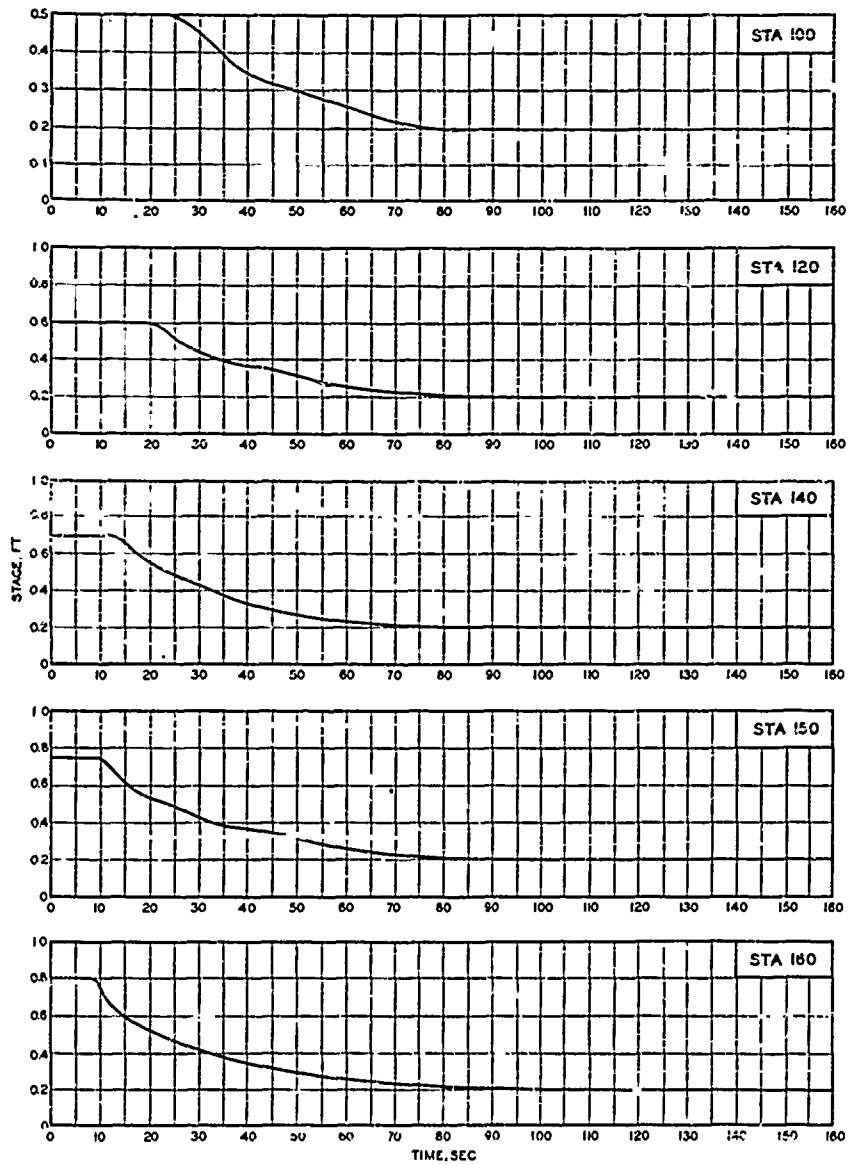
STAGE--TIME HYDROGRAPHS
STATIONS 150, 160, 172, 176, AND 180
TEST CONDITION 1.1 (10)



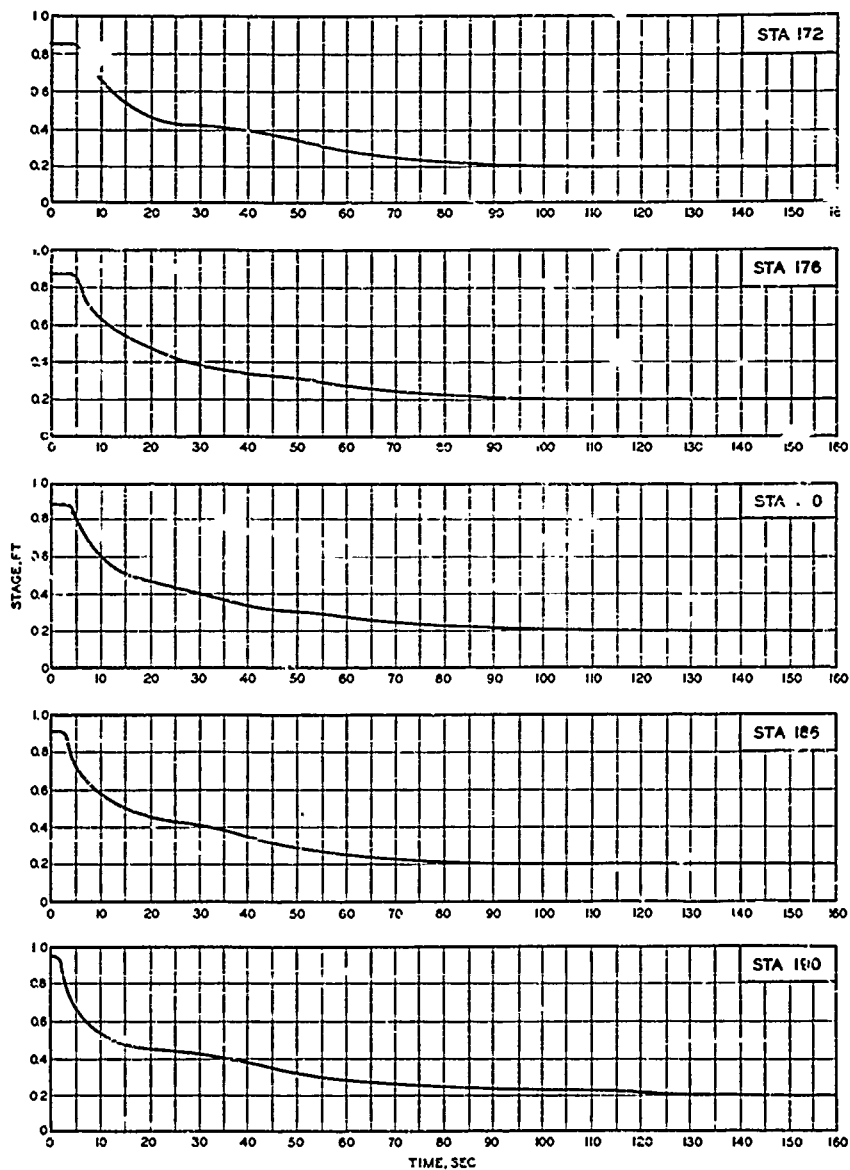
STAGE-TIME HYDROGRAPHS
STATIONS 186, 190, 196, 198, AND 200
TEST CONDITION 11 (10)



STAGE-TIME HYDROGRAPHS
STATIONS 225, 280, AND 350
TEST CONDITION 1.1 (10)



STAGE-TIME HYDROGRAPHS
STATIONS 100, 120, 140, 150, AND 160
TEST CONDITION 1.1 (20)



STAGE-TIME HYDROGRAPHS
STATIONS 172, 176, 185, 186 AND 190
TEST CONDITION 1.1 (20)

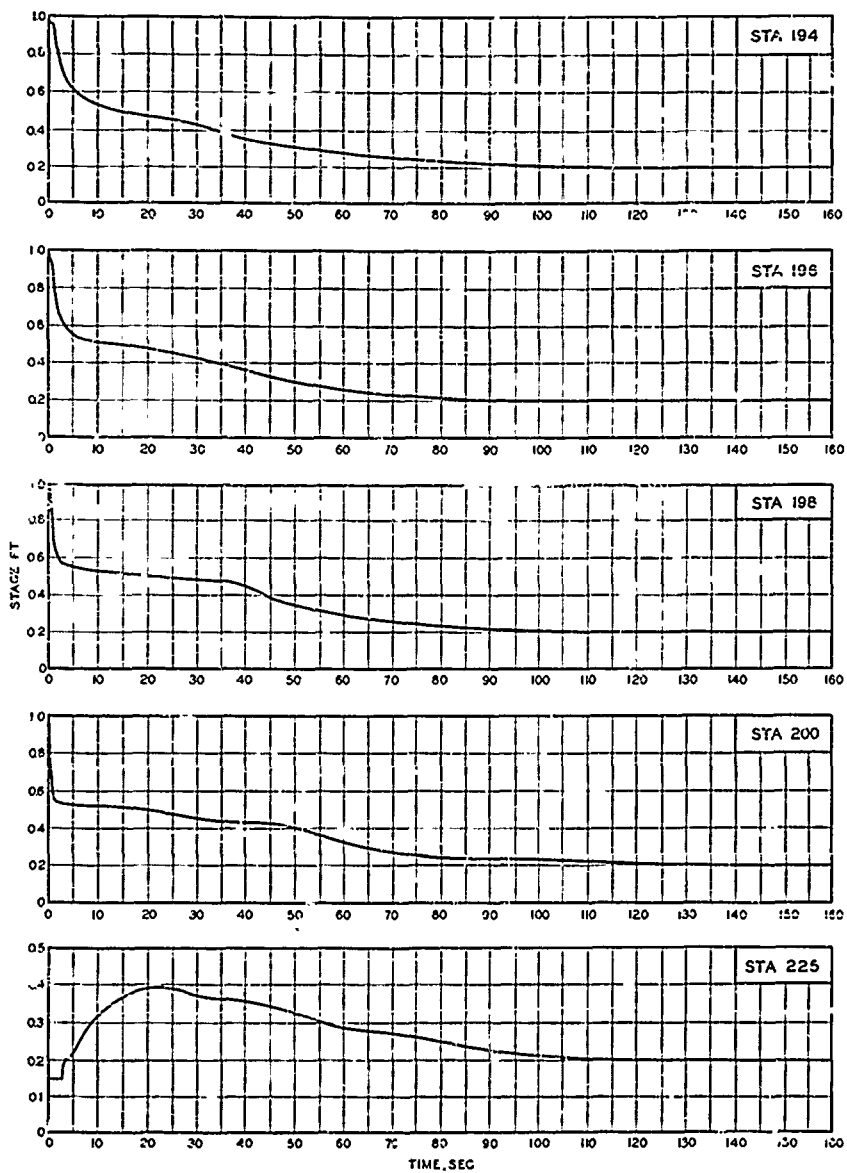
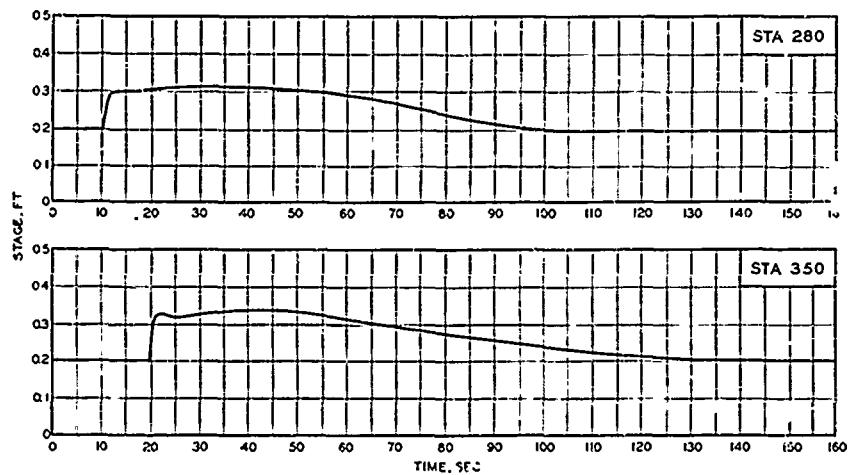
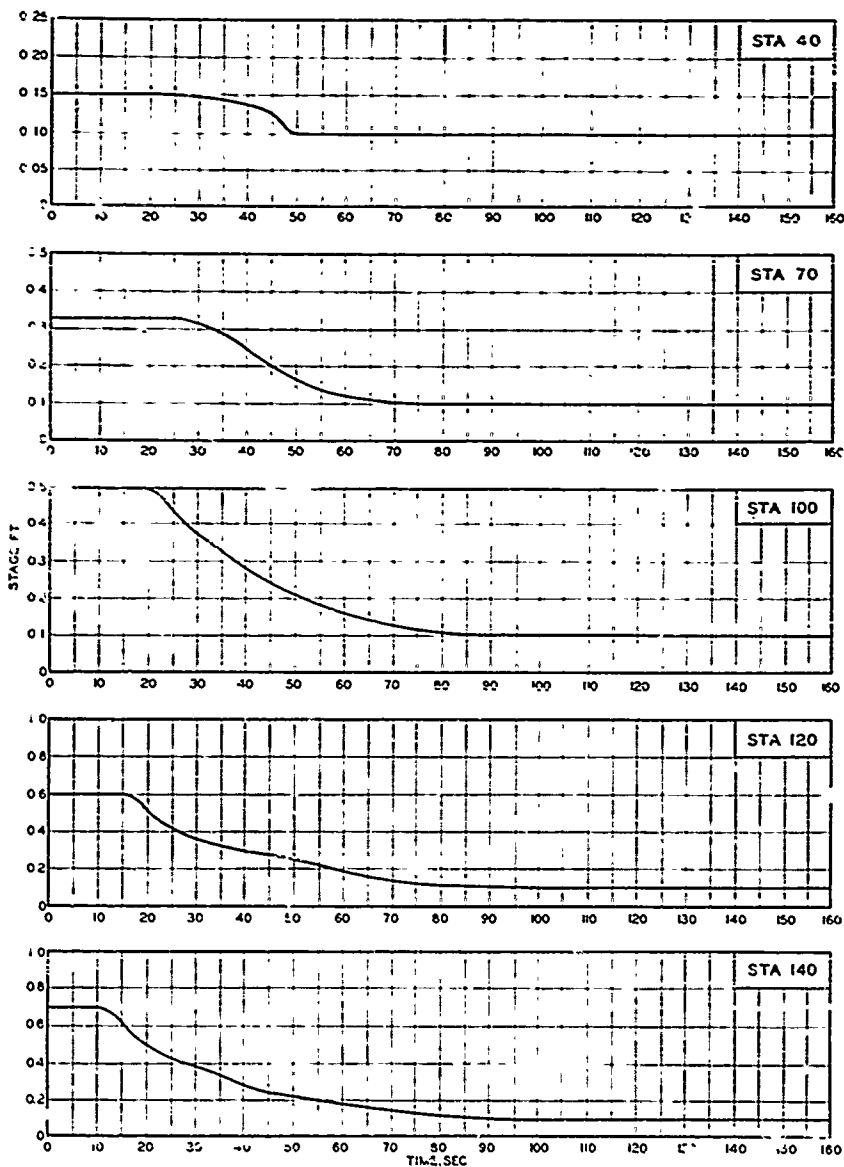


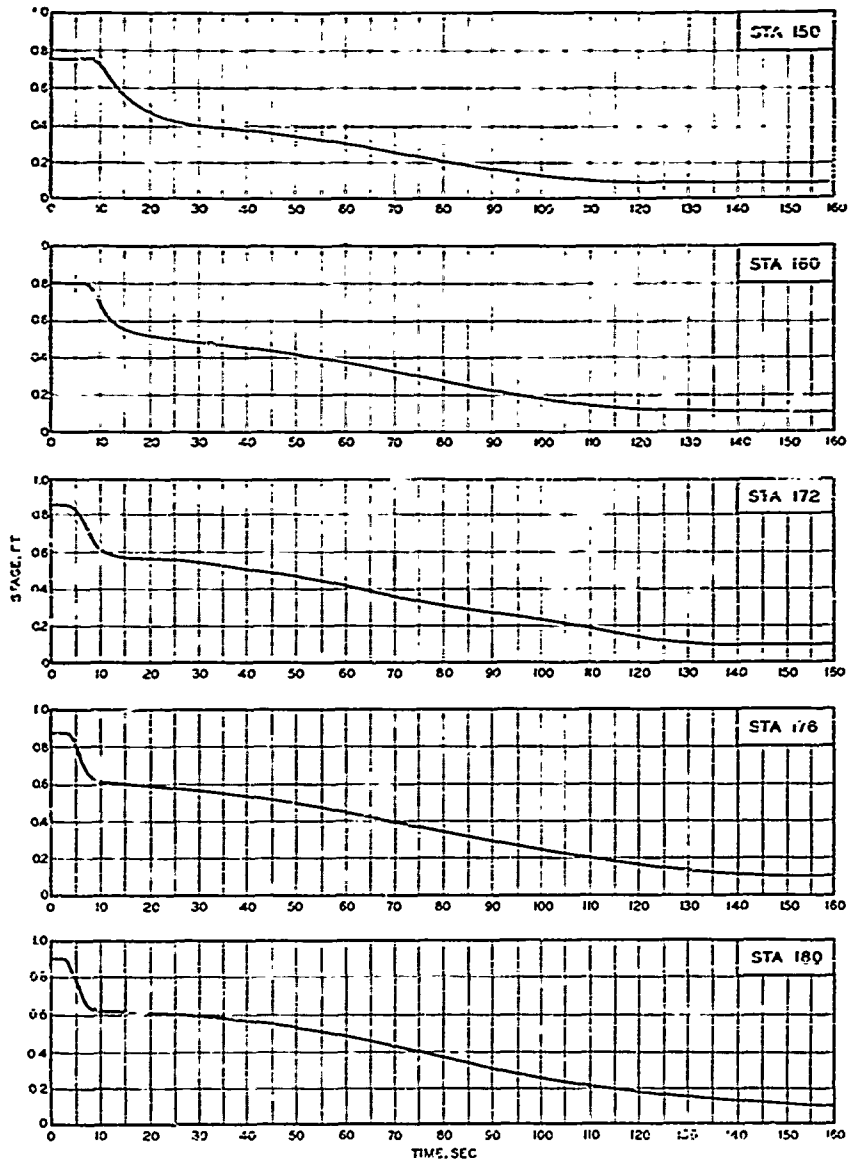
PLATE 68



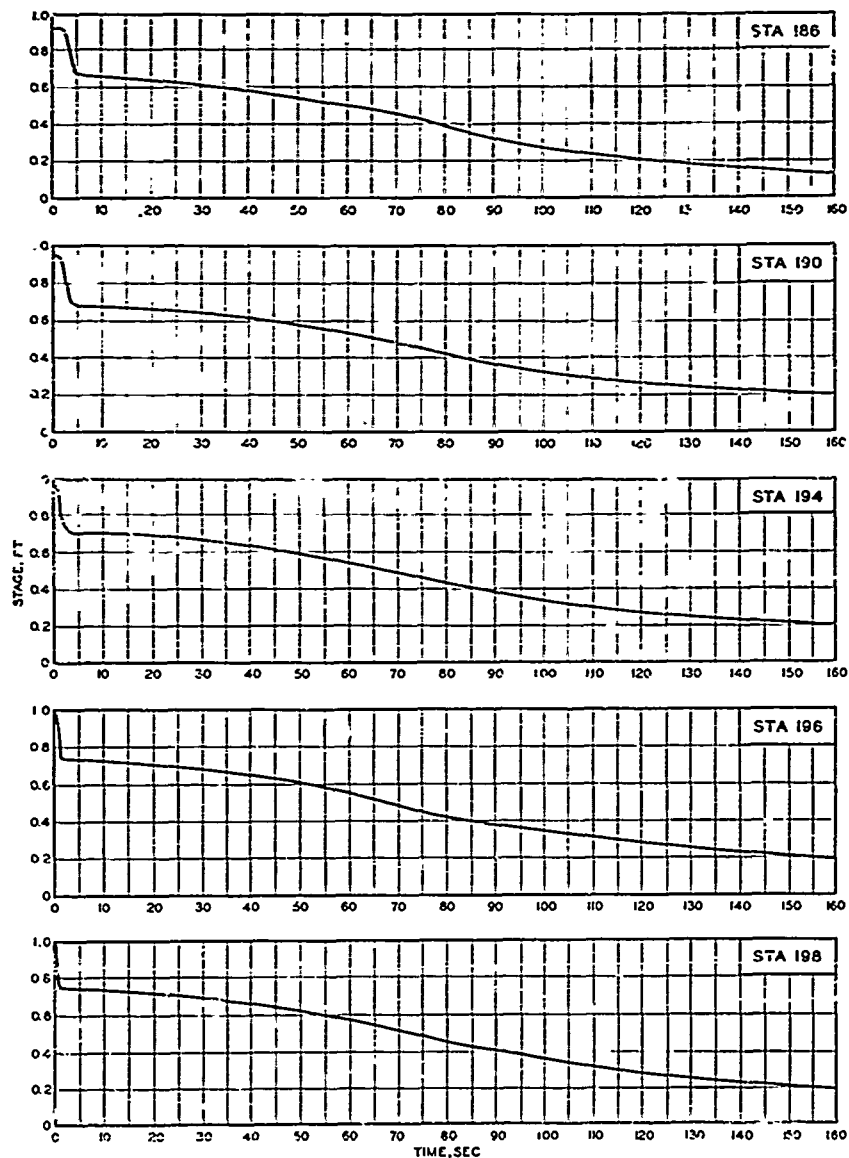
STAGE-TIME HYDROGRAPHS
STATIONS 280 AND 350
TEST CONDITION 1.1 (20)



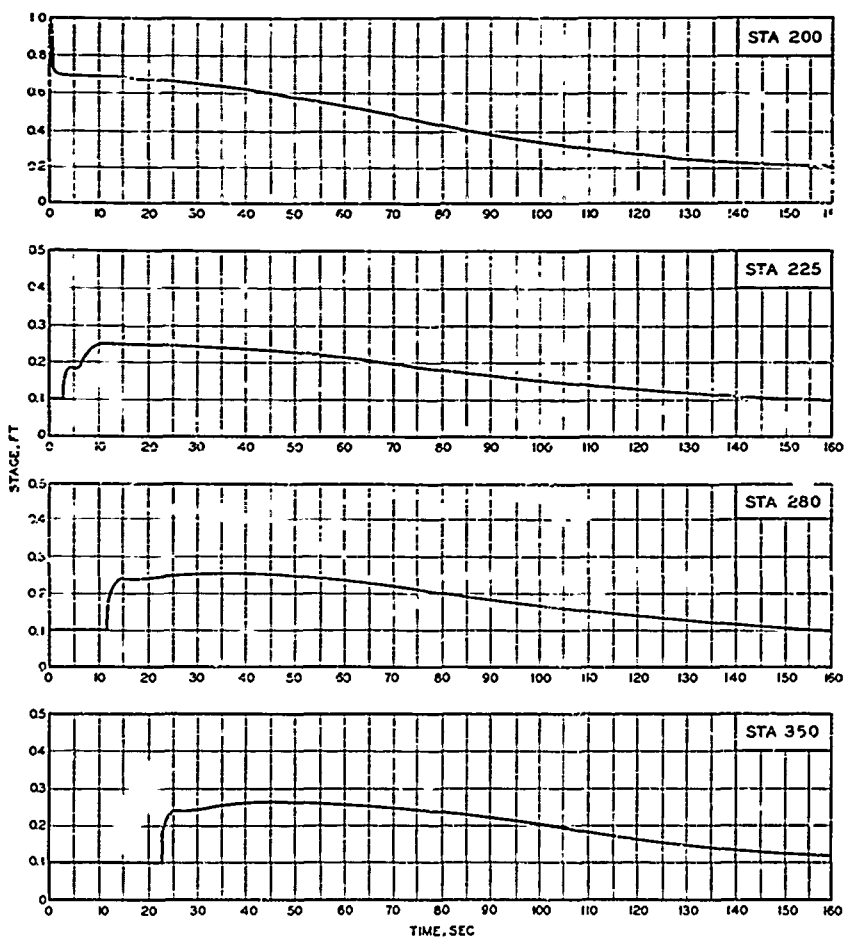
STAGE-TIME HYDROGRAPHS
STATIONS 40, 70, 100, 120 AND 140
TEST CONDITION 2 I (10)



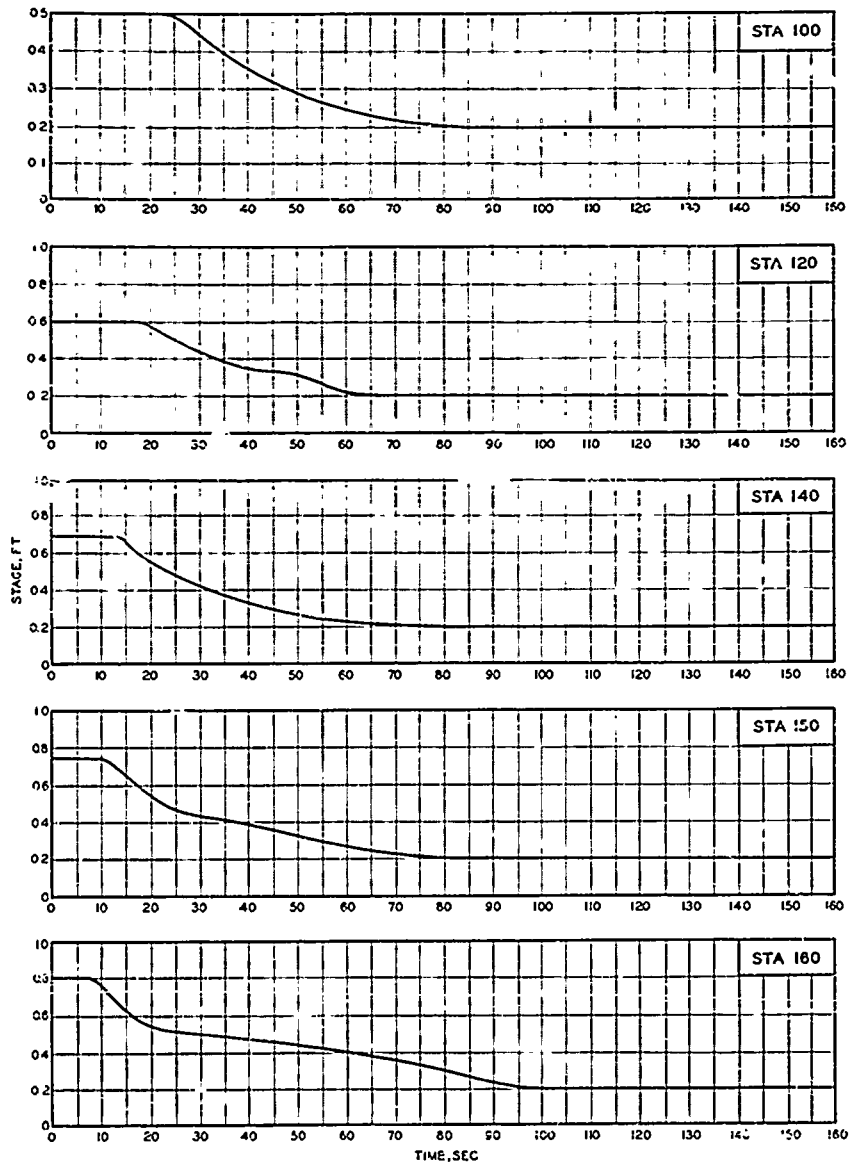
STAGE-TIME HYDROGRAPHS
STATIONS 150, 160, 172, 176, AND 180
TEST CONDITION 2.1 (10)



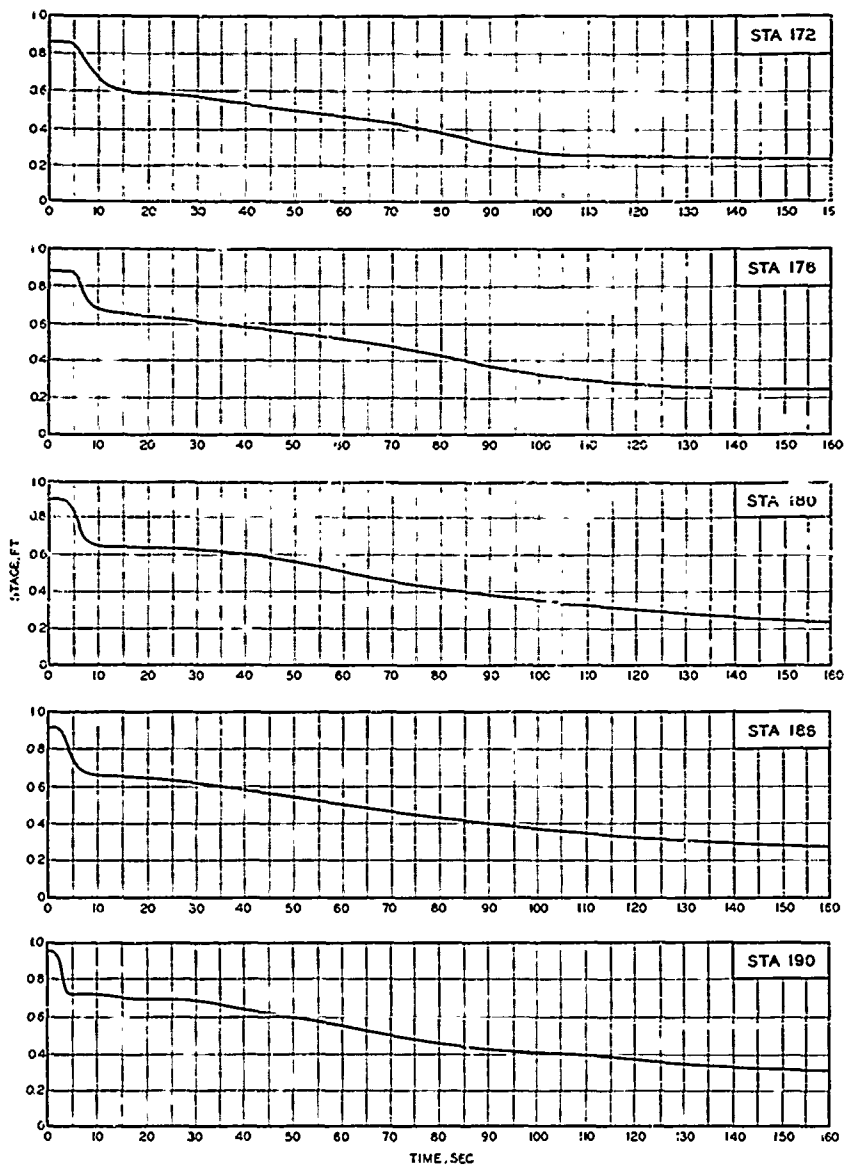
STAGE-TIME HYDROGRAPHS
 STATIONS 186, 190, 194, 196, AND 198
 TEST CONDITION 2.1 (10)



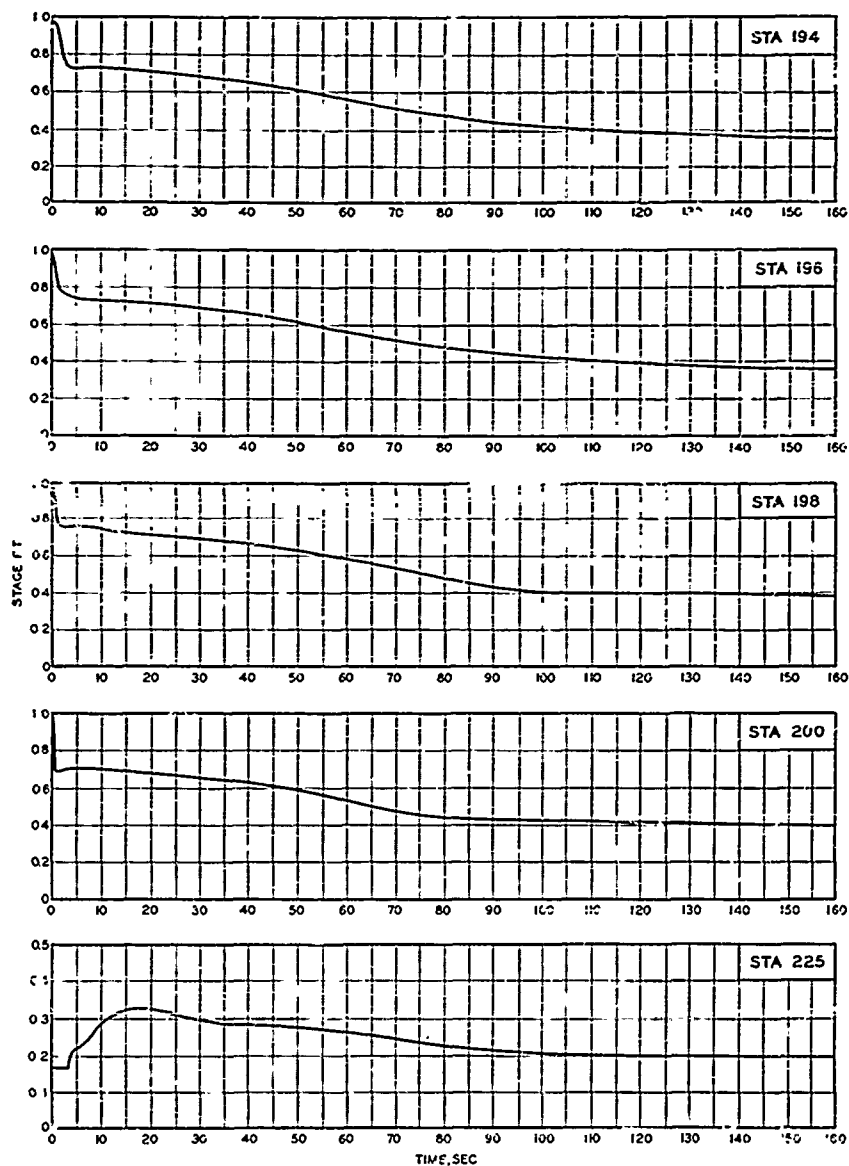
STAGE-TIME HYDROGRAPHS
STATIONS 200, 225, 280, AND 350
TEST CONDITION 2.1 (10)

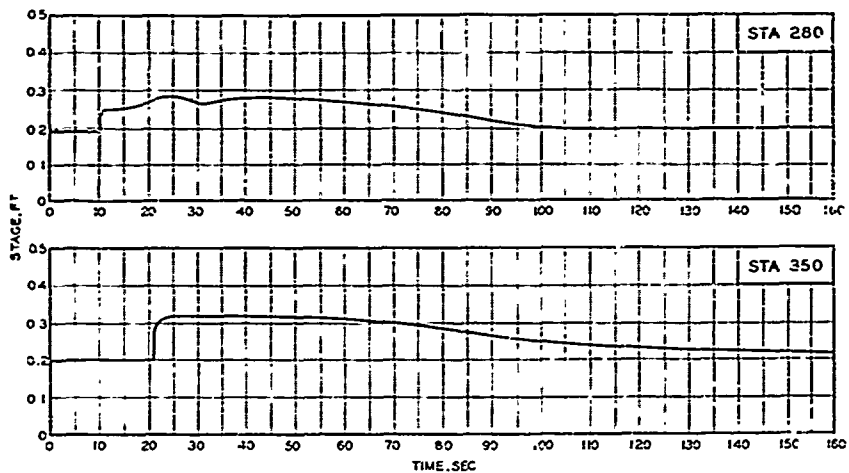


STAGE-TIME HYDROGRAPHS
STATIONS 100, 120, 140, 150, AND 160
TEST CONDITION 2.1 (20)

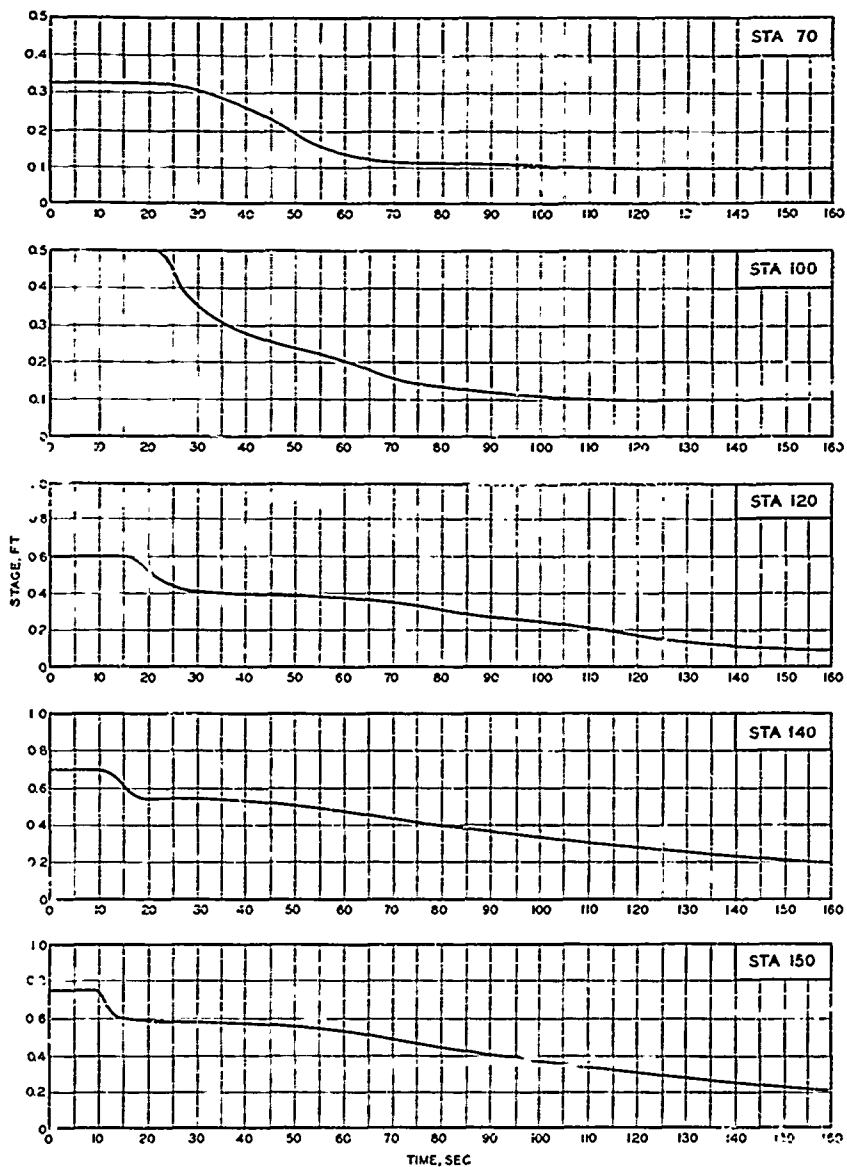


STAGE-TIME HYDROGRAPHS
STATIONS 172, 176, 180, 185, AND 190
TEST CONDUCTION 21 (20)

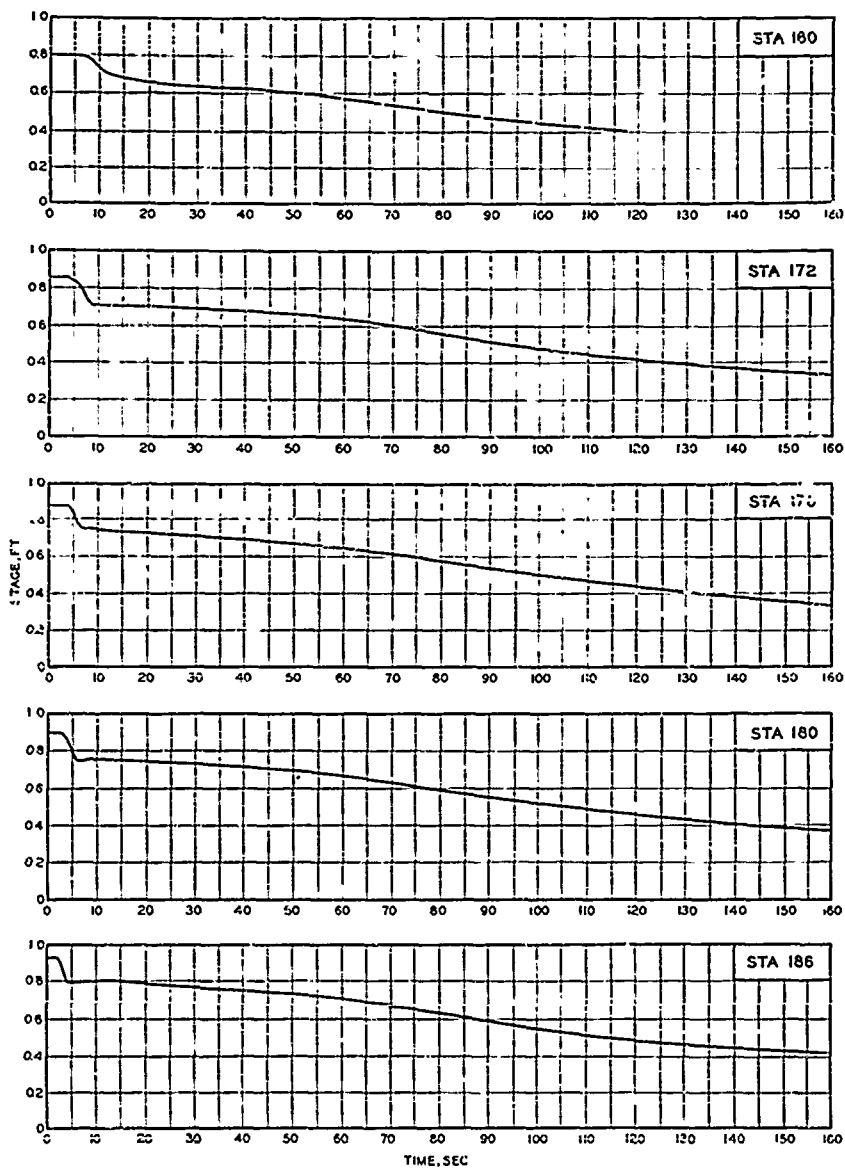




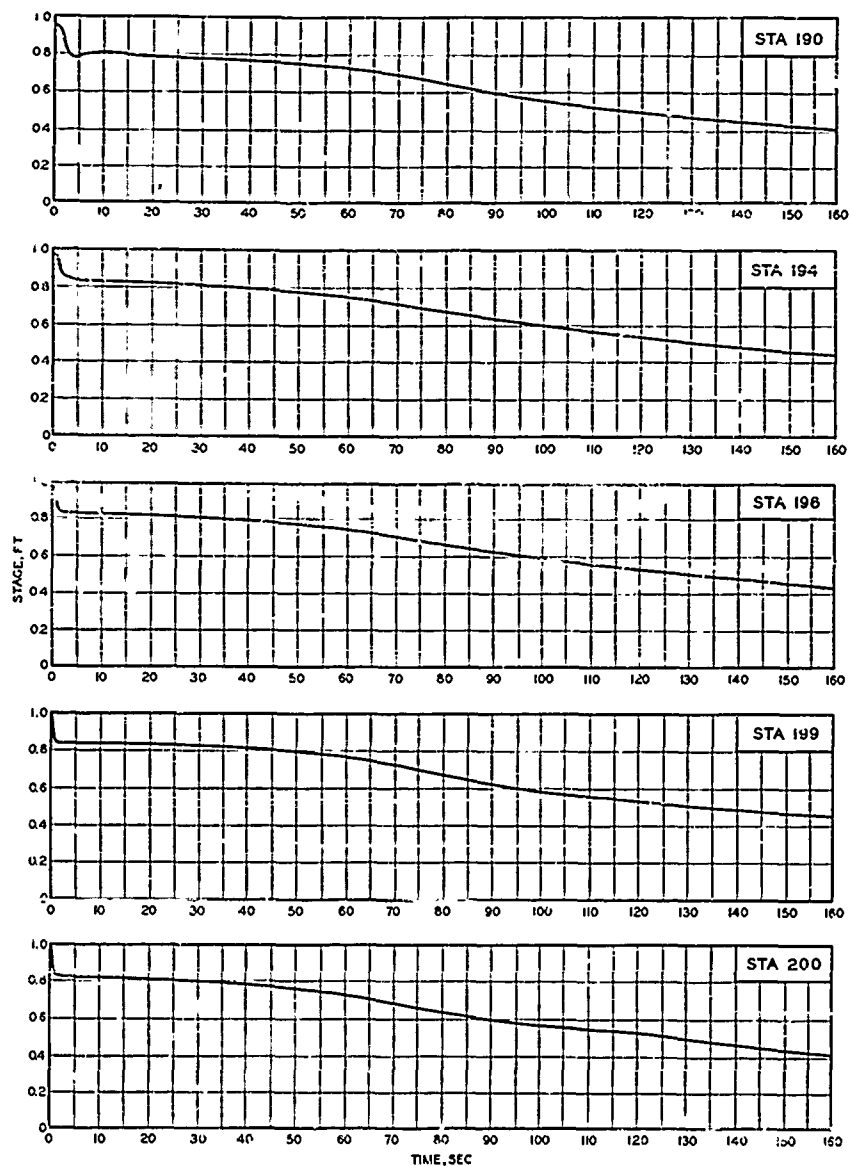
STAGE-TIME HYDROGRAPHS
STATIONS 280 AND 350
TEST CONDITION 21(20)



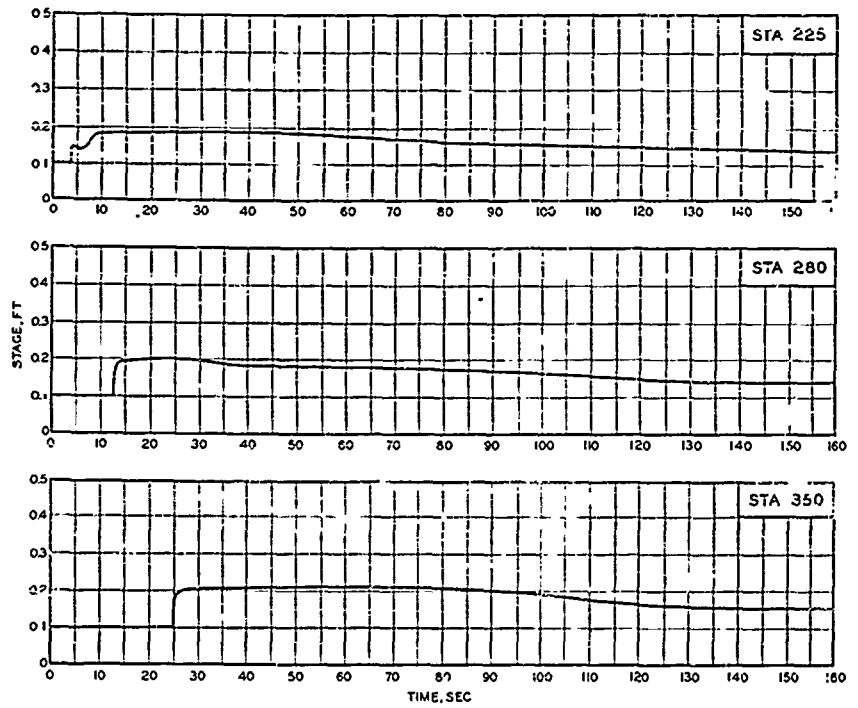
STAGE-TIME HYDROGRAPHS
STATIONS 70, 100, 120, 140 AND 150
TEST CONDITION 3.1 (10)



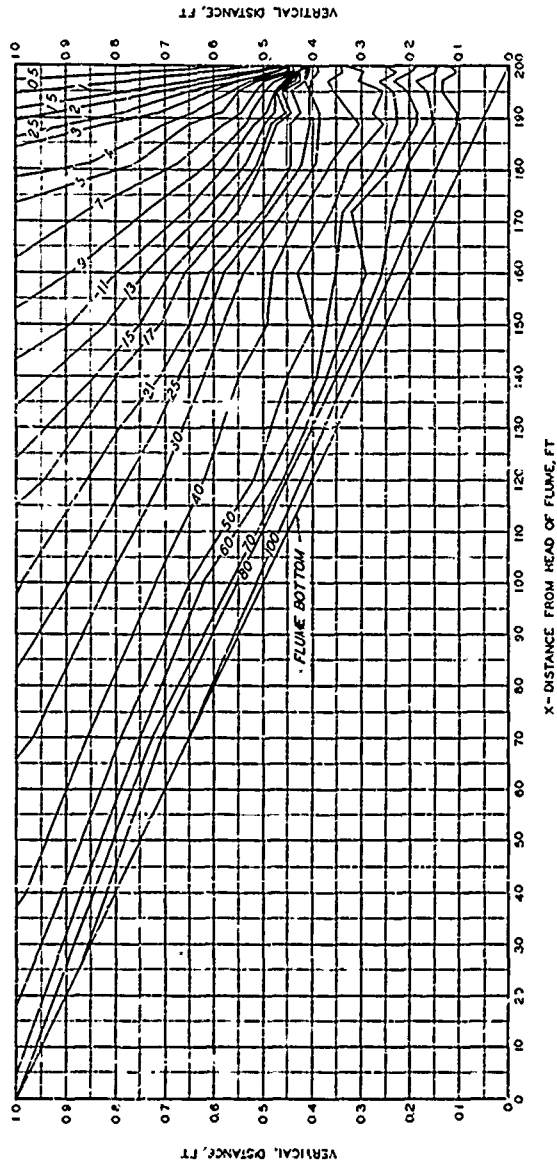
STAGE-TIME HYDROGRAPHS
STATIONS 180, 172, 170, 180 AND 186
TEST CONDITION 3.1 (10)



STAGE-TIME HYDROGRAPHS
STATIONS 190, 194, 196, 199 AND 200
TEST CONDITION 3.1 (10)

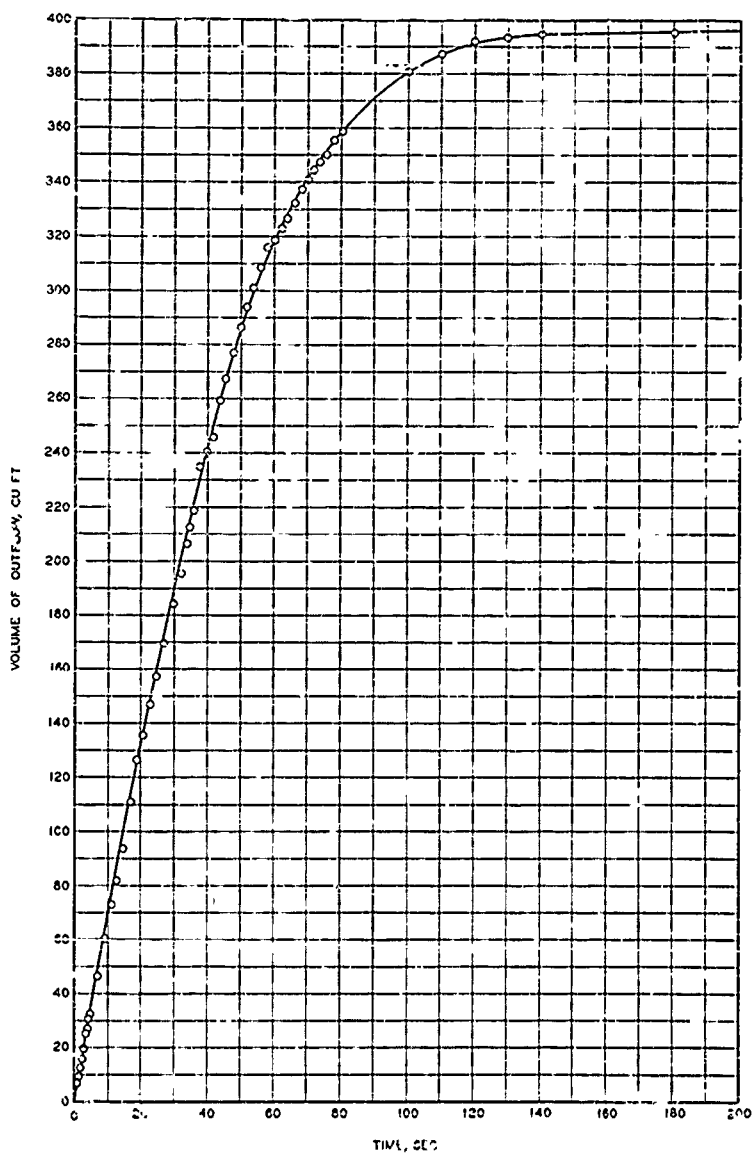


STAGE-TIME HYDROGRAPHS
STATIONS 225, 280, AND 350
TEST CONDITION 3.1 (10)

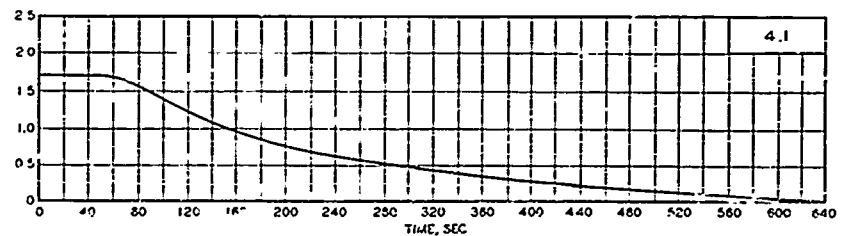
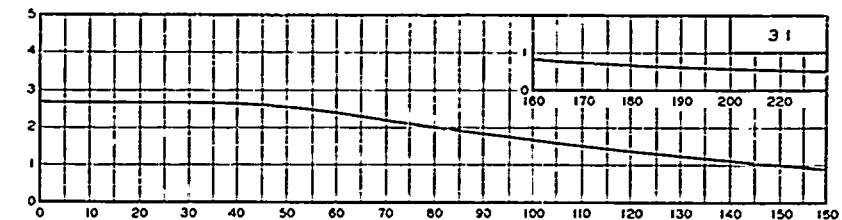
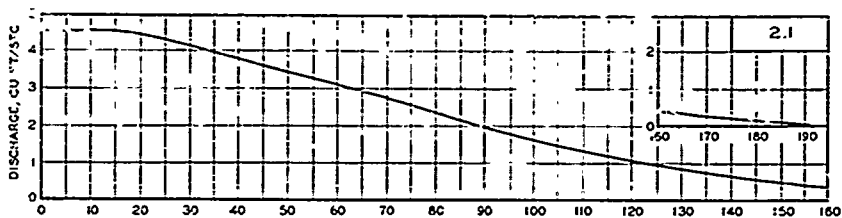
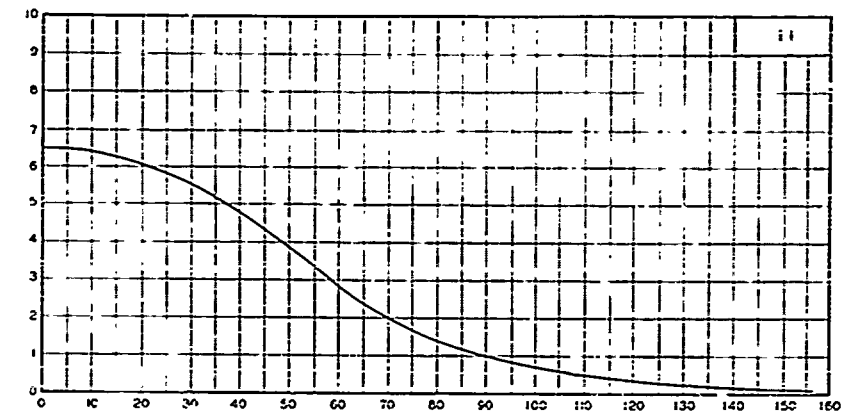


WATER-SURFACE PROFILES TEST CONDITION 1.1

"T": TIME IN SECONDS AS INDICATED

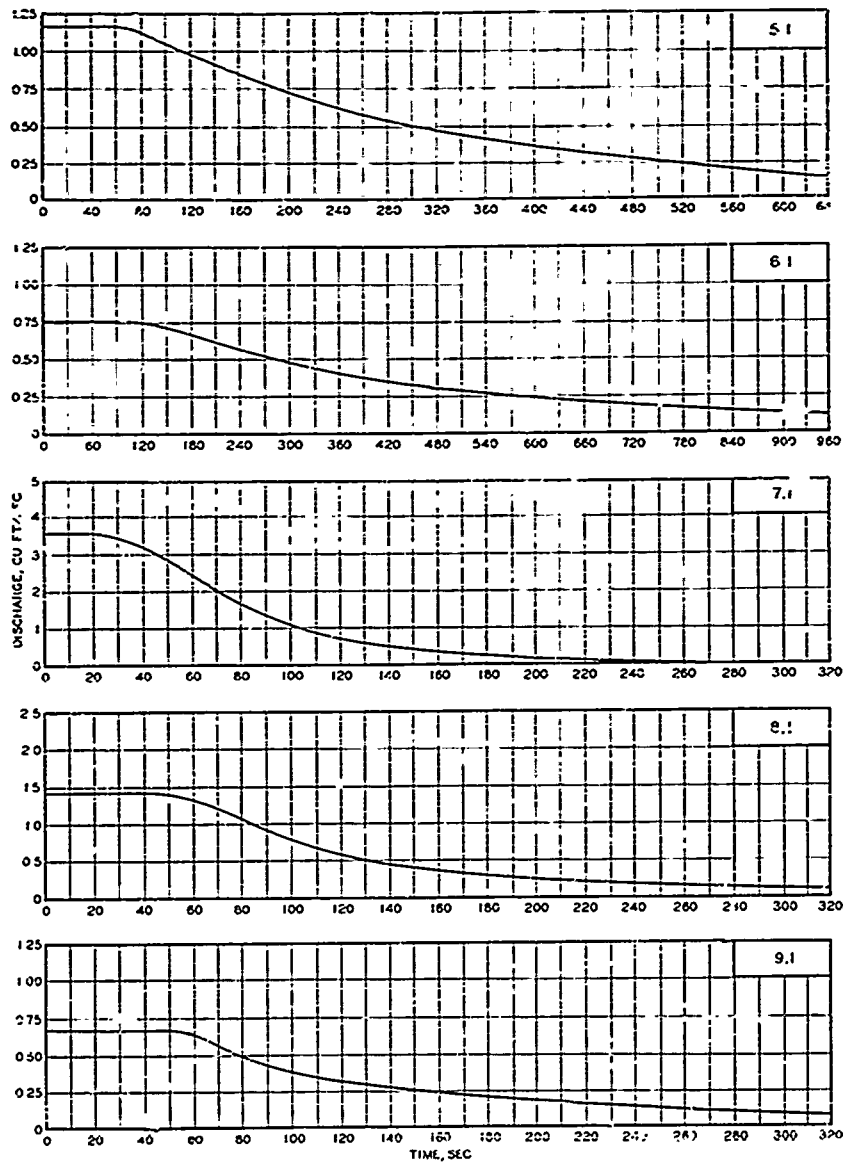


VOLUME OF OUTFLOW
AS A FUNCTION OF TIME
TEST CONDITION 1.1



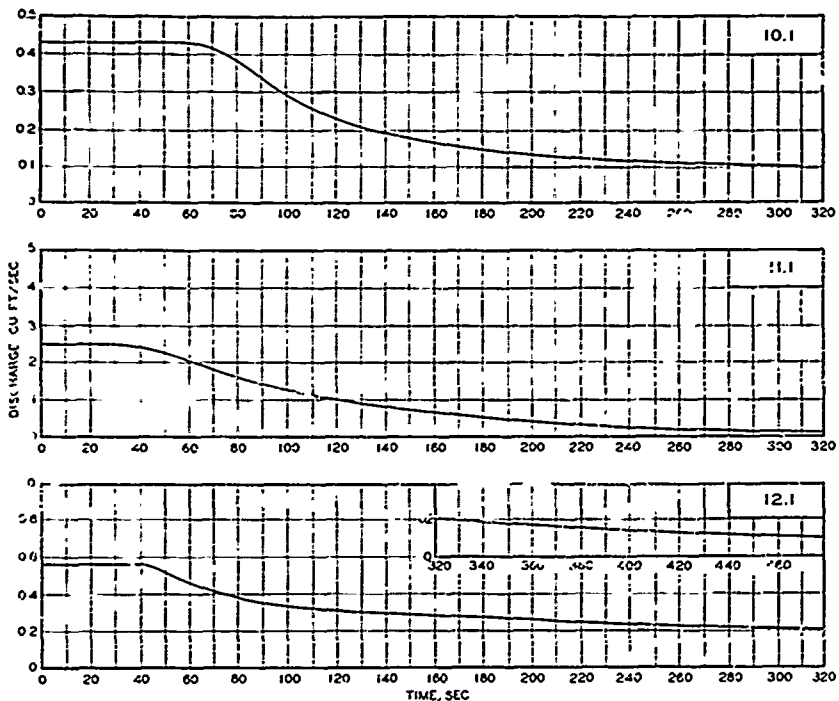
DISCHARGE-TIME HYDROGRAPH¹
AT STATION 200

TEST CONDITIONS 1.1, 2.1, 3.1, AND 4.1



DISCHARGE-TIME HYDROGRAPH AT STATION 200

TEST CONDITIONS 5.1, 6.1, 7.1, 8.1, AND 9.1

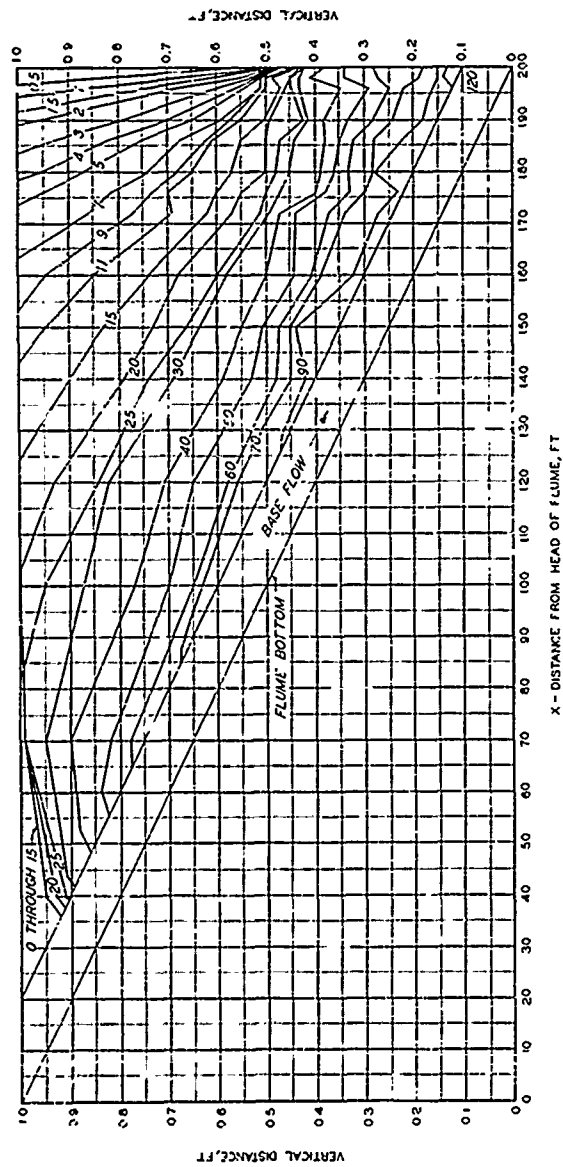


DISCHARGE-TIME HYDROGRAPH
AT STATION 200

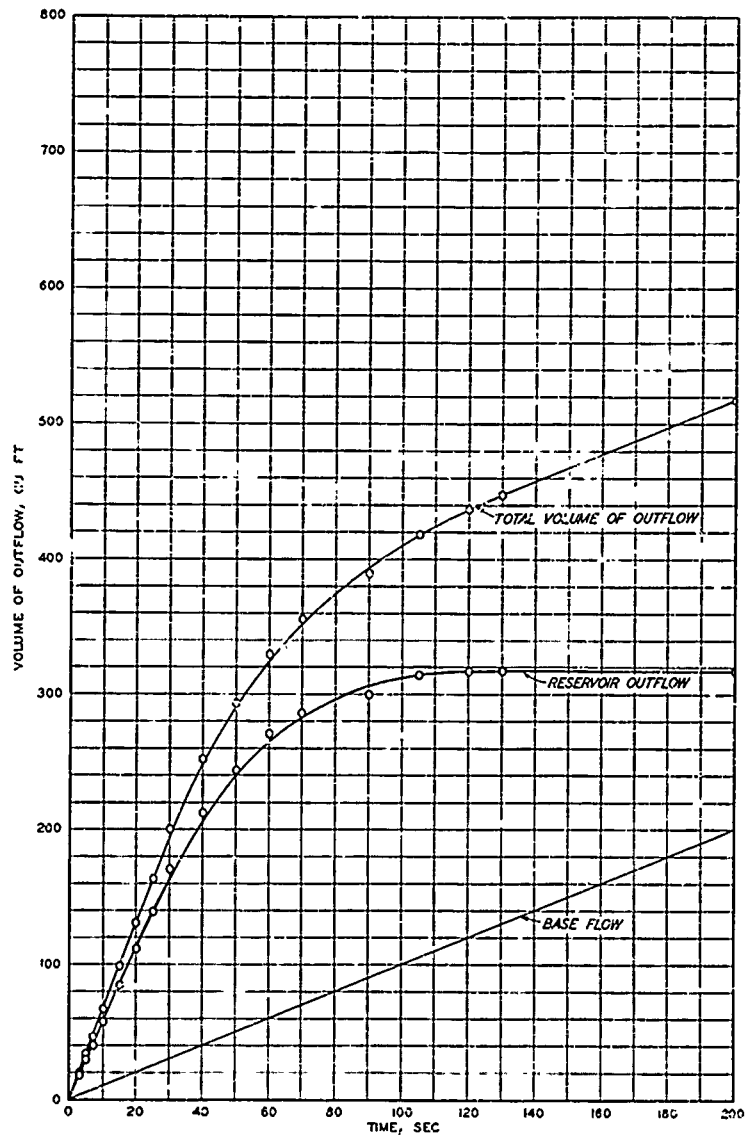
TEST CONDITIONS 10.1, 11.1, AND 12.1

WATER-SURFACE PROFILES

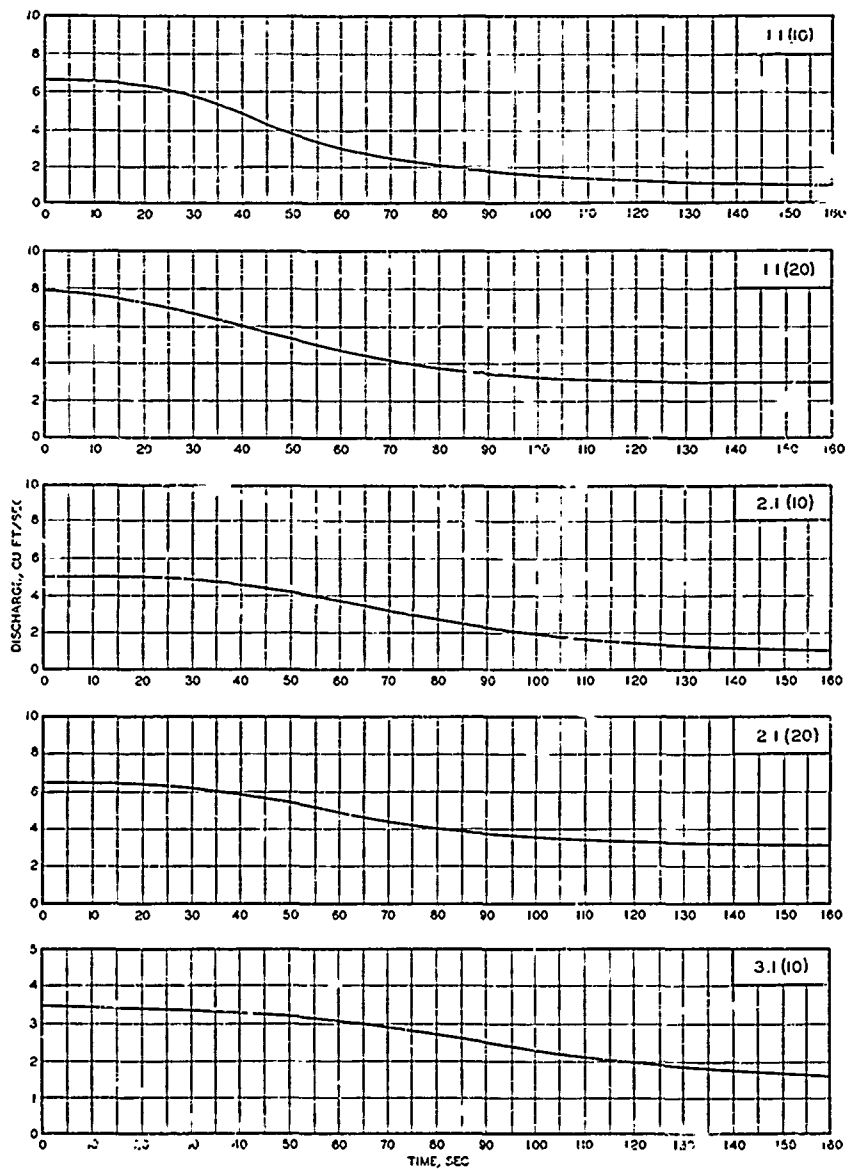
TEST CONDITION 1.1 (10)



NOT: TIME IN SECONDS AS INDICATED

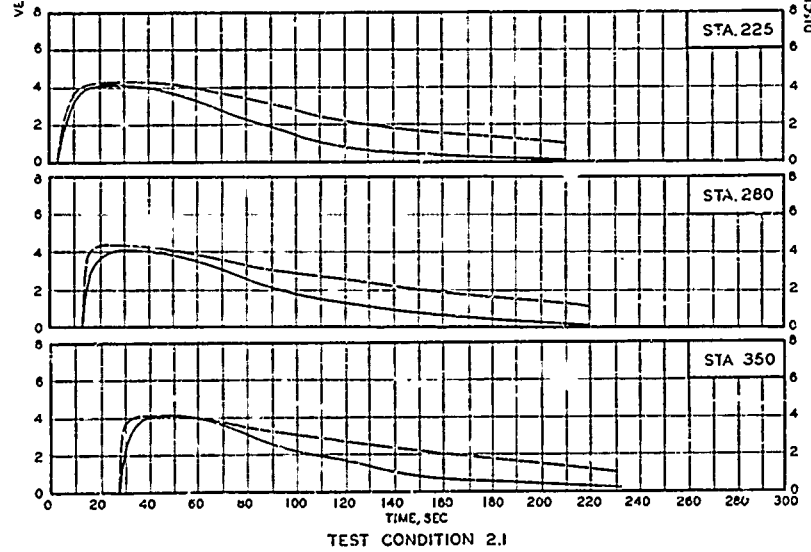
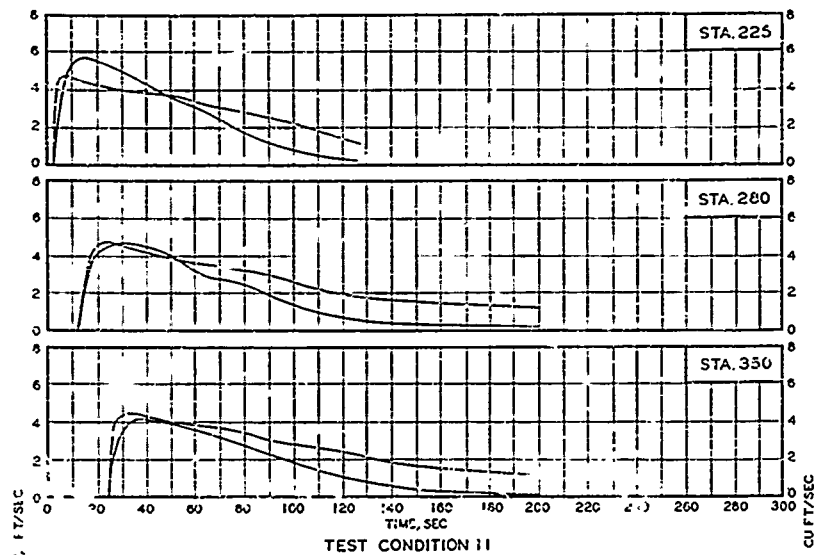


VOLUME OF OUTFLOW
AS A FUNCTION OF TIME
TEST CONDITION II (10)



DISCHARGE-TIME HYDROGRAPH
AT STATION 200

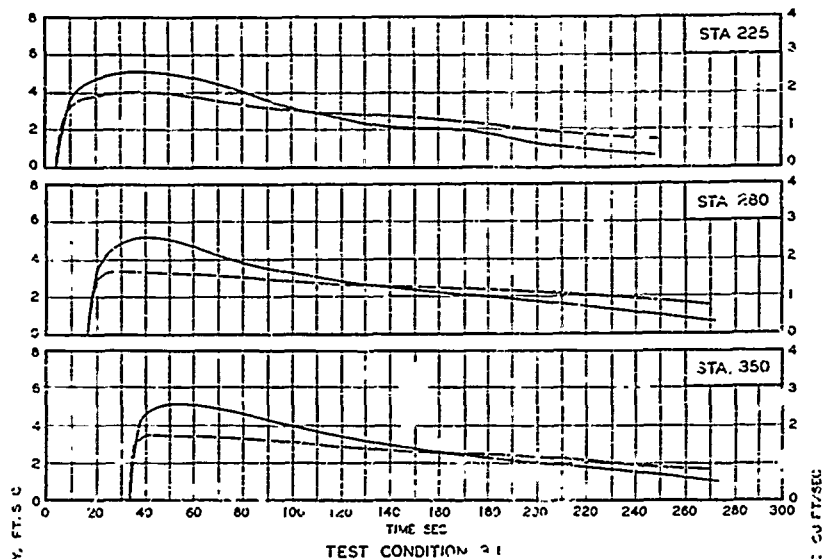
TEST CONDITIONS 1.1 (10), 1.1 (20),
2.1 (10), 2.1 (20), AND 3.1 (10)



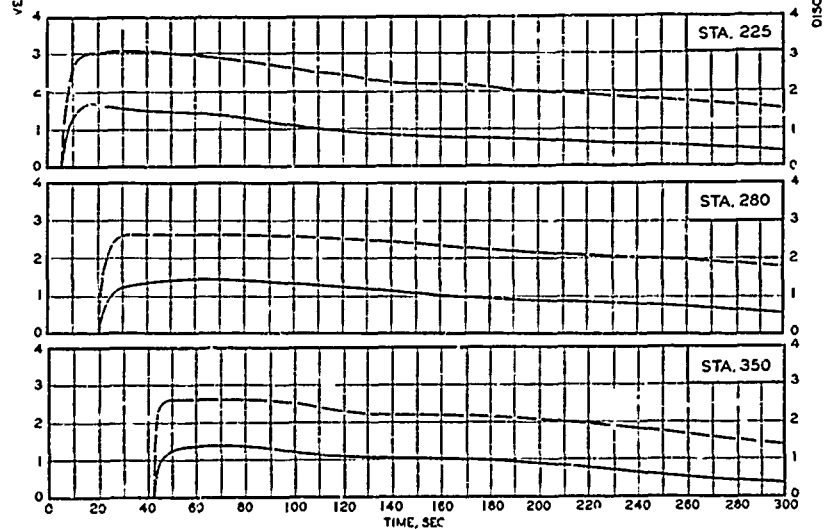
VELOCITY-DISCHARGE-TIME HYDROGRAPH FOR VARIOUS STATIONS

TEST CONDITIONS 1.1 & 2.1

— VELOCITY
- - DISCHARGE



TEST CONDITION 3.1

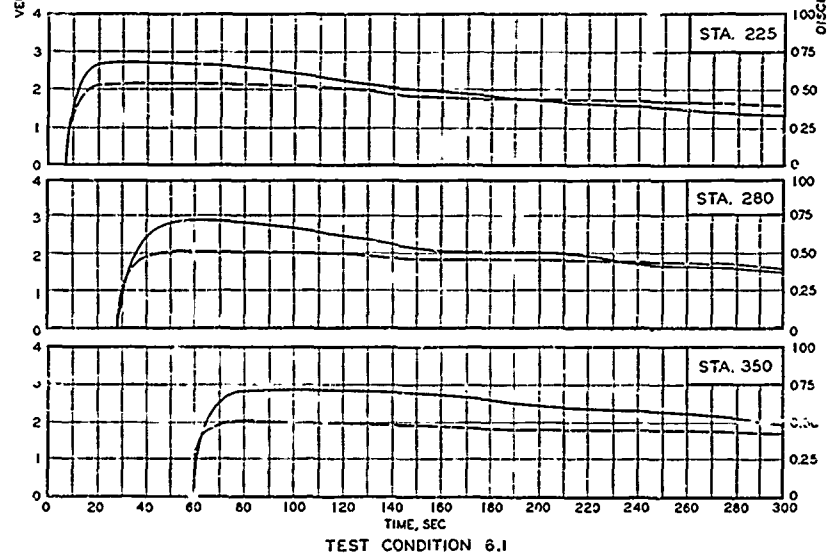
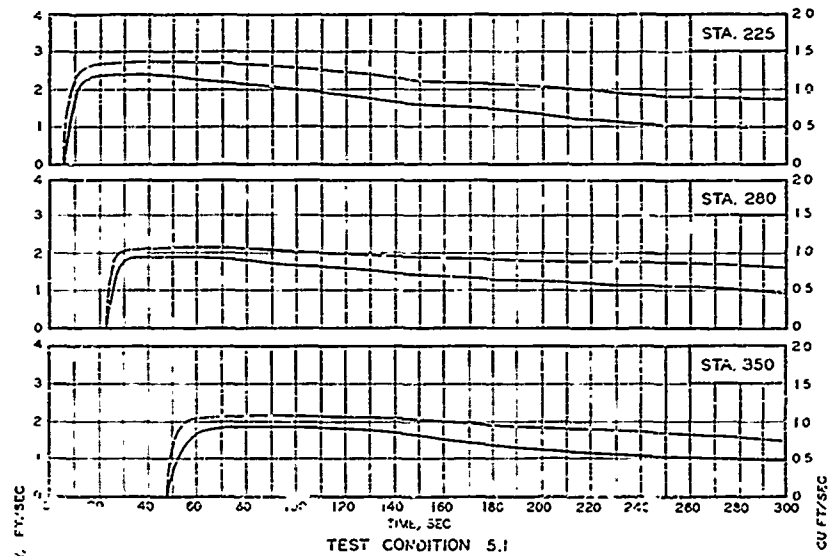


TEST CONDITION 4.1

VELOCITY-DISCHARGE-TIME HYDROGRAPH FOR VARIOUS STATIONS

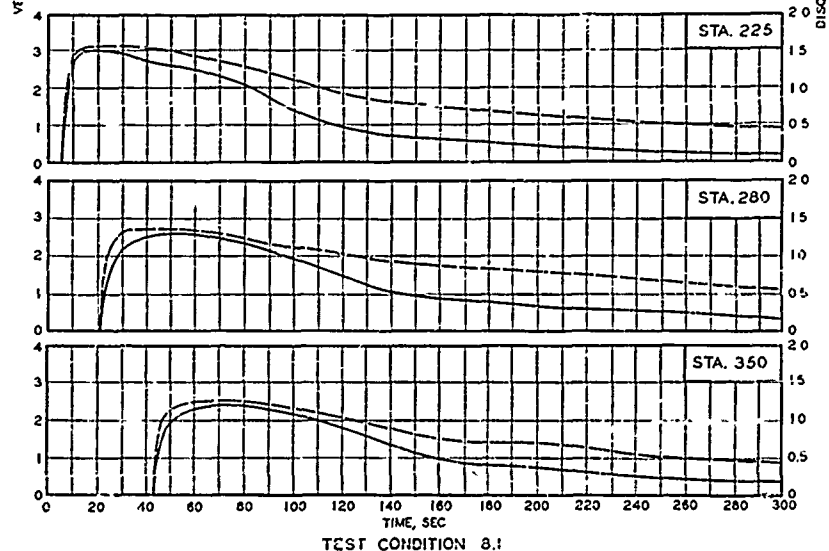
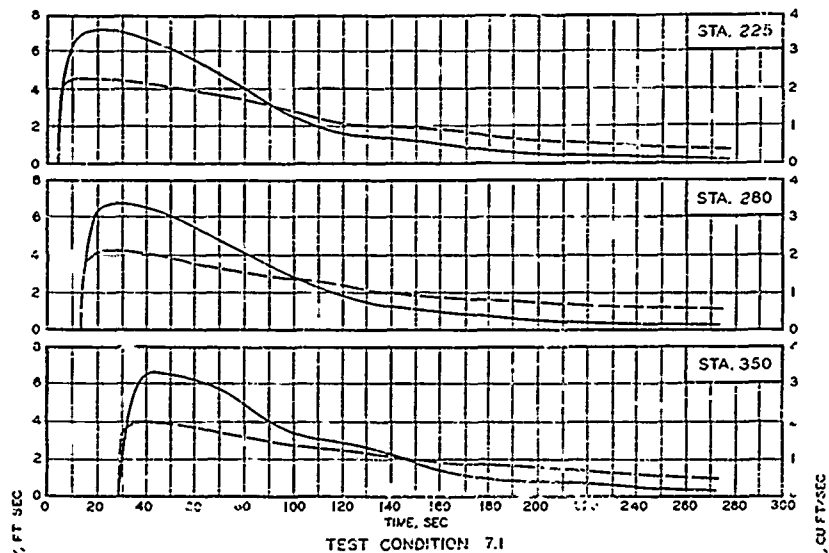
— VELOCITY
- - DISCHARGE

TEST CONDITIONS 3.1 & 4.1



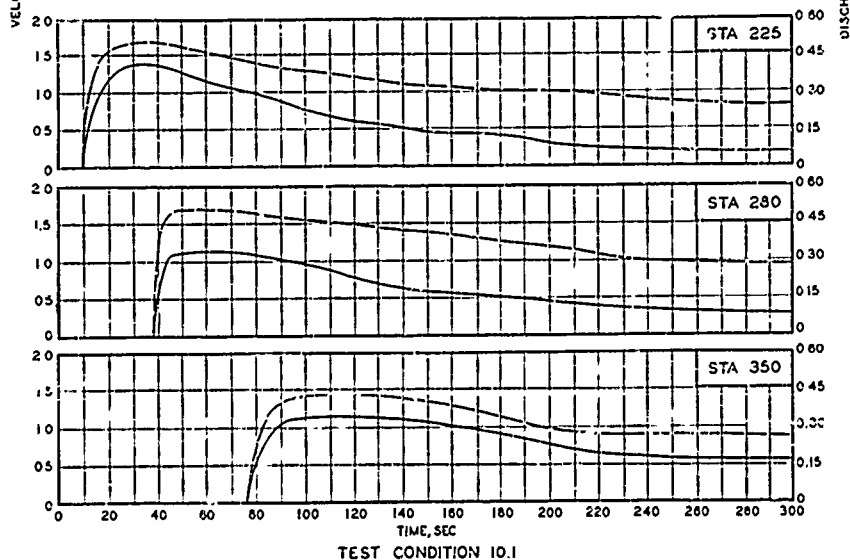
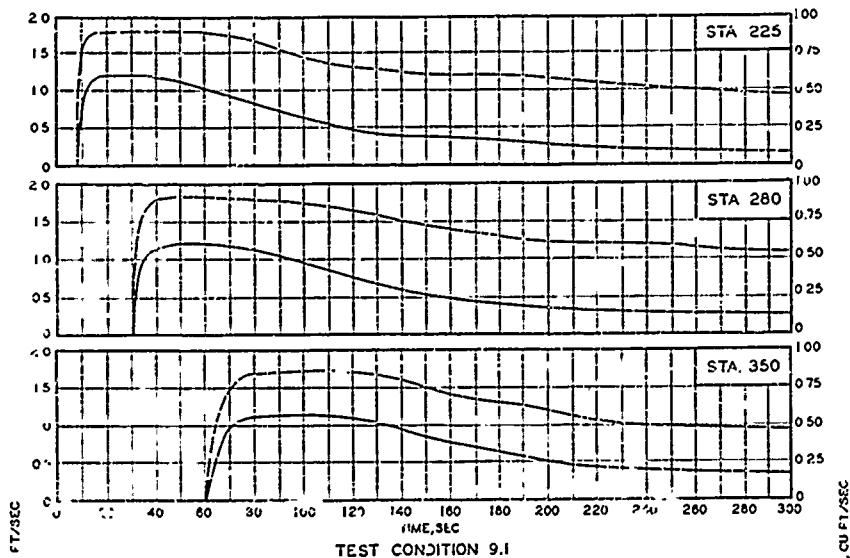
VELOCITY-DISCHARGE-TIME HYDROGRAPH
FOR VARIOUS STATIONS
TEST CONDITIONS 5.1 & 6.1

--- VELOCITY
— DISCHARGE



VELOCITY-DISCHARGE-TIME HYDROGRAPH
FOR VARIOUS STATIONS
TEST CONDITIONS 7.1 & 8.1

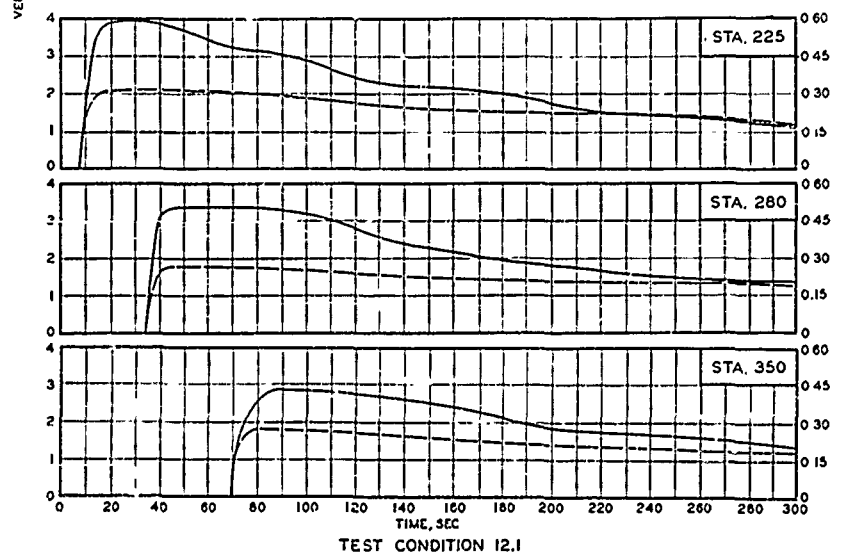
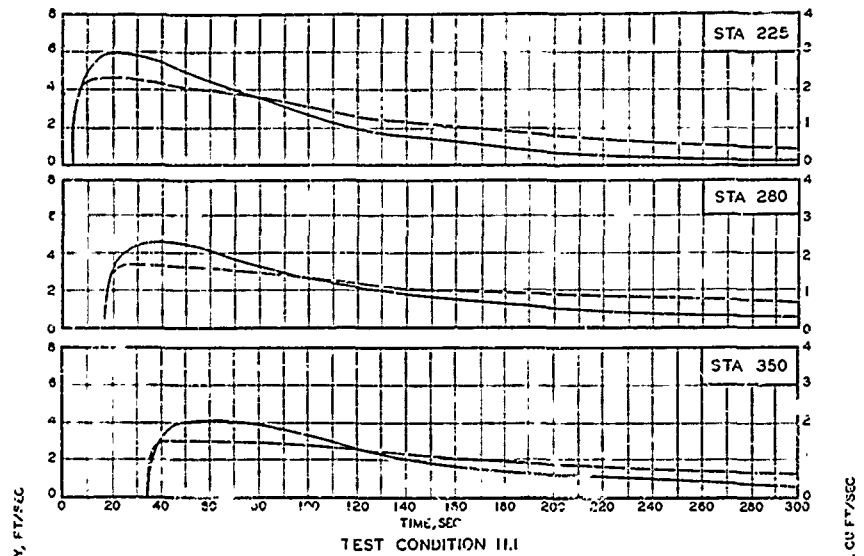
— VELOCITY
— DISCHARGE



VELOCITY-DISCHARGE-TIME HYDROGRAPH FOR VARIOUS STATIONS

TEST CONDITIONS 9 & 10.I

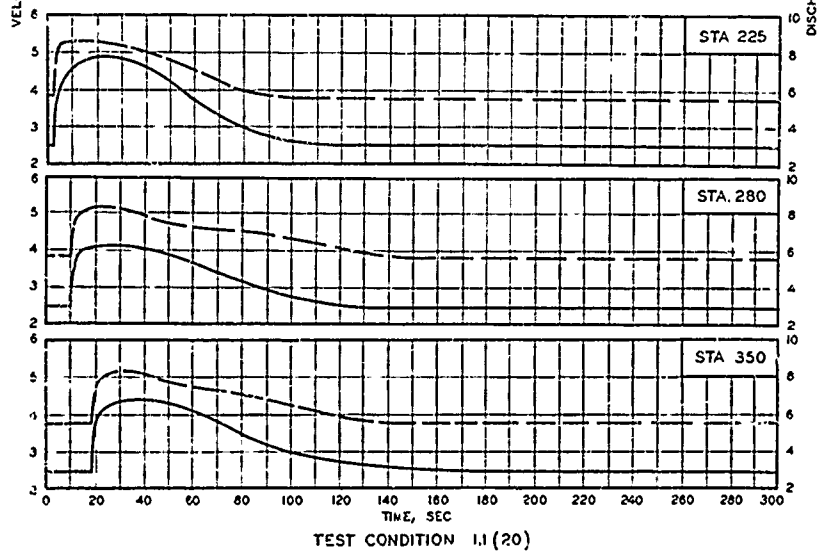
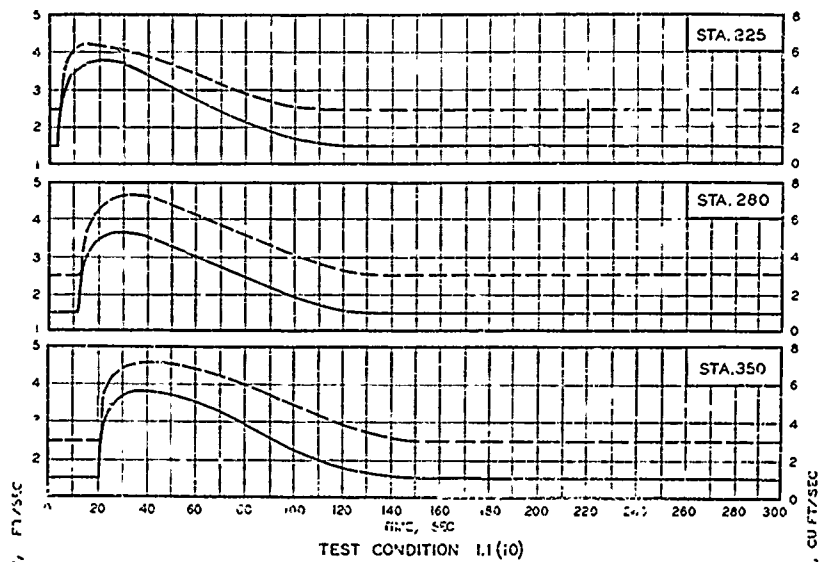
--- VELOCITY
--- DISCHARGE



VELOCITY-DISCHARGE-TIME HYDROGRAPH FOR VARIOUS STATIONS

TEST CONDITIONS 11.1 & 12.1

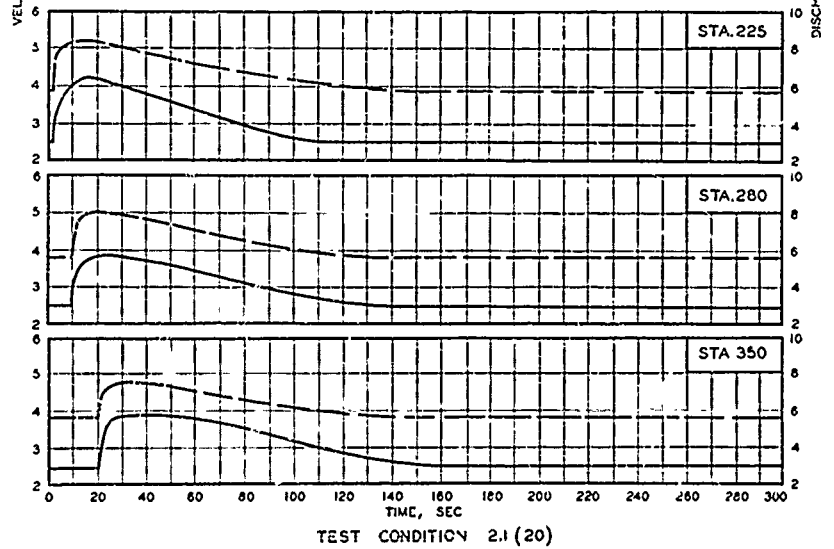
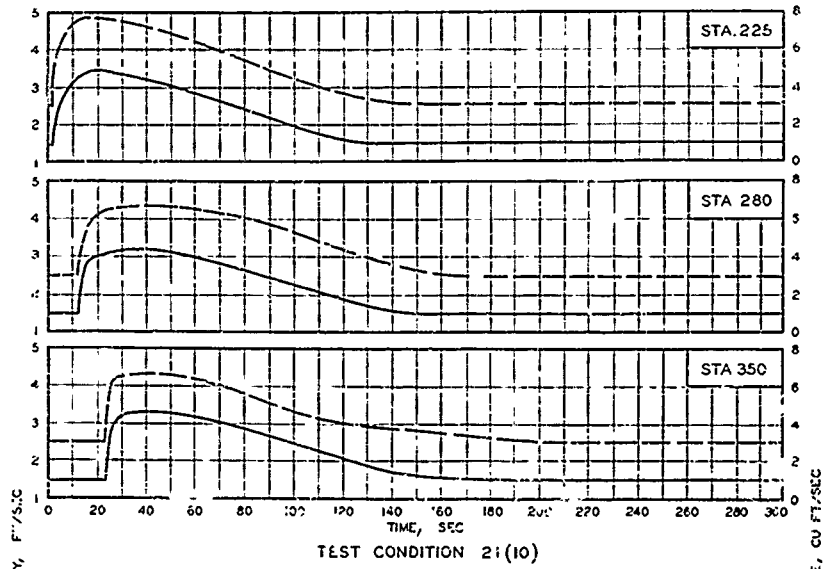
— VELOCITY
— DISCHARGE



VELOCITY-DISCHARGE-TIME HYDROGRAPH FOR VARIOUS STATIONS

TEST CONDITIONS I.1 (10) & I.1 (20)

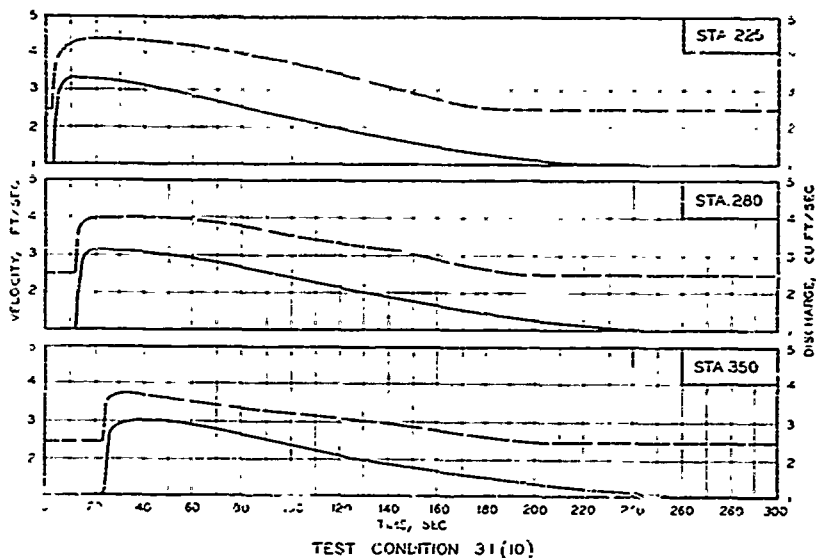
— VELOCITY
- - DISCHARGE



VELOCITY-DISCHARGE-TIME HYDROGRAPH
FOR VARIOUS STATIONS

TEST CONDITIONS 2.1(10) & 2.1(20)

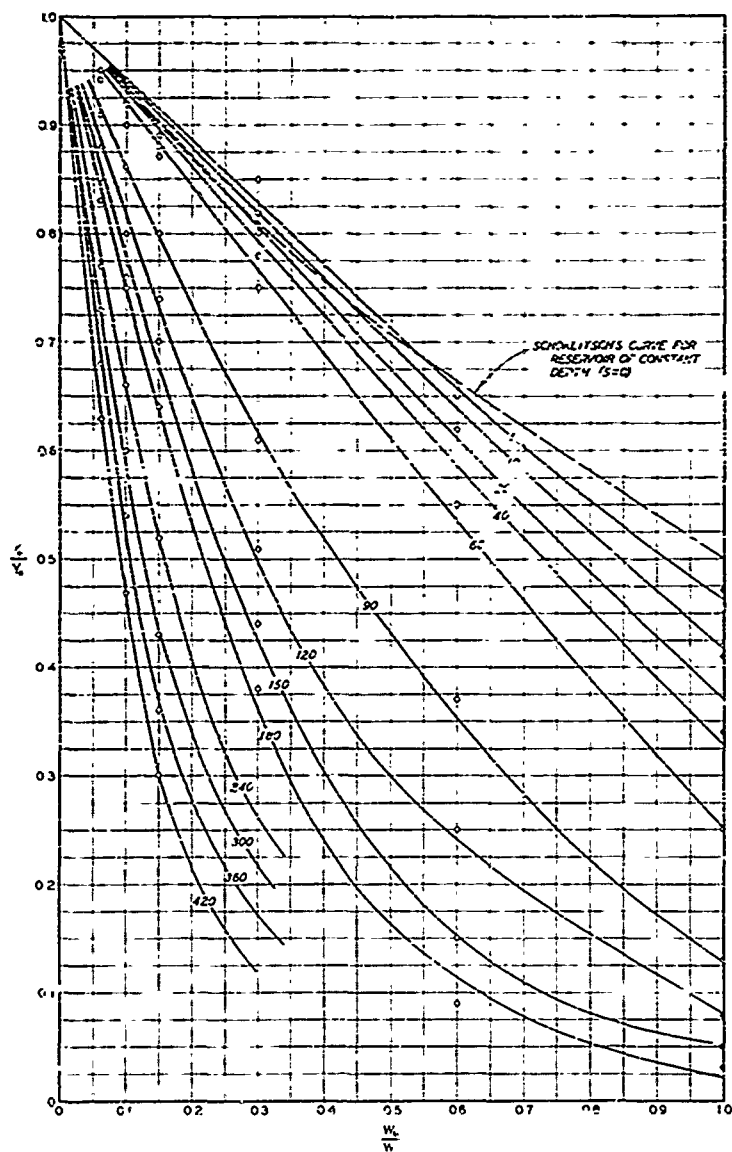
— VELOCITY
— DISCHARGE



VELOCITY-DISCHARGE-TIME HYDROGRAPH
FOR VARIOUS STATIONS

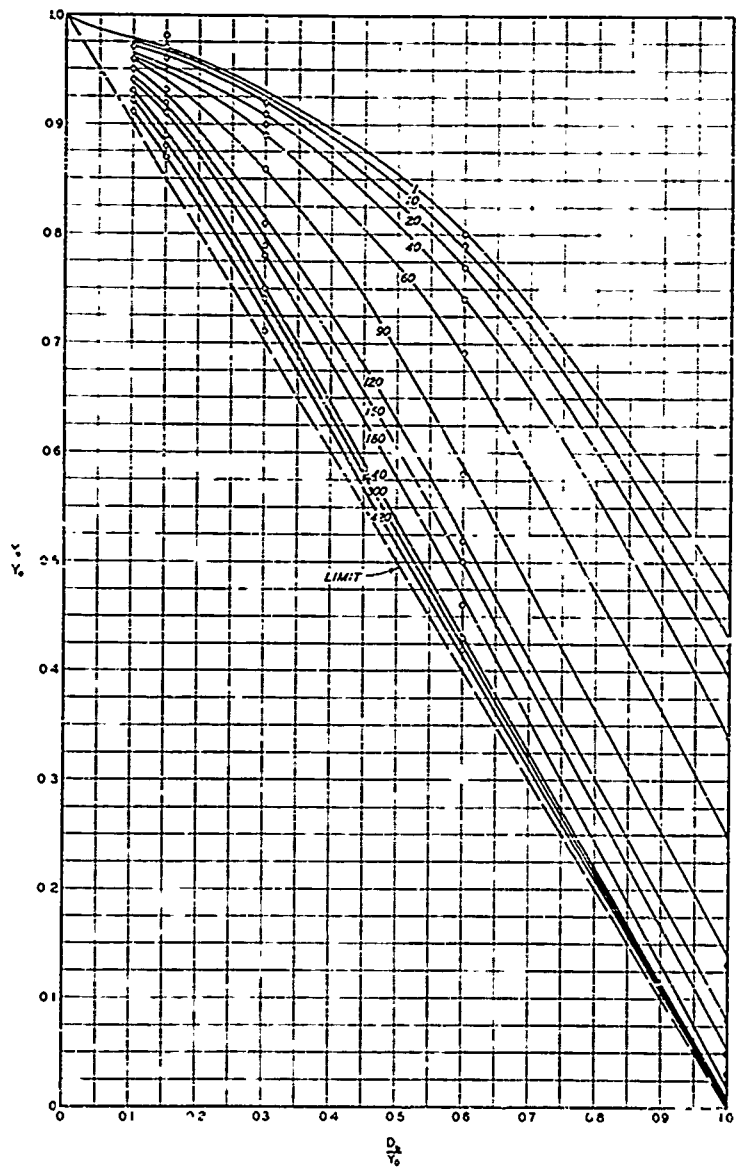
TEST CONDITION 31(10)

— VELOCITY
- - DISCHARGE



NOTE NUMERICAL VALUE ON EACH CURVE
INDICATES TIME IN SECONDS

EFFECT OF BAFLE WIDTH
ON OUTFLOW DEPTH
 $D_0/h_0=1$



NOTE: NUMERICAL VALUE ON EACH CURVE
INDICATES TIME IN SECONDS

EFFECT OF BRACH DEPTH
ON OUTFLOW DEPTH
 $W_b/W_d=1$

PLATE 100

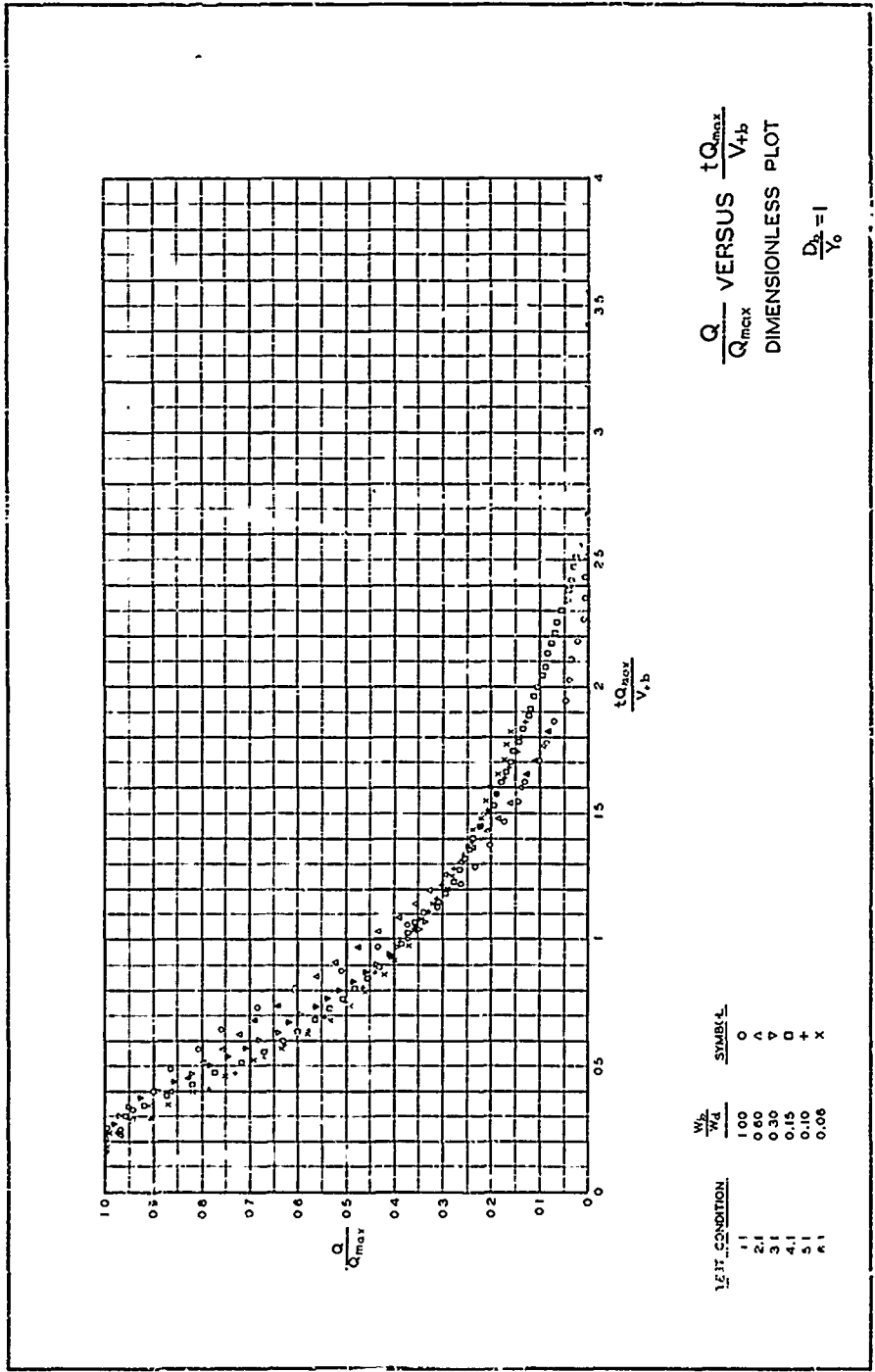
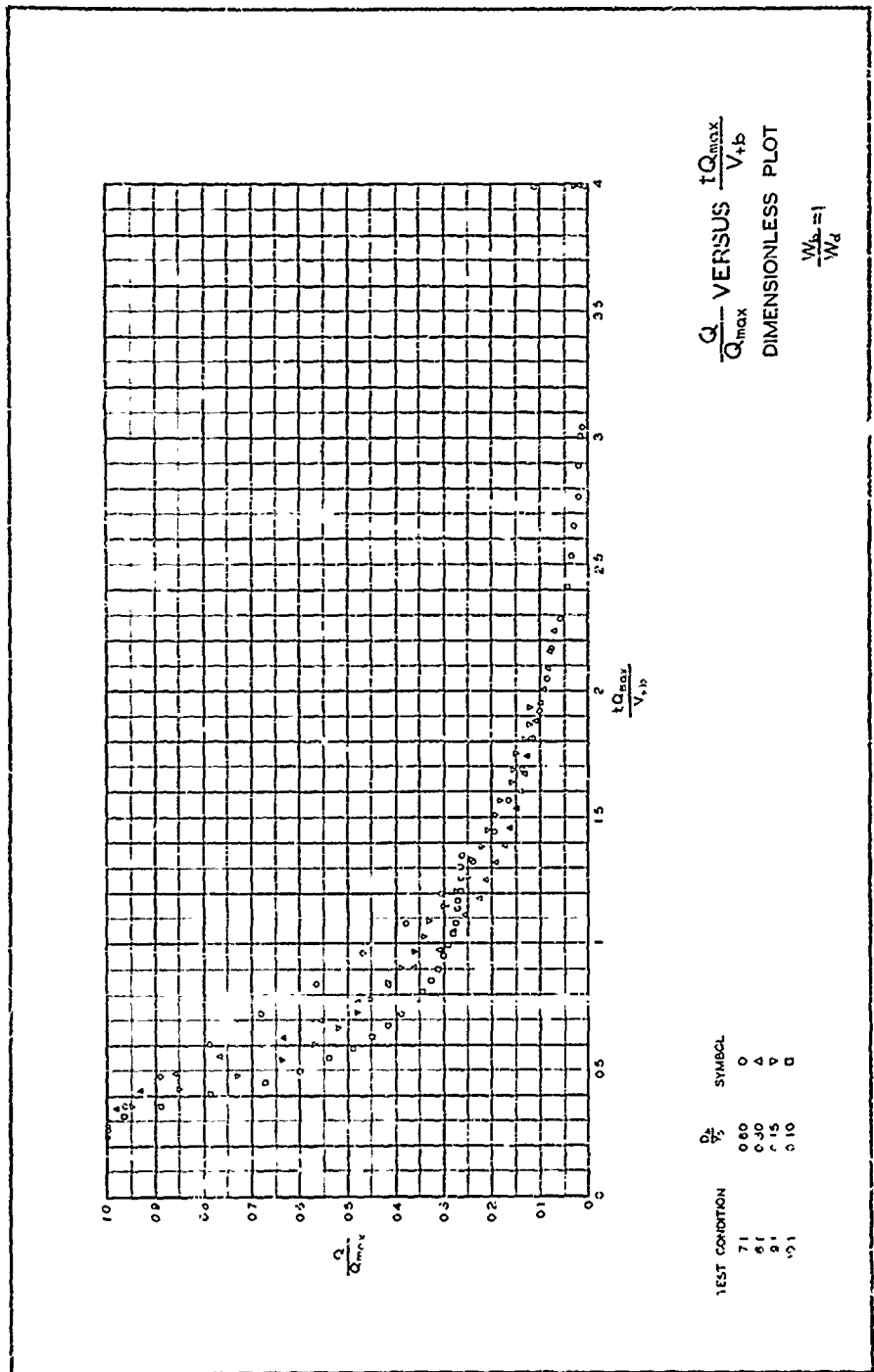
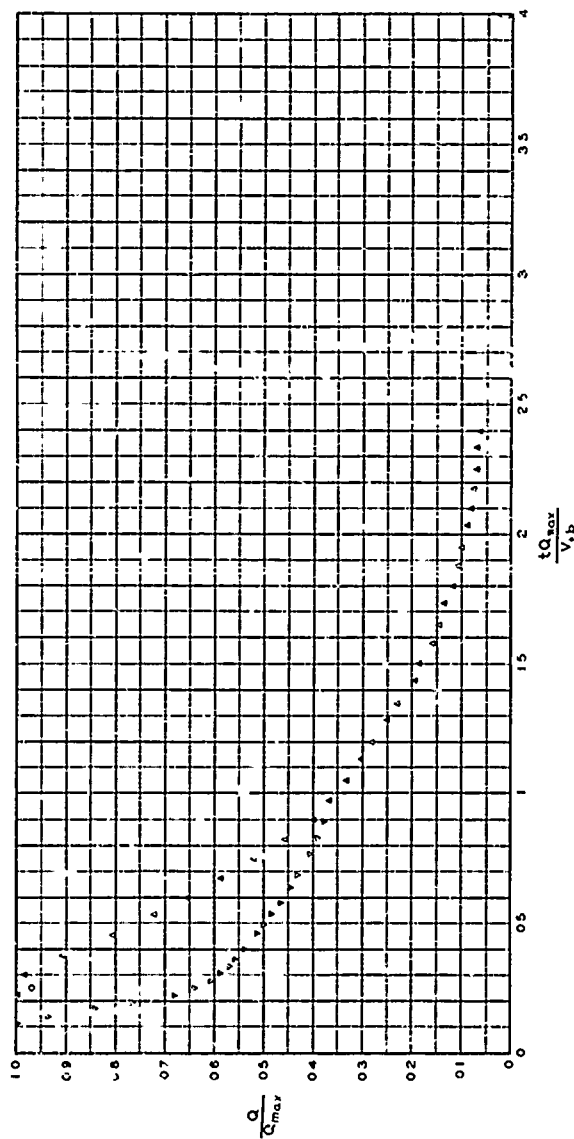


PLATE 102

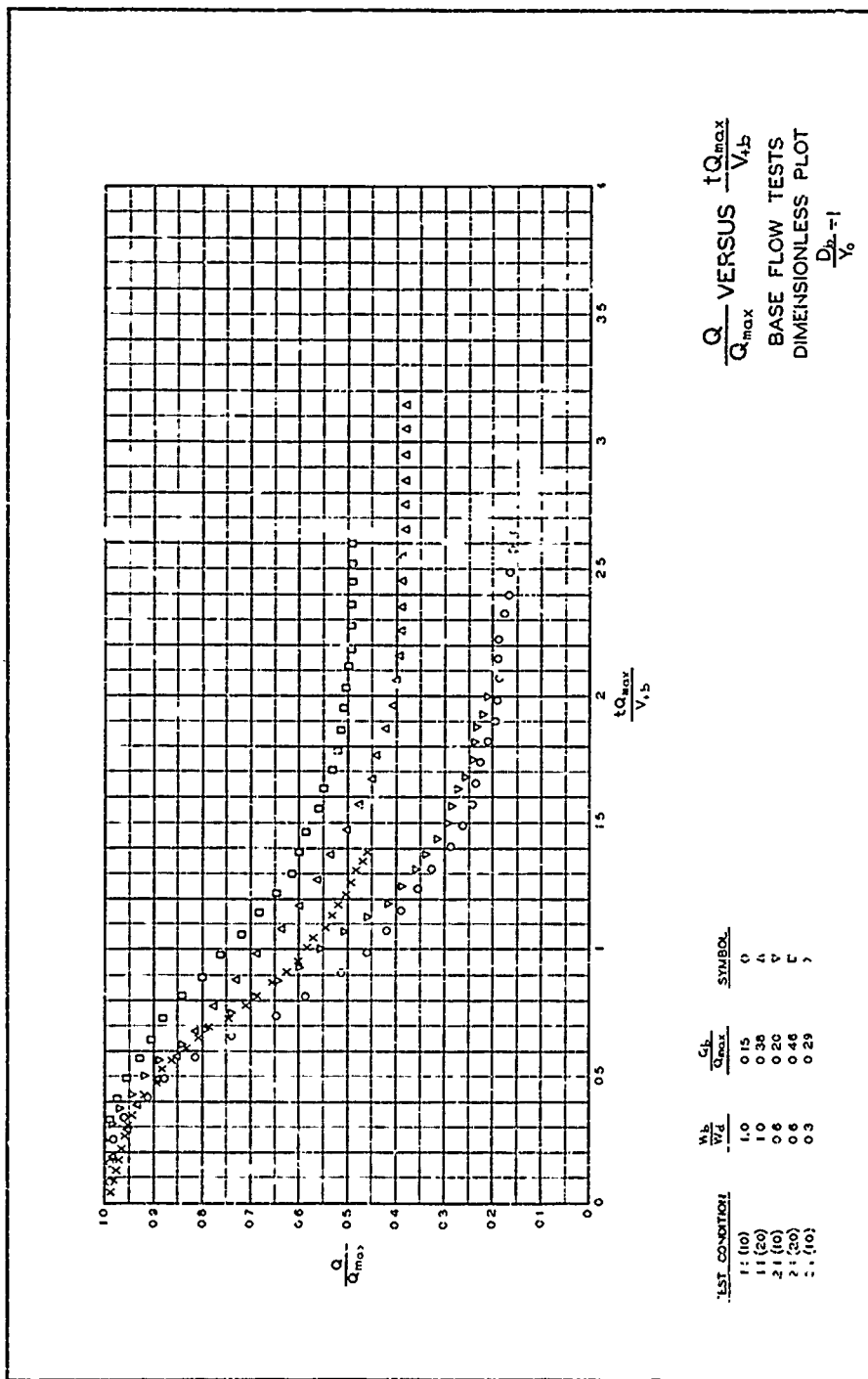


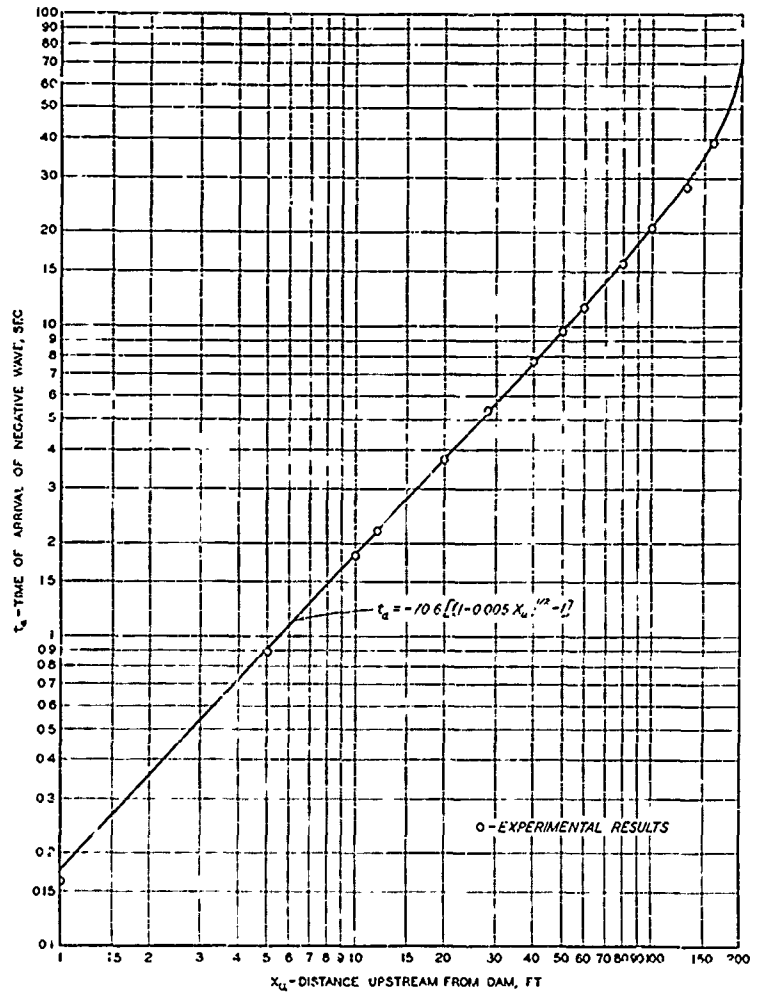


$\frac{Q}{Q_{max}}$ VERSUS $\frac{tQ_{max}}{V_b}$
 DIMENSIONLESS PLOT
 $\frac{D_b}{Y_0} = \frac{W_b}{W_i}$

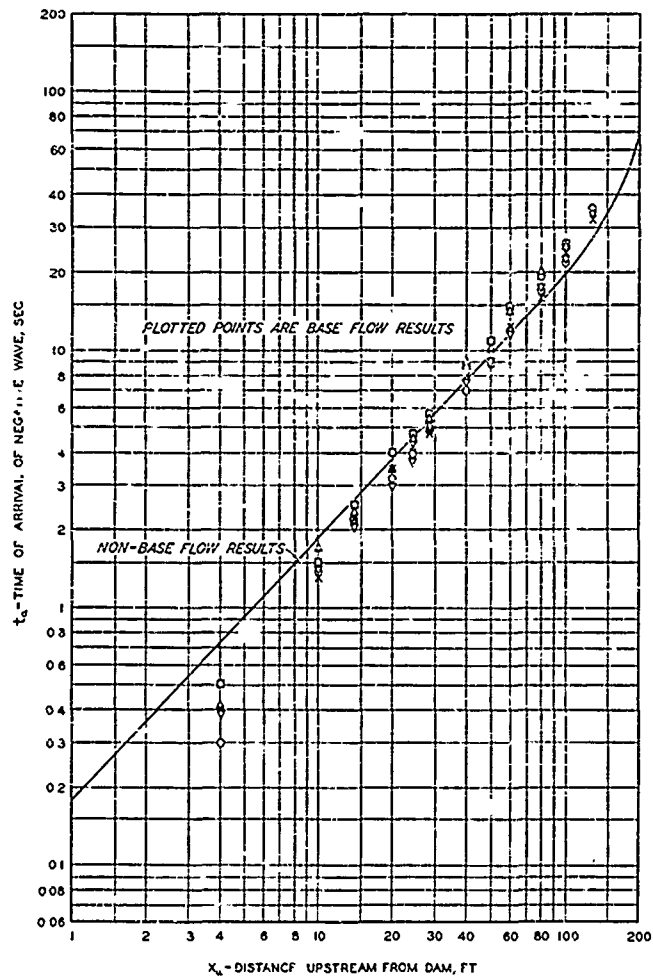
EXPERIMENTAL CONDITION	$\frac{P}{P_0}$	$\frac{W_b}{W_i}$	SYMBOL
11.1	0.36	0.09	Δ
12.1	0.36	0.09	Δ

PLATE 104





ARRIVAL TIME OF NEGATIVE WAVE
AS A FUNCTION OF DISTANCE

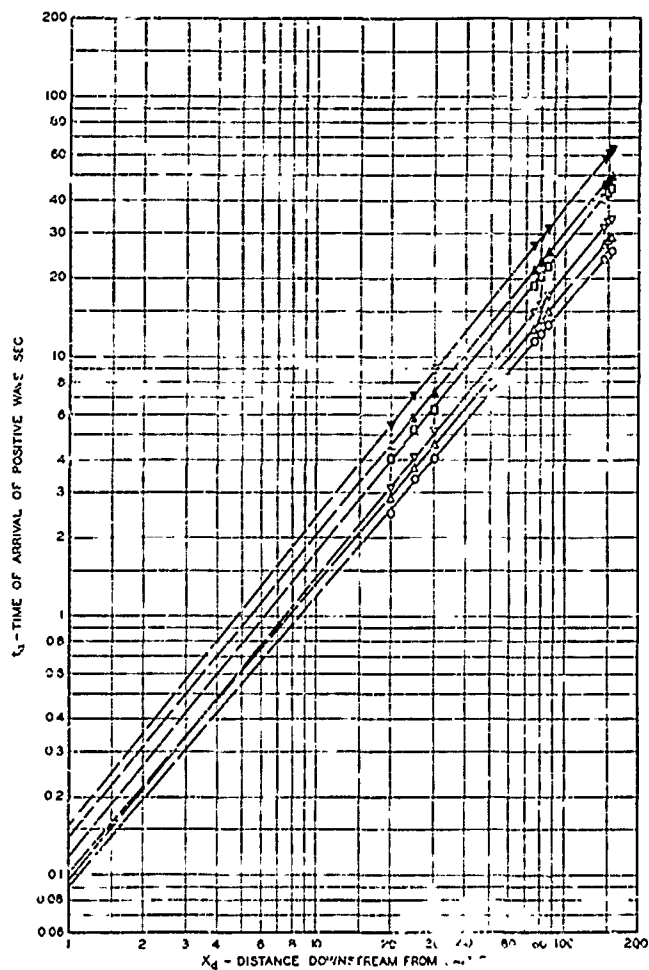


SYMBOL	TEST CONDITION
O	11 (10)
Δ	11 (20)
▽	21 (10)
□	21 (20)
X	31 (10)

ARRIVAL TIME OF NEGATIVE WAVE
AS A FUNCTION OF DISTANCE

BASE FLOW TESTS

PLATE 106

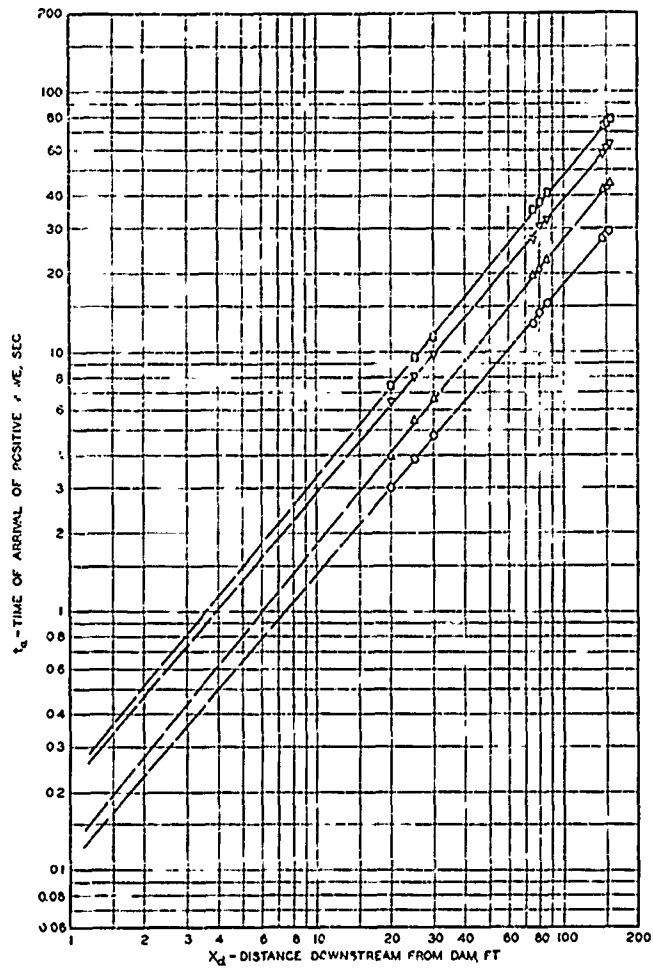


LEAST SQUARES EQUATIONS AND SYMBOLS

CONDITION	EQUATION	SYMBOL
11	$t_a = 0.606(X_d)^{1.18}$	O
21	$t_a = 0.095(X_d)^{1.18}$	Δ
31	$t_a = 0.094(X_d)^{1.17}$	V
41	$t_a = 0.118(X_d)^{1.16}$	D
51	$t_a = 0.135(X_d)^{1.17}$	▲
61	$t_a = 0.154(X_d)^{1.16}$	▼

ARRIVAL TIME OF POSITIVE WAVE
AS A FUNCTION OF DISTANCE

$$\frac{D_B}{V_0} = 1$$

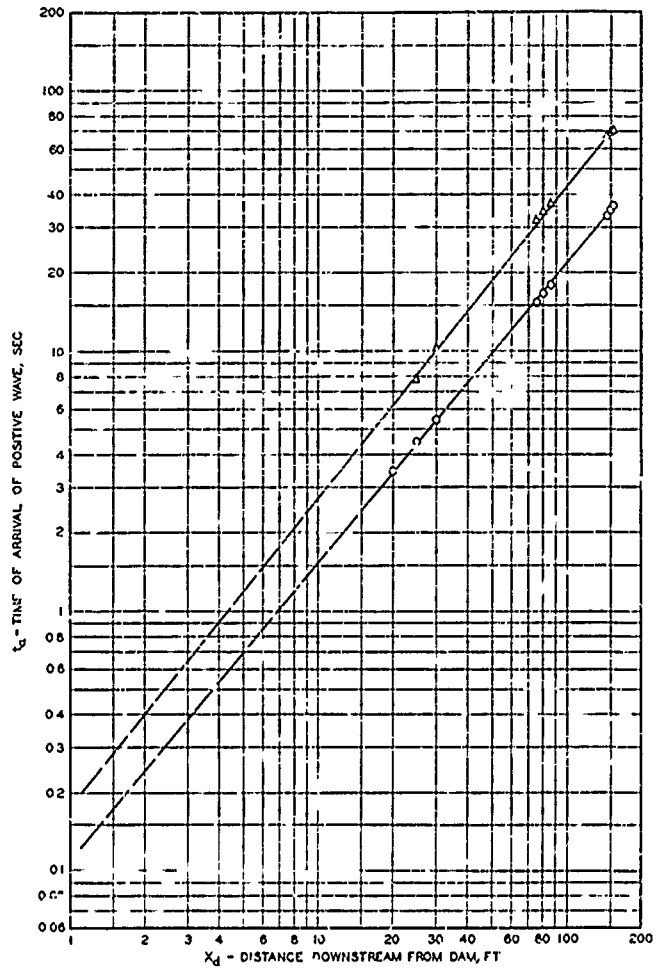


LEAST SQUARED EQUATIONS AND SYMBOLS

<u>CONDITION</u>	<u>EQUATION</u>	<u>SYMBOL</u>
7.1	$t_a = 0.104 (X_d)^{1/2}$	O
8.1	$t_a = 0.20 (X_d)^{1/2}$	Δ
9.1	$t_a = 0.218 (X_d)^{1/2}$	▽
10.1	$t_a = 0.223 (X_d)^{1/2}$	□

ARRIVAL TIME OF POSITIVE WAVE
AS A FUNCTION OF DISTANCE

$$\frac{V_{1D}}{W_d} = 1$$

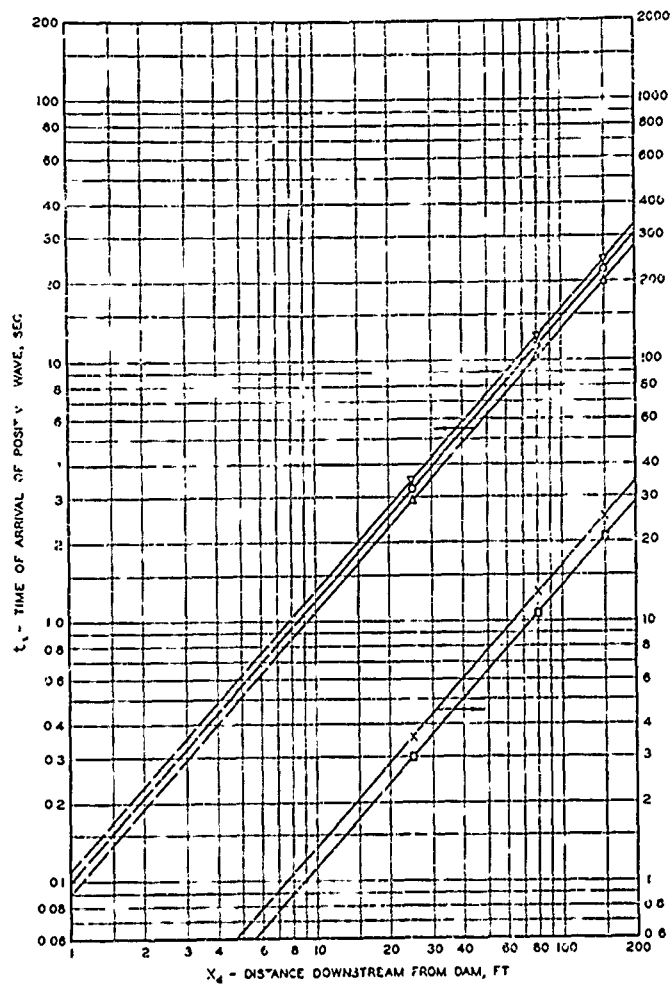


LEAST SQUARES EQUATIONS AND SYMBOLS

CONDITION	EQUATION	SYMBOL
111	$t_b = 0.001 (X_d)^{1.15}$	O
121	$t_b = 0.170 (X_d)^{1.20}$	Δ

ARRIVAL TIME OF POSITIVE WAVE AS A FUNCTION OF DISTANCE

$$\frac{t_b}{Y_0} = \frac{W_b}{W_0}$$



CONDITION	EQUATION	SYMBOL
1 1(10)	$t_a = 0.100 (X_d)^{0.68}$	O
1 1(20)	$t_a = 0.090 (X_d)^{0.68}$	Δ
2 1(10)	$t_a = 0.105 (X_d)^{0.68}$	▽
2 1(20)	$t_a = 0.092 (X_d)^{0.68}$	D
3 1(10)	$t_a = 0.112 (X_d)^{0.68}$	X

ARRIVAL TIME OF POSITIVE WAVE
AS A FUNCTION OF DISTANCE

BASE FLOW TESTS

$$\frac{L_d}{V_0} = 1$$

PLATE 110